Bulletin
of
The Geological Society of America

VOLUME 62 February 1951 NUMBER 2

CONTENTS

	Pages
Statistical methods applied to the study of rock fractures. By Howard J. Pincus	81–130
Radioactivity of the Bourlamaque, Elzevir, and Cheddar batholiths, Canada. By W. N. Ingham and N. B. Keevil	131–148
Structural analysis of the west border of the Durham Triassic Basin. By John W. Harrington	149–158
Differentiation in lavas of the Keweenawan series and the origin of the copper deposits of Michigan. By Henry R. Cornwall	159–202
Triassic to Tertiary stratigraphy near Cerro de Pasco, Peru. By William F. Jenks	202–220

Subscription $15 per year.

Publication Office: Mt. Royal & Guilford Aves., Baltimore 2, Md.

Communications for publication should be addressed to The Geological Society of America, Dr. H. R. Aldrich, Secretary, 419 West 117th Street, New York 27, N. Y.

NOTICE.—Four weeks notice of change of address is necessary. In accordance with the rules established by the Council, claims for non-receipt of the preceding number of the Bulletin must be sent to the Secretary of the Society within three months of the date of the receipt of this number in order to be filled gratis.

Entered as second-class matter in the Post-Office at Baltimore, Md., under the Act of Congress of July 16, 1894.

Accepted for mailing at special rate of postage provided for in Section 1103, Act of October 3, 1917, authorized on July 8, 1918

PAPERS IN PRESS FOR FORTHCOMING ISSUES

GEOLOGY OF THE BARRILLA MOUNTAINS, TEXAS. By G. K. Eifler

MEASUREMENT OF PALEOTEMPERATURES AND TEMPERATURES OF THE UPPER CRETACEOUS OF ENGLAND, DENMARK, AND SOUTHEASTERN UNITED STATES. By H. C. Urey, H. A. Lowenstam, S. Epstein, and C. R. McKinney

CARBONATE-WATER ISOTOPIC TEMPERATURE SCALE. By Samuel Epstein, Ralph Buchsbaum, Heinz Lowenstam, and Harold C. Urey

MECHANICAL BASIS FOR CERTAIN FAMILIAR GEOLOGIC STRUCTURES. By M. King Hubbert

GEOLOGY OF THE WOODSVILLE QUADRANGLE, VERMONT–NEW HAMPSHIRE. By W. S. White and M. P. Billings

MINOR MORAINES IN SOUTH DAKOTA AND MINNESOTA. By Charles S. Gwynne

IRON FORMATION AND ASSOCIATED ROCKS IN THE IRON RIVER DISTRICT, MICHIGAN. By Harold L. James

GLOBAL STRAIN ACCUMULATIONS AND RELEASE AS REVEALED BY GREAT EARTHQUAKES. By Hugo Benioff

MECHANISM OF WEATHERING. By A. F. Frederickson

YOUNGER INTRUSIVE ROCKS OF PLATEAU PROVINCE, NIGERIA, COMPARED WITH THE ALKALIC ROCKS OF NEW ENGLAND. By Robert Greenwood

ST. PAUL GROUP: A REVISION OF THE "STONES RIVER" GROUP OF MARYLAND AND ADJACENT STATES. By Robert B. Neuman

BULLETIN OF THE GEOLOGICAL SOCIETY OF AMERICA
VOL. 62, PP. 81-130, 24 FIGS. FEBRUARY 1951

STATISTICAL METHODS APPLIED TO THE STUDY OF ROCK FRACTURES

Quantitative Comparative Analysis of Fractures in Gneisses and Overlying Sedimentary Rocks of Northern New Jersey

By Howard J. Pincus

Abstract

A quantitative analysis of fracture-orientation data collected in Precambrian gneisses and overlying lower Paleozoic sedimentary rocks in three northern New Jersey areas yields the following results: (1) The data, as plotted on both rectangular co-ordinates and the Schmidt equal-area net, show definite clustering for all localities studied; the Poisson Exponential Binomial Limit is applied to test for significant departure of the diagrams from isotropism, to estimate mean orientations of fracture sets (mean fracture planes), and to aid in interpreting the rectangular point diagrams. (2) Fractures and foliations in the crystalline rocks do not appear to be genetically related. (3) Most localities have two principal joint sets, but there are proportionately more Precambrian than Paleozoic localities with three sets. (4) The Paleozoic localities show more concentrated clustering on the point diagrams. (5) The dihedral angle between mean fracture planes and bedding is typically near 90 degrees; the dihedral angle between mean fracture planes and foliation has no typical value. (6) The angle of fracture in both rock types appears to be independent of the nature of the rock. (7) Contrasts in rock type (metamorphic vs. overlying sedimentary) are usually accompanied by striking differences in point-diagram patterns. (8) The measurement of a few large fractures gives no better approximation of the mean fracture planes than the measurement of an equal number of fractures of any size. (9) The trends of mean fracture planes conform with linear features visible on air photographs. (10) A high proportion of fractures dip steeply; dips in the crystalline rocks are systematically smaller than those in the overlying sedimentary rocks.

The fractures in the gneisses are probably older than those in the sedimentary rocks.

The deformation of the gneisses seems to have taken place through mechanisms fundamentally different from those involved in deforming the overlying sedimentary rocks.

CONTENTS

	Page
Introduction	82
Acknowledgments	82
I—Geological setting	83
1.—General geology	83
2.—Geology of the areas selected for study	85
Gladstone-Peapack (Area I)	85
Oxford (Area II)	86
Bowling Green Mountain (Area III)	86
II—Collection and statistical treatment of the quantitative data	90
1.—Selection of localities	90
2.—Principles used in collecting field data	91
3.—Method of plotting the data on rectangular co-ordinates	93
General discussion	93
Interpretation of contour patterns	94
Strike and dip frequency distributions	96
Rectangular co-ordinates and the Schmidt equal-area net: Their properties compared	96
Size of grid squares	98
4.—Number of observations required at each locality	99
5.—Statistical analysis of the data on point diagrams	101
III—Analysis of mean fracture planes	105
1.—Overall aspects of mean fracture planes	105
2.—Number of clusters at each locality	110
3.—Frequency values of maxima on the point diagrams	111
4.—Dihedral angle between mean fracture planes and bedding or foliation planes at the respective localities	114
5.—Dihedral angle between mean fracture planes at each locality	116
6.—Comparison of contour diagrams of localities in structurally similar positions	117
7.—Use of large fractures in reconnaissance	118
8.—Relation of mean fracture planes to features visible on air photographs (Area III)	120
9.—Geometric erasure of the Paleozoic deformation: Validity and implications of an arbitrary method of structural restoration	120
Paleozoic sedimentary rocks	120
Precambrian gneisses	121
Discussion of areas	122

Page

IV—Angle of dip of fractures in the gneisses and the sedimentary rocks 123
General statement 123
Dips of individual fracture planes 123
Dips of mean fracture planes 124
V—Summary and conclusions 124
Appendix. Annotated bibliography of selected papers 127
References cited 128

ILLUSTRATIONS

Figure Page

1. Index map of New Jersey 83
2. Gladstone-Peapack (Area I) map 84
3. Oxford (Area II) map 86
4. Bowling Green Mountain (Area III) map .. 90
5. Rectangular co-ordinate diagram 93
6. Interpretation of contoured diagrams 95
7. Effect of cutting the abscissa of a cyclic variable frequency curve at different points 96
8. Comparison of methods of plotting 97
9. Effect of the addition of successive increments of fracture orientation data 100
10. Problem of cluster borders: Identification and evaluation 103
11. Rectangular co-ordinate diagrams with "A" and "B" contours, and the associated strike and dip frequency distributions—Area I 106
12. Rectangular co-ordinate diagrams with "A" and "B" contours, and the associated strike and dip frequency distribution— Area II .. 107
13. Rectangular co-ordinate diagrams with "A" and "B" contours, and the associated strike and dip frequency distribution—Area III .. 108
14. Overlay of Figure 2: bedding, foliation, and mean fracture planes—area I 109
15. Overlay of Figure 3: bedding, foliation and mean fracture planes—Area II 110
16. Overlay of Figure 4: bedding, foliation, and mean fracture planes—Area III 111
17. Summary picture of the mean fracture planes and foliation planes for the three areas 112
18. Number of clusters at each locality 113
19. Frequency values of maxima on the contoured point diagrams 113
20. Dihedral angle between mean fracture planes and bedding and foliation 114
21. Dihedral angle between mean fracture planes at each locality 116
22. Comparison between large and other fractures as estimates of mean fracture planes .. 119
23. Rotated fracture data 121
24. Angle of dip in the sedimentary rocks and in the gneisses 124

TABLES

Table Page

1. Properties of grid squares of different sizes .. 98
2. Bedding, foliation, and mean fracture planes of all localities in the three areas 104
3. Angle between strike of mean fracture planes and strike of bedding and axis of fold 115

Introduction

Fracture patterns in sedimentary and crystalline rocks have been studied in many regions, but some of the results obtained have uncertain meaning. Literature on field techniques suggests that some data may have been collected with considerable selectivity. Several papers do not mention field techniques; the meaning of the data is doubtful because the method of measuring is unknown, and comparisons with other studies are hazy.

The desire for a more objective, standardized approach has led to the application of statistical methods. The writer suggests modifications of previous methods and explains some new techniques. (The Appendix is an annotated bibliography of selected papers in which comparable quantitative methods are applied to the study of rock fractures, structural petrology, and sedimentology.)

Another difficulty in interpretation of the results of some of the earlier papers attaches to the meaning of fracture patterns in Precambrian crystalline rocks, since most of these rocks have been deformed more than once. Here, the writer compares the fractures in the Precambrian rocks with those in the overlying Paleozoic sedimentary rocks; both groups of rock were involved in later deformations in the areas studied. To the writer's knowledge, the type of comparative study presented here has not been undertaken before.

Acknowledgments

Dr. Walter H. Bucher suggested the subject of this paper and gave advice and much time in connection with the preparation of the final manuscript.

Dr. Howard Levene of the Department of Mathematical Statistics, Columbia University,

provided much valuable information on statistical techniques. He suggested the use of the Poisson Exponential Binomial Limit in the analysis of the point diagrams (II, 5).[1]

Dr. Meredith Johnson, State Geologist of New Jersey, gave valuable information and secured access to various properties.

The costs of the field work were defrayed in part by a grant from the Kemp Memorial Fund.

For all this help and co-operation the writer is deeply grateful.

I—Geological Setting

General Geology

The fracture orientation data were obtained in the New Jersey Highlands (Fig. 1). Structurally, the area consists of comparatively gently folded lower Paleozoic rocks; Precambrian crystalline rocks appear along anticlinal axes. The topography is a function chiefly of structure and lithology: gneisses in anticlines form ridges of moderate slope, and limestones in synclines underlie the valleys between. Quartzites form the steepest features. The rocks providing the fracture data range from Precambrian to lower Silurian. A generalized section of this part of the column is as follows (Kümmel, 1938–1940):

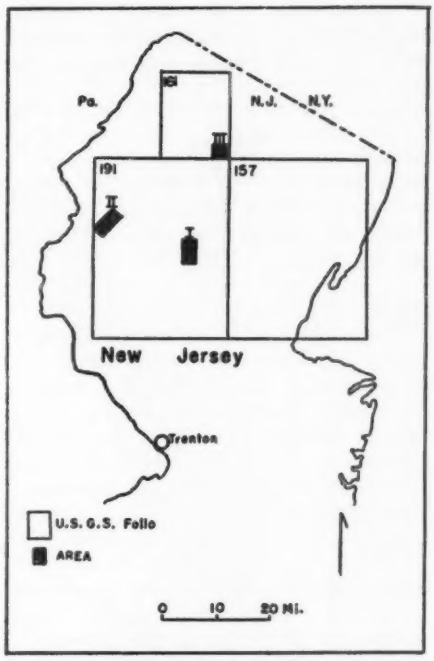

Figure 1.—Index Map of New Jersey

			Feet
Silurian	* Green Pond conglomerate†	(Sgp)	1200–1500
Ordovician	Martinsburg Shale	(Omb)	3000
	Jacksonburg limestone	(Ojb)	125–300
	* Kittatinny limestone	(COk)	2500–3000
Cambrian	* Hardyston quartzite	(Ch)	5–200
Precambrian	* Losee gneiss	(Lgn)	(Age relation of gneisses unknown)
	* Byram gneiss	(Bgn)	

* Formations providing fracture data.

† Lies unconformably on the pre-Cambrian rocks in the Bowling Green Mountain area.

After extensive deformation, metamorphism, and erosion of the Precambrian rocks in the New Jersey Highlands, an invasion of the sea, beginning in Cambrian time and ranging through the Ordovician, resulted in the deposition of a thick series of sediments. The Hardyston and the Kittatinny formations lie at the base of this series.

[1] (II, 5) refers to Part II, Section 5 of this paper. This type of notation is used throughout the paper.

Near the close of the Ordovician, the land was uplifted, and the sea withdrew. In eastern New York and western New England the Taconic disturbance produced extensive folding and thrusting. The extent and degree of this folding in northern New Jersey has not been determined.

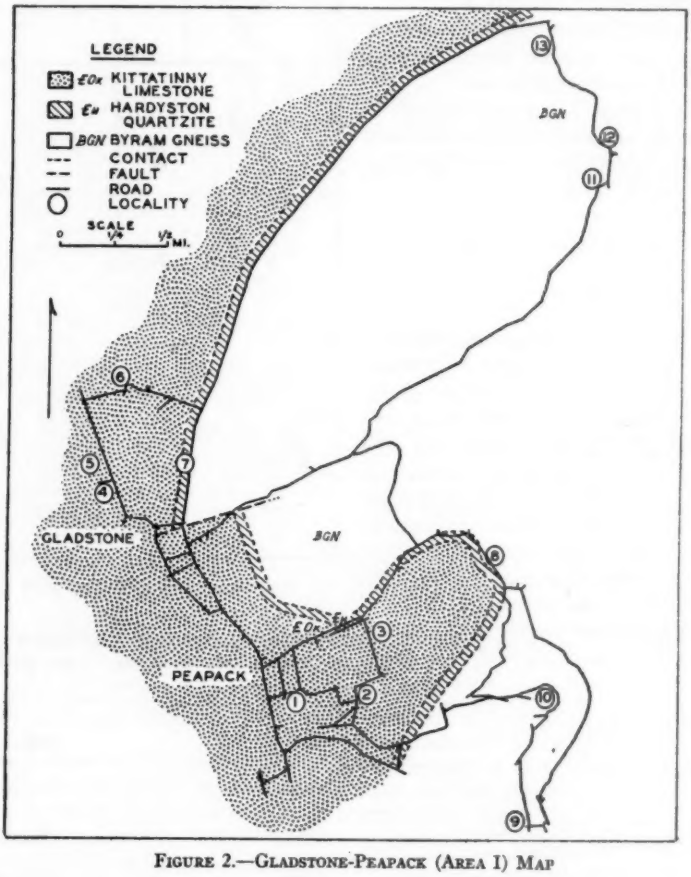

FIGURE 2.—GLADSTONE-PEAPACK (AREA I) MAP

The Green Pond and Shawangunk conglomerates, generally conceded to be of the same age (lower Silurian), were deposited after the Cambrian and Ordovician formations had been so eroded that, in the Green Pond syncline, the conglomerates lie directly upon the Precambrian gneisses. At the northern end of the syncline, northeast of Skunnemunk Mountain in New York, they lie upon the upper Ordovician Hudson River shales. North of Macopin Lake, on the east side of Kanouse Mountain, the Green Pond conglomerate lies upon the Cambro-Ordovician dolomite. Southwestward from Bowling Green Mountain along the band of sedimentary rocks which are bounded by crystalline rocks on both sides, only remnants of the conglomerate remain in the vicinity of Carey, Kenvil, and Rustic. From the geologic map (Bayley, Kümmel, and Salisbury, 1914) it appears that here the patches of Green Pond conglomerate are underlain by the Cambro-Ordovician Kittatinny limestone. Still farther southwest along the same synclincal axis,

the Silurian rocks have been removed, and the Kittatinny beds are the youngest in the German Valley.

Thus the tracing of this one band of sedimentary rocks demonstrates that the surface of erosion below the lower Silurian cuts across the older rocks from the upper Ordovician Hudson River shales to the Precambrian gneisses. It shows further that the axis of the Siluro-Devonian, Green Pond-Skunnemunk syncline coincides largely with the axis of the earlier syncline of Cambro-Ordovician rocks. Such a preservation of a fold axis through more than one period of folding is a common orogenic phenomenon.

Geology of the Areas Selected for Study

General geology.—The following areas in the New Jersey Highlands were investigated for study:

(1) Gladstone-Peapack (anticline and syncline).
(2) Califon* (anticline).
(3) Washington* (anticline and syncline).
(4) Oxford (anticline and syncline).
(5) Vienna† (anticline).
(6) Bowling Green Mt. (anticline).

In the three areas selected, data were collected in Pre-cambrian gneisses and in the sedimentary rocks immediately above. At Gladstone-Peapack and Oxford, exposures of Hardyston quartzite are rare. Here the Kittatinny serves as the principal source of data in the Paleozoic sediments. Similarity in structural behavior, at least insofar as fracturing is concerned, is believed to obtain for the rocks of these two formations (III, 6).

Each of the three areas displays unique structural features. Although the Gladstone-Peapack and Oxford areas involve folding in the same kinds of rock, minor faults transect the folds of the former. In both areas, the foliation in the gneisses is generally quite indistinct, and at some points it appears to be missing (Figs. 2, 3).

The part of the Bowling Green Mountain studied consists of a sharply broken anticline of Green Pond conglomerate with linear limbs and a considerably shattered nose. The foliation in the gneissic core is more distinct than that in the other two areas, but in some exposures it is not easily determined (Fig. 4).

Gladstone-Peapack, Oxford, and Bowling Green Mountain areas are referred to as "Areas I, II, and III" respectively. Exposures studied within each area are designated "Localities" and are identified on the map and in the text by arabic numerals.

Area I (Gladstone-Peapack) (Fig. 2): The area was mapped on a scale of about 1:6800 (1 inch:100 paces) by means of a tripod-mounted Brunton; the small scale and early date of published maps (Bayley, Kümmel, and Salisbury, 1914, on base map of 1908) rendered them unsuitable for this study. A mosaic was constructed of closed traverses chiefly along roads. Because the road cuts in this region provide the most useful exposures of crystalline rocks, the two tasks of base mapping and geological reconnaissance were performed concurrently.

The available air photographs of suitable scale and definition were taken when heavy foliage masked most exposures, and were therefore of little help in reconnaissance.

Large local exposures, such as quarries, in which fracture data were collected, were mapped by closed traverses on a scale of 1:680 (1 inch:10 paces). The positions of points of collection along such exposures were entered accurately on these local maps to prevent duplication of data if, for any reason, it might be necessary to return later for additional readings.

Also, the localities were mapped to determine their principal dimensions with respect to distances along the strike between them. It was necessary to keep these dimensions small with respect to the distances between localities, say 1:10, so that the localities could be considered as points not partaking of systematic areal variations. In addition, interpretation of data diagrams for the localities is simplified by following this rule (III, 1).

Where fracture data were taken from a group of small exposures of gneiss near a road or along a road cut, closed traverses were not run. Detailed notes were taken, and the length

* Rejected for collection of data because of paucity of suitable exposures.

† Rejected for collection of data because of paucity of suitable exposures and magnetic effects of the crystalline rocks.

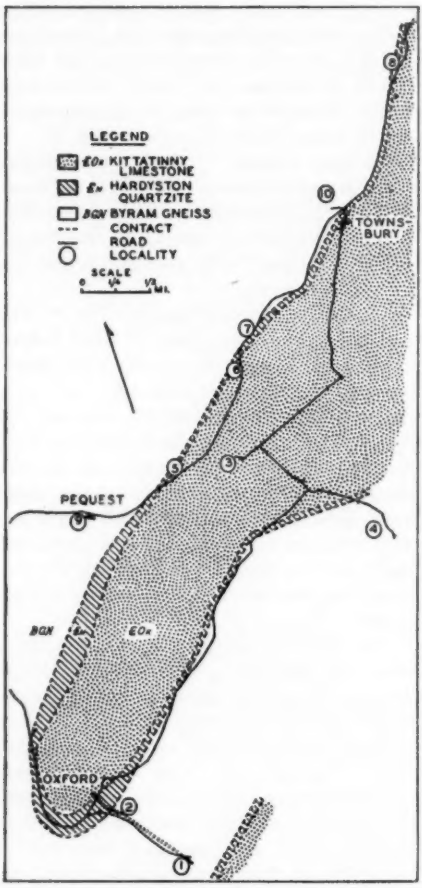

FIGURE 3.—OXFORD (AREA II) MAP

and direction of the maximum dimension of the locality were recorded.

The heavy soil mantle and abundant glacial debris hampered the discovery of suitably large and desirably situated exposures. Although the Byram and Losee gneisses underlie topographic highs, hilltops usually lack exposures of rock in place. Road cuts are the best single source of exposures of Precambrian rocks. There is little danger that road construction has produced fractures that might be confused with natural joints.

The fractures in the gneisses lack regularity, frequently disappear into continuous rock, and occasionally run into each other in a somewhat confusing manner. They resemble quite closely the cracks in a deformed mass of clay. The fracture surfaces show considerable slickensiding, although weathering has almost obliterated this feature on many surfaces.

The Hardyston quartzite was very rarely seen in outcrop; its presence was inferred from the location of loose quartzite boulders and occasional low linear swells along valley borders. The fractures in the quartzite are small, regular, and well defined.

Since the Kittatinny forms valleys, quarries are the best sources of information for this unit. The fractures in the Kittatinny are generally regular and well defined and are larger than those in the quartzite. The fractures in the shalier beds are more closely spaced than those in the purer carbonates.

The presence of cherts on hilltops underlain by gneisses seems to bear out the contention (Kümmel, 1938–1940) that the Kittatinny blanketed the older rocks; the cherts are similar to those found in the Kittatinny and are interpreted as solution residuals.

AREA II (OXFORD) (Fig. 3): The mapping procedure here was identical with that in the Gladstone-Peapack area.

U. S. Route 46 (N. J. 6) provides cuts through Kittatinny, Hardyston, and Precambrian rocks. The last group is also exposed in cuts of the Delaware, Lackawanna, and Western Railroad.

In this area, as in Area I, the Hardyston quartzite is rarely seen in place.

The fractures in the gneisses and the sedimentary rocks display the same properties as those in Area I, except that in the Hardyston quartzite, which is more vitreous in Area II, the fractures are subconchoidal.

AREA III (BOWLING GREEN MOUNTAIN) (Fig. 4): Air photographs, used as a base map in this area, show many details of geologic interest which are visible because the photographs were taken when foliage was absent; also, outcrops are especially prominent on the resistant conglomerate. For example, the air photographs show that the western limb of the anticline runs almost due west, abutting against an area of crystalline rocks, while the U. S. Geological Survey map (Kümmel, Spencer, and Weller, 1908) shows a syncline formed by the conglomerate swinging around to the

DETAILED NOTES—AREA I

Locality	Formation	Description	Remarks
1—Peapack Quarry	Kittatinny	Bluish-gray, medium- to fine-grained magnesian limestone; bedding up to 3–4 feet thick, with occasional interlayering of shaly and sandy members.	Close fracturing of thin shaly interbeds closely follows the larger, more widely spaced joints of the carbonate layers. Locally, tiny veinlets of deep-red carbonate. Quarry in operation. Dry.
2—Quarry	Kittatinny	Gray and more massive than beds in No. 1.	Few shaly beds present are closely fractured. Abandoned and flooded.
3—Quarry	Kittatinny	Similar to No. 2.	Abandoned and overgrown.
4—Quarry	Kittatinny	Reddish, medium- to fine-grained magnesian limestone; argillaceous laminae 3–4 feet apart; becomes redder, sandier, and shalier in lower beds, with quartz geodes occurring in the oldest beds.	Selected close to Nos. 5 and 7 for comparison of fracture orientations. Fault N.87°W., 90-degree dip in southern part of quarry. Displacement on north side about 30 feet to the west. Quarry abandoned.
5—Quarry	Kittatinny	Bluish-gray to reddish-gray, medium- to fine-grained magnesian limestone, with some sandy layers.	Abandoned.
6—Quarry	Kittatinny	Bluish-gray to gray, medium- to fine-grained magnesian limestone. Some cross-bedding.	Some banding shows lensing which may be cross-bedding in section. Close fracturing in shaly layers. Fault N.81°W., 68°W., in center of quarry; displacement on north side about 10 feet to west. Abandoned and partly flooded.
7—Hyatt Property	Hardyston	Fine- to medium-grained gray quartz matrix with white subrounded to rounded quartz grains up to sand size. Occasionally feldspathic.	Fractures are smaller in area than those measured in any other locality, but are regular and well defined. Small exposure.
8—Road west of North Branch, Raritan River, and east of Blairsden estate.	Byram	Yellowish-brown to brown, medium- to coarse-grained, traversed by black bands of hornblende and biotite. Contains much feldspar (including orthoclase) and quartz.	Road cut. Small amount of data collected due to small size of exposure. Is approximately in line with synclinal axis cutting through Peapack.

DETAILED NOTES—AREA I—*Continued*

Locality	Formation	Description	Remarks
9—Road from south gate into Blairsden estate.	Byram	Same as No. 8, but somewhat finer-grained, becoming coarser-grained to the north. Foliation not distinct and frequently absent.	Many diversely oriented fracture surfaces are slickensided. Immediate impression of fractures is that orientations are random. Road cut.
10—Blairsden road, west of the main house.	Byram	Same as No. 9 but foliation is even less distinct, and the grain is coarser.	Same as No. 9.
11—Schiff Scout Center road, near bridge. Old quarry?	Byram	Coarse-textured, occasionally with graphic intergrowths; gross composition and color similar to No. 8; foliation very faint.	Many slumped blocks required careful examination of exposures before readings were taken.
12—Near Schiff Scout Center	Byram	Coarse-textured, but not generally as coarse and feldspathic as No. 11.	Road cut and hill side.
13—West end of dirt road road leading to Schiff camp. Just south of dam.	Byram	Same as No. 9.	Foliation locally dips west, but is dominantly east. Fractures cut across swirls in foliation.

northeast. The writer's field work indicates that the interpretation drawn from the photographs is correct (Fig. 4).

Furthermore, the western "contact" of the Losee and Byram gneisses within the anticline, as shown on the U. S. Geological Survey map, coincides with a prominent line on the photographs which, when extended northward, coincides with a fault zone cutting the Green Pond conglomerate. Probably this "contact" is actually a long shear zone; its trend is almost parallel to the trend of the large fault to the west which truncates the western limb of the anticline (Fig. 4).

The Green Pond conglomerate in this area is a fairly uniform, grayish to grayish-purple quartzitic conglomerate with angular to moderately rounded white quartz pebbles up to 2 inches long. The size of the pebbles gradually increases toward the contact with the underlying gneisses. The matrix is vitreous and highly quartzose. Prominent cross-bedding is common. Cracks in the pebbles are usually parallel to the larger fracture surfaces. No evidence was seen of intraformational bedding-plane slippage.

The fractures in the conglomerate are generally regular and well defined, cutting quite smoothly across the cross-bedding. A somewhat puzzling feature is the existence, very close to each other, of fractures of parallel orientation, some of which are quartz-filled, while others are empty and closed. Small en echelon fractures are also present, lying in zones parallel to cross fractures; some of these en echelon fractures are quartz-filled, while others are not. Possibly the quartz-filled fractures resulted from locally more prolonged deformation which caused the fractures to gap and fill with vein quartz.

Between the belt of exposures of conglomerate and the scattered outcrops of the underlying crystalline rocks is a narrow draw which is quite prominent in the east limb of the anticline, and locally present in the west limb. Loose blocks, consisting mostly of conglomeratic talus, abound in the depression. The draw may be the surface expression of a crush zone developed along the gneiss-conglomerate contact, and along which considerable slippage and shattering took place during the break-folding of the Green Pond conglomerate.

DETAILED NOTES—AREA II

Locality	Formation	Description	Remarks
1—South entrance, Oxford Tunnel, west side of cut.	Byram	Yellowish-brown to brown, medium- to coarse-grained, with foliation visible only on a few fresh surfaces. More linear than platy. Same gross composition as Area I.	Slickensides of steplike character somewhat obscured by weathering and grime. Fractures generally well defined.
2—North entrance, Oxford Tunnel, east side of cut.	Byram	Same as No. 1.	Same as No. 1.
3—Quarry	Kittatinny	Gray, fine to medium-grained, thick-bedded, magnesian limestone.	Fractures large and well defined. Abandoned and overgrown.
4—Stewart Gap	Byram	Coarse-grained, highly feldspathic, with no visible foliation. Some rocks in the vicinity noticeably magnetic.	Great irregularity of some fracture surfaces resulted in use of smaller proportion of fractures than in other localities. Some sheeting present, but not in exposures used as sources of data.
5—Southernmost limestone exposure on N.J. 6, north of branch road to Pequest.	Kittatinny	Similar to No. 3.	Road cut.
6—Green farm, N.J. 6.	Kittatinny	Similar to No. 3.	Abandoned quarry bordering road.
7—First gneiss exposure north of No. 6 along N. J. 6.	Byram	Grayer than Nos. 1 or 2, with foliation more apparent, some bands resembling bedding.	Road cut.
8—N.J. 6, south of Great Meadows.	Hardyston	Gray, fine-graned quartzite, with vitreous matrix.	Subconchoidal fracture surfaces difficult to measure.
9—Pequest railroad crossing.	Byram	Same as No. 1.	Same as No. 1.
10—Townsbury granite quarry, north of N.J. 6.	Byram	Grayer and coarser than Nos. 1 and 2; foliation faint to absent.	Some fractures quite large and regular.

The Byram gneiss is similar to that in Areas I and II. The Losee gneiss contains more light-colored feldspar and quartz than the Byram and is finer-grained and lighter-colored on the weathered surface.

In this area, the foliation, which is not always easy to determine, is more distinct than in Areas I and II. It is less distinct in the Losee than in the Byram. Fairly persistent pegmatitic sheets from a fraction of an inch up to a foot or more thick lie parallel to the foliation.

The fractures display the same characteristics as those in the gneisses in Areas I and II, but, in addition, near No. 4 there is an exposure with some very persistent partings which bear a striking resemblance to flat-lying bedding planes. Close inspection, however, re-

veals that the partings cut the foliation almost at right angles. The partings are almost parallel to the bedding of the conglomerate in the curvature. However, there is enough change between the localities in each area to define adequately the overall structure so that frac-

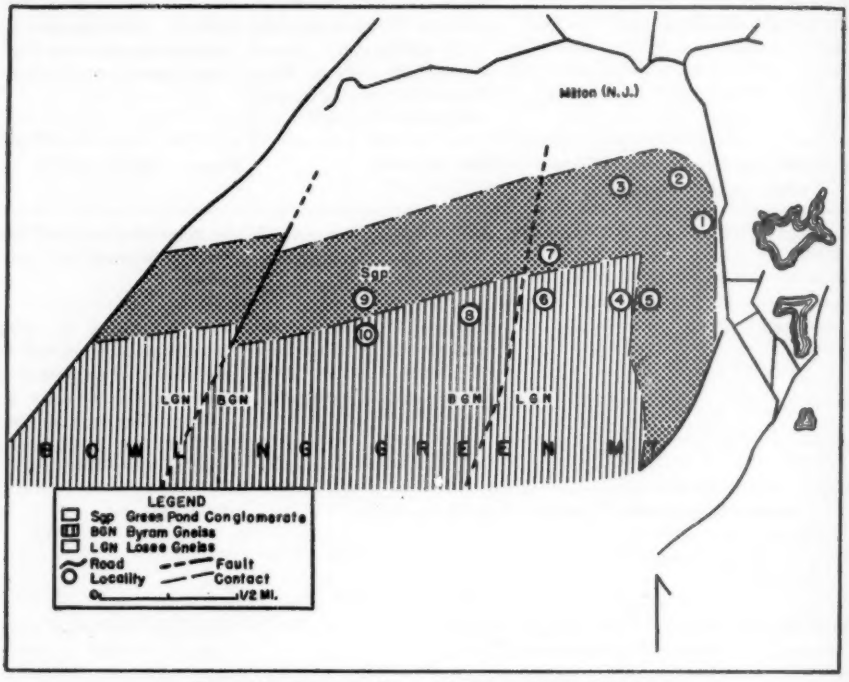

FIGURE 4.—BOWLING GREEN MOUNTAIN (AREA III) MAP

adjacent locality, No. 5. Could they be the result of frictional resistance to differential movement of the overlying conglomerate along the contact with the gneisses?

Here, slickensiding is not so apparent as in the other two areas, probably because the exposures are natural and old, and, therefore, have been weathered considerably more.

II—COLLECTION AND STATISTICAL TREATMENT OF QUANTITATIVE DATA

1.—*Selection of the Localities*

In each area studied, localities were selected in the lowest continuous Paleozoic rocks representative of the changing trend around the structure. The lack of exposures of sufficient size, or of any exposures, prevented complete definition of all significant changes in trend and ture orientations may be investigated as a function of structure. Additional localities not showing significant changes in trend were introduced in some instances to provide reference data with which localities in structurally similar positions could be compared. (*See* Area I, Nos. 4 and 5; Area III, Nos. 6, 8, and 10.)

Localities in the Precambrian gneisses were placed, insofar as possible, across the strike from and in structural positions corresponding to those of the localities in the overlying Paleozoic sediments. Where this was impossible, it was usually feasible to select localities somewhat offset parallel to the Paleozoic trend and in comparable structural positions. (*See* Area II, north limb of syncline.)

The largest linear dimension of any locality is approximately 110 yards (100 meters); the average maximum dimension is less than half that amount.

DETAILED NOTES—AREA III

Locality	Formation	Description	Remarks
1—East limb of anticline	Green Pond	Described in text	Some gapped surfaces are filled with milky quartz. Some movement along fracture surfaces indicated.
2—Nose of anticline	Green Pond	Described in text	Same as No. 1
3—West limb of anticline	Green Pond	Described in text	Same as No. 1
4—Just west of contact with conglomerate in east limb (No. 5)	Losee	Light-colored, fine-grained, weathering grayish white or brown. Foliation fairly apparent, although not obvious.	Fractures resemble cracks in clay, as described in text.
5—At base of conglomerate of east limb	Green Pond	More large pebbles than in Nos. 1 and 3	
6—Just south of contact with conglomerate in west limb (No. 7)	Losee	Typical Losee Foliation visible	Quartz veinlets are roughly parallel to larger fracture surfaces.
7—At base of conglomerate of west limb	Green Pond	Described in text	
8—West of No. 6 and in similar structural position	Byram	Typical Bryam composition. Some coarse-grained, more feldspathic bands lie parallel to foliation.	In the coarse bands is some faint fracture cleavage bearing northeast.
9—West of No. 7 and in similar structural position	Green Pond	Described in text	Cracks in pebbles are parallel to larger fracture surfaces.
10—West of No. 8, and in similar structural position, and south of No. 9	Byram	Somewhat finer-grained than the typical Byram, with bands of the more typical texture interspersed. The bands are parallel to faint foliation.	In the coarser bands is some fracture cleavage bearing east-northeast.

The distance between localities along the strike within a given rock type is usually at least 10 times the average maximum dimension of the localities.

Thus, insofar as possible, the Paleozoic localities were chosen far enough apart so that the data sources could be considered as points, and close enough to represent the amount of curvature along the trend; Precambrian localities were tied to structurally comparable Paleozoic localities wherever possible. Other Precambrian localities, as for example Area I, Nos. 11 and 12, Area II, Nos. 1 and 2, Area III, No. 8, were set up for purely geological reasons involving the possible detection of structures within the gneisses which may be related to and antedate Paleozoic and later deformation (III, 9).

2.—*Principles Used in Collecting Field Data*

Orientations of all fractures were measured at small exposures; at large exposures such as quarry walls, all fractures within reach along the most convenient traverse were measured,

until sufficient data had been accumulated (II, 4). Thus, the attempt was made to eliminate subjective selection of primary data.

Müller (1933), in recognizing the problem of obtaining an impartial sample, states that the best method is to measure all joints.

In this study, data were not collected on orientations of fracture surfaces (1) cutting rocks not definitely determined to be in place, (2) too small in area (*i.e.*, measured in terms of but a few square inches or less), (3) which are the small, irregular components of large surfaces, (4) which are so irregular that they could not be approximated by a plane, (5) close to recognized faults. Thus the possibility of local stresses affecting the mode of fracture as recorded is lessened. Wager (1931) presents a quantitative study of such an effect.

Quantitative data on the spacing of fractures were not collected. In some quarries the spacing of dominant fractures is related, at least in part, to the lithology. In the more argillaceous carbonate rocks, parallel fractures are more closely spaced than in the purer carbonate rocks, sometimes by a factor of as much as 5. The fact that the impure beds are usually thinner than the pure also enters into the problem of spacing.

King (1948) believes the spacing of joints depends on the nature of the rocks and particularly on tectonic relations. In more highly deformed areas, fractures are more closely spaced. However, evidences of the effect of varying degrees of deformation on the spacing of joints were not observed in the present study.

The possibility that the character and orientation of fractures at the weathered surface may differ from those at depth has been considered by King (1948) and Müller (1933). In this study, almost all observations in Areas I and II were made in quarries and road cuts in which weathering could not have exerted much influence on the fractures. In Area III, both the sedimentary rocks and the underlying crystallines have been subjected to much weathering, and therefore comparison of fractures between the two rock types does not involve the unintentional comparison of weathered with unweathered material.

The writer believes that weathering produces, at most, only a trigger action along predetermined planes of weakness. The observation of Appleby (1942), that fractures in dynamited exposures correspond closely with those of normal exposures, is compatible with this contention. The differences with depth reported by King (1948) and Müller (1933) may be more apparent than real, since the same planes of weakness may exist throughout the vertical extent of a rock mass, but weathering could result in the "birth" of fractures at the surface which obscure the fewer sets below.

Some cautions to be observed in collecting fracture data are:

(1) Fractures almost parallel to foliation or bedding tend to be overlooked once the orientation of the foliation or bedding is known.

(2) The techniques of the investigator may vary with time. During the course of a field season, efficiency may be increased by modifying methods, but such modifications should be instituted only if the later body of data does not have a meaning different from the earlier. Such a difference could come about, for example, in the measurement of irregular surfaces if, in midseason, in the interest of speed it were decided to measure the largest smooth part of the surface rather than the overall orientation. Whether or not such a modification should be made would depend on geological considerations and quantitative tests.

It is highly desirable to plan the field procedure carefully in advance. Methods should be based on the investigator's experiences, modified by the techniques of others. A "test run" of a few days in the area to be studied will often help considerably in approaching an adequate level of standardization and may save considerable time and lessen confusion.

Some of the personal factors involved in collecting fracture data are considered by Müller (1933).

(3) All data should be collected by one worker; data of more than one observer should be accepted only after the results obtained in a test area prove comparable. The test area should involve situations requiring typical decisions concerning what to use and what to reject.

(4) Very large fracture surfaces may be inadvertently measured many times and therefore tabulated as that many fractures. This effect may be minimized by standing off at a distance

from the exposure to view it in its grosser aspects before approaching it to make measurements. On the other hand, such large features may be overlooked if they form the face of a quarry wall or cliff of imposing dimensions. Cizancourt (1947) has considered this problem.

(5) In sedimentary rocks, one should observe if there are variations in fracture patterns from bed to bed, and in that case data should be collected separately for the different beds. Lumping of such data would "blur" the point diagrams (II, 3), and the values of the co-ordinates of concentrations would be subject to suspicion (II, 5).

3.—*Method of Plotting the Data on Rectangular Co-ordinates*

General discussion.—In this paper, fracture orientations have been plotted as points on rectangular co-ordinate diagrams, the abscissa and the ordinate denoting strike and dip values, respectively (Fig. 5). The origin represents north-south strike and vertical dip.

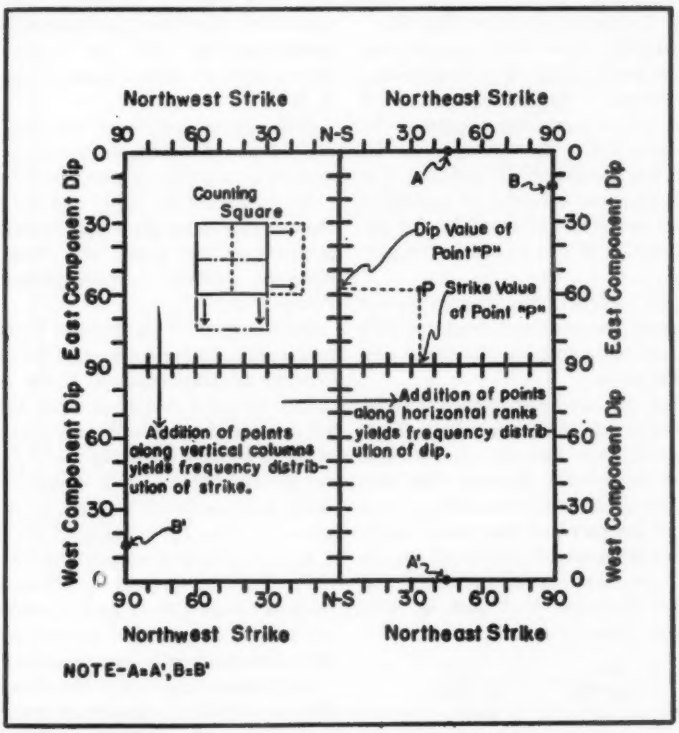

FIGURE 5.—RECTANGULAR CO-ORDINATE DIAGRAM

Northwest strikes up to N.90°W. and northeast strikes up to N.90°E. are shown to the left and right of the origin, respectively; dips with east and west components are plotted above and below the origin, respectively. Equal linear distances along each axis represent equal angular increments of strike and dip.

A rectangular grid system is superimposed on the diagram, with grid lines oriented parallel to the axes. The spacing of the grid lines depends on the number of points plotted and on the desired resolution of the pattern (II, 4). These lines intersect to form equal squares or grid cells over the extent of the diagram.

An easily manipulated table of numerical values becomes available when the points in each grid cell are added, and the sums are entered in the corresponding cells in an identi-

cal grid. The addition of numbers in ranks, *i.e.*, parallel to the abscissa, yields a frequency distribution of dips; the addition of numbers in columns, *i.e.*, parallel to the ordinate, yields a frequency distribution of strikes (Fig. 5).

In the diagrams, points falling on grid lines have been arbitrarily assigned to the adjoining squares according to the following rules: (1) If the point lies on a grid line parallel to the abscissa, it is added to the square below; (2) if on a grid line parallel to the ordinate, it is added to the square to the right; (3) it is added to the square below and to the right if it lies on the intersection of two grid lines ("Right-below" rule).

Because the borders of the diagram do not really represent discontinuities, fractures with either east-west strike or horizontal dip require special consideration.

In addition, fractures with east-west strike are not covered by the previously outlined rules of plotting, since their dips do not have east or west components. If north dips were assigned to the upper half of the ordinate, and south dips to the lower, or vice versa, faulty groupings would result. Consider the result when the former arrangement is used, and assume three fractures, k, l, and m, with orientations as follows:

	Strike	*Dip*
k	N.87°E.	50°N.W.
l	E.-W.	50°N.
m	N.87°W.	50°N.E.

Although these three orientations are similar, k and m fall in widely separated squares. The position of l is indefinite until the method proposed in the next paragraph is applied; then only does it fall close to the others.

If r joints dip north p degrees, then plot $r/2$ points at N.89°W., p degrees E., and $r/2$ points at N.89°E., p degrees W.; if s joints dip S. q degrees, then plot $s/2$ points at N.89°W., q degrees W., and $s/2$ points at N.89°E., q degrees E. Half of the vertical joints are plotted at N.89°W., 90°, and the other half at N.89°E., 90°.

The reason for this procedure is that fractures which strike east-west and dip north are intermediate between fractures which strike northwest and dip northeast, and those which strike northeast and dip northwest; east-west striking fractures which dip south are intermediate between fractures which strike northeast and dip southeast and those which strike northwest and dip southwest. Thus, points near either side border, and diagonally opposite points near the other side border, represent planes which are almost parallel (Fig. 5, Points B, B′).

Although no horizontal fractures were encountered in this work, the method of handling such data may be properly considered here.

All points on the upper and lower borders represent the same plane (horizontal), and all points near the upper and lower borders represent similarly oriented planes (Fig. 5, Points A and A′).

Since horizontal planes have no strike, the points representing them must be distributed in some arbitrary manner. If the number of such planes in a locality be equal to n, then k points, such that $k = n/2r$, are plotted in each of the $2r$ squares bordering the 0° dip lines at the top and bottom of the diagram. Thus, no strike value is favored over any other strike value, and the dip values are little disturbed.

In the plotting of vectors instead of planes, north- and south-plunging vectors present a problem comparable to that of east-west striking planes, and vertical vectors require the same treatment as horizontal planes.

To evaluate graphically the co-ordinates of clusters of points, a system of smoothed contouring is used in which a unit square, say $t^o \times t^o$, is passed over the entire area of the diagram in steps of $t^o/2$ measured parallel to the axes (Fig. 5). Moving squares which run off the edge of the diagram so that only half the square falls within the graph proper are treated similarly to points with east-west strike co-ordinate or zero dip co-ordinate, as the case may be, except that instead of splitting points as above the counting boxes are split.

The number of points in each position of the moving square is plotted at the center of the square, and contours are drawn on the basis of these numbers. The third dimension indicated by the contours represents frequency.

Interpretation of contour patterns.—Several types of deformation may produce distinctive contour patterns.

Consider a horizontal slab of material warped cylindrically so that the axis of the

cylinder is horizontal and strikes northwest (Fig. 6, 1a).

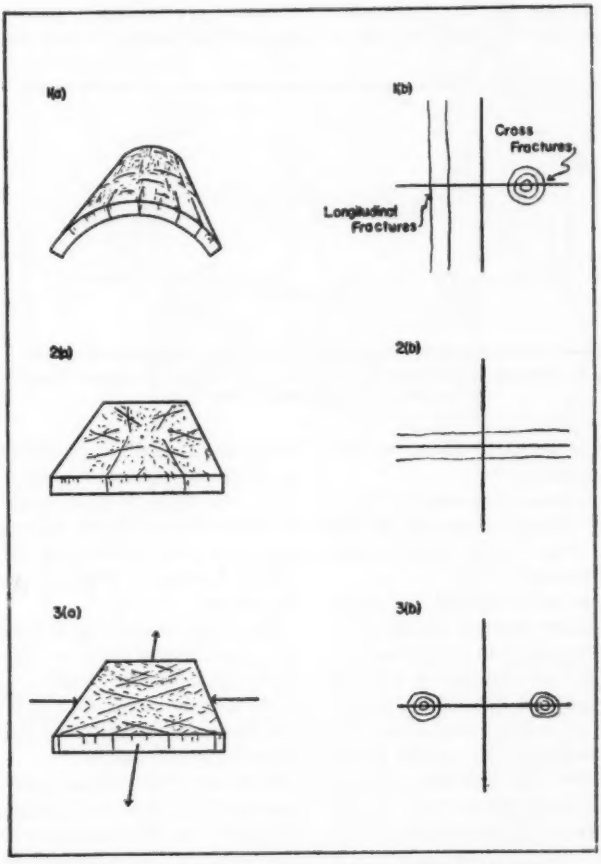

FIGURE 6.—INTERPRETATION OF CONTOURED DIAGRAMS

The resulting two sets of tension fractures (Fig. 6, 1a), when plotted on rectangular coordinates, yields the contour pattern of Figure 6, 1b.

Pairs of vertical conjugate shear fractures, arranged radially about a center in a horizontal plane (Fig. 6, 2a), produce the pattern of Figure 6, 2b.

Figure 6, 3b depicts the distribution of points brought about by the presence of two sets of vertical conjugate shears such as shown in Figure 6, 3a.

The point diagrams of Figure 6, 1b, 2b, 3b do not represent unique situations and are not *prima facie* evidence of the particular areal pattern shown with each (Fig. 6, 1a, 2a, 3a). Thus, the pattern produced by the radial fractures of Figure 6, 2a could be produced by other planes which dip vertically and strike in directions distributed evenly around the compass circle, with the spatial arrangement of the fractures allowed to vary in any manner desired. The plotting of clusters for all localities in one area, or for a number of areas combined, involves so many possibilities of space arrangement that the likelihood of useful interpretation is small (III, 1).

If the contours in any diagram yield a "pla-

teau-like" picture, the investigator should refer to his primary data to see if he has mixed readings from two strata with only slightly similar fracture patterns (II, 2). This precaution will eliminate the "blending" of two or

work fairly well unless the curve is badly skewed or bimodal.

The graphically determined mode is easily estimated and sufficiently precise for the purposes of this paper, at least for the dip dis-

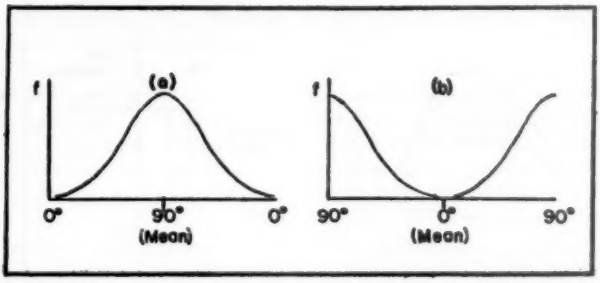

FIGURE 7.—EFFECT OF CUTTING THE ABSCISSA OF A CYCLIC VARIABLE FREQUENCY CURVE AT DIFFERENT POINTS

three peaks which are close enough so that their "foothills" overlap.

Strike and dip frequency distributions.—Separate frequency distributions have been derived for each locality (Figs. 11–13). They are used for graphical interpretation only.

The two ends of each principal axis of the rectangular co-ordinate diagram represent but one point, since the angular range from one end of an axis to the other end is 180°. In effect, then, the separate distribution of each variable, *i.e.*, dip or strike, is drawn on a cylinder with the frequency axis parallel to the axis of the cylinder. For depiction on a flat surface, the distribution cylinders for dip and strike are "cut," one on the 0° dip line, and the other on the east-west strike line, and each is then "unrolled."

The class width in these distributions is equal to $180°/k$,[1] where k equals the number of grid squares in each diagram.

The conventional treatment of these distributions as simple frequency curves may lead to spurious results. Figure 7 shows that the value of the mean depends, in part, on where the abscissa has been "cut." To compute arithmetic means and other statistical measures, Krumbein (1939) suggests that the modal value be used to "center" the distribution with respect to its abscissa. This adjustment should

tributions (IV); the strike distributions, most of which show much dispersion and usually have more than one mode, must be examined in their entirety. Strike distributions of this type have been used by Pia (1924), Teichert (1927), Kaufmann (1931), Stehmann (1934), and others.

The writer is planning a separate study of these distributions based on the methods proposed by Krumbein (1939). Structural processes inferred from this approach will be compared with those deduced from the present three-dimenional analysis.

Rectangular co-ordinates and the Schmidt equal-area net: their properties compared.—The introduction of the rectangular system of plotting points calls for a comparison with the use of the familiar Schmidt equal-area net. Figure 8 provides a graphical comparison of the two methods of plotting; the same body of data (Area I, No. 1) is used in each.

(1) The equal-area net is a device for graphical representation, while the rectangular coordinates, besides being graphical, provide easy computation. If separate frequency distributions for dip and strike were to be secured from the Schmidt net, the summing of ranks and columns, respectively, or a comparable numerical operation would have to be performed anyway.

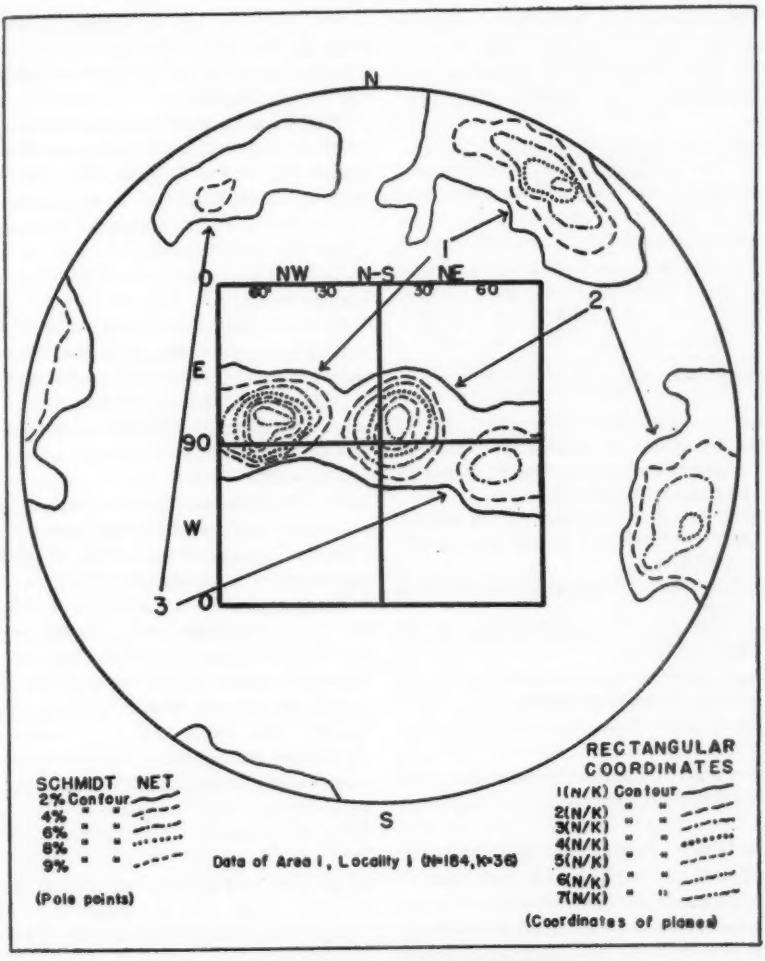

FIGURE 8.—COMPARISON OF METHODS OF PLOTTING

(2) On the rectangular diagram, equal increments of angle, whether of strike or dip, are represented by equal linear increments parallel to the axes, no matter where plotted. Equal increments of angle on the equal-area net are represented by distances which vary according to a trigonometric function.

(3) Inspection of the rectangular grid for critical values (II, 5) is very simple owing to the equal size of the squares and their arrangement in rows and columns. Similarly, points are plotted with greater rapidity, and the co-ordinates of clusters are more quickly evaluated than in the Schmidt net.

(4) A rectangular grid is readily constructed on any standard rectangular co-ordinate paper, or with scale and triangle on blank paper. The equal-area net must be reproduced from previously drafted forms, or may be constructed only with some difficulty.

(5) The equal-area net is familiar to most geologists, while the rectangular system is not.

(6) The rectangular co-ordinate diagram sacrifices the great advantage of the Schmidt net, *i.e.*, that of immediately conveying true space relationships and compass directions.[2]

TABLE 1.—PROPERTIES OF GRID SQUARES OF DIFFERENT SIZES

t°	k	r	a	m	N
60	9	30	11.1	5†	45
45	16	22.5	6.25	5†	80
30	36	15	2.8	5†	180
20	81	10	1.24	5†	405

t = length of one side of the counting square, in degrees.
k = number of grid squares per diagram.
r = distance in degrees between the centers of adjacent, overlapping squares, measured parallel to the axes, (=t/2)
a = percentage of the total area of the diagram which is contained in one grid square. (=100/k)
m = minimum expected number of points for each square.
N = the total number of points required for the diagram. (=km)

* These dimensions give an integral number of equal squares, all of convenient size.

† II, 4.

However, when one becomes accustomed to the rectangular system, interpretation is rapid and simple.

(7) In both methods, points falling along the outer edge of the graph or projection must be distributed arbitrarily. The rectangular system as here used requires two ways of splitting, one for zero dips and the other for east-west strikes; the equal-area net requires only one type of splitting.

Size of the grid squares.—The size of the squares to be used plays an important part in the design of the rectangular co-ordinate diagram. The size of the grid square selected depends chiefly on the desired "resolution" of the contour diagram.

In addition, if the investigator establishes a minimum expected number of points for each square (II, 4 and 5), then the size of the squares, which determines *k*—*i.e.*, the number of squares—will also fix the minimum number of readings per diagram.

Table 1 shows the relationship between the various factors.

Thus the total data required increases more rapidly for a given change in the side of the counting square when it is small than when it is large. Furthermore, the area of the square decreases asymptotically with a decrease in the side of the square, little change taking place below $t = 30°$.

The 45-degree and 30-degree squares appear to be the most useful for the present study. Of course, increasing the number of squares is analogous to increasing the resolution of an optical system. Thus, features not visible at low power, *i.e.*, with smaller number of boxes per diagram, might show up at higher power. When the writer applied the 16-square grid to the first 80 points of Area I, No. 1, two distinct maxima were visible (Fig. 9, d); when a 36-square grid was applied to 184 points from the same locality, including the first 80 mentioned, an additional "high" appeared (Fig. 9, f). This raised the question of whether the appearance of the third maximum was due to the use of a finer grid, or simply to the increased number of observations (II, 4). When the "higher-power" 36-square grid was applied to the original 80 points only, the third maximum showed up clearly also (Fig. 9, e). The same technique has been applied to the data of Area I, No. 9, which is in crystalline rocks, while Area I, No. 1, is in sedimentary rocks; similar results were obtained. (*See* lower half of Fig. 9; d, e, f.)

The writer then applied 36-square grids to the higher concentration areas of all 16-square diagrams; a 16-square grid was similarly applied to the one 9-square diagram (Area I, No. 8). (The diagrams using the 36-square grid in the original form were not examined with an 81-square system.) In performing this operation, not only were additional maxima sought, but the co-ordinates of the recognized

[2] Also, an isotropic distribution of points on rectangular co-ordinates does not have the same meaning as an isotropic distribution on the Schmidt net. In this study, however, the same statistical test, when applied to identical data plotted in both systems, yields virtually identical results (II, 5). Whether or not the application of either system is inherently more *valid* than the other, at least as regards structural planes, is a problem to be solved by geological considerations beyond the scope of this paper; isotropism, *per se*, can be defined in an infinity of ways.

"high" were re-evaluated; thus one might "see" the maxima in slightly different positions due to the increased resolution. Of some 70-odd maxima so checked, over half had no change in co-ordinates; the remainder, with the exception of three, had corrections no greater than 5° in either strike or dip. Of the three larger corrections, all could have been made by using the 16-square diagram, with the unit square moving in jumps equal to ¼ of one side. No additional maxima were detected other than that in the first diagram (Fig. 9) discussed.

In Figure 8, where $k=36$ and the area of the counting square equals 2.8 per cent of the total area of the diagram, the maxima agree very closely with those determined by the 1 per cent circle on the Schmidt net.

In several localities where two highs of nearly the same value are present, the application of "higher-power" examination resulted in the switching of the relative heights of peaks (Area III, No. 10). However, these "heights" are still so close in magnitude after switching that this aspect of the "higher-power" grid system appears to be unimportant.

Müller (1933) discusses the effect of varying the size of the moving circle in an analogous discussion of the Schmidt net.

4.—*Number of Observations Required at Each Locality*

In this problem, as in others involving quantitative information, the question arises, "How many data should one collect?" There is no clear-cut answer.

Probably the best single method of determining the minimum number of observations required is to utilize one's own experience in the particular field being studied, and that of others in comparable fields.

Mathematical statistics offers no magic formula which establishes one minimum amount of data in the study of the size of a flora, another for the shot patterns of artillery pieces, and still another for the analysis of rock fractures. The methods of mathematical statistics do, however, enter into these considerations, since the statistical test to be applied may require some minimum amount of data below which the sensitivity of the test would be insufficient, or below which the approximations used in deriving the test might not hold. The choice of which statistical tests are to be used depends on the questions which are to be put to the body of data, and the amount of labor necessary to apply the method.

There is no maximum number of observations one should make other than that dictated by convenience and by the fact that more data increase sensitivity to smaller-order changes. The investigator should be aware, however, that the error of the mean of a sample varies inversely with the square root of the number of items in the sample (Hoel, 1947) and therefore, as this number increases beyond, say 30, the additional precision gained is small compared to that obtained when a similar increase is made with fewer items.

Many workers have discussed rock fractures; those who have done quantitative work have, in general, not stated why they used the number of observations listed.

Müller (1933) has considered the problem of deciding upon the number of observations to be made at each locality. He mentions the work of Stiny (1925), who advocated 80–100 observations, and Völker (1927), who used 300–600 observations per locality. Müller arrives at the figure of 200 observations but states that one needs more data in areas of unknown character and fewer data where conditions are known.

In the writer's previous unpublished study (Pincus, 1948) of prominent fractures in the Poundridge (N. Y.) granite and gneiss it became quite evident that, when data for one area were plotted, very little change in pattern was observed after the first 60 points were entered on the diagram. This observation led him, in the earlier study, to delay plotting the points until the field work had been completed, for he feared that this early clustering might be the result of an unconscious selection of surfaces oriented similarly to the most frequently occurring fractures previously measured.

In the present study, it was decided to collect data in increments of 20 within one locality for each of the two chief rock types—*i.e.*, dolomitic limestones and gneisses—much in the manner of a sequence of motion picture frames, until the point pattern no longer changed in configuration. The danger of unconscious

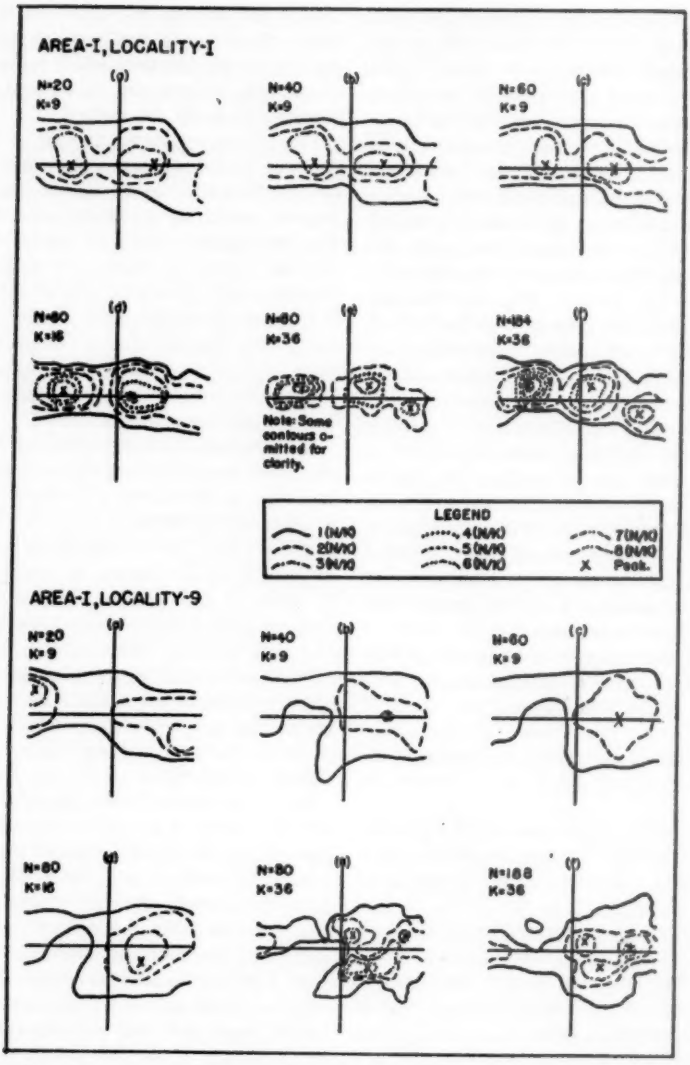

FIGURE 9.—EFFECT OF THE ADDITION OF SUCCESSIVE INCREMENTS OF FRACTURE-ORIENTATION DATA

selection was virtually eliminated by the method of measuring all joints above the minimum size on an exposure (II, 2).

The changes brought about by the addition of successive increments of data are illustrated in Figure 9. Apart from the effect of changing the size of the grid squares, the general pattern is well established with the first 60 points plotted, and the remaining important details show up after 80 points have been plotted. Also, the pattern for the sedimentary rocks appears to be stabilized with fewer points than does the pattern for the gneisses.

While a graphic analysis of this method is

presented only for the first large locality encountered for each rock type, the principle was applied to several localities and was kept in mind throughout the period of measurement. No great departures were observed from the effects seen in these first plots, except that the point diagrams of some localities appeared to reach their final configurations when fewer than 60 points had been plotted.

To provide a margin of safety, a minimum of 80 points per locality were collected, wherever possible.

The total number of joints measured is no indication of the adequacy of the amount of data collected; the areal distribution of the readings must always be considered. Several thousand arbitrarily selected fracture orientations collected in small numbers at each of many scattered exposures would have a considerably different meaning from an equivalent number collected according to the principles outlined in this paper—*i.e.*, standardized collecting at critically situated and carefully outlined localities, with an empirically derived minimum number of readings per locality.

Since the number of grid squares used most frequently for *initial* examination is 16, and the minimum data level is 80 points per locality, the number of points which would fall into each square, if all points were evenly distributed over a diagram, is 80/16, or 5. ($=m$). This figure, which is the "minimum expected value", has been used for all diagrams, regardless of the number of grid squares.

In poorly foliated Precambrian rocks, the minimum amount of data per locality was set at 100 for the 16 square grid. These additional data (*i.e.*, > 80) were collected to compensate for data lost by deletion, owing to later information showing that some "fractures" are, in fact, foliation planes.

5.—*Statistical Analysis of the Data on Point Diagrams*

Assuming that all points (N) on a rectangular diagram are evenly distributed (*i.e.*, isotropic) throughout its extent, and a grid system of k equal squares is applied, then the expected number of points in any one square is N/k. To derive some value A, such that the presence of A or more points in any one box indicates that the assumption of even distribution (isotropism) is so unlikely as to warrant rejection (A-test), the Poisson Exponential Binomial Limit is employed; its use for this purpose is as an approximation which is easily evaluated, and which is adequate for the present requirements. This function is explained in most elementary statistical texts (Fisher, 1948).

Let P_A = the probability that a particular box will have A or more points.

$1-P_A$ = the probability that a particular box will not have A or more points.

$(1-P_A)^k$ = the probability that k independent boxes will not have A or more points.

If 1 per cent be taken as the arbitrary level of probability that at least one cell will have A or more points—*i.e.*, in random sampling of an evenly distributed population—the chance of getting A or more points in any one box is one in 100, then

.01 = 1 − the probability that no box will have A or more points,

and $.01 = 1-(1-P_A)^k$.

In this problem the boxes are not independent, as assumed above: if one box has many points there are fewer left for the other boxes. This will tend to reduce the probability desired, but the resulting error in the value of A will be one of increase and is therefore on the safe side.

Knowing k for any diagram, P_A is evaluated. Referring to tables of the Poisson function (Molina, 1947) in which P_A is evaluated from the equation

$$P_A = \sum_{x=A}^{\infty} \frac{e^{-N/k}\left(\frac{N}{k}\right)^x}{x!},$$

in which x = the number of points falling in any one box. A may then be evaluated, since N/k is known.

When P_A falls between two probability figures in the tables, the higher value of A is taken. Thus the probability of a Type I error (or level of significance) is less than or equal to .01, *i.e.*, the probability that any cluster of

points is designated as such when it does not really exist is less than or equal to .01.[3]

In this study, all diagrams show significant departure from uniformity of distribution (isotropism)—*i.e.*, the A values are reached or exceeded in every case. A fixed grid has been used for the test of significance, but moving squares supply the numbers for drawing the actual A contours, which surround the centers of all squares containing A or more points (Figs. 11, 12, 13).

At this point, devotees of the Schmidt net might argue that isotropism on rectangular co-ordinates is not equivalent to isotropism on the reference sphere, and therefore that all conclusions based on this initial condition are invalid. The first part of the statement is correct, but the conclusion is incorrect, for isotropism is a ***defined*** condition, and the conclusions reached in this internally consistent system are valid as long as the intervening steps in reasoning are legitimate. The writer concedes that isotropism on rectangular co-ordinates, as applied to rock fractures, may be shown to be empirically without basis, but this possibility exists also for isotropism on the Schmidt net, or for any other definition of isotropism. (***We still do not know how rocks break.***) Therefore, isotropism in terms of dip and strike on rectangular co-ordinates is not *incorrect*; in fact, it has much in its favor in terms of ease of statistical operations and related thought processes, especially when one has become accustomed to its properties.

As an experiment in method, the writer has applied the A-test to the clusters plotted on the Schmidt net; unit counting circles were chosen such that their areas are in the same proportion to the total area of the Schmidt net as the areas of the unit squares are to the total area of the rectangular co-ordinate diagram.[4]

The tests are identical, except for the type of plot. For each of the 33 localities, the A-test applied to the Schmidt net shows significant departures from isotropism; further, high-point densities on the Schmidt net occur in positions corresponding to those of the clusters on the rectangular co-ordinate diagram. (Figure 8 shows this similarity of position, even where a 1 per cent counting circle is used.) This result does not warrant the conclusion that both methods are, after all, identical, for the high-point densities within clusters cause the close correspondence; large discrepancies might result from more dispersed data. The rectangular co-ordinate system is used, wherever applicable, throughout the remainder of this paper.

Once significant departure from the defined isotropism has been established, it is helpful to outline the borders of clusters (Fig. 10) in order to facilitate the evaluation of co-ordinates and the interpretation of contour patterns (II, 3). To this end, the following method is used:

---

[3] The A-test is somewhat similar in principle to Winchell's (1937) tests. He defines an isotropic model, and the observed data are then tested to determine the probability that they have been drawn from the isotropic parent population. The method outlined in the preceding paragraphs (A-test) attacks the same problem in a somewhat different sequence of steps, for here the comparable probability is assigned a fixed value, and from this the value of A is derived, such that the occurrence of A or more points in any one square indicates that the parent population of the observed distribution does not conform to isotropism, as defined.

Furthermore, both of Winchell's tests (*i.e.*, zone and general) use the chi-square test, which means that the number of points actually falling in *each* square or zone is compared with a theoretical value. This is a tedious operation (Pincus, 1948), and the test is possibly too sensitive (Chayes, 1949).

The A-test is quite easily applied, especially if the values of k and P_A are repeated for a number of tests. In contrast with chi-square comparisons, the A-test does *not* consider each unit area of the diagram, but rather it tests the *general* distribution of points over the area of the diagram, such that the occurrence of A or more points *any place* on the diagram warrants rejection of the isotropic parent population, as defined, *no matter how the N-A points outside the critical unit area are distributed.* Obviously, the results of each of these tests have different meanings; the selection of a test depends on the aims of the investigation and the amount of data to be processed.

Both Winchell's test and the A-test make assumptions about the distribution of directional elements in the parent population; Chayes' (1949) use of the correlation coefficient as a measure of preferred orientation neatly avoids this assumption, but the writer wonders if one does not think in terms of the nature of distributions in parent populations in formulating hypotheses and theories. Chayes' correlation method indicates, ".. that adjacent areas of the grid do or do not generally contain similar numbers of points."

[4] For Schmidt net of 10 cm. radius, the following equivalences were established:

Unit Circle	*Unit Square*
(1) $r = 1.67$ cm.	(1) $30° \times 30°$ ($k = 36$)
(2) $= 2.5$	(2) $45° \times 45°$ ($k = 16$)
(3) $= 3.33$	(3) $60° \times 60°$ ($k = 9$)

For empirical reasons, P_B, the probability that a box has B or more points, is arbitrarily set equal to .05, and, knowing N/k, the cluster border value, B, is evaluated from the tables

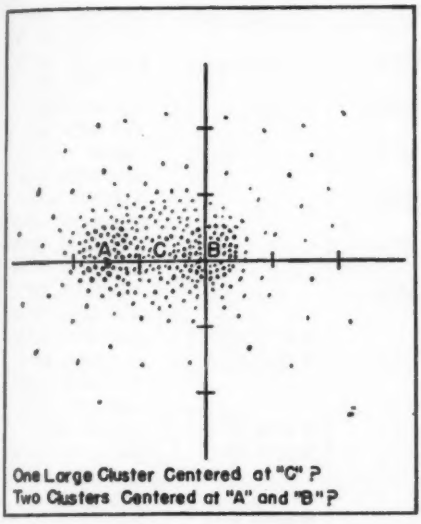

FIGURE 10.—PROBLEM OF CLUSTER BORDERS: IDENTIFICATION AND EVALUATION

of the cumulated Poisson function (Molina, 1947). Thus, once it is known that a cluster exists and its border contour has been drawn surrounding the centers of all squares containing B or more points, the probability, P_B, of wrongly including a particular box in the cluster is less than or equal to .05.[5]

Those clusters containing values of A or greater are used not only as indicators of significant departures from isotropism, but also as significant "highs," the co-ordinates of which are to be evaluated. The cluster border value, B, aids in evaluating these co-ordinates by indicating asymmetry with respect to the peak and the area bounded by the A contour. The measure of central tendency used is the mode (Hoel, 1947; Arkin and Colton, 1939), which is taken off center from the peak according to the degree and direction of asymmetry indicated by the B contours; this system is analogous to the 2-dimensional "difference method" (Croxton and Cowden, 1940). Co-ordinates are evaluated graphically to the nearest 5°.

The "form" contour determined from the cluster border value, B, may be used to aid in deciding if two closely spaced highs (of value A or greater, and separated by a trough with values less than A) are parts of the same cluster or are two different clusters (Area I, No. 6). A similar problem arises when there are two elongated clusters lying end to end. Here, one must decide if there are two distinct clusters capable of being evaluated by simple sets of co-ordinates, or if there is really a belt with one co-ordinate value fixed and the other with a wide range of values (Area II, No. 2). Such decisions, however, are largely subjective; the writer has depended upon such factors as the shape of form contours, the relative relief between peaks and troughs, and the closeness of peaks. However, the number of subjective decisions made here is very few. More refined methods of identifying and outlining clusters are beyond the scope of this paper.

Before the writer applied the A-test to the data, he studied the diagrams, all of which had been contoured in multiples of the expected value, and made estimates of which clusters were "significant," and what their co-ordinate values should be; later application of the Poisson function and the use of the A and B values yielded results very similar to the purely graphical method. The advantage of using the statis-

[5] Since moving squares have been used in drawing the B contours, there is some departure from the stated probability figure, at least insofar as points falling within those contours are concerned.

The probability of a Type I error is less than the stated figure (.05) only if a fixed grid is used. A fixed grid with 45 degree squares has 16 independent units; if a 45 degree square is moved in steps of 22½ degrees, there are 64 overlapping positions. The chance that one of these 64 squares will contain B points is clearly greater than the chance that one of the 16 fixed squares will contain B points, but less than the chance of a square containing B points if there were $4k$ fixed squares and $4N$ points.

In this study, the discrepancy is of little consequence, since levels of significance are not involved in the B probability figure; as stated above, this figure has only empirical justification. Also, sketches (not here included) of B contours, based on fixed and moving squares for identical sets of data, show differences in smoothness rather than differences in gross patterns.

There is no such departure from the stated level of significance for the A values, since, as stated previously, fixed squares have been used for the test of significance, while the moving squares have been used only as a smoothing device.

TABLE 2.—BEDDING, FOLIATION, AND MEAN FRACTURE PLANES OF ALL LOCALITIES IN THE THREE AREAS

Area I

Locality No.	No. of readings (N)	Formation	Bedding Strike Dip	Foliation Strike Dip	Mean fracture planes Strike Dip
1	184	Kittatinny	N 9°W, 20°W		(1)N 60°W, 75°E (2)N 15°E, 80°E (3)N 65°E, 75° W
2	100	Kittatinny	N 26°E, 20°W		(1)N 10°W, 80°E (2)N 85°E, 90°
3	80	Kittatinny	N 68°E, 12°E		(1)N 10°W, 90° (2)N 80°W, 90°
4	82	Kittatinny	N 26°E, 65°W		(1)E-W, 75°S (2)N 10°W, 50°E
5	93	Kittatinny	N 31°E, 50°W		(1)N 5°E, 50°E (2)N 80°W, 85°W
6	180	Kittatinny	N 51°E, 70°W		(1)N 55°W, 70°W (2)N 30°W, 50°E
7	108	Hardyston	N 31°E, 40°W		(1)N 10°W, 50°E (2)N 80°W, 70°W
8	57	Byram		N 51°E, 60°E	(1)N 20°W, 85°E
9	188	Byram		N 50°E, 60°E	(1)N 60°E, 85°E (2)N 25°E, 75°W (3)N 10°E, 75°E
10	155	Byram		N 56°E, 50°E	(1)E-W, 80°S
11	102	Byram		N 71°E, 89°E	(1)N 55°W, 70°W (2)N 35°E, 70°W (3)N 30°E, 45°E
12	110	Byram		N 60°W, 81°E	(1)N 35°W, 90° (2)N 80°E, 80°E
13	80	Byram		N 66°E, 70°W	(1)N 20°W, 75°W (2)N 75°E, 35°E

Area II

1	135	Byram		N 89°W, 70°W	(1)N 85°W, 85°W (2)N 60°E, 35°W (3)N 40°E, 65°E
2	131	Byram		N 41°W, 80°E	(1)N 75°E, 85°E (2)N 35°W, 90°
3	90	Kittatinny	N 81°E, 25°W		(1)N 60°E, 70°E (2)N 55°W, 75°W (3)N 25°E, 80°E
4	98	Byram			(1)E-W, 90° (2)N 80°W, 75°W
5	81	Kittatinny	N 86°E, 20°E		(1)N 85°W, 85°W
6	90	Kittatinny	N 76°E, 65°E		(1)N-S, 65°W (2)N 30°W, 45°E
7	80	Byram		N 41°E, 75°W	(1)N 75°W, 70°E
8	80	Hardyston	N 66°E, 10°E		(1)N 35°E, 75°E (2)N 80°W, 65°W
9	90	Byram		N 81°E, 60°E	(1)N 15°W, 70°E (2)N 50°E, 65°E
10	111	Byram		N 65°W, 79°W	(1)N 70°W, 80°W (2)N 40°E, 70°E (3)N 65°E, 85°E

TABLE 2—*Continued*

Area III

Locality No.	No. of readings (N)	Formation	Bedding Strike Dip	Foliation Strike Dip	Mean fracture plane* Strike Dip
1	85	Green Pond	N 11°E, 30°E		(1)N 80°E, 80°W (2)N 25°W, 65°W
2	80	Green Pond	N 59°W, 25°E		(1)N 65°E, 65°E (2)N 10°W, 90°
3	85	Green Pond	N 84°W, 40°E		(1)N 75°E, 60°E (2)N 10°E, 70°E
4	102	Losee		N 56°E, 80°E	(1)N 45°W, 65°W (2)N 30°E, 70°E
5	100	Green Pond	N 13°E, 40°E		(1)N 75°E, 70°W (2)N 10°W, 65°W
6	88	Losee		N 41°E, 80°E	(1)N 70°W, 60°W (2)N 60°W, 45°E
7	80	Green Pond	N 89°W, 35°E		(1)N 70°E, 65°E (2)N-S, 70°E
8	85	Byram		N 51°E, 80°E	(1)N 50°W, 65°W
9	81	Green Pond	N 89°W, 35°E		(1)N-S, 80°E (2)N 85°W, 55°W
10	80	Byram		N 46°E, 80°E	(1)N 70°W, 40°E (2)N 70°W, 55°W

* Mean fracture planes ranked according to the "height" of the maxima on the point diagrams.

tical method is that a definite statement concerning probabilities can be made, and any two people using this system on one body of data should arrive at virtually identical results. Furthermore, the *A* and *B* contours provide standardized distribution pictures that can be directly used in comparing data from different localities (III, 6).

The contour diagrams and the associated strike and dip frequency distributions appear in figures 11, 12, and 13. Peak values, not to be confused with the final values of co-ordinates used to describe the clusters, are indicated on the diagrams with an "X"; cluster co-ordinates are listed in Table 2.

The cluster co-ordinates define the attitude in space of a plane which is used as a summary, descriptive figure; this plane is hereafter referred to as the "mean fracture plane" of a given cluster of points.

The attitude in space and the areal relations of bedding, foliation, and mean fracture planes are depicted in Figures 14, 15, and 16, which are overlays of the maps of Figures 2, 3, and 4, respectively. The method of depiction is that of the stereographic projection (Bucher, 1944); face poles on the *upper* hemisphere are used. Instead of using points, the various planes are distinguished as follows:

B—Bedding; *F*—Foliation;

1, 2, 3—Mean fracture planes, the number indicating relative heights of maxima in each corresponding point diagram.

III—ANALYSIS OF THE MEAN FRACTURE PLANES

1.—*Overall Aspects of the Mean Fracture Planes*

The mean fracture planes for each locality are plotted as points on the rectangular co-ordinate diagram (Fig. 17). The data for all three areas have been plotted on one set of axes.

In interpreting this diagram, one must remember that the co-ordinates of each point are average values of distributions subject to a higher order of dispersion than points representing individual fracture planes. Also, the degree of dispersion of one cluster of primary data may be fairly high, *i.e.*, it may appear as

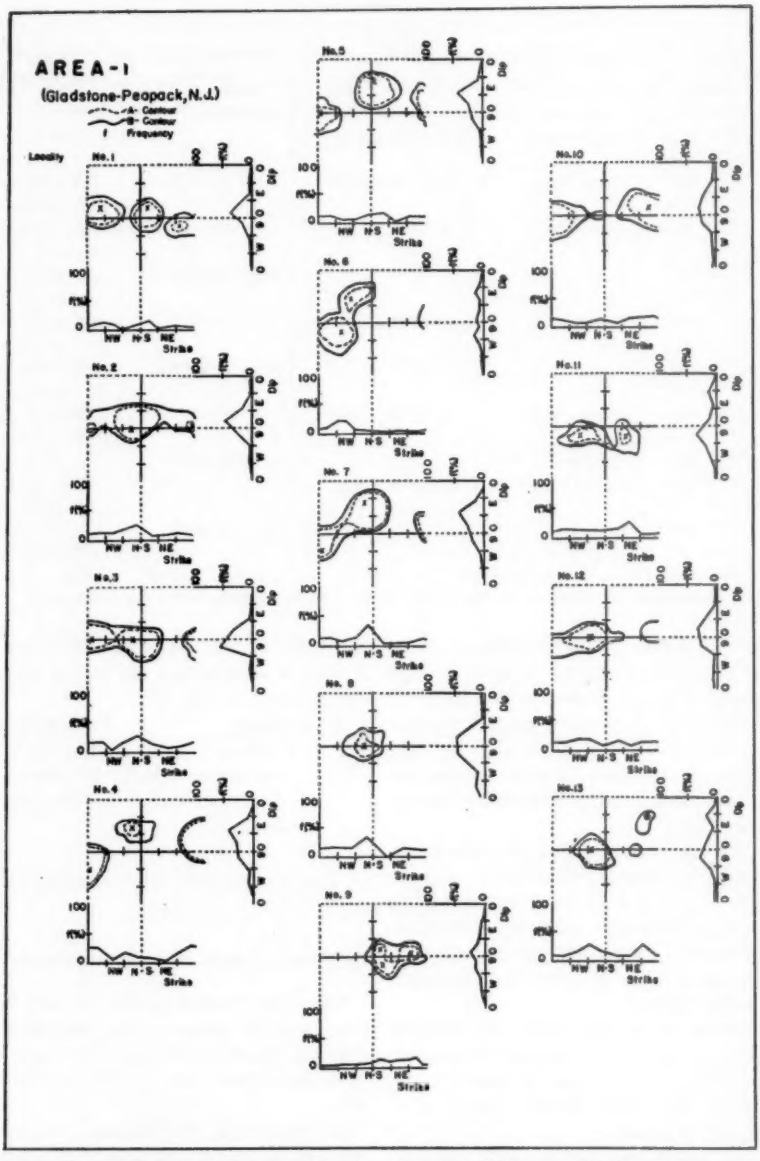

FIGURE 11.—RECTANGULAR CO-ORDINATE DIAGRAMS WITH "A" AND "B" CONTOURS, AND THE ASSOCIATED STRIKE AND DIP FREQUENCY DISTRIBUTIONS—AREA I

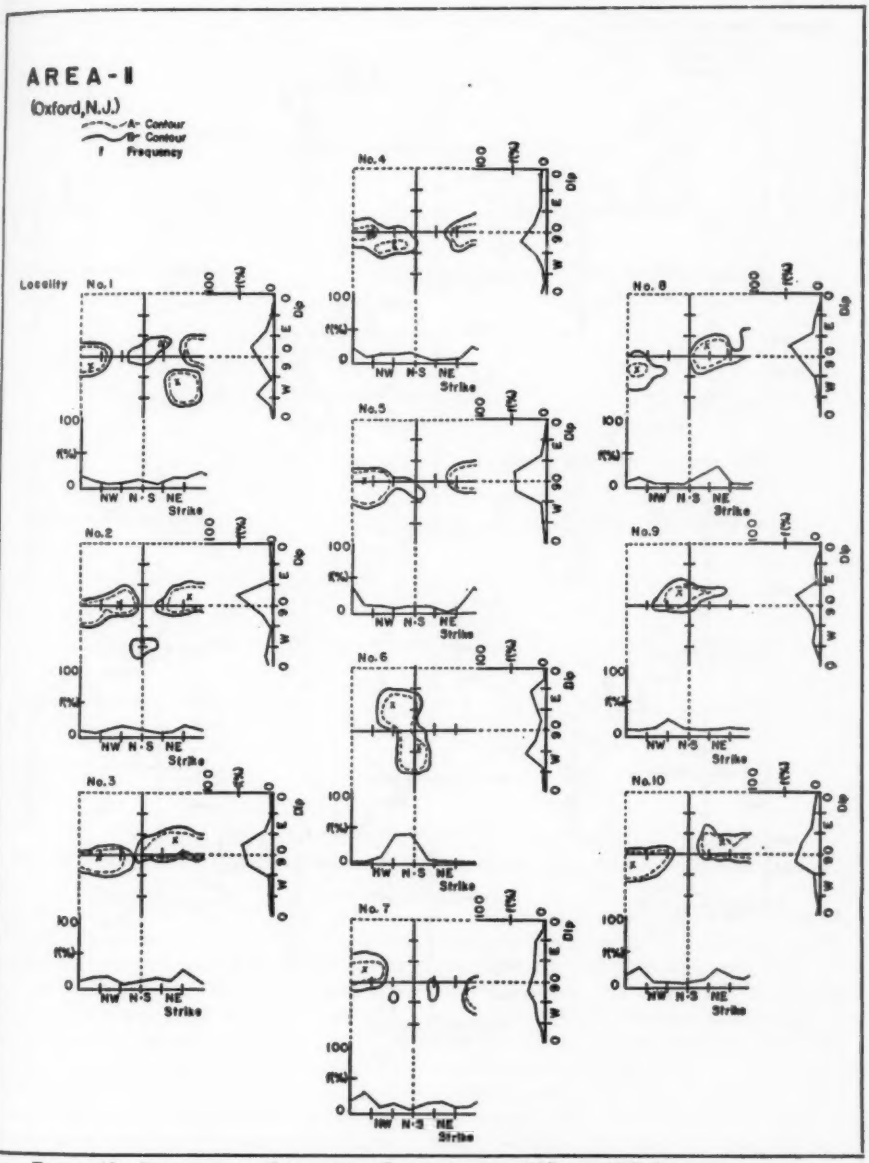

FIGURE 12.—RECTANGULAR CO-ORDINATE DIAGRAMS WITH "A" AND "B" CONTOURS, AND THE ASSOCIATED STRIKE AND DIP FREQUENCY DISTRIBUTIONS—AREA II

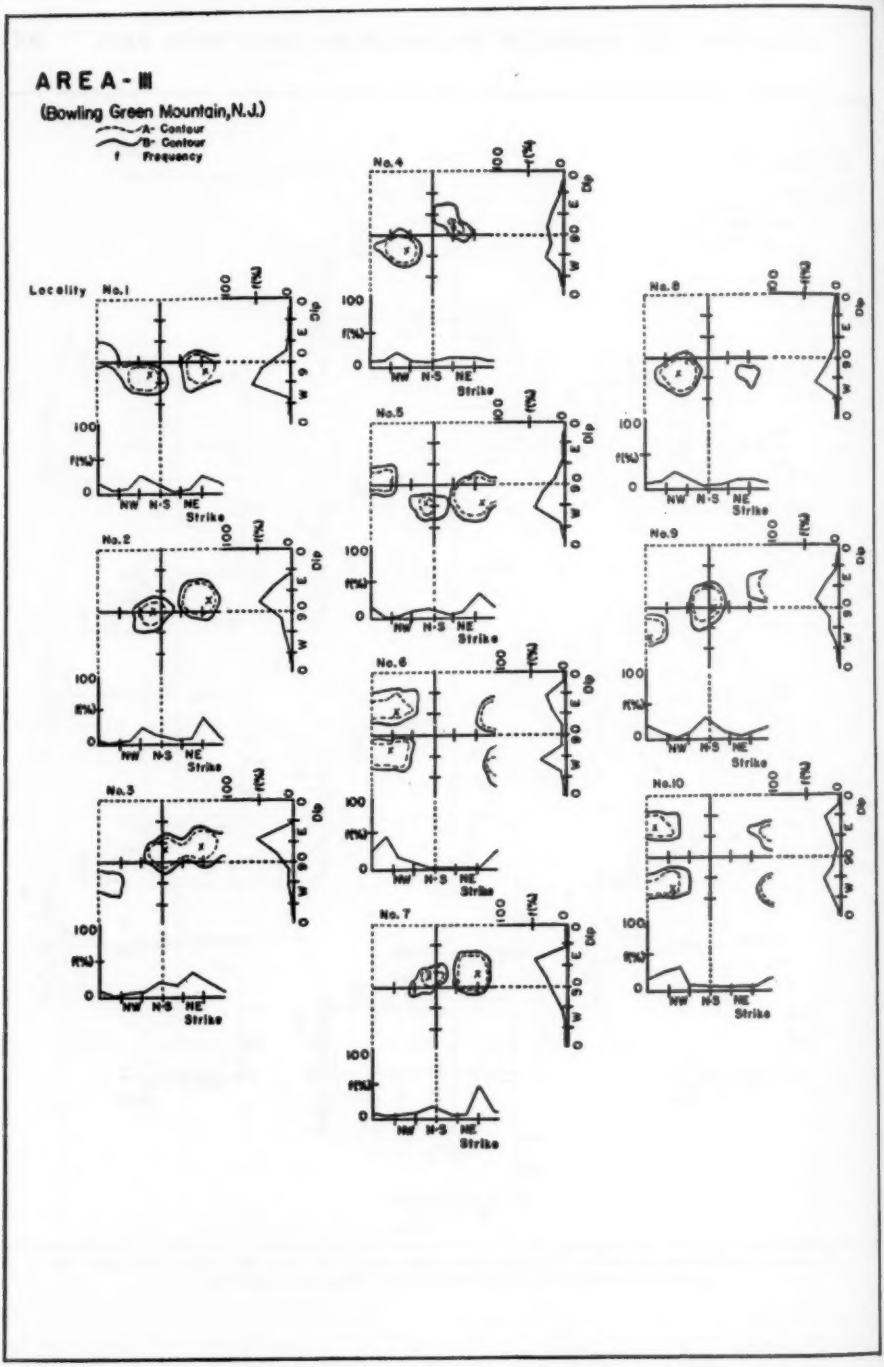

FIGURE 13.—RECTANGULAR CO-ORDINATE DIAGRAMS WITH "A" AND "B" CONTOURS, AND THE ASSOCIATED STRIKE AND DIP FREQUENCY DISTRIBUTIONS—AREA III

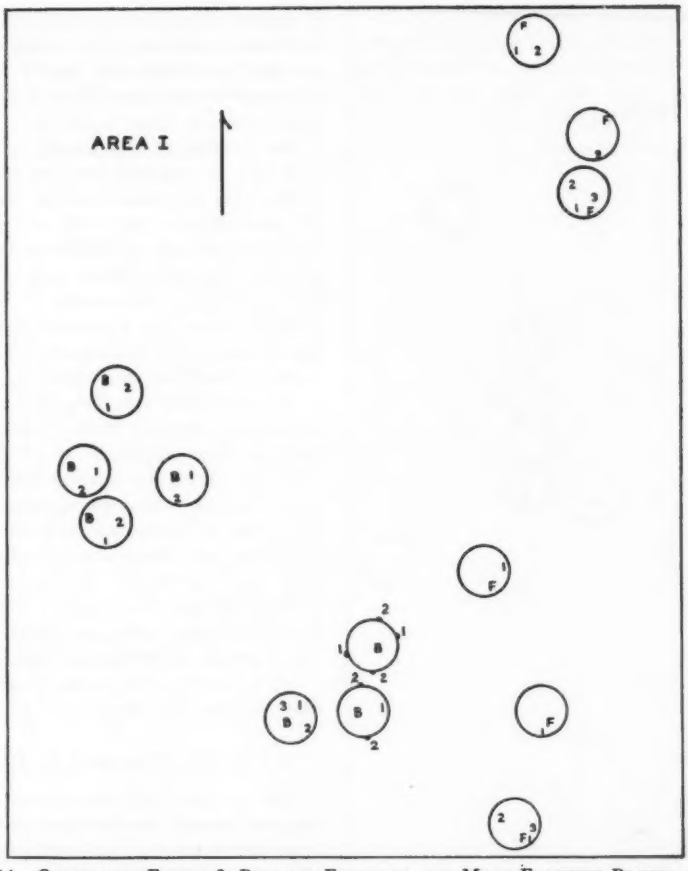

FIGURE 14.—OVERLAY OF FIGURE 2: BEDDING, FOLIATION, AND MEAN FRACTURE PLANES—AREA I

a gentle high on the locality point diagram, while the dispersion of another cluster may be small, *i.e.*, it may appear as a sharp peak on the locality diagram (Area I, No. 6). Yet, both such clusters are represented as single points in this composite diagram.

In addition, the structural positions of localities have not been selected at random (II, 1). For instance, two or more localities are recorded on one limb of a fold (*e.g.*, Area III) because those are the positions for which data were desired. Thus, if the same orientation pattern should exist at the similarly situated localities, it is counted several times in compiling the overall picture.

In view of these considerations, the writer has chosen to examine the overall diagram merely for the tendency to cluster in, say, one quadrant, for either or both rock types, or for the tendency to cluster in bands. The application of the Poisson test to this diagram does show a significant departure from uniformity of point distribution.

Although only the diagram for all three areas is presented here, the writer has examined similar separate plots for each area; the patterns for Areas I and II closely resemble the combined diagram, the points showing a rough banding parallel to and lying symmetrically about the abscissa. These relations obtain for both rock types. Area III shows the same banding as the other two areas, if both rock

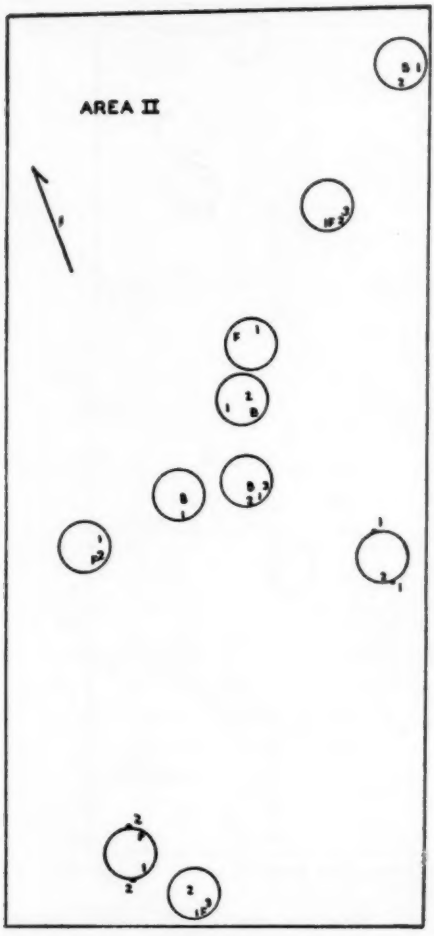

FIGURE 15.—OVERLAY OF FIGURE 3: BEDDING, FOLIATION, AND MEAN FRACTURE PLANES—AREA II

types are considered together. However, fracture groups in the crystalline rocks cluster within the range of strikes from N.35°W. to N.70°W., while no Paleozoic fracture groups lie within this range. The clustering of the crystalline data is undoubtedly due to the fact that all but one of the crystalline localities lie in structurally similar positions, *i.e.*, west of the axis of the anticline expressed in the overlying conglomerate.

The tendency toward steep dips is apparent in all these data. The fact that the strike values show no marked central tendency is not surprising if one recalls that the bearings of the structural trends in the Paleozoic rocks assume a wide range of values (Table 2).

The banding of the overall fracture data (Fig. 17), as compared with the more circular highs of the individual localities (Figs. 11, 12, 13) demonstrates that as the area under scrutiny increases, the possibility of useful interpretation decreases. When such addition has been performed, the circular clusters of the localities blend into a continuous band along the abscissa; such banding could be produced by many combinations of clusters.

It is somewhat surprising that the orientations of the foliations in the Precambrian rocks show a rough similarity in all three areas (Fig. 17), while the fracture orientations do not. This large-scale view appears to indicate that, if the foliations were produced or oriented by stress, this stress was not identical with that which produced the fractures in the gneisses. Whether or not either of these hypothetical stresses bears any relation to those which produced folding and fracturing in the overlying sedimentary rocks is considered in other sections (III, 6, 4, 9).

2.—*Number of Clusters at Each Locality*

The fact that each rectangular co-ordinate diagram studied shows a significant departure from isotropism has been established (II, 5). The manner in which this departure takes place may be investigated along several lines (III, 3, 5, 6); one method of approach is to study the number of clusters, *i.e.*, the number of point concentrations with peak value greater than *A*.

The most frequent number of clusters at each locality is two, regardless of rock type (Fig. 18). The next most frequent, but considerably smaller number of clusters, is three. The Precambrian rocks have a higher proportion of localities with one and three clusters than do the Paleozoic localities; the proportion of Precambrian localities with three clusters is more than double those with one cluster. This tendency toward a higher number of sets of fractures in the more deformed rocks is familiar to the field geologist; both Van Hise

(1896) and King (1948) have observed the same phenomenon. The simplest explanation is that the Precambrian rocks have been subject to both the Paleozoic and earlier deformations.

If, on the other hand, the fractures in the Precambrian rocks were the direct result of the deformation which produced fracturing in the Paleozoic rocks, then some simple geometric relationship between the fractures in both rock types should exist, even if the angle of fracture varies with the nature of the material involved. This statement is based on the assumption that the materials of each rock type were structurally homogeneous just previous to fracturing, and that the boundary between the two materials exerted no modifying influence on the distribution of stresses. The possibility that such a geometric relationship exists is investigated (III, 6).

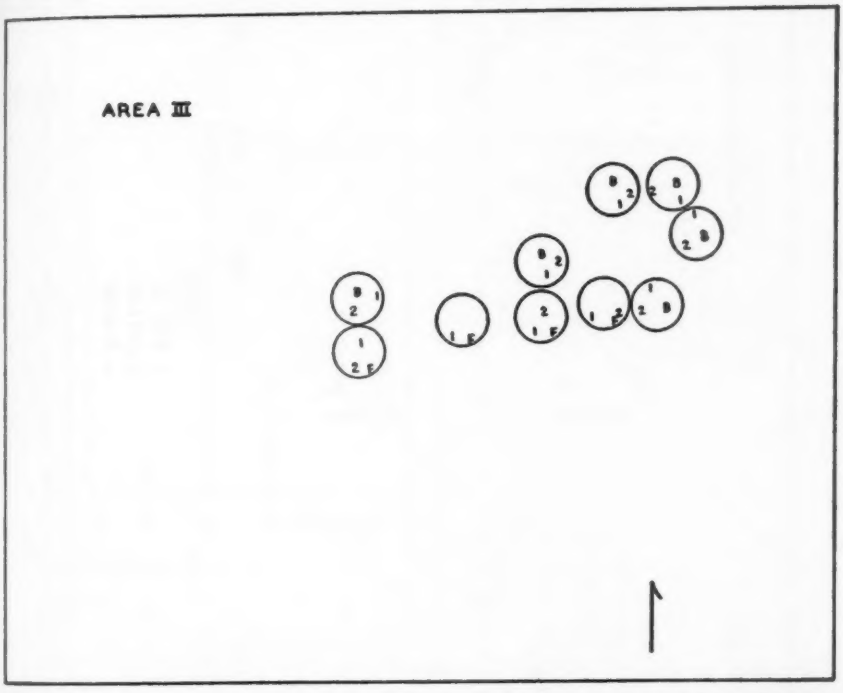

FIGURE 16.—OVERLAY OF FIGURE 4: BEDDING, FOLIATION, AND MEAN FRACTURE PLANES—AREA III

However, the number of fracture sets in the Precambrian rocks equals, in most instances, the number of fracture sets in the Paleozoic rocks (*i.e.*, two). If the fractures in the crystalline rocks are assumed to be the result of pre-Paleozoic deformation, then the deformation which produced the fractures in the Paleozoic rocks did not, in general, introduce more sets into the Precambrian than already existed. The prominence of slickensiding on the Precambrian fracture surfaces compared with its relative absence on the surfaces in the overlying sedimentary rocks is consistent with this hypothesis; thus, probably the later (Paleozoic) deformation resulted in movement along pre-existing fracture surfaces, in place of additional rupturing.

3.—*Frequency Values of Maxima on the Point Diagrams*

Another method of investigating the manner in which the point diagrams depart from uniformity is to study the "heights," or frequency

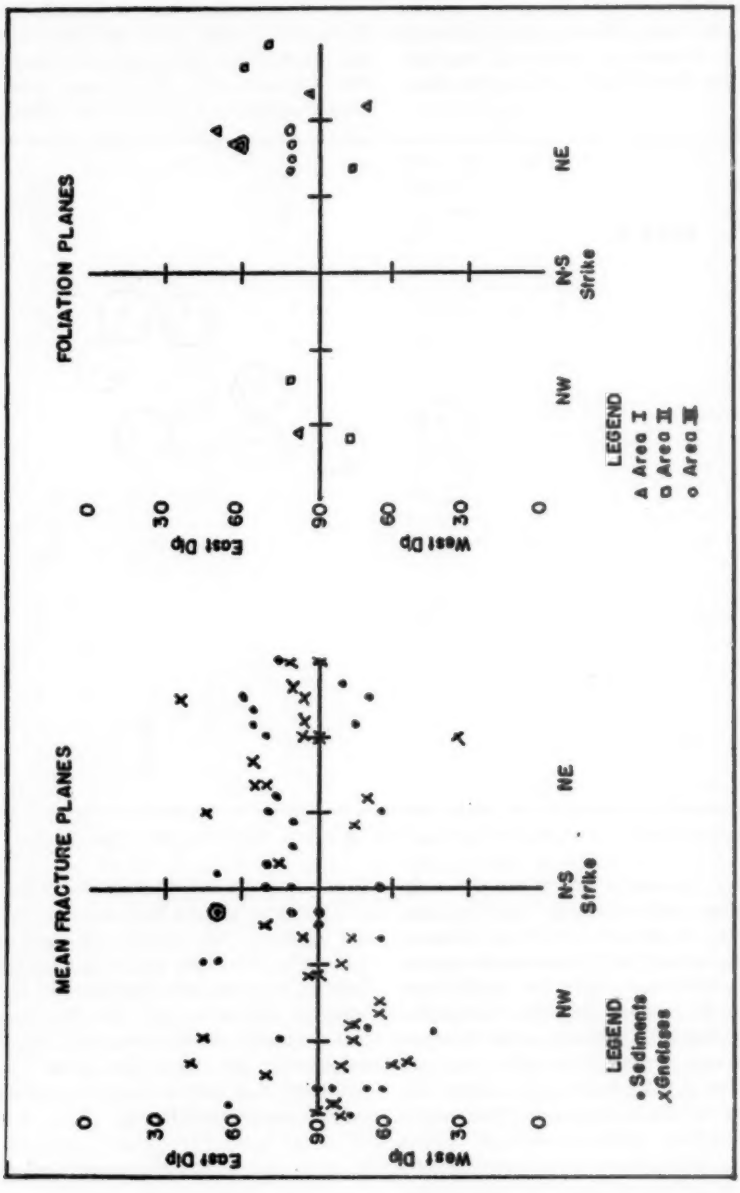

FIGURE 17.—SUMMARY PICTURE OF THE MEAN FRACTURE PLANES AND FOLIATION PLANES FOR THE THREE AREAS

values, of the maxima of the point diagrams. For ease of comparison, the "heights" are taken as the ratio of the absolute frequency value, *i.e.*, the locally largest number of points

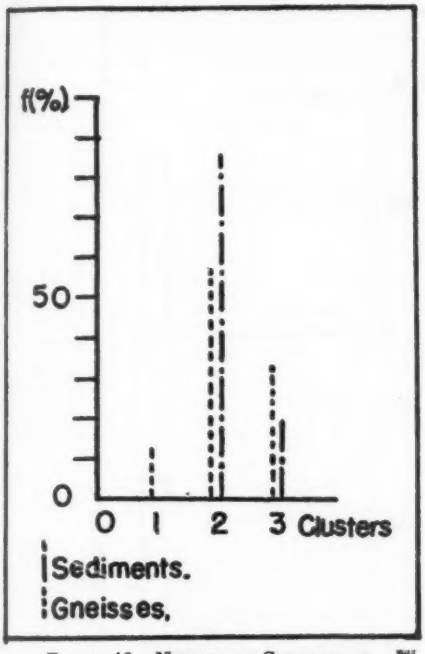

FIGURE 18.—NUMBER OF CLUSTERS AT EACH LOCALITY

tallied with the counting square, to the expected value (N/k). Only the first- and second-ranking highs for each diagram are here considered, since third-ranking highs are few in number (III, 2) and are of much lower frequency value than either of the other two maxima.

When placed in the form of two frequency distributions, one for the Precambrian and the other for the Paleozoic, the heights ratios for both the first- and second-ranking maxima have larger modal values in the Paleozoic rocks (Fig. 19). For example, the mid-point of the model class of the first-ranking high is 5.5 for the Paleozoic rocks, and only 4.5 for the Precambrian. If the modal values were adjusted for skewness, the contrast would be somewhat greater (Croxton and Cowden, 1940).

In the case of the second-ranking maxima, the mid-points of the modal classes of the two rock types are equal; however, adjustment for

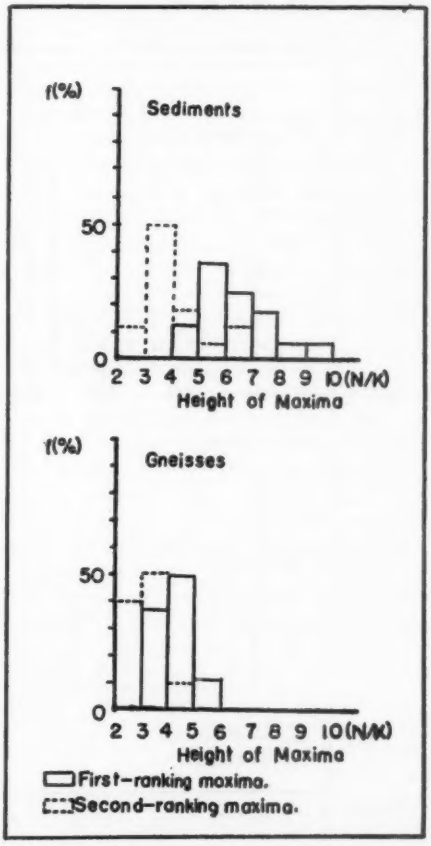

FIGURE 19.—FREQUENCY VALUES OF MAXIMA ON THE CONTOURED POINT DIAGRAMS

skewness of the distributions yields a slight difference in modal value which is in the same direction as that for the first-ranking highs.

The fact that the Precambrian localities have a higher proportion of three fracture sets (III, 2) is not the principal reason for having lower maxima, since Precambrian localities with but two sets of fractures also have lower maxima than Paleozoic localities with two sets.

The contrast between the levels of the Precambrian and Paleozoic peaks can be explained if one assumes that the fractures, actual or

incipient, in the Precambrian were earlier than the deformation which produced the Paleozoic fractures. When the later deformation occurred, the fractures in the Precambrian were rotated differentially with respect to each other, resulting in the dispersion of orientations which had been very nearly equal.

An alternate assumption is that the Precambrian rocks may have fractured originally in a more heterogeneous manner than the Paleozoic rocks. Reasoning based on this assumption could then place the fracturing of the Precambrian earlier than or contemporaneous with the fracturing of the Paleozoic.

The two highs of any one diagram do not rise to the same level, and the difference in level between the first- and the second-ranking maxima is less in localities of gneiss than in Paleozoic localities (Fig. 19). This contrast could be explained by the first assumption, since the cluster with the greater density of points would, of course, show the effects of subsequent deformation more than would a less dense concentration; therefore, the later deformation would reduce the difference in the levels of the peaks representing the fracture sets, as originally formed.

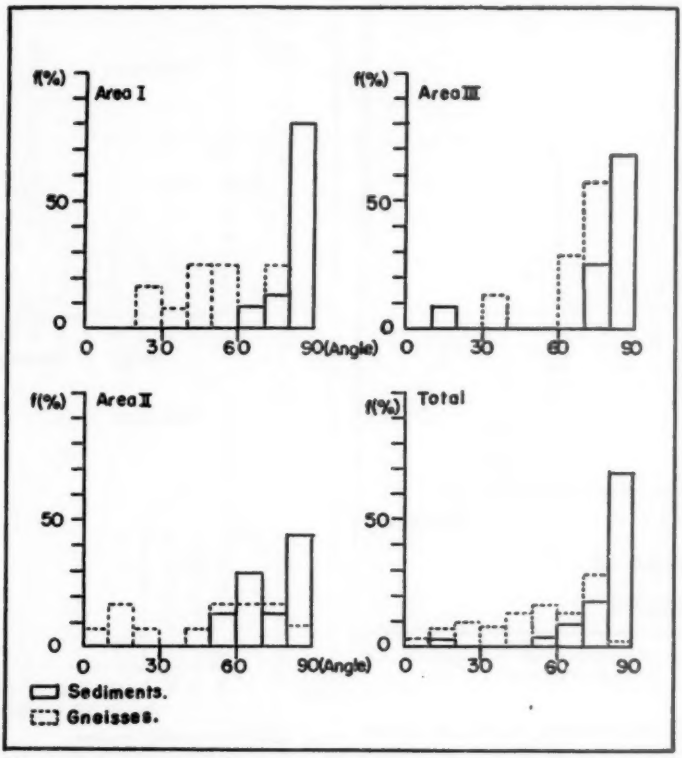

FIGURE 20.—DIHEDRAL ANGLE BETWEEN MEAN FRACTURE PLANES AND BEDDING AND FOLIATION

4.—*Dihedral Angle Between Mean Fracture Planes and Bedding or Foliation Planes at the Respective Localities*

If central tendency is characteristic of the frequency distribution of the dihedral angles between mean fracture planes and some structural plane, *e.g.*, bedding or foliation, then that

angular relationship must have some structural significance. The modal value of the dihedral angle can then be used as an aid in attempting to deduce the genetic significance of the relationship.

TABLE 3.—ANGLE BETWEEN STRIKE OF MEAN FRACTURE AND STRIKE OF BEDDING AND OF AXIS OF FOLD

Angle value	Frequencies of:	
	(1) Angle between strike of mean fracture plane and strike of bedding	(2) Angle between strike of mean fracture plane and bearing of axis of fold
0–10°	0	1
11–20	2	3
21–30	3	4
31–40	4	3
41–50	2	4
51–60	3	2
61–70	4	3
71–80	6	3
81–90	2	3
	—	—
	26	26

The value of the dihedral angle is computed by means of the stereographic projection (Bucher, 1944). The value of the acute dihedral angle is recorded.

Frequency distribution of these angles have been prepared for each of the three areas studied and for all three areas combined (Fig. 20). The angles between mean fracture planes and bedding planes, and those between mean fracture planes and foliation are grouped separately.

All the distributions of the dihedral angles between bedding and mean fracture planes show a strong tendency to assume the largest value possible, *i.e.*, close to 90°. In other words, by far, most of the mean fracture planes stand approximately normal to the bedding planes in the sedimentary rocks. This justifies the inference that the axes of greatest tension[6] lay parallel to the bedding planes.

Rock fractures at right angles to bedding planes have been reported by many workers (Parker, 1942; King, 1948).

Since one can draw an infinite number of planes through a normal to a given plane, the question arises whether there are preferred directions among the mean fracture planes which are almost perpendicular to the bedding. Table 3 shows (1) the difference in angle between the strike of the mean fracture planes and the strike of the bedding at the respective cloalities, and (2) the difference in angle between the strike of the mean fracture plane and the bearing of the axis of the fold in which the fractures occur.

Surprisingly, there is no marked central tendency in either distribution; thus, the trends of the inferred axes of tension bear no systematic geometrical relation to the strike of the bedding and the trend of the fold axes.

In contrast to the preponderance of angles close to 90° between mean fracture planes and bedding, the distribution of the angles made with foliation (Fig. 20) shows no such striking central tendency. Note, however, that Area III does have a distribution with a strong mode in the 71°–80° class, that is, in the class of second largest magnitude of dihedral angle.

In the discussion concerning foliation planes, it should be noted that the accuracy of measuring the orientation of foliation planes was, in some cases, not so great as in the case of fracture surfaces, *i.e.* 5°, the order of error ranging up to 15°, in some instances. The foliation of Area III, the area with the best central tendency in figure 20, is more accurately measured than that of the other two areas; therefore, it might be argued that the lack of central tendency in the distributions of Areas I and II is due to large errors of measurement rather than to an inherent dispersion. However, the histograms of figure 20 show so much dispersion (Areas I, II, and Total) that it seems difficult to explain the observed spread, even if one assumes that the previously mentioned order of error (15°) occurs everywhere.

It is believed, therefore, that the stresses which produced the fractures in the gneisses were not identical with or even similar to those which could have produced or oriented the foliation. Furthermore, the foliation, which is cut by the fracture planes and is, therefore, older, had no appreciable influence on the dis-

[6] Tension is used here in the relative sense, *i.e.*, the axes of least compression are equivalent to axes of tension.

tribution of stresses which resulted in fracture. This same conclusion was reached through the overall plot (III, 1), and it is really the same approach; but it is pointed out in greater detail through the examination of the data from individual localities.

Appleby (1942), in postulating lines of stress from the orientations of the bisectors of acute dihedral angles between selected fractures in the crystalline rocks of the New Jersey Highlands, concludes that the joints in the gneisses are not related to Precambrian folding.

5.—*Dihedral Angle between Mean Fracture Planes at Each Locality*

As a means of examining the behavior of the two principal types of material involved, *e.g.*, unmetamorphosed sedimentary rocks and gneisses, frequency distributions of the dihedral angle between mean fracture planes at each locality have been prepared for Areas I, II, and III individually, and for all three combined (Fig. 21).

Only the dihedral angle between the mean fracture planes that correspond to the first- and second-ranking maxima at each locality have been computed; third clusters, when they exist, are so much less prominent than the other two that it would not be proper, for the purposes of this study, to group their dihedral angles with that produced by the first two clusters. In addition, since three dihedral angles exist between three planes, while only one exists between two planes, localities with three maxima would exert a disproportionately large influence on the grouped results.

The histograms of Figure 21 show that (1) by far most of the dihedral angles measure between 60° and 90°, and (2) though the frequency pattern is quite distinctive for each area, those of the two rock types show fairly

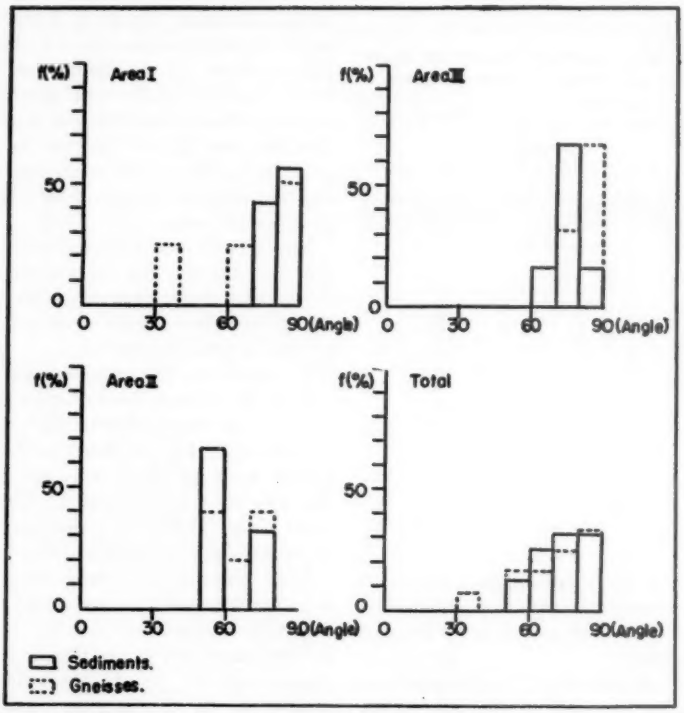

FIGURE 21.—DIHEDRAL ANGLE BETWEEN MEAN FRACTURE PLANES AT EACH LOCALITY

good agreement on each histogram. This suggests that fracture angles are largely independent of the nature of the rock. How far this may be generally true cannot be determined, of course, from these few cases; careful attention in future studies is warranted.

data have been treated several ways, but there has been no consideration of any aspects of the individual patterns as such. These patterns will now be compared for localities in structurally similar positions (Figs. 2, 3, 4, 14, 15, 16), as follows:

(1) Localities of the same general age and lithology

	Gneisses	*Sediments*
Area I	No. 9 compared with No. 10	No. 4 compared with Nos. 5 and 6
Area II	No. 7 compared with No. 10	No. 5 compared with No. 6
Area III	No. 8 compared with No. 10	No. 1 compared with No. 5; Nos. 3, 5, and 7 compared

(2) Localities of different general age and lithology

	Gneisses *Sediments*
Area I	Nos. 9 and 10 compared with No. 2
Area II	No. 7 compared with No. 6 No. 9 compared with No. 5 No. 10 compared with No. 8
Area III	No. 6 compared with No. 7 No. 10 compared with No. 9 No. 4 compared with No. 5

(3) Localities of the same general age but of different lithology

	Gneisses	*Sediments*
Area I	No. 11 compared with No. 12	No. 7 compared with Nos. 4, 5, 6
Area II		No. 6 compared with No. 8
Area III	No. 6 compared with Nos. 8 and 10	

For determining areal structural relations, more is needed than the mere angle of fracture; the orientation in space of the fracture planes must be considered. These space relations are considered in the section which follows (III, 6).

6.—*Comparison of Contour Diagrams of Localities in Structurally Similar Positions*

The preceding sections (III, 1–5) have been concerned with the data derived from the contour diagrams of the individual localities; these

The diagrams of Figures 11, 12, and 13 are compared for (1) similarity in position and configuration of the "*A*" and "*B*" form contours and (2) similarity in position of the peaks within the "*A*" contours. These graphic comparisons reveal:

(1) The contour patterns agree fairly well for all but one of the comparisons of localities of the same general age and lithology. The one conspicuous disagreement applies to Area II, Nos. 5 and 6. The dips of the bedding differ by 45° (Table 2), while the strikes are essentially the same. In the other comparisons, dips

and strikes are similar. Thus, the attitude of the bedding as well as the structural position must be considered in such comparisons.

(2) All but one of the comparisons of crystalline with sedimentary rocks show little or no agreement. The one good agreement (Area II, No. 8 and No. 10) shows as good correspondence of patterns as do comparisons between localities of the same rock type.

(3) For comparison of localities of the same general age, but of different lithology, not so many data are available. In spite of careful search, the writer found only two localities in the Hardyston quartzite suitable for this type of fracture study. The fracture pattern of one of these (Area I, No. 7) is no more different from that of the corresponding localities of dolomitic limestone (Area I, No. 4, 5, and 6) than the latter are from each other. The other quartzite locality (Area II, No. 8) has as its nearest neighbor the one in the dolomites (Area II, No. 6) mentioned above as deviating from the normal behavior of the dolomite fracture patterns. The next nearest usuable locality of dolomite (Area II, No. 5) is almost 4 miles (Fig. 3) from No. 8; if the pattern of No. 6 should actually be aberrant, the comparison of Nos. 5 and 8 might be accepted as showing moderate agreement. But no compelling conclusions can be drawn from such a comparison.

The comparison of localities in the gneiss with somewhat different lithologies yields fairly good agreement. In Area I, the contrast between No. 11 and No. 12 is one of texture and composition within the Byram gneiss (I, 2); agreement in fracture pattern (Fig. 11) is fair. In Area III, the comparison between No. 6, which is in the Losee gneiss, and Nos. 8 and 10 in the Byram gives fair agreement with No. 8, at least one cluster, and excellent agreement with No. 10.

In summary, therefore, it appears that contrasts in the lithology within the same rock type, *i.e.*, crystalline or sedimentary, may not contribute appreciably to differences in contour diagram patterns; contrasts in rock type, on the other hand, are accompanied by striking contrasts in the contour diagrams. On the basis of these and the results obtained from the analysis of the angle of fracture (III, 5), it is reasonable to infer that the fractures in the crystalline rocks differ from those in the sedimentary rocks because of differences in the stresses involved, rather than differences in lithology.

7.—*Use of Large Fractures in Reconnaissance*

The question frequently arises whether the measurement of large fractures might not be sufficient for recognizing the dominant fracture orientations of a region, or "Do the orientations of a few large fractures tend to assume values appreciably closer to the orientations of the mean fracture planes of clusters than do the orientations of all other joints"? If they do, then the measurement of large fractures may be an efficient reconnaissance method in structural studies.

In this study, large joints are those that are conspicuously larger than the rest at any given locality.

The orientations of large fractures have been plotted on rectangular co-ordinates (Fig. 22) for two localities of dolomitic limestone and two localities of gneiss (Area I, Nos. 1, 2; Area I, Nos. 11, 13) selected from the areas of this report. Separate plots have been made (Fig. 22) for all other fractures for each locality; the number of these smaller fractures in each diagram equals the number of large fractures plotted. Thus, in Area I, No. 1, 184 fractures have been measured, of which 38 are large. Of the remaining 146 fractures, every fourth reading has been plotted so that 38 points appear on the diagram.

Points representing the mean fracture planes of the respective localities are plotted as "X" on both sets of diagrams; contours have not been used because of the fewer points represented.

The plots of the large fractures do not provide a better estimate of the mean fracture planes than do the smaller fractures (Fig. 22). In fact, there is some indication, *e.g.*, Area I, No. 1, that the reverse might be true. As long as the number of points plotted falls below the established minimum (II, 4), *i.e.*, 80, the estimate is not reliable, regardless of the size of the surface measured.

Müller (1933) indicates that there is no known relation between the size of joints and their orientation. This is illustrated also in this

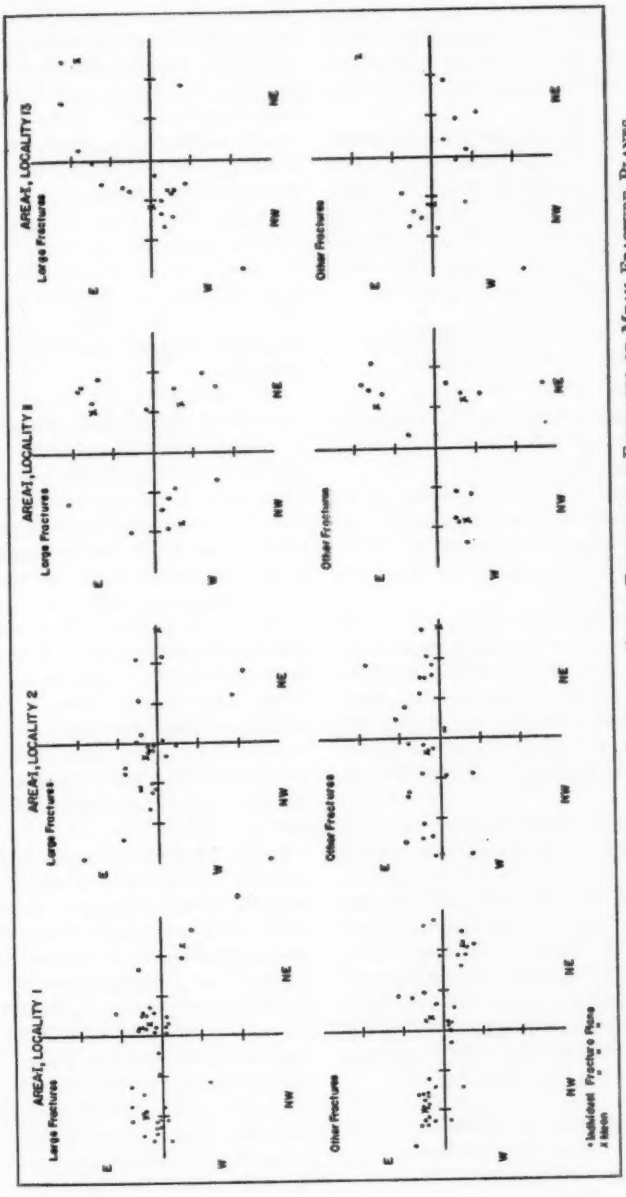

FIGURE 22.—COMPARISON BETWEEN LARGE AND OTHER FRACTURES AS ESTIMATES OF MEAN FRACTURE PLANES

paper (III, 6), where it is shown that the fracture pattern of Area I, No. 7, is very much like that of Area I, Nos. 4, 5, and 6. The surface areas of the fractures in No. 7 are smaller than those of the fractures in the other group by a factor of 10 or more.

(Features of single or a few fractures, other than the surface area, may bear some relation to mean fracture planes. In Area III, quartz-filled fractures (No. 1) and cracks cutting pebbles (No. 9) in the Green Pond conglomerate are roughly parallel to some of the mean fracture planes at the respective localities.)

8.—*Relation of Mean Fracture Planes to Features Visible on Air Photographs (Area III)*

The air photographs of Area III, which were used as a base map in this study (I, 2), reveal the following features:

At Nos. 7 and 9, both of which are on the anticline outlined by the conglomerate, the cross joints which are oriented N.–S., 70°E., and N.–S., 80°E., respectively, are discernible on the air photographs.

The regional structural grain, *i.e.*, north-northeast, is shown in the gneiss areas as distinctive lines, some of which are of considerable length. Some less conspicuous lines trending west-northwest roughly agree with the orientations of the mean fracture planes at Nos. 8 and 10 (N.50°W. and N.70°W., respectively).

The two sets of intersecting lines which appear in the nose of the anticline are roughly parallel to the bedding in both limbs and may represent lines of yielding imposed by the bedding planes when the stiff quartzitic beds broke to form the fold. This is borne out by observations on the ground and by the orientation of mean fracture planes near the nose: in each limb there is a rough parallelism between one mean fracture plane and the bedding plane of the opposite limb (Nos. 1, 5, 3, 7).

9.—*Geometric Erasure of the Paleozoic Deformation: The Validity and Implications of an Arbitrary Method of Structural Restoration*

Paleozoic sedimentary rocks.—It has been shown (III, 4) that, in all frequency distributions of the dihedral angles between bedding and mean fracture planes, the angles tend to assume the largest values possible, *i.e.*, values close to 90°. The difference in angle between the strike of the bedding and the strike of the mean fracture planes which are perpendicular to the bedding, and the angle between the strike of these fracture planes and the axis of the particular fold show no marked central tendency. Thus, while the predominance of fracture planes perpendicular to the bedding indicates that two of the principal stresses responsible for forming them were parallel to the bedding planes, the orientations of the fracture show no obvious relationship to present structure.

One may ask next if it is possible to "erase" the effect of the Paleozoic deformation in such a way as to enable recognition of original structural patterns in the sedimentary rocks which are not now apparent. The very fact that recognition would become possible might be taken to indicate that new insight has been gained into the mechanism of the deformation of the sedimentary rocks.

The geometric process here used is that of rotating the mean fracture planes in the direction of and by an amount equal and opposite to the inferred deformation of the Paleozoic rocks at the respective localities; the deformation is defined as the amount and direction of dip. The rotation was performed by means of the stereographic projection (Bucher, 1944; Melton, 1929).

In applying the rotation process, it is assumed that the primary dips of the sediments are negligible, so that rotation by an amount equal to the entire dip angle, which equals the primary dip plus the dip due to deformation, will not introduce an appreciable error. This assumption is justified, at least in Areas I and II, by the work of Kümmel (1938–1940), who states that the Hardyston and Kittatinny covered the gneisses over a large area; therefore, surfaces of deposition must have been essentially horizontal. The widespread areal occurrence of rocks of Green Pond age and lithology indicates that the original dip of the Green Pond conglomerate (Area II) was probably small.

Correction for the horizontal displacement involved in the restoration process, like that

used in the construction of palinspastic maps (Kay, 1945), is not necessary for areal interpretation in this study because most bedding dips are fairly flat (Table 2), and therefore the horizontal displacement produced is correspondingly small.

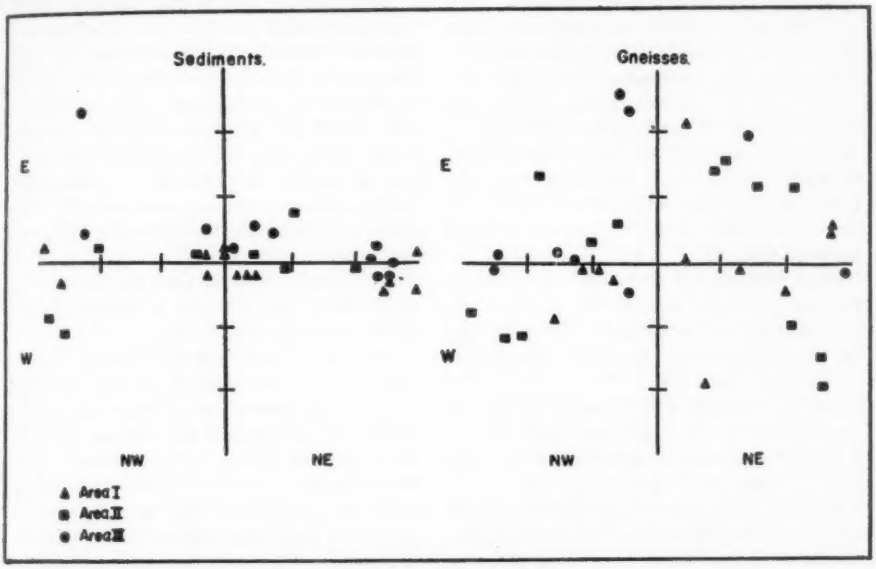

FIGURE 23.—ROTATED FRACTURE DATA

Before considering the data yielded by rotation, the reader is cautioned that the number of localities in each area is too small for completely definitive data; however, the method is discussed to show the possibilities for future investigations and to suggest to what processes the tentative results may point.

Points representing the rotated mean fracture planes in the sedimentary rocks have been plotted on rectangular co-ordinates (Fig. 23). Comparing this diagram with that for unrotated data (Fig. 17), it is obvious that the rotation produces a marked steepening of dips. This result is to be expected, since, in the areas studied, bedding and mean fracture planes are so often perpendicular to each other (III, 4).

In the plots for Areas I and III there are two clusters of rotated data; the diagram shows no clustering for Area II, but rather a rough banding parallel to and centered about the abscissa. The data for all three areas combined show two distinctive clusters at approximately N.5°E., 85°E., and E.-W., 90°. Therefore, the process of restoration appears to produce two sets of mean fracture planes which are perpendicular to each other, and most of which are perpendicular to the bedding. Similar relations are common in jointed plateau rocks. It must be remembered, of course, that the clusters of Figure 23, like those of Figure 17 (Fractures), consist of points each of which is itself a summary point, or mean fracture plane. Thus the diagram is really a second-order generalization.

It appears likely from the fracture data that the sedimentary rocks were broadly warped either along a roughly N.-S. or E.-W. axis prior to the actual folding; the warping produced no master fractures of large dimensions, but minor rectangular joints scattered through the rock. As a consequence of the later folding, the early minor fractures were developed to their present dimensions

Precambrian gneisses.—It was pointed out (III, 4) that the mean fracture planes in the gneisses show no apparent systematic relationship to the foliations, nor do the orientations

of the fracture planes show any appreciable similarity to the orientations of the mean fracture planes in the sedimentary rocks which are in structurally comparable positions (III, 6).

However, the frequency distributions of the dihedral angles between mean fracture planes at the various localities (III, 5) show no appreciable difference between gneisses and sedimentary rocks. This observation, which indicates that lithology need not have an important effect on the angle of fracture, is supported by the close correspondence between contour patterns for structurally comparable localities with rocks of the same general age and of different lithology (III, 6).

Thus, the dihedral angle between the mean fracture planes is roughly the same in the gneisses and the sedimentary rocks, but the attitude in space of the fractures in the gneisses is not easily explained.

Are the fractures in the gneisses older than the fractures in the sediments? Since the deformation which has contorted the sedimentary rocks has also acted upon the gneisses, would a rotation process like that used on the former so "erase" the effect of the Paleozoic deformation that original patterns not now apparent, may be recognized in the fractures and foliations?

In applying the rotation process to the gneisses, it is assumed that the paths through space of small elements of the upper and outer portions of the crystalline mass have been similar to those of the corresponding elements of the overlying sedimentary rocks. Since little is known of the path through space of particles or small elements of large masses of rock under differential confining stress, this assumption must be used with caution.

Another assumption required by this method of restoration is that fracturing occurred as soon as folding began, or, as an alternative, later, but stresses were distributed within the crystalline rocks along surfaces roughly parallel to the overlying sedimentary bedding planes or parallel to the nearly flat ground surface.

An important factor is that the accuracy of the rotation process in the gneisses is lower than it is in the sedimentary rocks. Some of the localities of gneiss are far from exposures of the overlying rocks; inference of the attitudes of the now-absent beds needed to determine the direction and amount of Paleozoic deformation imposed on the gneisses involves further assumptions and the subsequent incorporation of additional error in the results.

Despite these uncertainties and the small number of usable localities, the writer has applied the restoration to the foliations and fractures in the three areas studied (Fig. 23). If the rotation process is of any value, its application should produce some structural pattern in either or both the foliations and the fractures, and the scatter of points on the rectangular diagram should be less for rotated mean fracture planes than for the corresponding unrotated data.

The foliation is older than the fractures in the gneisses; the foliation is everywhere cut by the diversely oriented fractures.

Discussion of areas.—In *Bowling Green Mountain* (*Area III*), air photographs show the presence of long, linear zones of shear in the gneiss parallel to the trend of the foliation (III, 8). In the field, en echelon fractures between foliation zones (I, 2: Detailed notes, Area III) is independent evidence of differential movement along such zones. This suggests that the crystalline basement has been deformed in part by differential movement on these shear planes; but this cannot be the dominant mode of deformation because well-defined joint sets are also present (Fig. 13).

The foliation planes are almost parallel to each other in their present attitude (Fig. 17); rotation produces an anticlinal structure which is similar, with respect to the direction of plunge, to the present fold in the conglomerate. However, the derived fold is subject to suspicion because if such a fold existed before the sedimentary rocks were deformed, why would the later deformation be so selective as to bend the various elements of the structure into almost perfect parallelism?

While the rotation, therefore, probably does not demonstrate actual conditions, it may rectify, in a general way, the attitude of the fracture planes produced by the Paleozoic deformation. Applied to the mean fracture planes, the most important sets become more nearly parallel and nearly vertical (Fig. 23) and are approximately perpendicular to the axis of the anticline.

If the fractures had been steep initially (IV),

and if the application of the rotation process has any meaning, these results are reasonable. Thus, there is support for the conclusion (III, 2, 3) that the fractures in the gneisses are older than those in the sedimentary rocks.

Therefore, the deformation of the gneisses in Area III seems to have taken place through the mechanisms of (1) differential movements on shear planes, and (2) fracturing within and across the plates between the shear planes before bending similar to that of the sedimentary rocks produced the present attitudes of the fractures.

Extensive petrofabric studies, using material collected along different parts of the same plates and across corresponding parts of different plates, might help one draw more positive conclusions, if these results were used in conjunction with the fracture data.

In the *Gladstone-Peapack (Area I) and Oxford (Area II)* areas the foliation in its present attitude (Fig. 17) is not uniform like that in Area III. The rotation of foliation and fracture planes produces some indication of areal structural patterns, but so few localities are involved that the conclusions are largely subjective.

Plots of the rotated fracture data in the gneisses for each of the two areas (Fig. 23) show greater spread about the abscissa than do the corresponding unrotated data (Figs. 11, 12; Table 2). This result is in conflict with the assumptions that the fractures in the gneiss were originally steep (IV), that the rotation process is valid, and that the fractures in the gneiss are older than those in the sediments.

Actually, rotation does not clarify the structural picture in Areas I and II but, rather, confuses it.

Thus the process of rotation, which gives simplified results with sedimentary rocks cannot be applied to the gneisses.

It rather seems that in these two areas the Paleozoic deformation of the crystalline rocks consisted of diversely directed movements of individual blocks between pre-existing fractures, possibly with a certain amount of permanent deformation of the blocks themselves. Deformation by this mechanism has been postulated by C. W. Wilson (1934). To describe this process, the term "crush mobility" has been suggested to the writer by W. H. Bucher.

The net effect of these movements would have been an upward surge in anticlinal areas and a downward movement beneath synclines.

IV—Angle of Dip of Fractures in the Gneisses and the Sedimentary Rocks

General Statement

The preponderance of steeply dipping fractures in both the gneisses and the sedimentary rocks is observable in the dip distributions of Figures 11, 12, and 13. That this is reflected in the attitude of the mean fracture planes is indicated in Figure 17.

One may then ask if dips of fracture planes are initially steep, and, therefore, would the dips of fractures in more-deformed rocks be flatter than those in less-deformed rocks in the same area because subsequent deformation would produce greater dispersion of dips?

Dips of Individual Fracture Planes

In the following analysis the percentage of all fractures with dips greater than 45° is evaluated for each locality, and frequency distributions of these percentages for each of the two rock types are compiled (Fig. 24). The frequency axis is given in per cent to make the results comparable for the two rock types.

The percentages of dips greater than 45° in the Precambrian rocks are systematically smaller than those of the dips in the Paleozoic rocks (Fig. 24). This, then, is consistent with an affirmative answer to the question above.

However, the fractures which came into being in rock bodies devoid of bedding surfaces serving as gliding planes may initially display a higher proportion of flatter dips.

The first alternative above requires that the fractures in the Precambrian rocks be older than those in the Paleozoic, while the latter alternative makes no such age restrictions.

Some conclusions in Part III of this paper appear to agree with the first alternative, but do not provide proof of its correctness. The final choice between these two alternatives as explanations of the magnitude of dip in the fracturing of crystalline rocks may be decided by a quantitative, comparative study of rock fractures in pure granites of the same region

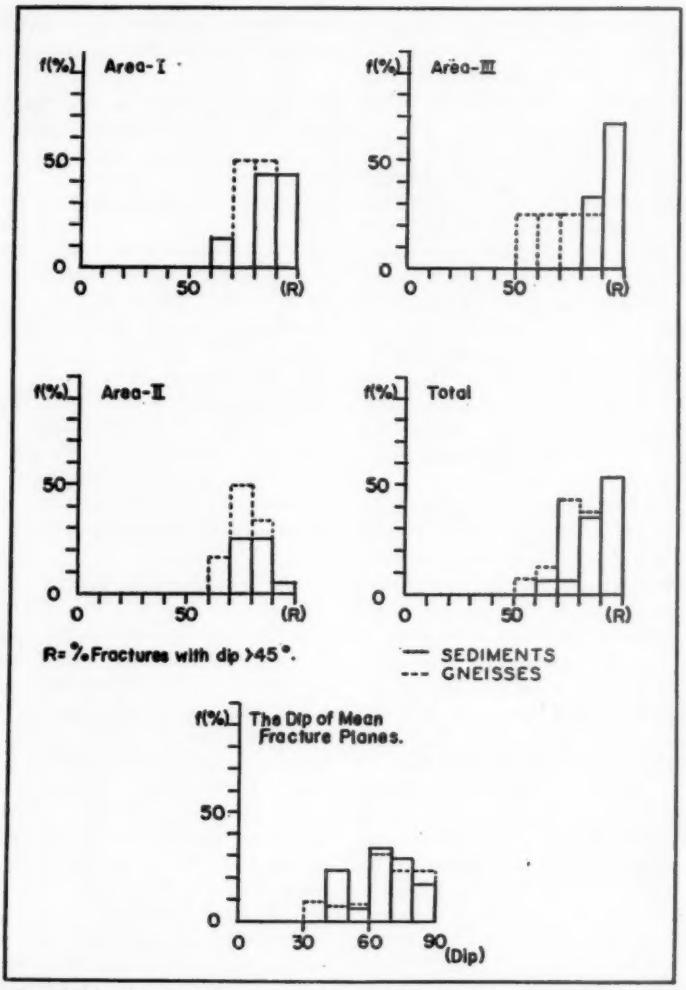

FIGURE 24.—ANGLE OF DIP IN THE SEDIMENTARY ROCKS AND IN THE GNEISSES

which have undergone different degrees of deformation due to differences in age.

Dips of Mean Fracture Planes

A frequency distribution of the dips of mean fracture planes from all three areas is presented in the lower part of Figure 24. There is no great difference between the data of the gneisses and those of the sediments; the slight difference that does exist is in the same direction as that discussed above, *i.e.*, the dips in the older rocks are flatter.

The close correspondence between the two sets of summary data, in contrast with the greater disparity when individual planes are considered, as above, indicates that the use of summary data alone may obscure significant results.

V—SUMMARY AND CONCLUSIONS

An analysis of fractures in lower Paleozoic rocks thrown into open folds, and in the underlying Precambrian gneisses has been approached from a quantitative point of view.

A minimum of approximately 80 measurements of fracture orientations in each locality provides, at least in this study, an adequate picture of the presence and attitude of dominant fracture sets in both the gneisses and the sedimentary rocks (II, 4).

A simple statistical device has been used to decide whether or not points plotted on a rectangular co-ordinate diagram depart significantly from isotropism; in these diagrams strikes and dips are represented on the abscissae and ordinates, respectively. The same device has been used to outline the borders of clusters of points; this enables one to evaluate co-ordinates of clusters, *i.e.*, orientations of mean fracture planes, and to draw form contours for easy reading of the diagrams (II, 3, 5).

The method of plotting points on rectangular co-ordinates yields essentially the same results as those of the Schmidt net, but the former lends itself more easily to numerical statistical operations. The disadvantage of the rectangular system is that it fails to give an immediate visual picture of the orientation of the planes (II, 3).

All localities studied show significant departures from uniform point distributions, *i.e.*, from isotropism, for data plotted on both rectangular co-ordinates and on the Schmidt net (II, 5).

An overall plot of mean fracture planes for all areas shows that steep dips predominate (Fig. 17). While the attitude of foliations is roughly similar in all three areas studied, the fracture patterns in the Precambrian rocks are not. This suggests that the two may not be genetically related (III, 1).

Most localities have two principal joint sets, regardless of rock type (III, 20). However, there are proportionately more Precambrian than Paleozoic localities with three sets of fractures; possibly the Precambrian rocks show the effects of the Paleozoic deformation, in addition to those recorded before the beginning of Paleozoic time. The fact that there is not an even higher proportion of Precambrian localities with three principal sets may be attributed to the substitution of movement along pre-existing fractures in place of additional fracturing.

The clusters of the point diagrams of Paleozoic localities have higher frequency values than those of the gneisses (III, 3); the difference in frequency value between the two most important maxima in the various localities are less in the gneisses than in the sedimentary rocks. This result suggests that the fractures in the Precambrian and Paleozoic rocks represent two periods of deformation: the frequency pattern of the earlier, *i.e.*, the Precambrian, was dispersed by the effect of the second deformation.

There is a marked central tendency in the frequency distributions of the dihedral angle between the mean fracture planes and the bedding planes (III, 4); this implies that the latter played a significant role in the formation of the fractures. The fact that the modal value of the angle is near 90° indicates that two of the axes of principal stress were parallel to the bedding planes. In contrast, the distributions of the angle made with the foliation planes show little or no central tendency; this implies that the planes of foliation exerted little or no influence on the orientations of the fractures. The same conclusion was reached through the overall plot (III, 1); the method here is similar, but more detailed.

Though the frequency distribution pattern of the dihedral angle between the mean fracture planes at each locality is quite distinctive for each of the three areas, those of the two rock types show fairly good agreement with each other (III, 5). This points to the conclusion that the angle between fracture planes, *i.e.*, the angle of fracture, may be largely independent of the nature of the rock.

The attitude in space of the angle of fracture is one of the considerations in comparing the contoured point diagrams of individual localities in structurally similar positions. It is indicated that contrasts in lithology within the same rock type, *i.e.*, sedimentary or crystalline, do not contribute appreciably to difference in contour-diagram patterns; contrasts in rock type, on the other hand, usually produce strikingly different diagrams (III, 6). On the basis of these results, and the previous conclusions with respect to the similarity in the angle of fracture in the two rock types, it is reasonable to infer that the fractures in the crystalline rocks differ from those in the sedimentary rocks owing to differences in the stresses involved, rather than because of lithologic differ-

ences. Whether the differences in the stresses involved are due primarily to differences, with respect to time, in the mode of external application of the stresses, or to differences in internal stress distributions which are concurrent, or both, is not ascertainable from these data.

The measurement of a few large fractures gives no better results, at least in this study, than the measurements of an equal number of fractures of any size. As long as the number of points plotted falls below the established minimum, the estimate of the mean fracture plane is not to be considered reliable (III, 7).

An arbitrary, geometric process for removing the effects of the Paleozoic deformation of the sedimentary rocks results in the steepening of dips of the mean fracture planes, and the data cluster into two groups representing fracture planes which are approximately perpendicular to each other (III, 9). Probably these fractures resulted from a broad warping which occurred prior to the actual folding.

When the same process of removing the effects of the Paleozoic deformation is applied to the gneisses (III, 9), serious doubts arise as to the validity of applying this method, since little is known of the path through space of individual points in the crystalline basement during the deformation which throws the overlying sedimentary rocks into open folds. Assumptions involving estimates of the amount and direction of the Paleozoic deformation of the Precambrian gneisses must be made in order to apply the geometric restoration; but the very use of these assumptions casts doubt on the accuracy and the validity of the process.

The deformation of the gneisses in Area III seems to have taken place through the mechanisms of differential movements on shear planes, and fracturing within and across the plates between the shear planes before bending similar to that of the overlying sediments produced the present attitudes of these features.

In Areas I and II the Paleozoic deformation of the gneisses seems to have consisted of diversely directed movements of individual blocks between pre-existing fractures, possibly with a certain amount of permanent deformation of the blocks themselves. The total effect of these movements would have conformed with folds in the overlying beds.

A high proportion of all fractures measured in this study dip more steeply than 45°. The percentages of dips greater than 45° in the Precambrian rocks are systematically smaller than those of dips in the Paleozoic rocks (IV). If it could be proved that the dips in the gneiss were originally as steep as those in the sediments, the conclusion would be warranted that the majority of the fractures in the gneiss are older than those in the sedimentary rocks.

Expressed as a geologic sequence of events, the results outlined above take this form, *subject to the doubts and qualifications attached to each item in the preceding pages:*

(1) The fractures in the Precambrian gneisses came into being after the development of the foliation and complicated structural detail in the metamorphic sequence. The foliation planes seem to have exerted no influence on the orientation of the fractures.

(2) After peneplanation of the Precambrian surface and the subsequent deposition of the Paleozoic sediments, the region was gently warped; the warping produced no master fractures of large dimensions, but rather minor joints scattered through the rock. During this deformation, adjustments probably took place along the pre-existing fracture surfaces in the underlying crystalline rocks.

(3) As a consequence of later folding, chiefly post-Taconic, the minor fractures in the sedimentary rocks developed to their present dimensions, while the Precambrian rocks were deformed by (a) movement along the pre-existing fractures and the deformation of the solid blocks between the fracture planes, or by (b) differential movements on large shear planes with fracturing between and across the shears, followed by some bending similar to that of the overlying beds.

(4) Subsequent minor movements and weathering further enlarged the fractures to their present dimensions.

Clearly, additional quantitative studies of rock fractures are required for more complete comprehension of the nature of rupture in rocks. Data must be culled from a wide variety of structural situations and lithologies, and methods of treating these data must be applied as the particular situation requires.

If the methods of collection, treatment, and

analysis of the data in this study indicate some new lines of approach to the study of rock fractures and other fields which may be studied quantitatively as well as qualitatively, and if the inferences drawn from the results of this study provide a stimulus for further work in related structural fields, then this paper has served its principal purposes.

Appendix

Annotated Bibliography of Selected Papers

Melton, F. A. (1929) *A reconnaissance of the joint systems in the Ouachita Mountains and Central Plains of Oklahoma*, Jour. Geol., vol. 37, p. 733–738.

The bedding is rotated back around the line of strike, together with the included joints, to the horizontal position; another set of rotations is made about a vertical line until all bedding strikes coincide in the north-south line of the figure. The two dominant joint systems so derived are analyzed graphically. The direction of slickensides are used to confirm the direction of deformation deduced from the adjusted orientation of the joints.

Müller, L. (1933) *Untersuchungen über statistische Kluftmessung*, Geol. u. Bau., Jahrg. 5., Heft 1, p. 206, 207, 214–216, 227–228, 231, 233, 234.

This is a comprehensive paper covering methods of measuring the orientations of joints, importance of three-dimensional considerations, number of measurements to be made, use of the Schmidt net, effect of varying size and movement of the unit counting circle used on the Schmidt net, graphic evaluation of mean fracture orientation, and a history of the quantitative study of rock fractures.

The methods outlined are applied to 4,000 joint measurements collected in the vicinity of Salzburg.

An important problem is which joints to measure. The tendency to increase maxima (Fischer, 1926) does not cancel the effects of the tendency to look for differences (Teichert, 1927); the best method is to measure "completely blindly."

There is no known relation between the size of the joints and their orientation.

Winchell, H. (1937) *A new method of interpretation of petrofabric diagrams*, Am. Mineral., vol. 22, p. 15–36.

Theoretical random distributions are set up for points on the Schmidt net; then the actual distributions are compared with the theoretical distributions.

(1) General test: The number of points per square (on the Schmidt net) are counted, and then the number of squares containing 0, 1, 2, etc., points are determined. The theoretically most probable number of squares containing 0, 1, 2, etc., points are calculated from the Poisson exponential function; this represents the theoretical random distribution. The chi-square test is then used to calculate the probability that the actual distribution has been drawn from a population with the theoretical random distribution.

(2) Zone test: A circle with diameter equal to that of the fabric diagram is divided into 10 concentric rings of equal area, the rings representing zones of equal area on the scatter diagram, and the number of points in each zone is counted. The theoretical distribution is isotropic; the theoretical frequency is the same in each zone, and is equal to the total number of points divided by the number of zones (10). The chi-square test is used to calculate the probability (P) that the observed distribution has been drawn from an isotropic population. The test circles must be oriented on the basis of field evidence; relative values of P in different aspects give some indication of the direction of concentration.

Krumbein, W. C. (1939) *Preferred orientation of pebbles in sedimentary deposits*, Jour. Geol., vol. 47, p. 673–706.

Two methods are presented for describing frequency distributions of azimuth or of dip. (Two-dimensional analysis).

(1) Radius vector summation method: The data are combined into azimuthal classes extending over 180°; the value of each class mid-point is doubled to maintain the cyclic nature of the distribution. For each angle class, a radius vector is drawn from a common origin; its direction is determined by the value of the doubled class mid-point, and its length is proportional to the frequency in the class. Each radius vector is then resolved into a horizontal and vertical component; the ratio of the sums of the horizontal to the vertical components equals the tangent of twice the mean angle. Thus, a mean angle is evaluated, but the method is tedious and the determination of dispersion involves complications.

(2) Moment analysis: A histogram is constructed on rectangular coordinates; the distribution is adjusted so that the modal class falls at the center of the abscissa. Conventional methods are used to find the arithmetic mean, the standard deviation, and higher moments.

In studying the orientation of the long axis of pebbles, it is found that sometimes the particles have neither marked azimuthal nor plunge concentrations, yet a combination of the two produces pronounced concentrations on the petrofabric diagram.

Cizancourt, H. de (1947) *Quelques problèmes de tectonique géometrique*, Extrait de la Rev. d. l'Inst. Fr. d. Pétrole et Ann. de Comb. liq., vol. II, no. 1, p. 3–24; no. 2, p. 81–98; no. 3, p. 141–154; no. 5, p. 252–254.

The nature of flow and rupture in rocks is outlined, and the orientation data of rock fractures in the foreland of the Pyrenees are analyzed graphically. The data are plotted on a modified stereographic projection, the diameter of the circle representing somewhat more than 180°; this construction eliminates the difficulties involved in studying peripheral contours.

The joints in the granites of the axial zone of the Pyrenees have contour diagrams similar to those of the encasing sedimentary rocks.

A comprehensive bibliography is included.

King, P. B. (1948) *Geology of the Southern Guadalupe Mountains, Texas*, U. S. Geol. Survey, Prof. Paper 215, p. 114–115, 117, 124.

The spacing, appearance, and error of measurement of joints in this area are discussed. The number of joint sets and the trends of the joints are contrasted between two adjoining areas which were deformed to different degrees.

Pincus, H. J. (1948) *Statistical techniques applied to the study of rock fractures* (unpublished), Masters Thesis, Columbia Univ. Library.

Strike and dip of joints and foliation in the granite and gneisses of the Ward Poundridge Reservation, New York, are plotted on rectangular coordinates The chi-square test is used to determine the probability that the points plotted are drawn from a parent population which is isotropic over a rectangular grind. This method is very tedious and is possibly too sensitive for joint studies.

A method is proposed for comparing the patterns of any two diagrams by means of Spearman's coefficient of rank correlation. The significance of the results obtained will remain doubtful until additional knowledge has been acquired of the theoretical properties of this coefficient.

Chayes, F. (1949) *Statistical analysis of two-dimensional fabric diagrams*, in Fairbairn, H. W. (1949) *Structural petrology of deformed rocks*, Addison-Wesley Press, p. 297–307.

Two-dimensional anisotropy, once established by the chi-square test, may be described according to the method of Krumbein (1939), if the distribution is unimodal.

Theoretical compass rose diagrams comparable to some actual sample distributions are reproduced from Schmidt (1918), and Schmidt's system is briefly discussed.

Chayes, F. (1949) *Statistical analysis of three-dimensional fabric diagrams*, in Fairbairn, H. W. (1949), Addison-Wesley Press, 308–326.

The definition of isotropism is extended to cover a third dimension.

The zone test of Winchell (1937) is discussed; Winchell's concern about the orientation of the zones is unnecessary, for it is the adequacy of the *isotropic model* which is being tested.

In the empty space test, the total area of the fabric diagram is divided into two parts, one containing all of the points and the other containing none. The chi-square test is applied to determine the probability that the observed distribution has been drawn from an isotropic population, i.e., one which should yield samples such that the number of points falling in each of the two parts are proportional to their areas. It is shown that, "....remarkably small empty areas are sufficient to render a sample incompatible with our isotropic model," i.e., the test is much too sensitive.

Concerning the general test of Winchell (1937), "....the test takes no account of the spatial distributions of the various cell frequencies and very little of the size of individual discrepancies between observed and theoretical frequencies."

Correlation as a measure of preferred orientation (Chayes, 1946) is compared with the foregoing methods. The correlation is determined between the number of points in a unit area (square) and the number in each of the four nearest squares. The tendency to cluster will yield a significantly positive correlation coefficient. Thus, this method avoids, "....*a priori* assumptions about the frequency distributions of fabric elements in unoriented rocks."

The same data are studied by inspection, the empty space test, the correlation test, and the Winchell general test. The results are tabulated and compared.

References Cited

Appleby, A. N. (1942) *Joint patterns in highly folded and crystalline rocks, with particular reference to northern New Jersey* (An abridgement), New York Univ., p. 9–12, 14.

Arkin, H., and Colton, R. (1939) *An outline of statistical methods*, Barnes and Noble, New York.

Bayley, W. S., Kümmel, H. B., and Salisbury, R. D. (1914) *Raritan (N. J.) Folio*, U. S. Geol. Survey, Geol. Atlas of U. S., Folio 191, Scale 1:125,000.

* Becker, G. F. (1893) *Finite homogeneous strain, flow, and rupture of rocks*, Geol. Soc. Am., Bull., vol. 4, p. 13–90.

* Bubnoff, S. von (1931) *Zur Deutung des Südbaltischen Kluftlentzes*, Geol. Rundsch., vol. 22, p. 306–308.

* Bucher, W. H. (1920–1921) *The mechanical interpretation of joints*, Jour. Geol., vol. 28, p. 707–730, vol. 29. p. 1–28.

—— (1944) *The stereographic projection, a handy tool for the practical geologist*, Jour. Geol., vol. 52, p. 196, 199–201, 209.

*—— (1949) *Fault pattern and fault movement*, Am. Assoc. Petrol. Geol., address (Distinguished Lect. Ser.).

Chayes, F. (1946) *Application of the coefficient of correlation to fabric diagrams*, Am. Geophys. Union, Tr., vol. 27, p. 400.

—— (1949) *Statistical analysis of two-dimensional fabric diagrams*, and *Statistical analysis of three-dimensional fabric diagrams*, in Fairbairn, H. W. (1949) *Structural petrology of deformed rocks*, Addison-Wesley Press, Cambridge, p. 297–307, 308–326.

Cizancourt, H. de (1947) *Quelques problèmes de tectonique géometrique*, Rev. d. l'Inst. Fr. d. Pétrole et Ann. d. Comb. liq., vol. 2, no. 1, p. 3–24, no. 2, p. 81–98, no. 3, p. 141–154, no. 5, p. 252–254.

* Cloos, H. (1925) *Einführung in die tektonische Behandlung magmatischer Erscheinungen(Granitektonik), 1-Das Riesengebirge*, Bornträger, Berlin.

Fisher, R. A. (1948) *Statistical methods for research workers*, 10th ed., Hafner Pub. Co., New York, p. 54–55.

* Furse, G. D. (1948) *The McIntyre Mine (Porcupine gold area)*, in *Structural geology of Canadian ore deposits, a symposium*, Geol. Div., Canad. Inst. Min. Metall., p. 492.

* Griggs, D. T. (1936) *Deformation of rocks under high confining pressures*, Jour. Geol., vol. 44, p. 541–547.

Hoel, P. G. (1947) *An introduction to mathematical statistics*, John Wiley and Sons, New York, p. 18, 65, 186–191.

* Significant reference not specifically mentioned in text.

* Johnston, W. D., Jr., and Cloos, E. (1934) *Structural history of the fracture systems at Grass Valley, California*, Econ. Geol., vol. 29, p. 39–54.

* Kaiser, E. (1926) *Ganginjektionen und Faltung*, N. Jahrb. f. Mineral., Beil. Bd. 54, Abt. B, p. 1–16.

Kaufmann, R. (1931) *Die Klufttektonik des Kambrosilurs von Gotland, Oeland, und dem Kalmargebiet*, Geol. Rundsch., vol. 22, p. 292–306.

Kay, Marshall (1945) *Paleogeographic and palinspastic maps*, Am. Assoc. Petrol. Geol., Bull., vol. 29, p. 433.

King, P. B. (1948) *Geology of the southern Guadalupe Mountains, Texas*, U. S. Geol. Survey, Prof. Paper 215, p. 114–115, 117, 124.

* Korn, D. (1929) *Tektonische und gefügeanalytische Untersuchungen im Grungebirge des Böllsteiner Odenwaldes*, N. Jahrb. f. Mineral., Beil Bd. 62, Abt. B, p. 171–254.

* Korn, L. (1935) *Tektonische und gefügeanalytische Untersuchungen im kristallinen Vorspessart*, Mineral. Petro. Mitt., vol. 43, p. 1–44.

Krumbein, W. C. (1939) *Preferred orientation of pebbles in sedimentary deposits*, Jour. Geol., vol. 47, p. 673–706.

Kümmel, H. B. (1938–1940) Revised and rewritten version of Lewis, J. V., and Kümmel, H. B. (1914) *The geology of New Jersey*, State of N. J., Dept. Conserv. Devel., Geol. Ser., Bull. 50, p. 54–70.

—— and Weller, S. (1902) *The rocks of the Green Pond Mountain region*, N. J. Geol. Survey, Ann. Rept. State Geol. for 1901, p. 1–56, map.

——, Weller, S., and Spencer, A. C. (1908) *Franklin Furnace (N. J.) Folio*, U. S. Geol. Survey, Geol. Atlas of U. S., Folio 161, Scale 1:62,500.

* Lovering, T. S. (1928) *The fracturing of incompetent beds*, Jour. Geol., vol. 36, p. 709–717.

* Lowe, K. E. (1946) *An improved method of counting out petrofabric diagrams*, Geol. Soc. Am., Bull., vol. 57, p. 1215.

* Mackin, J. H. (1947) *Some structural features of the intrusions in the Iron Springs district*, Utah Geol. Soc., Guidebk. to Geol. Utah, no. 2, p. 26–43.

Melton, F. A. (1929) *A reconnaissance of the joint systems in the Ouachita Mountains and Central Plains of Oklahoma*, Jour. Geol., vol. 37, p. 733–738.

Molina, E. C. (1947) *The Poisson exponential binomial limit*, D. Van Nostrand Co., New York, Introd. and Table II (*Cumulated terms.*)

Müller, L. (1933) *Untersuchungen über statistische Kluftmessung*, Geol. u. Bau., Jahrb. 5, p. 206, 207, 214–216, 227–228, 231, 233, 234.

* Nadai, A. (1931) *Plasticity*, McGraw-Hill Book Co., New York, p. 291–305, 328–331.

* Osborne, F. F., and Lowther, G. K. (1936) *Petrotectonics at Shawinigan Falls, Quebec*, Geol. Soc. Am., Bull., vol. 47, p. 1343–1370.

Parker, J. M. (1942) *Regional jointing in slightly deformed sedimentary rocks*, Geol. Soc. Am., Bull., vol. 53, p. 382–384.

Pia, J. von (1924) *Über einen neuen Versuch zur Anwendung statistischer Methoden in der Tektonik*, Geol. Rundsch., vol. 15, p. 123–143.

Pincus, H. J. (1948) *Statistical techniques applied to the study of rock fractures*, (unpublished), Masters thesis, Columbia Univ. Library.

* Salomon, W. (1911) *Die Bedeutung der Messung und Kartierung von gemeinen Klüften und Harnischen, mit besonderer Berücksichtigung des Rheintalgrabens*, Deutsch. Geol. Ges., Zeitsch., vol. 63, p. 496–521.

* Schmidt, W. (1925) *Gesteinsumformung*, Denkschr., Naturh. Mus., Vienna.

* —— (1926) *Gefügesymetrie und Tektonik*, Jahrb. Geol. Bund., Vienna, vol. 76, p. 407–430.

* Schmidt-Thomé, P. (1938) *Heligoland und Hoheneggelsen-Mölme, ein Vergleich zweier saxonischer Aufwölbungen*, Geol. Rundsch., vol. 29, p. 491–510.

* Seitz, O. (1914–1917) *Über die Tektonik der Luganer Alpen*, Verh. Naturh. Med. Ver. N. F. Heidelberg, vol. 13.

* Shaler, N. S. (1887–1888) *The geology of Cape Ann, Mass.*, U. S. Geol. Survey, 9th Ann. Rept., p. 537–611.

Sheldon, P. (1912) *Some observations and experiments on joint planes*, Jour. Geol., vol. 20, p. 54, 55, 63.

* Spitz, W. (1913) *Versuch eines Schemas zur Darstellung von Kluft- und Harnischbeobachtungen*, Jahrb. Mitt. Oberrhein. Geol. Ver., Karlsruhe, vol. 3, p. 48–57.

* Stach, E. (1922) *Die stereographische Darstellung tektonischer Formen im Würfeldiagramm auf Stereo-Millimeter-Papier*, Deutsch. Geol. Ges., Zeitschr., vol. 74A, p. 277–309, vol. 74B, p. 332.

Stehmann, E. (1934) *Das Unterkambrium und die Tektonik des Paläozoikums auf Bornholm*, Geol. Pal. Inst. Ernst-Moritz-Arndt-Univ. Greifswald, Abh., no. 14, pl. 7, fig. 2.

Stiny, J. (1925) *Gesteinsklüfte und Alpine Aufnahmsgeologie*, Jahrb. Geol. Bund. Anst., Vienna, p. 97–127.

* —— (1926a) *Kluftmessung und Erdgeologie*, Internat. Zeitschr. Bohrtech., Jahrg. 34, p. 137–138.

* —— (1926b) *Kluftmessung und Quellenkunde*, Internat. Zeitschr. Bohrtech., Heft 13.

Teichert, G. (1927) *Die Klufttektonik der Kambrosilurischen Schichtentafel Estlands*, Geol. Rundsch., vol. 18, p. 244–263.

Van Hise, C. R. (1896) *Principles of Pre-Cambrian North American geology*, U. S. Geol. Survey, 16th Ann. Rept., pt. I, p. 668–672.

* Ver Steeg, K. (1944) *Some structural features of Ohio*, Jour. Geol., vol. 52, p. 131–138.

Völker, I. (1927) *Untersuchungen über die Klüfte und Fluidaltexturen der Porphyre im östlichen Odenwald und im mittleren Schwarzwald*, Centralbl. Mineral., Abt. B, no. 6, p. 251–263.

Wager, L. R. (1931) *Jointing in the Great Scar limestone of Craven and its relation to the tectonics of the area*, Geol. Soc. London, Quart. Jour., vol. 87, p. 392–424.

Wilson, C. W. (1934) *A study of the jointing in the Five Springs Creek area, east of Kane, Wyoming*, Jour. Geol., vol. 42, p. 498–522.

Winchell, H. (1937) *A new method of interpretation of petrofabric diagrams*, Am. Mineral., vol. 22, p. 15–36.

* Wisser, E. (1936) *Formation of the north-south fractures of Real del Monte area, Pachuca silver district, Mexico*, Am. Inst. Min. Metall., Tr., vol. 126, p. 442–487.

OHIO STATE UNIVERSITY, COLUMBUS, OHIO

MANUSCRIPT RECEIVED BY THE SECRETARY OF THE SOCIETY, SEPTEMBER 14, 1949.

BULLETIN OF THE GEOLOGICAL SOCIETY OF AMERICA
VOL. 62, PP. 131-148, 7 FIGS. FEBRUARY 1951

RADIOACTIVITY OF THE BOURLAMAQUE, ELZEVIR, AND CHEDDAR BATHOLITHS, CANADA

W. N. INGHAM AND N. B. KEEVIL

ABSTRACT

Differentiation of the Elzevir magma into eight phases progressed with the concentration of radioactive elements in later, more acidic members, and culminated with relatively radioactive pegmatites and weakly active veins. The distribution of radioactivity in related rock types is such that it has correlative value. The results of several hundred determinations of radioactivity have shown a tendency for the heaviest elements to concentrate in the periphery of batholiths or stocks. In intrusives greater than 2 miles across, a core zone of lower than average radioactivity may be present if erosion has removed the roof.

Several variables must be considered if sampling for radioactivity research is to be representative. Regional differences in radioactivity suggest a steeper geothermal gradient in southeastern Ontario than in western Quebec. Local differences in the radioactivity of batholiths may be important in influencing the course of differentiation, syntexis, and refusion at depth.

CONTENTS

	Page
Introduction	132
Acknowledgments	132
Bourlamaque batholith	132
General geology	132
Petrography	132
Radioactivity	133
Experimental procedure	133
Areal distribution	135
Variation with depth	135
Associated rocks	135
Elzevir batholith	136
General geology	136
Petrography	136
Gray granite	136
Gabbro-diorite-syenite-granite series	138
Quartz diorite-syenite	138
White granite	138
Aplitic granite	138
Associated dikes	138
Radioactivity	138
General statement	138
Distribution of radioactivity in the gray granite	138
Distribution in the white granite	140
Distribution in the syenite	140
Distribution in the quartz diorite and gabbro-diorite series	140
Aplitic granite	141
Associated rocks	141
Synopsis of distribution	141
Cheddar batholith	142
General geology	142
Petrography	142
Radioactivity	142
Radio-petrogenetic considerations	144
Distribution of radioactivity in batholiths	144
Contrast between core and contact zones	144
Effect of active accessory minerals	144
Influence of invaded rocks	145
Effects of granitization	145
Radioactivity of differentiation series	145
Basic to acidic rocks	145
Older to younger rocks	146
Local differentiation	146
Use in petrological correlation	146
Significance in geothermics	146
Radiogenic heat	146
Representative sampling	147
Summary of conclusions	147
References	148

ILLUSTRATIONS

Figure	Page
1. Location of batholiths in western Quebec and eastern Ontario	133
2. Radioactivity in the Bourlamaque batholith	134
3. Decrease of radioactivity with depth in the Bourlamaque batholith	135
4. Geology of the Elzevir composite batholith	137
5. Radioactivity in the Elzevir composite batholith	139
6. Generalized radioactivity profiles across the central part of the Elzevir gray granite	140
7. Radioactivity in the Cheddar batholith	143

TABLES

Page
1. Radioactivity of Bourlamaque batholith and associated rocks 136
2. Distribution of radioactivity in the Elzevir, Cheddar, and Bourlamaque intrusives .. 141
3. Average radioactivities of components of the Cheddar batholith 142
4. Differentiation of radioactive elements as a function of size of intrusive 145
5. Radioactivity of the differentiates of the Elzevir magma 146

Introduction

Evidence from the radioactivity of meteorites, dunites, and other igneous rocks suggests that the radioactive elements were concentrated in the upper crust in the large-scale differentiation of the solidifying earth. Geothermal theory indicates that this surface layer is most important in determining the rate of cooling of the earth, and it is, therefore, desirable to know the rate of production of radiogenic heat in granitic and related rocks which are believed to be typical of the lithosphere.

The distribution of radioactivity within individual batholiths and stocks needs to be determined in order to learn something of the history of the radioactive elements during consolidation of the granitic magma, and to decide upon suitable methods of representative sampling. Accordingly, detailed investigations have been made on a granodiorite and two granitic batholiths of Precambrian age.

Acknowledgments

The authors were encouraged in this work by the interest and advice of Professor E. S. Moore. A grant-in-aid from the Penrose Bequest of The Geological Society of America assisted part of the study. The co-operation of Dr. G. W. H. Norman and the staffs of the Mines in the Val d'Or area also is gratefully acknowledged. The writers are indebted to Mr. F. J. Wank, and Mr. C. A. Barnes for their assistance in sampling the Cheddar area.

Bourlamaque Batholith

General Geology

The Bourlamaque granodiorite batholith is in Abitibi East county, western Quebec, 60 miles east of Noranda, in the Val d'Or mining district (Fig. 1).

The consolidated rocks of the district are all Precambrian. The Bourlamaque granodiorite intrudes Keewatin-type volcanics ranging from andesite to rhyolite, with the more basic rocks predominating. The volcanics are commonly severely altered as evidenced by varying degrees of chloritization, sericitization, carbonatization, silicification, and albitization, and the introduction of albite is most pronounced in the flows close to the batholith.

The Lamaque boss to the south, the altered Siscoe stock to the west, and a small body close to the southeastern extremity of the batholith appear to be satellites of approximately the same composition as the main granodiorite. Other bodies and dikes of albite granite, syenite porphyry, granodiorite porphyry, and granodiorite may be related to the main intrusive. Dikes of andesite porphyry, albitite, aplite, and lamprophyre cut the batholith. Gold-quartz-carbonate-tourmaline veins are developed within the contacts of the batholith at a number of mining properties along the western, southern and eastern boundaries.

Probably the Bourlamaque mass is of the same general age as the Palmarolle, Taschereau, Flavrian, and La Corne batholiths of the Rouyn-Bell River area. To the southwest, similar rocks are overlain by the Cobalt series, which suggests that the intrusives are Algoman. Helium age determinations made on some of the rocks are in accord with the Algoman assignment of age, except for the La Corne granodiorite which may be older. These considerations suggest that the Bourlamaque batholith is pre-Cobalt and post-Keewatin.

Petrography

The granodiorite is normaly a uniformly gray, coarse-grained rock. The grain size averages 5 mm., but some feldspar laths and hornblende prisms attain a length of more than 1 cm. An altered facies frequently displays a slightly greenish tinge due to secondary chlorite, epidote, and carbonatized plagioclase. In the localized hybrid basic border facies,

the proportion of ferromagnesian minerals is increased at the expense of felsic constituents, making the rock darker.

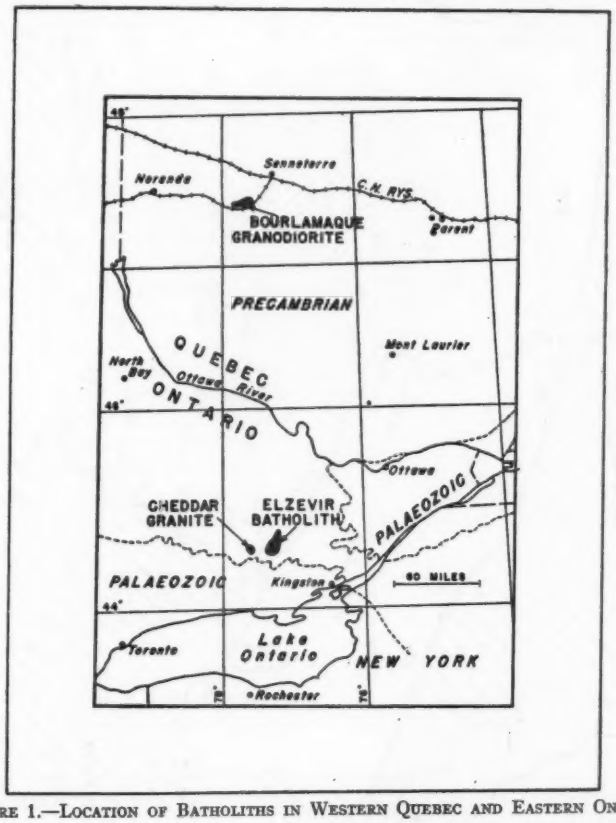

FIGURE 1.—LOCATION OF BATHOLITHS IN WESTERN QUEBEC AND EASTERN ONTARIO

Among the constituent minerals, albite, hornblende, and quartz are most abundant; apatite, ilmenite, magnetite, sphene, and zircon are accessories. Alteration products include chlorite, epidote, zoisite, and carbonates.

Gussow (1937a; 1937b) noted that the modes of the analyses recast as primary constituents indicate a remarkable uniformity in mineral composition throughout the Bourlamaque mass.

Radioactivity

Experimental procedure.—Hand specimens of rock carefully cleaned of surface contamination were broken into half-inch pieces and ground in a clean Braun Type UX mechanical pulverizer. About 1 gram of this product was finely ground in an agate mortar, suspended in alcohol, and deposited in films 92 mm. in diameter upon a copper disc. The rate of alpha-ray emission was determined by placing the disc in an ionization chamber and recording the amplified current impulses photographically continuously, and automatically for several hours. After correcting for the alpha-ray background of the ionization chamber and disc, the absolute activity was calculated or determined graphically (Keevil and Grasham, 1943). The instruments were calibrated with samples containing known amounts of uranium and thorium. The activity expressed in alpha-rays emitted per milligrams per hour, is related to uranium, U, and thorium content, Th.

$$a = 36.9 \times 10^4 U + 8.86 \times 10^4 Th \quad (1)$$

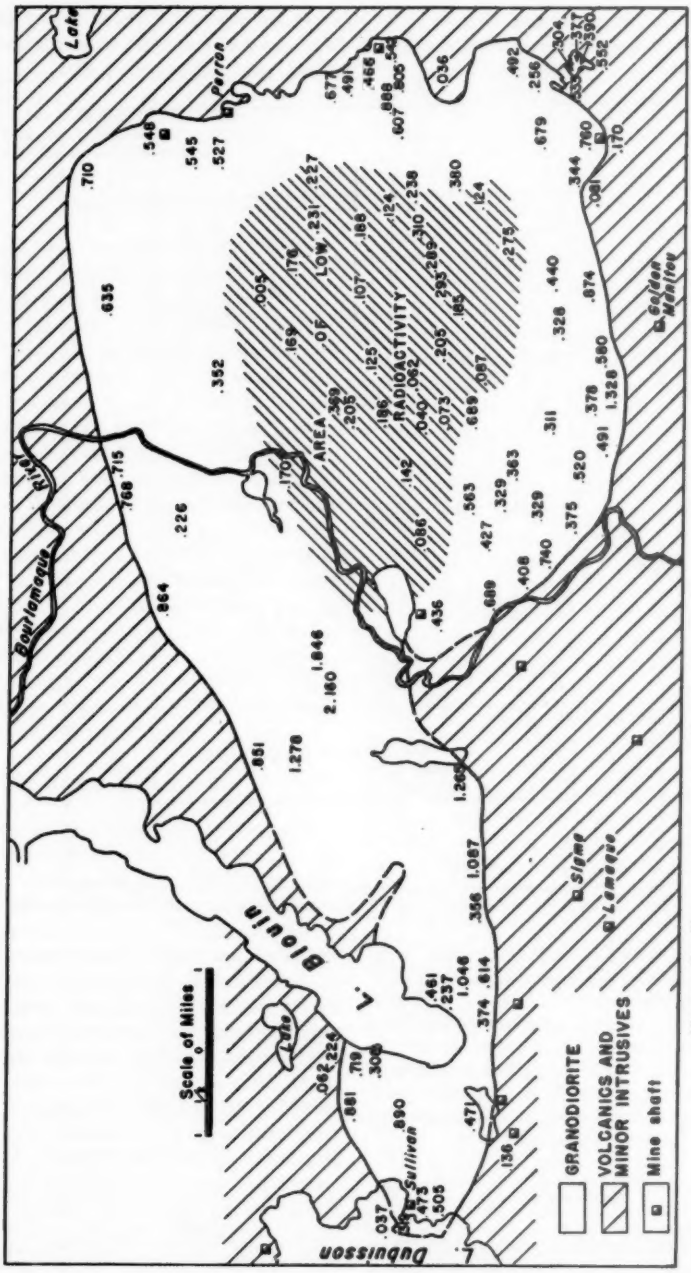

FIGURE 2.—RADIOACTIVITY IN THE BOURLAMAQUE BATHOLITH Expressed as alpha rays/mg./hr.

and to the rate of production of radiogenic heat (Keevil, 1943)

$$H = 2.15a + 22K \text{ cals./gm./M.y.} \quad (2)$$

or approximately

$$H = 2.60a \text{ cals./gm./M.y.} \quad (2a)$$

where K, Th, and U are concentrations in grams per gram, and $M.y.$ refers to millions of years.

Areal distribution.—The quantitative variation of the radioactivity of different parts of the Bourlamaque batholith has been carefully determined by analyses of some 150 specimens. The results for the granodiorite, plotted on Figure 2 according to locations in the intrusive, reveal a contrast in radioactivity between the core and border zones of the intrusive. Within the central region, the average activity is 0.116 alphas/mg./hr.; the average activity of the outer contact area is six times as high, 0.696. A heterogeneous distribution of activities is found in the intermediate zone, generally within the range 0.292–0.700.

Considered as a whole, there is a definite, but not uniform, decrease in radioactivity as the central portion of the mass is approached from its outer walls. This decrease does not culminate in a point of little or no radioactivity, but rather in a relatively large area comprising about a fifth of the exposed surface, in which the activity is considerably lower than the average for the whole intrusive.

Anomalous results were occasionally obtained. For instance, a mile northwest of Herbin Lake, a point 1½ miles from any known part of the outer edge of the intrusive, unusually high values of 2.16 and 1.84 were obtained for two specimens examined. A relatively high proportion of zircon observed in thin sections of these rocks may well account for the increased radioactivity. At the southeast corner of the batholith where the mass is especially basic, lower than average values for the border rocks were obtained, possibly because of assimilation of weakly active basic volcanics invaded by the granodiorite. The narrow western tongue of the batholith, as might be expected, tends to be more radioactive and variable than the main body of the intrusive.

Variation with depth.—For an indication of the depth variation of radioactivity, 21 samples were taken from drill holes and mines at depths to 1,650 feet. Around the main part of the intrusive, where the concentric distribution of radioactivity is evident, a decrease of activity with depth was found (Figure 3). These results are, however, inconclusive because of the small number of tests and the relatively shallow depths explored; and in the western border, where the surface distribution of radioactivity is erratic, opposite results were found.

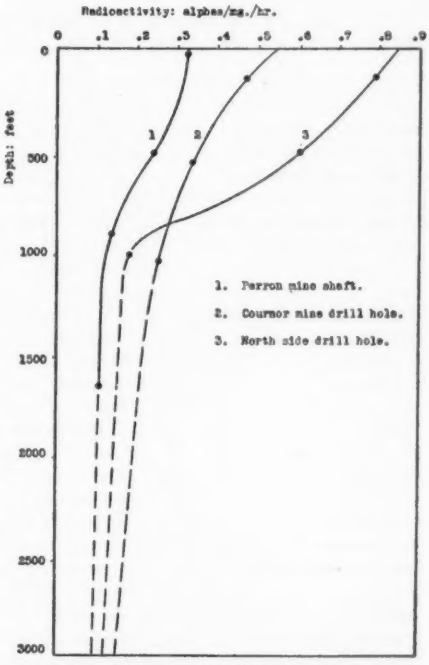

FIGURE 3.—DECREASE OF RADIOACTIVITY WITH DEPTH IN THE BOURLAMAQUE BATHOLITH

Associated rocks.—Comparison of the radioactivity of the Bourlamaque batholith with associated dikes and invaded rocks, with neighbouring intrusives, and with an average value for granodiorites is made in Table 1.

The average activity of the Bourlamaque batholith appears to be of the same order as that of other granodiorites in the region; all are considerably less than the average value for North American granodiorites (Keevil, 1943). While the radioactivity of late aplite

dikes associated with the Bourlamaque intrusives is relatively high, later quartz veins and pyrite are too weakly active to be detected by the alpha-ray counting method. The related area are Precambrian. The oldest rocks consist of severely metamorphosed, fine-grained greenstone, schists, biotite schists, massive and ellipsoidal lavas, and pyroclastics. Near the intrusive contact of the Algoman[1] batholith, these rocks are invaded by innumerable narrow stringers, seams, and lenses of granitic material along the planes of schistosity.

Granite pebbles in the Hastings conglomerate, the youngest Precambrian sedimentary rock, point to the existence of an earlier granite.

TABLE 1.—RADIOACTIVITY OF BOURLAMAQUE BATHOLITH AND ASSOCIATED ROCKS

Sample	Source	Activity alphas/mg./hr.
Bourlamaque batholith	Border zone	0.696
Bourlamaque batholith	Central core	0.116
Bourlamaque batholith	Average value	0.480
Unmineralized vein quartz	Sullivan Mine, Que.	0.000
Pyrite carrying gold	Cournor Mine, Que.	0.000
Aplite dikes	Intrusive into Bourlamaque	0.840
Adjacent granodiorite stock	S.E. of Bourlamaque batholith	0.36
Granite	Island, Flavrian Lake, Que.	0.43
Quartz	Separated from Flavrian granite	0.30
Feldspar	Separated from Flavrian granite	0.16
Hornblende	Separated from Flavrian granite	0.59
Diorite	N. of Flavrian Lake	0.18
Hornblende granodiorite	Vassan Tp., Que.	0.45
Granodiorite	E. of Lake La Motte, Que.	0.76
Granodiorite	Taschereau, Que.	0.31
Granodiorite	Average of 1000 samples*	1.4
Serpentinized peridotite	pre-Bourlamaque	0.041
Andesite	Inclusions in Bourlamaque	0.031
Andesite	Keewatin-type lava, S.E. of Bourlamaque	0.136
Tuff and Agglomerate	Keewatin-type lava, S.E. of Bourlamaque	0.08 to 0.50

* Study of North American rocks (unpublished).

granodiorite plug to the southeast is too small to show any zonal distribution of radioactivity.

The older basic rocks are generally less active, specimens of ultrabasic plutonics having activities of only 0.036, 0.037, and 0.057 alphas/mg./hr. The variable activities of tuff and agglomerate are not unexpected considering their varied nature and origin.

ELZEVIR BATHOLITH

General Geology

The Elzevir batholith lies 50 miles northwest of Kingston in southeastern Ontario at the southern edge of the Precambrian Shield (Fig. 1).

Except for a few small outliers of Paleozoic limestone, all of the consolidated rocks in the

Petrography

Gray granite.—The Elzevir composite batholith includes a number of lithologically distinguishable but intimately associated granitic rocks (Fig. 4). The most extensively developed is a gray granite, consisting mainly of quartz and orthoclase with considerable biotite and accessory sphene and apatite. It is distinctly foliated, especially near the

[1] post Hastings and pre-Ordovician

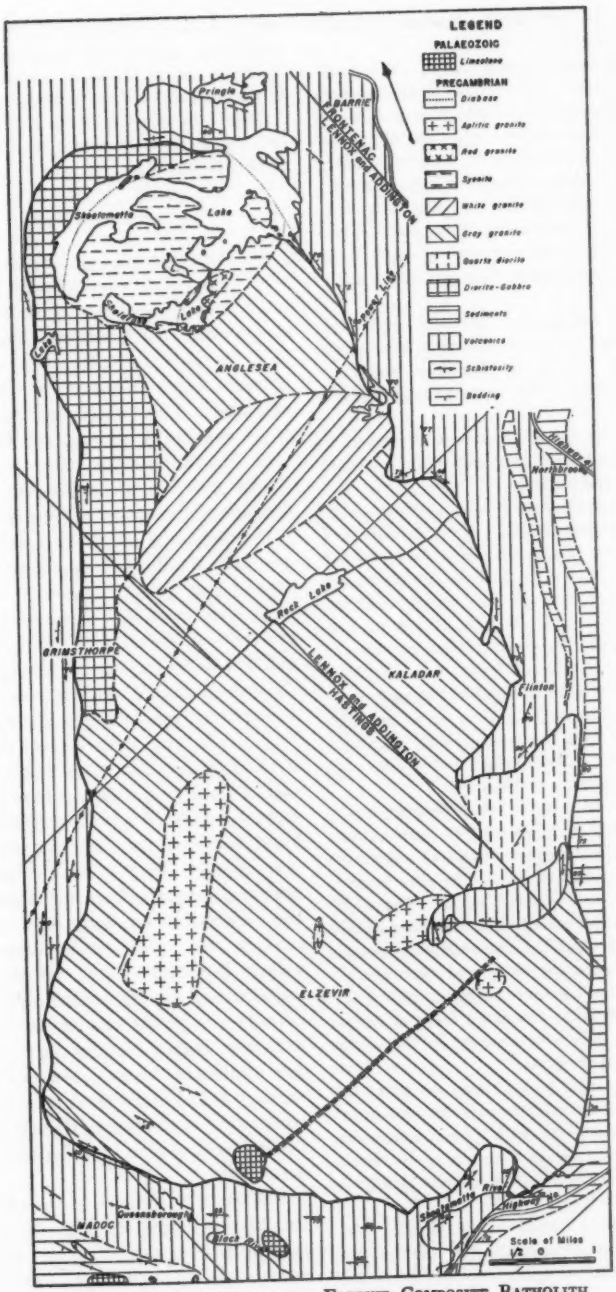

FIGURE 4.—GEOLOGY OF THE ELZEVIR COMPOSITE BATHOLITH

outer margin, but there are large areas of massive granite in the interior.

Gabbro-diorite-syenite-granite series.—A remarkable series of intrusive rocks occurs at the northern end of the composite batholith. This consists of gabbro, diorite, basic syenite, red syenite, and red granite with a complete gradation between the rocks. The diorite and gabbro probably represent an early product of the gray granite magma, their basic character being at least partly, if not chiefly, due to assimilation of intruded greenstones, many inclusions of which are found in them and in the neighboring granite.

The gradual change from diorite through basic syenite to syenite is accomplished by a reduction in plagioclase and increase in orthoclase, and by a reduction in amount of the ferromagnesian constituent.

The gabbro, an almost black rock of medium to coarse grain, is composed principally of carbonatized calcic andesine and augite.

A red biotite granite, the most acidic rock of the series, is composed mainly of orthoclase and quartz with about 10 per cent microcline and a few grains of albite. Magnetite, epidote, biotite, muscovite, apatite, tourmaline, and fluorite are accessories.

Quartz diorite-syenite.—A mass of rock ranging from quartz diorite to syenite crops out on the eastern side of the batholith. It is intruded by dikes of the gray granite and may represent an early basic differentiate of the granite magma, or an assimilation facies. The rock is coarse-grained, consisting chiefly of plagioclase, hornblende, and biotite, with minor sphene, quartz, and carbonate.

White granite.—A body of white biotite granite, 2½ miles wide and 5½ miles long, in southwestern Anglesea Township, is part of the main composite batholith. It appears to invade the gray granite, although gradational contacts occur. The white granite is a coarse-textured rock consisting largely of orthoclase, quartz, and biotite, with minor quantities of muscovite, apatite, pyrite, and carbonate.

Aplitic granite.—The seventh igneous rock in the Elzevir batholith is an elongated body of aplitic granite about a mile wide situated in the southwestern portion of the mass.

The aplitic granite is light gray to pink, the texture is saccharoidal, and the minerals present are albite, biotite, microcline, with sphene, muscovite, and zircon as accessories. The zircon is closely associated with biotite in which it forms pleochroic halos; apatite is lacking.

Associated dikes.—Narrow dikes of dark-gray biotite lamprophyre occasionally traverse the gray granite in the contact zone. The southeastern margin of the granite also contains dikes of coarsely crystalline pegmatite consisting chiefly of orthoclase, microcline, quartz, and muscovite. A late Precambrian dike of diabase is exposed intermittently in the southern part of the batholith for more than 5 miles in the direction N. 70° E. Numerous granitic and aplitic dikes are related to the intrusive rocks already described.

Radioactivity

General statement.—Radioactivity determinations have been made on nearly 200 rock specimens from the Elzevir intrusive and related rocks using the alpha-ray counting method (Fig. 5). Since the intrusion is composite, the different facies of the mass will be discussed separately. These contiguous granites appear to be genetically related, and it is worthy of note that their average radioactivities are sufficiently different to corroborate the field and petrographic evidence of their dissimilarity.

Distribution of radioactivity in the gray granite.—Like the Bourlamaque batholith, the large area of gray granite exhibits a zonal arrangement of radioactivity. The average of 31 determinations in the contact zone is 1.720 alphas/mg./hr., in contrast to an average of 0.497 in the central area. Within the intermediate zone, 40 scattered counts average 0.721 alphas/mg./hr.; 14 per cent of the values in the contact zone range between 0.5 and 1.0, but at least half of these were obtained from contaminated rock, samples of which invariably possess a lower radioactivity than the uncontaminated gray granite. In the intermediate zone, the activities range between 0.494 and 1.723, but the high values are found in areas where the contact zone also carries abnormally high values. The central area, 30 per cent of the total exposed surface, is uniformly low in radioactivity except for one or two minor inconsistencies. Such variations are not unexpected; the significant feature, revealed by a large number of radioactivity determinations, is the segregation of the radioactive elements into an active marginal zone around a relatively weakly active core.

Radioactivity profiles across two sections of the Elzevir batholith (Fig. 6) illustrate the generalized variations along east-west and north-south lines extending across the central part of the gray granite.

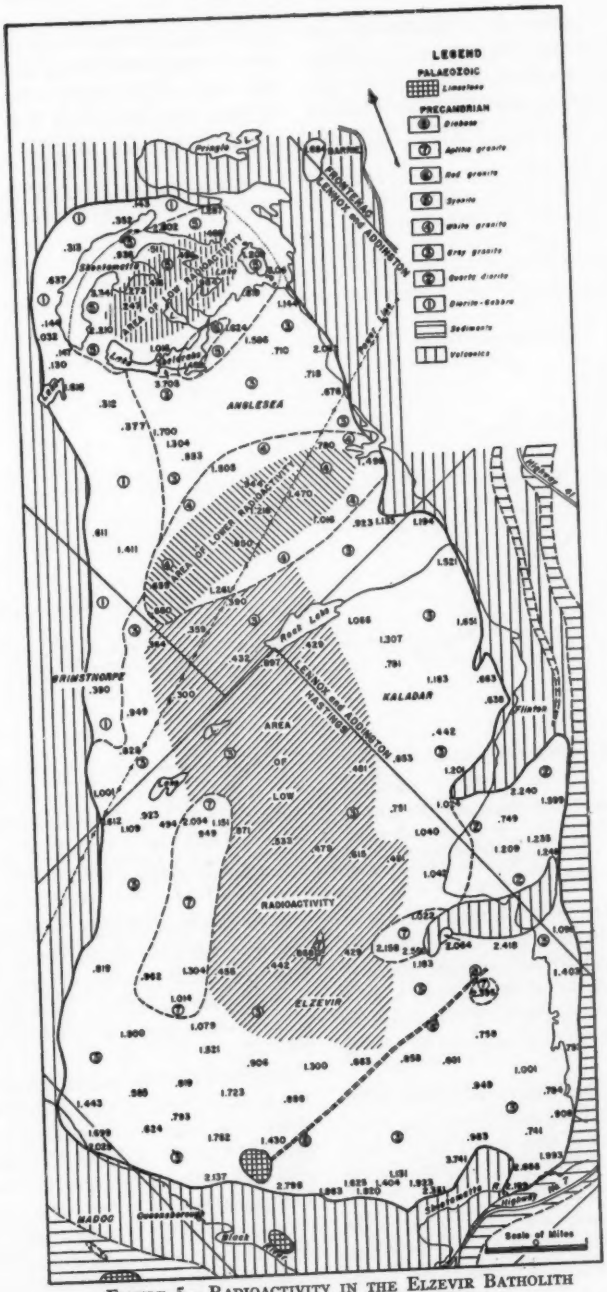

FIGURE 5.—RADIOACTIVITY IN THE ELZEVIR BATHOLITH
Expressed as alpha rays/mg./hr.

Distribution in the white granite.—In the mass of white granite lying within the northern part of the gray granite in Anglesea Township, the radioactivity was again found to be highest in the outer border, with an area of lower activities located inside it and extending to the western margin at the diorite contact (Table 2). The average activity of the border zone of white granite was found to be 1.319, compared to an average of 0.776 alphas/mg./hr. in the central area.

The salmon-colored quartz-rich phase, which is locally developed, especially near the center of the white granite, was found to be more radioactive (1.22, 1.47) approaching that of the red syenite and red granite.

Distribution in the syenite.—The circular body of syenite at the northern end of the batholith is also featured by an inner area of low radioactivity surrounded by a more radioactive border zone. In the central part, most of the values obtained were less than 0.50, while at the margin results as high as 3.70 alphas/mg./hr. were recorded. There is a slight tendency toward the development of a zone of intermediate radioactivity, as values of 0.82 and 0.94 were found between the core and the rim; in the other intrusives, some anomalies are superimposed upon the general core-border relationship.

Distribution in the quartz diorite and gabbro-diorite series.—Six determinations of radioactivity were made on specimens of the small body of variable quartz-diorite near Flinton (Fig. 5) with results ranging between 0.75 and 2.24 alphas/mg./hr. There is a vague suggestion of a core-border relationship, but this is uncertain both because of lack of uniformity in composition of the diorite and because of the small number of determinations. Furthermore,

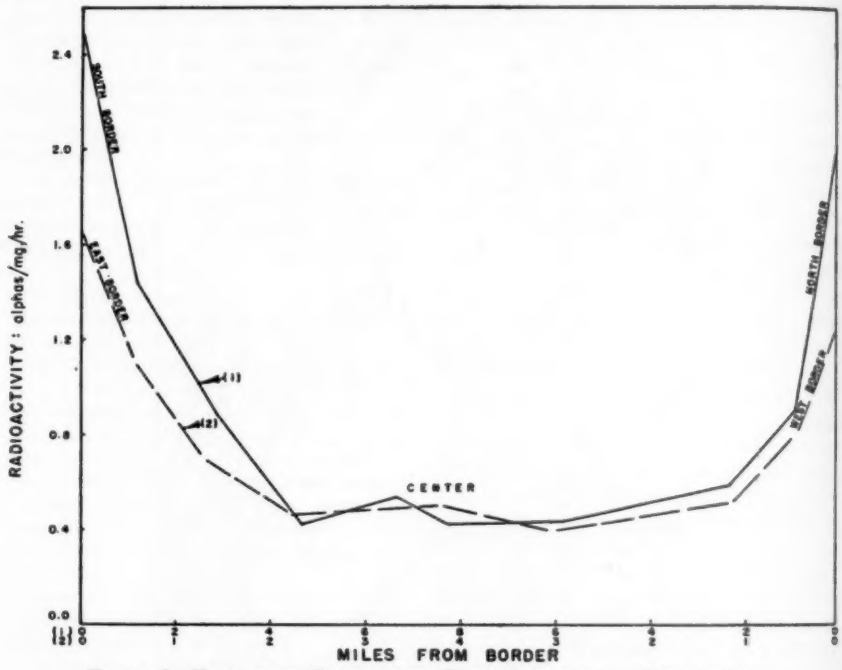

FIGURE 6.—GENERALIZED RADIOACTIVITY PROFILES ACROSS THE CENTRAL PART OF THE ELZEVIR GRAY GRANITE
(1) North-south profile across 16-mile length of batholith
(2) East-west profile across 8-mile width of batholith

the border value, 2.24, which is high for diorite, may be an effect of the near-by granite.

Most of the specimens studied from the northwestern and northern diorite-gabbro border zone of the batholith were low in radioactivity (near 0.3), but, where patches of granitic material were present, the activities were abnormally high (1.41, 1.62). The lowest values (0.03 to 0.14) were obtained from specimens taken near the outer contact, where the general basic character is due to assimilation of the basic weakly radioactive intruded volcanics. Higher values are obtained near the contact with granite and syenite, believed to be part of the differentiation series which includes the gabbro-diorite.

Aplitic granite.—The aplitic granite, regarded as the youngest facies of the batholith, possesses the highest average radioactivity of any of the rocks studied in this series: 1.690 alphas/mg./hr., with 40 per cent of the values exceeding 2.00. The larger area of this relatively zircon-rich rock, in the southwestern part of the main intrusive, does not show any systematic distribution of the radioactive elements, nor do the smaller patches of aplitic granite.

Associated rocks.—A dike of red granite which invades the closely related mass of red syenite was the most active of all specimens examined, 5.54 alphas/mg./hr. Two dikes of pegmatite cutting the southeastern contact zone of the gray granite have activities of 2.71 and 3.25; and a dike of aplitic granite intruding quartz diorite has a value of 1.24.

Radioactivity determinations were made on a few specimens of the invaded volcanics in order to find their effect, if any, on the activity of the border phase. The average radioactivity of four samples of andesitic lava collected along the eastern margin of the main intrusive is 0.133 alphas/mg./hr. The radioactivity of a highly talcose volcanic rock near the southern boundary of the intrusive was too low to be measured by the methods employed. Basic greenstones from the vicinity of the western contact yielded values as low as 0.07 alphas mg./hr. The activity of a pebble of granite gneiss from the Hastings conglomerate in southeastern Elzevir Township was only 0.36 alphas/mg./hr., lower than that of any of the other granitic rocks here studied.

Synopsis of distribution.—The radioactivities of the several phases of the Elzevir batholith are summarized in Table 2. Where any par-

TABLE 2.—DISTRIBUTION OF RADIOACTIVITY IN THE ELZEVIR, CHEDDAR, AND BOURLAMAQUE INTRUSIVES

Rock	No. of determinations	Average activity, alphas/mg./hr.				
		All samples	Contact zone	Intermediate zone	Central area	Weighted average*
Dike rocks	4	1.2 to 5.5				2.98
Aplitic granite	12	1.690	No significant variation			1.69
Red granite	1	1.56	Not determined			1.56
Syenite	17	1.453	1.860		0.477	1.30
Quartz-diorite	6	1.37†	1.51		0.75‡	1.20
White granite	10	1.076	1.32	0.78		0.93
Gray granite	86	1.018	1.720	0.721	0.497	0.65
Diorite-gabbro	12	0.293	0.102	no significant variation		0.20
Older lavas	15	0.11				0.11
Cheddar granite	175	1.81	3.01	1.88	1.11	1.85
Bourlamaque granodiorite	127	0.480	0.696		0.116	0.37

* Assumptions made on the basis of structural investigations of relative volume of core and border phases at depth and that the core phase is representative of the batholith at depth.

† Activity probably increased by granitization.

‡ One value.

ticular distributions of radioactivity are indicated, the average for the different zones is given. Averages for the Bourlamaque and Cheddar batholiths are included for purposes of comparison.

TABLE 3.—AVERAGE RADIOACTIVITIES OF COMPONENTS OF THE CHEDDAR BATHOLITH

Rock	Number of specimens	Activity alphas/mg./hr.	
Quartz veins	4	0.66	
Granite and aplite dikes	4	5.41	
Pegmatites	14	3.28	
near batholith	2		3.96
within border phase	4		4.62
in interior zone	8		2.43
Coarse-grained border phase	28	3.01	
pegmatitic granite in interior	20		1.06
pegmatitic granite (total)	48		2.20
Medium-grained granite and gneissic granite	113	1.86	
massive pink granite	21		1.92
reddish granite	13		1.65
gneissic pink granite	32		1.76
hybrid pink granite	37		2.04
outlying granitic rock*	10		1.50
Intermediate zone	93	1.97	
Interior zone	36	1.11	
Paragneiss†	10	1.16	
Amphibolitic paragneiss	2	0.41	
Limestone	4	0.64	
Granitized limestone	1	2.07	

* Specimens of granite and granite gneiss in paragneiss near the contact; some of these may be within the batholith, the position of the contact not being exactly known in places.

† One specimen of biotitic paragneiss at the northwestern contact of pegmatitic granite, not included in the average, possessed an activity of 7.03 alphas/mg./hr.

CHEDDAR BATHOLITH

General Geology

The Cheddar granite mass is a roughly elliptical body about 5 miles in the east-west direction and 7 miles along the north-south axis. The center lies at Long. 78° 10′ and Lat. 45° 20′, 7 miles southeast by south of Wilberforce, Ontario.

The Cheddar stock, presumably Algoman in age, is less gneissic and more uniform in texture than the granite gneisses which are prominently developed in this region, however, while massive pink and reddish granites are common, gneissoid areas and included patches of the invaded schist occur within the mass. Much of the border zone is characterized by the development of a pegmatitic facies. The mass may be a cupola of a much larger batholith, but it is enclosed by sedimentary and volcanic rocks, and, whether or not a separate intrusive, it seemed of value to study the distribution of radioactivity in some detail, particularly since radioactive mineral occurrences have been found and mined in the Wilberforce district. Preliminary radioactivity data (25 samples) on other granite bodies in the district suggest that the Cheddar mass is more radioactive than these rocks, and may have a different origin.

Petrography

Several textural and mineralogical facies of granite can be recognized within the borders of the batholith. The western, southern, and southeastern border consists of a rim half a mile wide of pegmatitic granite, and small scattered patches of this type occur in the interior of the mass, particularly in the southern portion. This rock is medium to coarsely granular and pink, and consists of quartz, microcline, commonly perthitic, together with magnetite, sphene, biotite, muscovite, apatite, zircon, and tourmaline; minor alteration products include chlorite, epidote, and zoisite.

A number of facies of medium-grained pink and reddish granite occur rather indiscriminately throughout the stock. The massive pink granite contains about 80 per cent feldspar, 17 per cent quartz, and 3 per cent hornblende, biotite, and magnetite, with magnetite, sphene and apatite present as accessories.

In the hybrid facies which occupies most of the northwestern section of the batholith, small irregular patches and aggregates of hornblende and biotite constitute up to 15 per cent of the rock, scattered throughout a matrix of quartz and feldspar.

Radioactivity

The distribution of 200 radioactivity values plotted on Figure 7, and summarized in Table 3, again shows a relatively radioactive border zone except at the northeast boundary of the

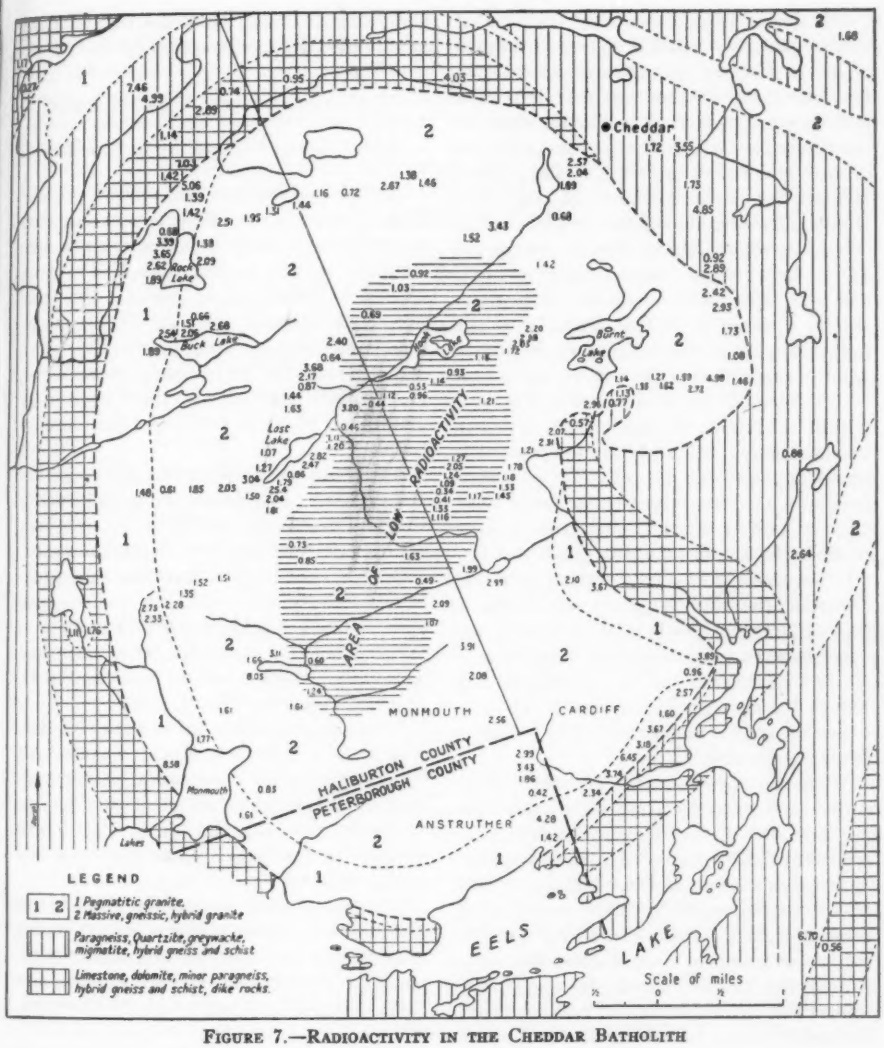

FIGURE 7.—RADIOACTIVITY IN THE CHEDDAR BATHOLITH

batholith; this conforms roughly with the distribution of pegmatitic granite. The radioactivity of the massive, foliated, and hybrid granite in the interior is somewhat irregular, but the average for the central area, 1.1, is lower than that for the intermediate zone between the core and the border facies, 2.0 alphas/mg./hr. This contrast in radioactivity is not so evident on Figure 7 as that between the coarse-grained border phase (3.01) and the remainder of the batholith (1.86) because of the more uniformly high radioactivity of the pegmatitic granite near the border.

In this connection it is noteworthy that the scattered pegmatitic granite in the interior is not particularly radioactive (1.06); furthermore, four pegmatites included in the border facies averaged 4.62 alphas/mg./hr., nearly twice as high as the average for eight pegmatites in the interior of the batholith, (2.43). Four specimens of the quartz from veins have an average activity of only 0.66.

The quartz veins, presumably representing residual magmatic material, were impoverished in radioactivity as were those associated with the Elzevir and Bourlamaque batholiths. The peak in concentration of radioactive elements was reached in associated pegmatites (3.28) and dikes of granite and aplite (5.41). The average radioactivity of 68 specimens of pegmatitic granite (2.2) taken throughout the whole batholith is only slightly higher than the average for 113 medium-grained granitic specimens (1.9); and this observation, together with petrographic evidence of deuteric alteration of the pegmatitic granite similar to that in the normal granite, suggests that the two are contemporaneous facies of the same intrusive. The core-border distribution of radioactivity, although less pronounced, holds whether the pegmatitic granite is developed or not. The pegmatitic granite in the outermost zone is nearly three times as high as that scattered in the interior of the batholith; and the pink granite exhibits a radioactivity in its central portion somewhat lower than that near its contact with peripheral pegmatitic granite. No general relationship was noted between composition, color, and texture of the pink granite and its radioactivity, although the more gneissic specimens showed a somewhat greater proportion of high values in frequency distribution curves.

While it is clear that the periphery of the intrusive is generally more radioactive than the core, the distribution of radioactivity is somewhat erratic. One reason for this appears to be irregularities in the distribution of zircon; the most active pegmatite (8.58) contains many small crystals of this mineral. In 14 other thin sections of granite, a trace of zircon was found in only one; and this sample was one of most radioactive of medium-grained granites (3.45). It should be remembered that the erratic nature of the distribution may be more apparent than real since the small one-third gram samples studied in the laboratory, even though quartered from large hand specimens, may not be truly representative of the outcrop. Such variations are generally much smaller than the major features of the distribution; for example, if one obtained values of 6.0 and 1.5 for two specimens of pink granite, it would be nearly certain that the former was a dike-rock. Similarly values of 3.0 and 0.8 for pegmatitic granite would suggest that the samples came from border and core, respectively.

Radio-Petrogenetic Considerations

Distribution of Radioactivity in Batholiths

Contrast between core and contact zones.—High radioactivities of the border as compared to the central area are indicated in six of nine intrusives studied in three areas. The contrast appears to depend upon erosional level and size of the intrusive, the most distinct gradation in radioactivity being found in the three largest areas, the Bourlamaque granodiorite, the Cheddar granite, and the Elzevir gray granite, all of which have been considerably eroded.

As none of the masses investigated were entirely uniform, but showed the common variation of Precambrian batholiths, it is not surprising that the results were somewhat erratic. When the number of radioactivity determinations are sufficient to provide a perspective view, however, the generalized distribution of radioactivity into an active border zone and impoverished core seems to be characteristic of larger batholiths (Figs. 2, 5, 6).

In smaller intrusives, the tendency for such a distribution seems to be absent, or is obscured by local fluctuations in radioactivity from specimen to specimen which may be due to a number of causes other than the differentiation into core and border zones of radioactivity (Keevil *et al.*, 1943).

The results (Table 4) suggest that less active cores are not evident in intrusives less than 2 miles across, and that in intrusives of comparable composition the contrast between core and border phases of larger batholiths increases with size of the intrusive.

Effect of active accessory minerals.—Certain accessory minerals may account for an appreciable proportion of the radioactivity of a rock; zircon, for example, may be hundreds or thousands of times as radioactive as the common mineral constituents of rocks (Keevil *et al.*, 1944). It is interesting to note that the relatively high activity of the aplitic granite is associated with numerous pleochroic halos surrounding zircon grains in biotite, and that only minor amounts of zircon were observed in the

other intrusive rocks represented in the Elzevir composite batholith. Similarly, two exceptionally high values for the activity of the Bourlamaque granodiorite (2.16 and 1.84) were associated with relatively high zircon content; and two values in the Cheddar stock, three times the normal radioactivity, were from the only specimens found to contain zircon.

Influence of invaded rocks.—Although the core-border radioactivity relationship is not determined by assimilation of invaded formations, local effects of contiguous rocks upon the radioactivity of the intrusives were noted in a number of instances. For example, in the southeastern part of the Bourlamaque batholith where the intrusive is locally more basic, activities of 0.26 and 0.34 alphas/mg./hr. were obtained, considerably lower than the average value, 0.696, for the border zone. Similarly in the Elzevir batholith, a number of border rocks with the lowest radioactivities in a fairly consistently active outer zone are the result of the local development of a more basic facies near the contact, where values of 0.03, 0.13 and 0.14 alphas/mg./hr. were found. The contaminated granitic rocks near the contact with the intruded schists at the northeastern border of the Cheddar stock are less radioactive than the average granite.

Effects of granitization.—At a number of places where granitization of invaded rocks occurred, higher than normal activities for the basic volcanics were observed. In some instances, radioactive elements appeared to have been introduced where little influence of the intrusive was visible in the field. To the southeast of the Bourlamaque batholith, specimens of lavas and volcanics, normally considerably less radioactive than 0.1 alphas/mg./hr. in this region, possessed activities as high as 0.55. It is possible that radioactive elements were introduced by relatively highly radioactive deuteric solutions derived from the albitic granodiorite magma.

In the Elzevir batholith, the variation of radioactivity in the gradational contact zones presents a rather special case of the influence of granitic magmas on invaded rock. Granitization of the diorite near Flinton, for example, is believed to account for its relatively high radioactivity.

TABLE 4.—DIFFERENTIATION OF RADIOACTIVE ELEMENTS AS A FUNCTION OF SIZE OF INTRUSIVE

Intrusive	Distance across intrusive, miles	Distance across weakly active central area, miles	Contrast in activity border: core
Bourlamaque, Que.			
Grainodiorite batholith	6.5	3	6
Related stock	0.3	—	none
Elzevir Tp., Ont.			
Gray granite	8	3.5	3.5*
Syenite	3	1.5	3
White granite	2.5	1.3	1.7
Quartz diorite	2	0.2 (?)	1.8
Diorite gabbro	1.5	—	none†
Aplitic granite	1	—	none
Monmouth Tp., Ont.			
Cheddar granite	5	1.5	2.8

* Distinct contrast between core, intermediate and border zones.

† Border phase low here due to assimilated volcanics of low activity.

Radioactivity of Differentiation Series

Basic to acidic rocks.—The closely related intrusives comprising the Elzevir mass provide an interesting series from early diorite through syenite to later granites of increasing acidity,

ending with pegmatites and veins as the final phase of magmatic activity. The concentration of radioactive elements increases until the pegmatitic stage is reached, and is insignificant by the time the vein-forming fluids are developed (Table 5).

TABLE 5.—RADIOACTIVITY OF THE DIFFERENTIATES OF THE ELZEVIR MAGMA

Differentiate, in order of increasing age	Average radioactivity	Estimated volume of magma	Proportion of radioactivity of primary magma
	alphas/mg./hr.	*per cent*	*per cent*
Veins	0.05	10^{-5}	6×10^{-5}
Pegmatites	2.98	10^{-4}	3×10^{-4}
Aplitic granite	1.69	4.4	10
Red granite	1.56	0.5	1
Syenite*	1.30	5	8
White granite*	0.93	10	13
Gray granite	0.65	70	64
Diorite	0.20	10	3

* The sequence of these closely related granitic rocks is uncertain but the white is younger than the gray granite and a dike of red granite cuts syenite; the gray granite is intimately related with the diorite which is intruded by dikes of the red granite and syenite, but is in gradational contact with the more massive facies of these rocks.

Although the later acidic rocks are most radioactive, the total radioactivity of these masses accounts for only 20 per cent of the radioactive elements associated with the primary magma. The gray granite of intermediate activity accounts for two thirds of the original radioactivity of the batholith as a whole.

Older to younger rocks.—In the Elzevir series, the younger members, as we have seen, are most highly radioactive. Older lavas in the region are much less radioactive, but it is of some interest to compare the radioactivity of the Elzevir granite with earlier intrusives of comparable composition in the region. The only granitic rock of proven antiquity is represented by pebbles in the Hastings conglomerate intruded by the Elzevir batholith. The radioactivity of a pebble of granite gneiss from this formation in southeastern Elzevir township was found to be considerably less than the younger granites (0.36 alphas/mg./hr.), confirming the general rule indicated by earlier and unpublished work that the younger granites of a region tend to be more radioactive.

Local differentiation.—It is difficult to assess the importance of local differentiation, because local changes in composition may also result from assimilation and granitization processes. However, the white granitic facies of the Elzevir batholith grades near the center of the mass into a quartz-rich, salmon-colored granite. The pink rock is more radioactive (1.35) than the central area of white granite (0.78), suggesting that the more potassic pink phase may represent the incipient stage of the next step in the differentiation series following white granite.

Use in petrological correlation.—A survey of the data for the Elzevir composite batholith shows that the radioactivity changes from one member to another in a characteristic fashion which serves to distinguish them about as well as their macroscopic differences and mineralogical compositions. For instance, at the south contact of the white granite, the activity is 1.26, whereas that of the adjoining core of the gray granite is 0.39. Similarly at the northern contact, the white granite possesses an activity of 1.50 as compared to 0.55 for the adjacent gray granite. At the contact between gray and aplitic granite, the activity changes in several places from 0.45 to 1.30, from 0.49 to 2.05, and from 0.43 to 2.16.

These examples suggest that radioactivity might be used occasionally as a tool in correlating igneous rocks.

SIGNIFICANCE IN GEOTHERMICS

Radiogenic Heat

While determinations of the radioactivity of rocks provide one of the most sensitive means of studying the geochemistry of the heaviest elements, they are perhaps most important in providing data on rate of production of radiogenic heat in the earth's crust (Eq. 2).

The uppermost granitic layer of major importance in determining the rate of cooling of the earth is known to be variable in thickness and in radioactivity. In the two regions studied, seismological evidence is not yet complete enough to determine the thickness of the granitic layer, but it is likely that they are not

much different. The radioactive heat-producing powers, however, differ considerably.

Elzevir and Cheddar areas, Southeastern Ontario: 2.9 cals./gm./M.y.[2]

Bourlamaque area, Western Quebec: 0.8 cals./gm./M.y.

The present surface heat flow depends largely on the radioactivity of the uppermost layers of the earth and is known to vary from region to region. It may be predicted, therefore, since the thermal conductivities of granite and granodiorite are not much different, that the surface heat flow in the Elzevir district is somewhat higher than that in the Bourlamaque area. In other words, if these masses are characteristic of large areas, the geothermal gradient in southeastern Ontario should exceed that in western Quebec.

Local differences in radioactivity such as are exhibited between the periphery and core of batholiths are probably of negligible effect upon major geothermal features such as the geothermal gradient. They may, however, play a small part in the particular geothermal history of the batholith. Consolidation of the magma at depth is undoubtedly a slow process and may require several million years. Near the final stages, the peripheral facies will contain a higher concentration of radioactive elements, and the neighboring rocks will be nearly in thermal equilibrium with the intrusive. The contribution of radiogenic heat would undoubtedly delay solidification slightly, the effect being greater the slower the crystallization process. This effect, though small, might be enough to influence the delicately balanced equilibrium in the final stages of consolidation, and may allow more complete differentiation and accumulation of metals from batholiths with a relatively highly radioactive border. It may also be a factor in assisting syntexis during magma emplacement.

The concentration of radioactive elements in the outer rim may also play an important role in the isostatic sinking and refusion of batholiths. The contrasts observed between the core and border zones are sufficient to permit the remelting of the border before the core in the first stages of refusion. These considerations are purely hypothetical, the magnitude of such effects would depend upon rates of differentiation, rates of heat transfer, and on the relative importance of convection currents.

[2] Million years (M.y.).

Representative Sampling

In the general study of the distribution of radioactivity in the rocks of the earth's crust, representative sampling is necessary to obtain reliable average radioactivities. Geologists, interested primarily in mapping contacts, marginal facies, and deposits around the borders of batholiths, are prone to collect samples of special interest near the border, rather than from the interior of the mass. This may be a contributing cause of the high average radioactivities indicated by early work.

To know the section of the batholith represented by the present erosional level, is important in estimating the radioactivity characteristic of the batholith at depth. Intrusives which have experienced only shallow erosion may be expected to yield considerably higher radioactivities than comparable masses which have been deeply eroded.

The influence of invaded rock must also be evaluated. Even where hybrids or contaminated facies are not evident at the margin of intrusives, it is desirable to study specimens of country rock both adjacent to the batholith and beyond the influence of invading magma.

Summary of Conclusions

(1) A concentration of radioactivity toward the outer margin of batholiths, not related to invaded rock, has been shown in six of nine intrusive studies in three areas.

(2) The difference in radiogenic heat-producing power of the rocks in southeastern Ontario (2.9 cals./gm./M.y.) and western Quebec (0.8 cals./gm./M.y.) should lead to observable differences in the geothermal gradient and the present surface heat flow.

(3) Representative sampling of batholiths for radioactivity investigations requires attention to all exposed parts, examination of invaded rock, and knowledge of the section represented by the present erosional level.

(4) In the series of related intrusives comprising the Elzevir composite batholith, an increase in specific radioactivity was found in

the change from basic to later acidic rocks, culminating with pegmatites; an intermediate gray granite, however, accounted for 64 per cent of the radioactivity of the primary magma.

(5) Characteristic radioactivities of members of an intrusive series may be used as a criterion for correlation.

References

Adams, F. D., and Barlow, A. E. (1910) *Geology of the Haliburton and Bancroft, areas*, Geol. Survey Canada, Mem. 6., 419 pages.

Auger, P. E., (1940) *Siscoe map area*, Quebec Bur. Mines, Adv. Rept., 12 pages.

Balk, R. (1937) *Structural behavior of igneous rocks*, Geol. Soc. Am., Mem. 5., 177 pages.

Bell, L. V. (1934) *Lamaque-Sigma mines and vicinity, western Bourlamaque Township*, Quebec Bur. Mines, Ann. Rept., pt. B., p. 3–60.

—— (1935) *Northern Dubuisson area, Abitibi County*, Quebec Bur. Mines, Ann. Rept., pt. B., p. 3–58.

—— and Bell, A. M. (1931) *Bell River headwaters area; Detailing the Pascalis-Louvicourt gold deposits*, Quebec Bur. Mines, Ann. Rept., pt. B., p. 59–128.

Denis, B. T. (1938) *Quebec Manitou-Fleming map-area*, Quebec Bur. Mines, Adv. Rept., 5 pages.

Gussow, W. C. (1937a) *Petrogeny of the major acid intrusives of the Rouyn-Bell River area, northwestern Quebec*, Ph.D. Thesis, Mass. Inst. Technol., 175 pages.

—— (1937b) *Petrogeny of the major acid intrusives of the Rouyn-Bell River area, northwestern Quebec*, Royal Soc. Canada, Tr., vol. 31, Sec. IV., p. 129–161.

Harding, W. D. (1939) *Geology of Kaladar Township*, Ont. Dept. Mines, Prelim. Rept., 2 pages.

Hawley, J. E. (1930) *Gold and copper deposits of Dubuisson and Bourlamaque Twnp., Abitibi County*, Quebec Bur. Mines, Ann. Rept., pt. C., p. 3–97.

Keevil, N. B. (1943) *Radiogenic heat in rocks*, Jour. Geol., vol. LI, no. 5., p. 287–299.

—— and Grasham, W. E. (1943) *Theory of alpha-ray counting from solid sources*, Canad. Jour. Res., vol. A21, p. 21–36.

——, Keevil, A. R., Ingham, W. N., and Crombie, G. P. (1943) *Causes of variation in radio activity data*, Am. Jour. Sci., vol. 241, p. 345–365.

——, Larsen, E. S., and Wank, F. J. (1944) *Distribution of helium and radioactivity in rocks. VI. The Ayer granite-migmatite at Chelmsford, Mass.*, Am. Jour. Sci., vol. 242, p. 345–353.

Meen, V. B. (1939) *Geology of the Anglesea-Barris area*, Ont. Dept. Mines, Prelim. Rept., 2 pages.

—— (1940) *Geology of Grimsthorpe and Elzevir townships*, Ontario Dept. Mines, Prelim. Rept., 3 pages.

Miller, W. G., and Knight, C. W. (1914) *The Precambrian Geology of Southeastern Ontario*, Ont. Dept. Mines, vol. 22, Pt. II., 151 pages.

Norman, G. W. H. (1941) *Vassan-Dubuisson map-area, Abitibi County, Quebec*, Geol. Survey Canada, Sum. Acc., 9 pages.

Wilson, M. E. (1926) *Madoc area*, Geol. Survey Canada, Map No. 559A

Quebec Bureau of Mines, Val d'Or, Quebec; Mining Geophysics Corporation, Ltd., 11 Jordan Street, Toronto, Ontario.

Manuscript Received by the Secretary of the Society, October 3, 1949.

BULLETIN OF THE GEOLOGICAL SOCIETY OF AMERICA
VOL. 62, PP. 149-158, 6 FIGS., 1 PL. FEBRUARY 1951

STRUCTURAL ANALYSIS OF THE WEST BORDER OF THE DURHAM TRIASSIC BASIN

By John W. Harrington

Abstract

The Durham Triassic Basin in Piedmont North Carolina is a lowland area floored with Triassic rocks and defined on the east and west by older Paleozoic slates and Carboniferous granites. A narrow strip along the western border of the sediments was mapped, and the relationship of the pre-sedimentation and post-sedimentation structural features determined. A reconnaissance method of multiple-surface analysis was used which suggests that linears in the Triassic-crystalline contact are buried fault scarps. The method was also applied to the graphic solution of two otherwise indeterminate rotational fault problems. A figure of 1800 feet is established as the probable minimum amount of erosional stripping in the basin and on the Piedmont since faulting. An integrated structural and geomorphic history for the formation and erosion of the western part of the basin is developed. Evidence suggests that the basin was never much wider than its present western limit and certainly did not extend as far west as the Dan River Triassic Basin.

CONTENTS

	Page
Introduction	149
Stratigraphy	149
Acknowledgments	151
Multiple-surface analysis	151
Division into structural units	151
Possible reflections of the border structure in the multiple-surface record	155
Use of the multiple-surface record in the analysis of rotational faults	155
Geomorphology	156
Conclusions	157
References cited	157

ILLUSTRATIONS

Figure	Page
1. Map of the North Carolina Triassic basins	150
2. Illustration of multiple-surface analysis	151
3. Map of Structural Unit 1	152
4. Map of Structural Unit 2	153
5. Map of Structural Unit 3	154
6. Multiple-surface record for the rotational faults	156

Plate	Facing page
1. Geologic map of the west border of the Durham Basin	156

Introduction

The Durham Triassic Basin in Piedmont North Carolina is one of the familiar faulted and filled graben structures which have been mapped from South Carolina to Nova Scotia. This basin extends southwestward from a point near Oxford in Granville County through Durham, Orange, and Chatham counties to a point in northern Lee County, where it blends with the Deep River Triassic Basin. The area investigated (Fig. 1) includes the western border facies of the sediments and a narrow belt of the adjoining crystallines. These more resistant rocks have been maintained as a low scarp which separates the basin plain from the beveled Piedmont surface. Relief varies from a minimum of 50 feet on a very gentle slope to a maximum of 350 feet with local slopes as high as 13°.

Stratigraphy

The stratigraphic and lithologic descriptions have been given by a number of workers. Holmes and Kerr in their Geologic Map of North Carolina (1887) grouped the metamorphosed and highly heterogeneous conglomerates, tuffs, breccias, igneous intrusives, volcanics, and apparently varved sediments as members of the Carolina Slate Series. On the Geologic Map of North America (Stose, 1946) they are correlated as Palezoic volcanic slates.

Intruding the slates are a number of equally heterogeneous phanerites which range from granite to diorite over very short distances. Xenoliths and cognate inclusions suggest that some of the variation may be due to assimilation of the heterogeneous slates. These intrusives have been correlated by Stose as Carboniferous in accord with similar intrusives of the other Atlantic States.

Triassic diabase dikes and sills are the youngest igneous rocks in the area. One large sill is 100 feet thick with perhaps 30 or 40 feet of its upper portion eroded. The dikes vary in thickness from a few inches to nearly 100 feet.

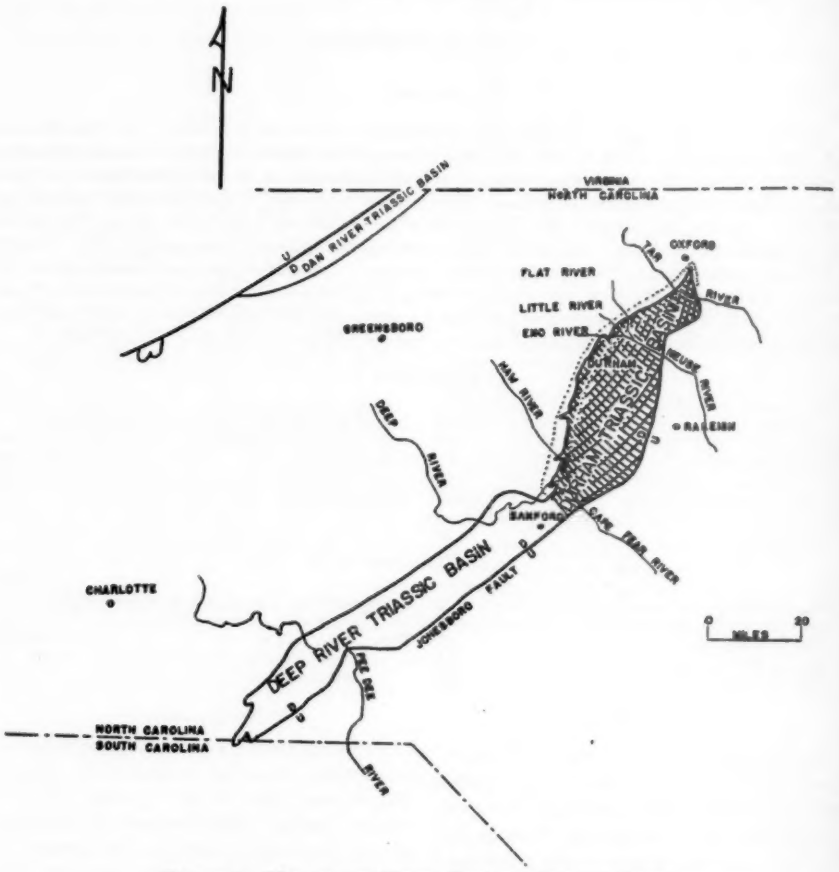

FIGURE 1.—MAP OF THE NORTH CAROLINA TRIASSIC BASINS
The investigated area is included inside the dotted line.

The Triassic sediments have been adequately described by Emmons (1856), Holmes and Kerr (1887), Russell (1892), Campbell and Kimball (1923), Goldston and Stuckey (1930), Prouty (1931), and most recently for the Deep River Basin by Reinemund (1949). In general they are red to buff arkosic sandstones, shales, and conglomerates with special characteristics reflecting the source material and conditions of deposition. Fanglomerates are common along the great Jonesboro fault bordering the basin on the east but are notably absent along the western border except at its juncture with the eastern fault.

Some of the streams which enter the basin from the west are flanked with terrace deposits as much as 40 feet thick. These are believed to be associated with the highest Coastal Plain terrace reported by Cooke (1930), and accordingly correlated as late Pliocene or Pleistocene. Lower flood-plain deposits are of recent

origin. The relationships of these various lithologic units are shown on the geologic map (Pl. 1).

outcrop of the Triassic sediments. One surface of each orientation was selected from each outcrop. Measurements of the strikes and dips of

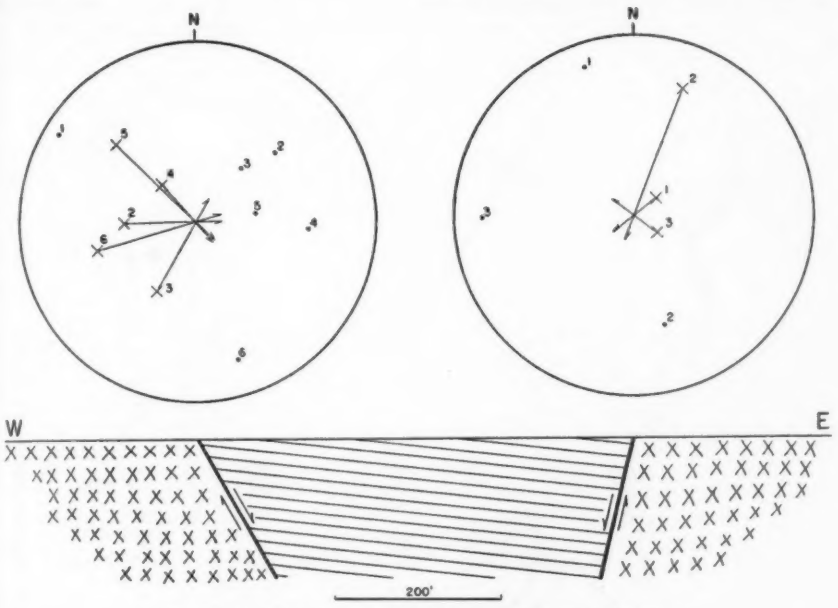

FIGURE 2.—ILLUSTRATION OF MULTIPLE-SURFACE ANALYSIS

This is a diagrammatic section of a small graben with the multiple-surface record for each footwall showing by dots the poles to the planes and by arrows the inferred direction of movement.

ACKNOWLEDGMENTS

The author is indebted to Professors G. R. MacCarthy, who directed this research, the late Wm. F. Prouty, W. A. White, and J. W. Huddle for their kind criticism and helpful advice.

MULTIPLE-SURFACE ANALYSIS

The geologic map shows that the border of the Durham Basin is marked by a number of very definite linears. An evaluation of these as unconformities and post-sedimentation faults was considerably facilitated by a reconnaissance system of the multiple-surface analysis developed by White (1948). The multiple-surface record consists of literally thousands of manganese oxide and colloidal clay casts of the slickensided fault planes. These occur both in the saprolite mantling the crystallines and in one

the planes and slickensides were plotted as stereographic projections. These were compared by inspection to the border lineations to determine the first approximation of the degree of correspondence.

The method is qualitative in that no measurements of the amount of displacement, the number of faults of the same strike, or the time of faulting were made. The only justifiable implication is that faulting occurred along a measured strike. Figure 2 illustrates the method and its interpretation in terms of adjacent structure. The small graben of Triassic sandstone between granite walls is reflected by the arrangement of the poles to the planes, and the arrows suggest the direction of movement.

DIVISION INTO STRUCTURAL UNITS

To determine the relationships between the multiple-surface record and the mapped struc-

FIGURE 3.—MAP OF STRUCTURAL UNIT 1

Average strike lines are superposed over the border linears. The numbered segments mark the zones from which the multiple-surface record was collected.

tures, the western border of the Durham Basin was divided into three entities based on the character of the Triassic-crystalline contact. Structural unit 1 extends from the southern end of the basin across Chatham County to show a contrast of lithologic type both in the conformable and downfaulted position. The faulting dropped fine-grained sediment from the lens and pocket area into contact with the crystallines.

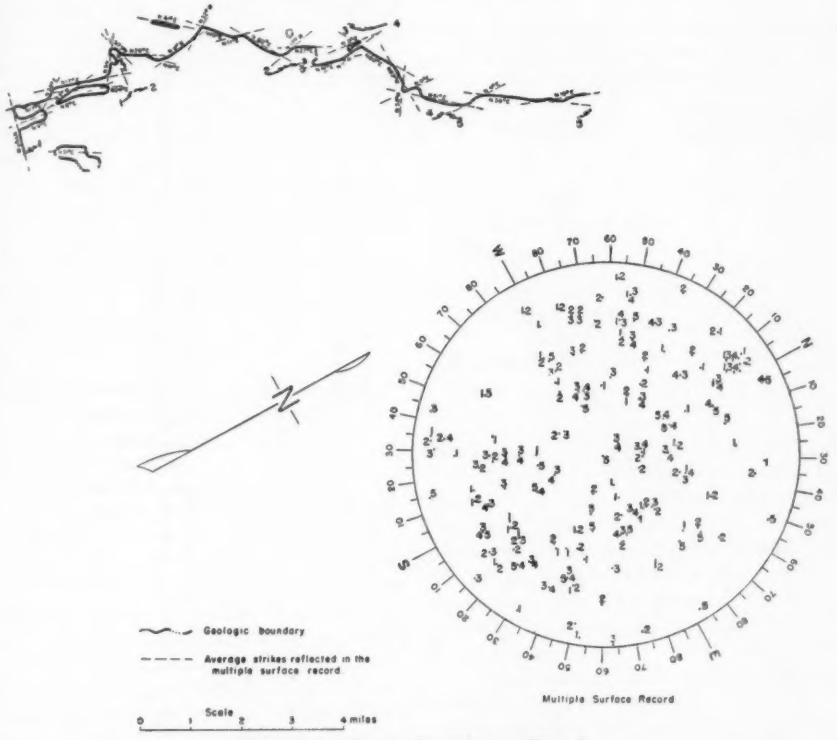
Geologic boundary
Average strikes reflected in the multiple surface record
Scale
0 1 2 3 4 miles
Multiple Surface Record

FIGURE 4.—MAP OF STRUCTURAL UNIT 2

Average strike lines are superposed over the border linears. The numbered segments mark the zones from which the multiple-surface record was collected.

Southern Orange County (Fig. 3). The Triassic-crystalline contact in this area is marked by a subrounded pebble and boulder conglomerate which rests upon the crystallines. The conglomerate seems to have been deposited in response to a change in gradient of the streams entering the Durham Basin from the west during Triassic time. The finer-grained sediments to the east reflect what Cotton (1941) has described as lens and pocket stratification on basin plains. Two post-sedimentation rotational faults in the central part of the unit

Structural unit 2 extending northward across Orange County to the sill in the vicinity of Durham (Fig. 4) comprises a series of post-sedimentation normal faults which mark the contact between the sediments and crystallines. Several small horsts of slate and granite surrounded by Triassic sandstone lie east of the border faults. Two grabens also show Triassic sandstone center blocks lying as isolated units in the slates west of the main border faults. The sandy textures and rarity of coarse components suggest very strongly that sediments

FIGURE 5.—MAP OF STRUCTURAL UNIT 3

Average strike lines are superposed over the border linears. The numbered segments mark the zones from which the multiple-surface record was collected.

in this unit represent a segment of the lens and pocket depositional facies which has been lowered into its present position. The implication is also that any coarser conglomeratic facies must have been eroded from the footwall blocks west of the present border faults.

Structural unit 3 extends northeastward across Durham and Granville counties to the intersection of the western border of the Durham Basin with the Jonesboro fault which marks the eastern border (Fig. 5). The Triassic-crystalline contact in an unconformity with a pebbly conglomeratic facies resting on the eroded slates and granites. At the extreme northern end of the basin the rounded pebbles give way to a coarse red fanglomerate. The massive nature of the conglomerates and their lack of regular bedding leads to the irregular-shaped outcrop areas of the thick sills which occur in this unit.

Possible Reflections of the Border Structure in the Multiple-Surface Record

Table 1 records coincidence between the strikes of border linears and the multiple-surface record. The linears of structural units 1 and 3 are primarily composed of lines of unconformity. The percentages of coincidence for these two units are appreciably lower than for unit 2 where the linears are due to post-sedimentation faulting. These figures agree with a hypothesis linking the multiple-surface record with both pre-sedimentation and post-sedimentation faulting. The lower values might be construed to reflect the effect of erosion on the fault scarps before burial.

The data at best suggests a genetic relationship among the linears, the multiple-surface record, and the geological history of the area.

Use of the Multiple-Surface Record in the Analysis of Rotational Faults

The two post-sedimentation rotational faults in the central part of structural unit 1 are quantitatively indeterminate on the basis of normal field evidence. The down-faulted sediments are irregularly cross-bedded, and exposures of the fault planes were poor. The multiple-surface records for these areas (Fig. 6) supplied the dips of the fault planes and the directions of movement on the planes. With this data and an estimate of the original slope of the floor of deposition the problems were solved. A slope of 8°E. was selected as representing the probable magnitude, based on evidence from a deep water well in Durham and from local slopes which may stand under the present conditions of weathering and erosion. The results indicate that Triassic sediments have been displaced downward at least 1800 feet at the eastern crystalline prominence of the southern fault and 1300 feet at the eastern crystalline prominence on the northern fault. These figures are equally valid as minimum estimates of the amount of erosion in this part of the Piedmont since faulting.

Table 1.—Percentage of Coincidence bewteen the Strikes of the Border Linears and the Multiple-Surface Record

Structural Unit	Tolerance within 1° on either side	Tolerance within 3° on either side
ONE Linears largely lines of unconformity	63	73
TWO Linears largely lines of post-sedimentation faulting	74	100
THREE Linears largely lines of unconformity	41	67

A number of factors of error could affect the data and the results. These have been examined rather carefully for the larger fault and their effects calculated. If the estimate of the deposition slope is too small the throw would be increased. A slope of 13° would give a calculated throw of 3200 feet. The conservative figure is believed to be more accurate. If the minimum slope set by the deep well is used the throw would be only 1000 feet. This figure is believed to be too small on the basis of the original cover necessary for the thick sills which have been intruded into the rocks of unit three. Errors of as much as 19° in the dip of the fault plane would change the throw by only about 100 feet. If the isolated crystalline mass shown in Plate 1 and Figure 4 is included

in the length of the fault, the throw would be increased to 2680 feet.

Reinemund (1949) calculated a throw of about 1500 feet for a similar fault striking in the same quadrant and only a few miles to the southwest. His determination was made on the basis of surface mapping and an extensive core-drilling program.

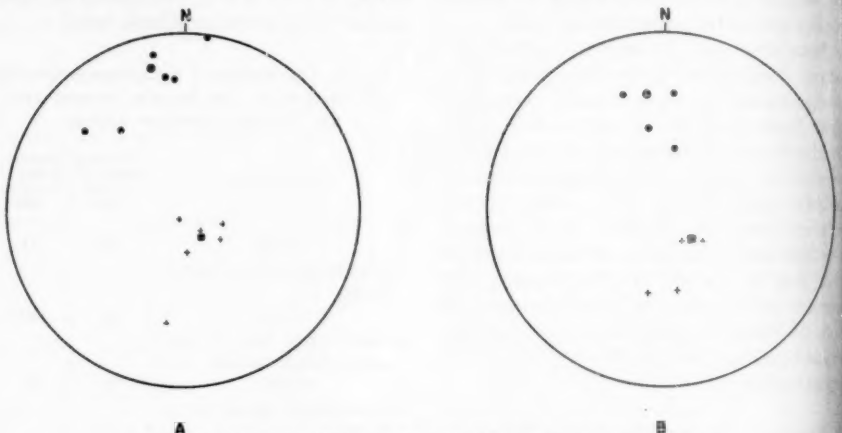

FIGURE 6.—MULTIPLE-SURFACE RECORD FOR THE ROTATIONAL FAULTS

P is the weighted position for the average pole. S is the weighted position for the average slickenside. Diagram A is the record for the Southern fault. Diagram B is the data for the Northern fault.

GEOMORPHOLOGY

The geomorphic, sedimentary, and structural histories of the basin are very closely integrated. The facies and post-sedimentation faults show that a westward extension of the basin existed before faulting. The question is whether this extension was great enough to include the Dan River Triassic Basin (Fig. 1) and support the well-known broad-warp hypothesis postulated for the Triassic Basins of Eastern North America. Wheeler summarizes this (1937). The fault analysis indicates that the basin need have been no more than 2½ miles wider than at present to accommodate the eroded sediments. The conglomeratic border facies seems to have been deposited in response to gradient change where sediment-laden streams entered the basin. The materials are apparently of a local origin and show no evidence of having been deposited in an extremely large basin and from a far distant source. The only mineral observed in the fill which is not represented in abundance among the western crystallines is a rather coarse-grained muscovite. Presumably the source of this material was a micaceous granite or schist in the portion of the Piedmont now completely eroded.

A chronological history may well begin with the normal faulting responsible for the development of the basin in Triassic time. Deposition accompanied and followed the faulting and erosion of the original fault surfaces. The result was a burial of fault scarps and perhaps the preservation of the general fault strikes as unconformity linears. Post-sedimentation normal faulting dropped finer clastics against the crystallines often depressing conglomeratic facies below the present erosion level. The erosional stripping of the basin was controlled by a slow degrading of the temporary base level imposed on eastward-flowing streams by the crystallines on the Atlantic side of the basin. One excellent example of superposition and examples of stream capture may be seen on the geologic map. The superposition is shown by the courses of the Haw River and Deep River as they cross alternate bands of easily eroded sediments and hard slates as they enter the main basin in structural unit 1. The segment of New Hope Creek which flows south-

ward along the west border scarp is believed to be an old tributary to the Haw River that worked headward during the etching of the basin to its present level. In this process it apparently tapped Morgan's Creek and the eastward-flowing segment of New Hope Creek in Orange County. Both of these streams show deep entrenched meanders in what is now the crystalline border scarp. This is certainly suggestive of their adjustment to an old age course following the eastward trend perhaps even into the Neuse River system before rejuvenation and capture.

A much later period of aggradation is marked by the deposition of the older alluvium. The present drainage systems were well established by this time. More recent uplift has permitted the entrenchment into these deposits so that they remain only as terraces.

Conclusions

(1) At least 1800 feet of Triassic sediments and a similar thickness of the Piedmont crystallines have been eroded since the time of rotational faulting.

(2) The Durham Basin probably never extended very far west of its present position.

(3) The technique of multiple-surface analysis developed by White offers a new tool for the solution of structural problems in the southeastern Piedmont where thick saprolite mantles and hides the rock. The value of the method has been partially shown by the application of multiple-surface data to the quantitative solution of faults and in the suggested interpretation of border lineations.

References Cited

Campbell, Marius R., and Kimball, Kent W. (1923) *The Deep River coal field of North Carolina*, N. C. Geol. Econ. Survey, Bull. 33.

Cooke, C. Wythe (1930) *Correlation of costal plain terraces*, Jour. Geol., vol. XXXVIII, p. 588.

Cotton, C. A. (1941) *Landscape*, Univ. Press, Cambridge, p. 179.

Emmons, Ebenezer (1856) *Geological report of the midland counties of North Carolina*, p. 227–254.

Goldston, E. F., and Stuckey, Jasper L. (1930) *The Jonesboro fault scarp west of Cary, North Carolina*, Elisha Mitchel Scientific Soc. Jour., vol. XLVI, no. 1, p. 67–68.

Holmes, Joseph Austin, and Kerr, Washington Caruthers (1887) *Geologic map of North Carolina*, N. C. Geol. Survey.

Prouty, Wm. F. (1931) *The Triassic deposits of the Durham Basin and their relation to the other Triassic areas of eastern United States*, Am. Jour. Sci., vol. XXI, p. 473–490.

Reinemund, John A. (1949) *Geology of the Deep River coal field, Chatham, Lee, and Moore counties, North Carolina*, U. S. Geol. Survey, Prelim. Map, Sheets 1, 2.

Russell, Israel C. (1892) *Correlation papers—the Newark system*, U. S. Geol. Survey, Bull. 85.

Stose, George W. (1946) *Geologic map of North America*, Geol. Soc. Am.

Wheeler, Girard (1937) *The west wall of the New England Triassic lowland*, Conn. State Geol. Nat. Hist. Survey, Bull. 58, p. 66–68.

White, Wm. A. (1948) *Molds of slickensides in saprolite* (Abstract), N. C. Acad. Sci., Elisha Mitchel Soc., Jour., vol. 46, No. 2.

——— (1950) *The Blue Ridge, a fault scarp*, Geol. Soc. Am., Bull., vol. 61, p. 1309–1346.

Southern Methodist University, Dallas, Texas

Manuscript Received by the Secretary of the Society, December 23, 1948

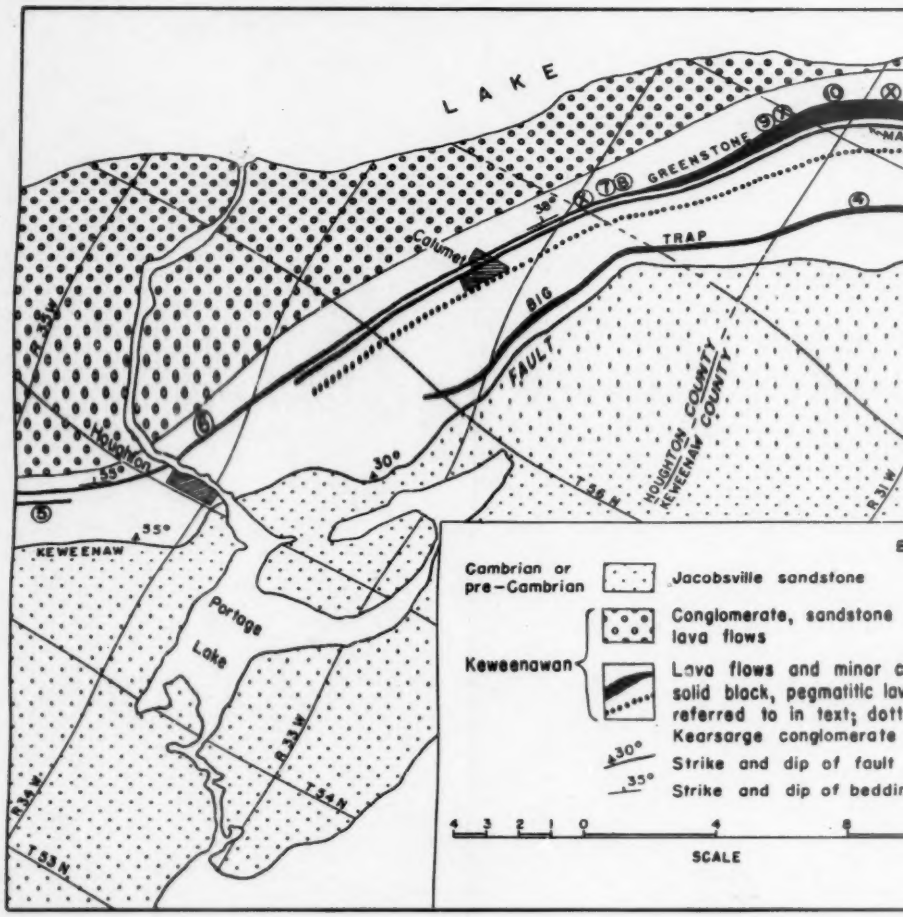

INDEX GEOLOGIC MAP OF SOME PEGMATITIC L

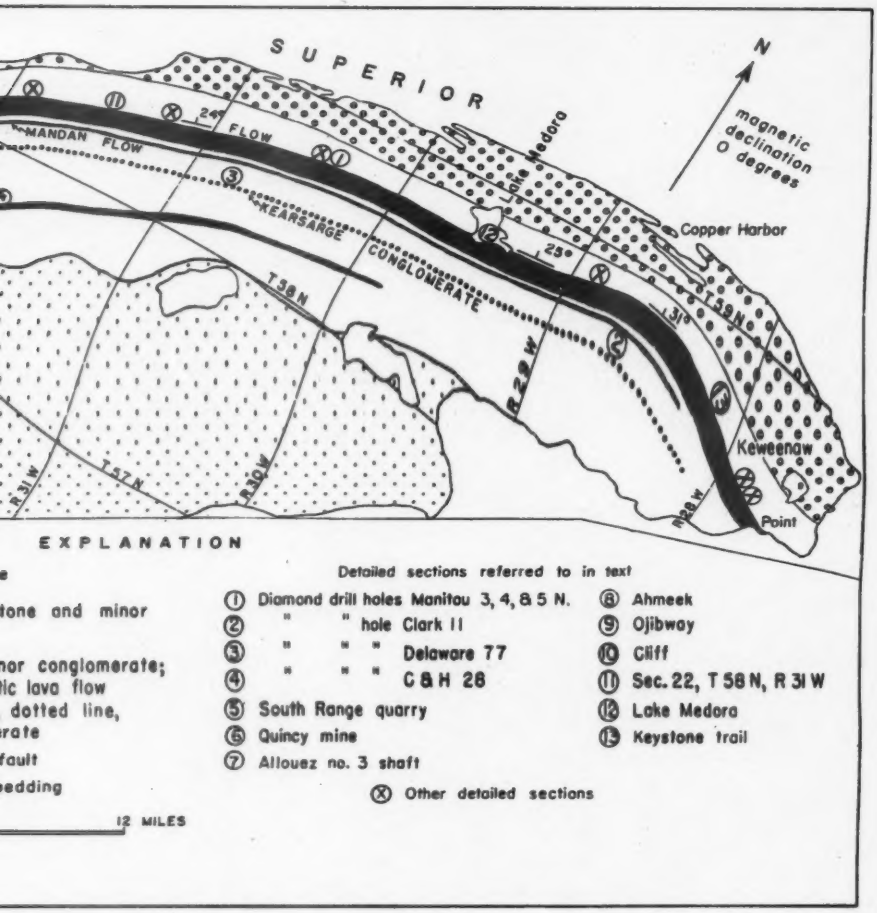

TIC LAVA FLOWS, MICHIGAN COPPER DISTRICT

BULLETIN OF THE GEOLOGICAL SOCIETY OF AMERICA
VOL. 62, PP. 159-202, 9 FIGS., 4 PLS. FEBRUARY 1951

DIFFERENTIATION IN LAVAS OF THE KEWEENAWAN SERIES AND THE ORIGIN OF THE COPPER DEPOSITS OF MICHIGAN

By HENRY R. CORNWALL

ABSTRACT

Five lava flows in the Keweenawan series of the Michigan copper district have been studied and chemical analyses made, with special attention to: (1) chemical and mineralogic variations within the upper, pegmatitic portions of the flows; (2) processes of differentiation; (3) comparison of the types of rocks found within a single flow with the types of flows that make up the lava series; (4) the relation of differentiation in the flows to the origin of the copper deposits.

The primary factors in the differentiation of the flows were probably: (1) cooling at a moderate rate, and predominantly from the top; (2) crystal sorting by differential settling; (3) migration and local concentration of volatiles; (4) periodic convective overturn of the magma. Convection currents probably were not active in the thinner flows and may not have been in the thicker. Alternate hypotheses have been presented, one assuming that convective overturn was important, the other that it was not.

All types of flows in the series can be approximated by differentiation products of the Greenstone flow, indicating that all the flows could have been differentiated from a magma similar to, but perhaps slightly more mafic than, that of the Greenstone flow.

In considering the origin of the copper deposits, the writer has briefly reviewed the literature and presented new evidence. The following modes or origin of the deposits appear still open to consideration: (1) The deposits are epigenetic, and formed by deposition from hot solutions ascending from an underlying intrusive. (2) The deposits are the result of a combination of syngenetic and epigenetic processes. Primary concentrations of copper in fumaroles, thermal springs, or playa lakes were reworked by later, ascending igneous emanations. (3) The amygdaloidal deposits are primarily syngenetic and have been only moderately modified by the action of later ascending solutions.

CONTENTS

	Page
Introduction	160
General geology	160
Classification of lavas	160
Purpose of investigation	161
Field and laboratory work	161
Previous work	162
Acknowledgments	162
Characteristic features of flows with pegmatitic segregations	162
Introduction	162
Ophitic basalt	162
Pegmatitic facies	163
Amygdaloid	163
Aplite dikes	163
Individual flows studied	164
Greenstone flow	164
General description	164
Settled blocks	164
Banded ophitic basalt	165
Planar structure of pegmatitic facies	166
Chalcocite mineralization of the amygdaloid	166
Mandan flow	167
Flow above Kearsarge conglomerate	168
Flow at South Range quarry	168
"Big" trap	168
Discussion of modes	169
General statement	169
Plagioclase	169
Pyroxene	171
Olivine	172
Ilmenite and magnetite	175
Minor constituents	175
Amygdaloids	177
Discussion of chemical analyses	177
Greenstone flow	177
Introduction	177
Distribution of elements	177
Magnesia—iron oxide ratio	178
Aplite	179
Norms	179
High olivine layers	180
"Big" trap	186
Differentiation	187
Basic facts	187
Process of differentiation	190
Summary	192
Differentiation at depth	193
Variation in lava series as a whole	193
General trends in the distribution of elements	196
Comparison with greenstone differentiates	196
Origin of the copper deposits	196
Hypotheses	196
Conclusions	199
References cited	200

ILLUSTRATIONS

Figure		Page
1.	Section across the Greenstone flow near the Allouez No. 3 shaft mine	164
2.	Section across the Greenstone flow at Cliff	164
3.	Modal variation in the Greenstone flow at Delaware	170
4.	Modal variation in the Mandan flow	171
5.	Modal variation in a pegmatitic flow above the Kearsarge conglomerate	172
6.	Modal variation in the "Big" trap	173
7.	Variation in the Greenstone flow of combined water, copper, sulphur, and the ratio of MgO to total Fe calculated as FeO	183
8.	Variation of norms in the Greenstone flow	184
9.	Variation of norms in the "Big" trap	187

Plate		Facing page
1.	Index geologic map of some pegmatitic lava flows of the Keweenawan series, Michigan copper district	159
2.	Ophitic basalt	166
3.	Pegmatitic facies	167
4.	Geologic map and section of a pegmatitic lava flow at South Range Quarry, Houghton County, Michigan	202

INTRODUCTION

General Geology

The writer has made a detailed petrologic and chemical study of five lava flows of the Keweenawan series that crop out on the Keweenaw Peninsula of upper Michigan in Houghton and Keweenaw counties (Pl. 1).

The native copper deposits of the Michigan copper district occur in basaltic lavas and interbedded felsitic conglomerates of the Keweenawan series that underlie the Keweenaw Peninsula of upper Michigan. The flows and sedimentary rocks dip northward, forming the southern flank of a large structural basin that is occupied by Lake Superior. These Keweenawan rocks are bounded on the south by a prominent, northward-dipping thrust fault. In the Michigan copper district, this fault, known as the Keweenaw fault, separates the Keweenawan series from the younger Jacobsville sandstone of Cambrian or Precambrian age.

The copper deposits and the flows studied by the writer occur in a part of the Keeweenawan series that is composed predominantly of lava flows. This part ranges in thickness from about 8000 feet at the west end of the district to 15,000 feet at the east end. It is overlain to the north by a series of conglomerates and sandstones with minor interbedded lavas and is bounded on the south by the Keweenaw fault.

Classification of Lavas

The bulk of the flows in the Keweenawan series of the Michigan copper district are basalts and basaltic andesites. Other types range from olivine-rich basalt through sodic andesite to rhyolite. A megascopic textural classification of the lavas and their differentiates, widely used in the district, gives a fair indication of the variation in chemical composition. Textural terms used to describe flows or parts of flows are: ophite, porphyrite, glomeroporphyrite, melaphyre, felsite, and dolerite (Lane, 1909; Butler, Burbank, *et al.*, 1929; Broderick, 1935).

Ophite. Crystals of pyroxene inclosing unoriented, euhedral plagioclase laths produce a mottled effect distinguishable on freshly broken surfaces, especially those of drill cores, and accentuated by weathering (Pl. 2). Ophitic texture is best developed in the more mafic flows.

Porphyrites and glomeroporphyrites contain phenocrysts of plagioclase which tend to clot together in the glomeroporphyrites.

Flows that are fine-grained throughout and have no distinctive texture are called *melaphyres.*

The *felsites* are reddish, fine-grained, equigranular or porphyritic rhyolitic rocks. Few small flows and intrusives have been seen, but felsite is the most prominent constituent in interbedded conglomerates.

In some of the thicker ophites and a few of the thicker porphyrites and glomeroporphyrites including the five flows described in this paper, the upper parts contain layers, lenses, or irregular masses in which the minerals, especially the plagioclases, are coarser-grained than in the surrounding rock, and are more or less intensely altered to albite, prehnite, chlorite, epidote, and pumpellyite. This altered rock is commonly amygdaloidal. These layers, lenses, and spots of altered, amygdaloidal, coarse-

grained rock have been called *"dolerites"* by previous workers. The term is confusing because "dolerite" is widely used in a different sense. W. Q. Kennedy (1933) uses the term "pegmatitoides", but this term is cumbersome and perhaps unfamiliar. The noun "pegmatitic facies" and the adjective "pegmatitic" will be used here.

Under the writer's classification (Table 1) the ophites are predominantly basalts, whereas the porphyrites, glomeroporphyrites, and melaphyres are predominantly basaltic andesites. The pegmatitic rocks have the composition of "albite diabase".

To correlate the textural terms of the Michigan copper district with the more common mineralogical terms, the writer proposes to use the mineralogical name with a textural adjective modifier wherever possible. For example an ophite with the composition of basalt will be called "ophitic basalt", or a glomeroporphyrite with the composition of andesite will be called "glomeroporphyritic andesite."

Purpose of Investigation

The purpose of this study was to get new, more-detailed information on the differentiation of the flows, and to determine, if possible, the relation of this differentiation to the occurrence of copper. Particular attention was paid to the pegmatitic portions of the flows studied, and differentiation trends in the successive pegmatitic layers within single flows were carefully investigated.

Field and Laboratory Work

The studies of three of the flows containing pegmatitic zones were based entirely on samples and specimens of diamond-drill core from holes that completely crossed each flow. These flows are the "Big" trap, an ophitic basalt immediately above the Kearsarge conglomerate, and the Mandan flow (Pl. 1).

A fourth flow, the Greenstone flow, was mapped during the summer of 1944, and suites of specimens were collected at a number of points throughout its thicker portion from Allouez (Pl. 1, loc. 7) east to the end of Keweenaw Point, a distance of 35 miles. It was also studied and sampled in a crosscut in the Quincy mine, 14 miles southwest of Allouez. A series of three diamond-drill holes cut the Greenstone at Delaware, where it is 1300 feet thick. T. M. Broderick (1935) sampled the core from these holes for his study of its differentiation, and the writer also logged and sampled the cores.

TABLE 1.—TEXTURAL CLASSIFICATION USED IN THE MICHIGAN COPPER DISTRICT

Following the quantitative mineralogical classification of A. Johannsen (1939).

Textural classification	Mineralogical classification
ophite	basalt*
	andesite
glomeroporphyrite	basalt
	andesite*
	dacite
porphyrite	basalt
	andesite*
	dacite
melaphyre	basalt
	andesite*
	dacite
	rhyodacite
felsite	rhyolite
aplite differentiate of doleritic ophite	granodiorite aplite
dolerite (pegmatitic facies of basalt)	albite diabase

*Predominant rock type of textural type. For example, ophites are predominantly basalts.

A fifth flow studied, an ophitic basalt at the South Range quarry, was sampled and mapped in detail. This flow is completely exposed on three faces cut in a glaciated hill, and approximately 50 per cent of the intervening hill top is exposed.

In the course of this study 222 thin sections were studied, and 125 modal analyses and 13 chemical analyses were made. In sampling for the chemical analyses of the pegmatitic layers in the Greenstone flow, half of the core length was split and the whole split was used; for the

"Big" trap the entire core of the pegmatitic layer was split and the whole split used.

Previous Work

Petrologic and petrographic studies of the lavas of the Michigan copper district have been made by Pumpelly (1873), Marvine (1873), Irving (1883), Hubbard (1898), Lane (1909), Butler, Burbank *et al.* (1929), and others. More recently T. M. Broderick (1935) studied the differentiation of single flows and discussed possible differentiation within the magma chamber, using detailed geochemical data for the first time. Using Broderick's samples and data, E. B. Sandell and S. S. Goldich (1943) have studied the distribution of rarer metallic constituents.

Acknowledgments

The writer is grateful to Dr. T. M. Broderick, Chief Geologist of the Calumet and Hecla Consolidated Copper Company, for encouraging the study, and for his valued suggestions and criticisms. Thanks are due also to Mr. E. R. Lovell, President of the Calumet and Hecla Consolidated Copper Company, for permission to study and sample diamond-drill core belonging to that company.

Drs. A. F. Buddington and H. H. Hess gave freely of their time and experience in discussing the problems involved in this study. The cost of chemical analyses and some of the thin sections were financed by a grant from Princeton University. The writer is likewise indebted to the U. S. Geological Survey for permission to use this petrologic study as a thesis for a doctorate at Princeton University. The work was carried out for the Survey as part of its program in the Michigan copper district. The writer appreciates the helpful criticism of Drs. R. S. Cannon, Jr., G. H. Espenshade, W. S. White, and other members of the Geological Survey.

Characteristic Features of Flows With Pegmatitic Segregations

Introduction

Flows with pegmatitic segregations make up only a small proportion of the total thickness of Keweenawan lavas, but they are found in all parts of the stratigraphic column. They reveal a more advanced stage of differentiation than the more common flows without pegmatitic segregations and therefore provide more evidence concerning the nature of the differentiation processes.

The five flows studied in detail by the writer may be fairly taken as representing this type of flow.

The flows with pegmatitic segregations have three distinct layers or zones. The lower half of each flow is ophitic basalt, here referred to as the "ophitic basalt zone". Above this zone and extending nearly to the top is the "pegmatitic zone", an alternation of layers of pegmatitic rock with layers of ophitic basalt. The rock in the uppermost 3 to 25 feet of each flow, above the pegmatitic zone, is amygdaloidal as in all types of Keweenawan lava flows, and this rock is called "amygdaloid". Two of the flows studied have scattered small concordant or discordant aplite dikes.

Ophitic Basalt

Ophitic basalt is the sole constituent of the ophitic basalt zone and the major constituent of the pegmatitic zone. Principal minerals in a typical flow are labradorite (An_{45-75}), augite, and moderate amounts of olivine. In addition to augite, certain flows contain small amounts of hypersthene and pigeonite. Common accessory minerals are ilmenite, magnetite, hematite, and chlorite. Ophitic basalt is dark green or gray (For photographs and photomicrographs of typical specimens see Butler, Burbank *et al.*, 1929, p. 36, Pls. 56, 57).

The pyroxene is generally fresh but locally slightly altered to chlorite and hematite. Plagioclase is slightly to moderately chloritized. Olivine is nearly completely altered to chlorite, serpentine (variety bowlingite), iddingsite, magnetite, and hematite.

Optical data indicate that the plagioclase is more calcic (Tables 7–12) in the ophitic basalt zone than in the ophitic basalt of the overlying pegmatitic zone. The n_β index of augite is quite uniform in all the flows studied, ranging from 1.691 to 1.704. Fresh olivine was found only in the Greenstone flow where its n_β index ranges from 1.727 at a point 150 feet above the base

of the flow to 1.741 at a point just above the middle of the flow. This represents a change of composition from $Fo_{64}Fa_{36}$ near the base to $Fo_{35}Fa_{65}$ near the middle of the flow.

In all the flows, the grain size of the ophitic basalt is coarsest near the center of the flow and decreases both upward and downward. The largest ophitic pyroxene crystals range from 50 mm. across in the thickest flow to 10 mm. in the thinner flows. In several of the flows, the ophitic basalt contains scattered plagioclase phenocrysts. The phenocrysts are commonly about 2 mm. long by 0.75 mm. wide, but in the Greenstone flow the largest phenocrysts are 15 mm. long.

Pegmatitic Facies

Pegmatitic facies interlayered with ophitic basalt characterize the pegmatitic zone of a typical flow. The pegmatitic material occurs in layers or lenses that range from 1 inch to over 50 feet thick and are oriented parallel to the plane of the flow. A flow normally contains 6 to 15 pegmatitic layers, and the total amount of pegmatitic material is 10 to 20 per cent of the pegmatitic zone.

The pegmatitic facies is notably coarser-grained than the ophitic basalt with which it occurs, and the texture is not ophitic (Butler, Burbank, *et al.*, 1929, p. 36, Pl. 56). The predominant mineral is albite-oligoclase (An_{8-18}) which occurs in euhedral laths with average lengths of 1 to 4 mm. and gives the rock a white or pinkish color. The interstices between the plagioclase laths are filled by augite, ilmenite, magnetite, chlorite, and apatite. Scattered vesicles throughout the rock are filled with epidote, quartz, prehnite, calcite, pumpellyite, and native copper. The pyroxene is slightly to moderately altered to chlorite, epidote, and hornblende. The plagioclase is moderately to intensely altered to prehnite, chlorite, pumpellyite, epidote, sericite, and kaolinite.

Amygdaloid

At the top of each flow is a zone, 3 to 25 feet thick, of fine-grained amygdaloidal andesite (Butler, Burbank, *et al.*, 1929, p. 36, Pls. 58, 59, 60, 61). The abundant 1- to 10-mm. vesicles are filled with chlorite, calcite, prehnite, quartz, epidote, pumpellyite, laumontite, and analcime. The andesite consists of 1- to 2-mm. glomeroporphyritic clots of albite-oligoclase laths and scattered 1-mm. altered olivine crystals in a groundmass of either microcrystalline augite and plagioclase or reddish, semiopaque material. The albite-oligoclase laths are commonly fresh, but the groundmass is moderately to intensely altered to hematite, chlorite, epidote, pumpellyite, quartz, and prehnite. The amygdaloids are reddened by the presence of abundant hematite.

Aplite Dikes

Fine-grained aplite dikes, granophyric differentiates of the flows in which they occur, have been found in the pegmatitic zones of the "Big" trap and Greenstone flows. The dikes, ranging from 1 inch to 1½ feet thick, can be separated into two groups, called for convenience the "silicic" and the "chloritic" types (analyses G-26 and 26-g4, respectively, of Table 8).

The silicic aplite is a reddish, fine-grained, granular rock that consists of oligoclase (An_{12}) phenocrysts 0.5–2 mm. long and 0.2–0.5 mm. wide in a matrix of quartz and semiopaque material (probably mostly kaolinite) with lesser amounts of augite, ilmenite, magnetite, apatite, chlorite, pumpellyite, epidote, zoisite, and calcite. The plagioclase is partly replaced by quartz, especially along cleavage cracks. It is also altered to kaolinite, sericite, chlorite, pumpellyite, epidote, and prehnite. The silicic aplite is locally altered to a dense, dark-green aggregate of pumpellyite, chlorite, epidote, and quartz. In some of the dikes, a planar structure is caused by a parallelism of the plagioclase laths in the plane of the dike.

Derivation of the silicic aplite from the enclosing flow is widely evident. The aplite occurs interstitially between the crystals, as larger irregular segregations in the pegmatitic layers and as dikes indiscriminately crossing pegmatitic and ophitic layers; there is complete gradation between these various types.

The chloritic aplite is almost black, fine-grained, and contains numerous oligoclase (An_{14}) phenocrysts, 0.2 to 1.5 mm by 0.1 to 0.7 mm, in a matrix of oligoclase fragments and chlorite. The matrix also contains some augite, ilmenite, magnetite, and zoisite.

Individual Flows Studied

Greenstone Flow

General description.—The Greenstone flow is an ophitic, slightly porphyritic basalt extending 55 miles from a point southwest of Houghton, Michigan, to the end of Keweenaw Point (Pl. 1). It is only 35 feet thick near Houghton but increases eastward to about 250 feet at Allouez. Northeast of Ahmeek, it increases abruptly, reaching 1400 feet at Cliff. From Cliff to the end of the Point, thickness ranges from 1150 to 1400 feet.

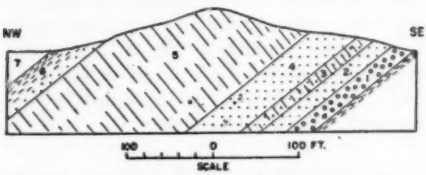

Figure 1.—Section Across the Greenstone Flow near the Allouez No. 3 Shaft Mine NE ¼ of section 31, T.57N, R32W

1. Allouez conglomerate
2–6. Greenstone flow
2. Fine- to medium-grained, banded, ophitic basalt
3. Medium-grained, ophitic basalt with rough, columnar jointing
4. Medium- to fine-grained ophitic basalt
5. Fine-grained basalt with pronounced columnar jointing
6. Fine-grained, ophitic basalt, overlain by cellular amygdaloid
7. Glomeroporphyritic andesite, Pewabic flow

Southwest of Ahmeek, the Greenstone flow consists of ophitic basalt and columnar basalt topped by cellular amygdaloid. In the 51st-level crosscut at the Quincy mine the flow is 55 feet thick and ophitic. The flow contains amygdaloidal inclusions and streaks, the latter nearly parallel to the plane of the flow, and there is a thin amygdaloid at the top. The cross section near the Allouez No. 3 shaft mine (Fig. 1) is probably typical of the thinner part of the Greenstone. The middle part of the flow (zone 5 in the cross section) is fine-grained, columnar, nonophitic basalt; the upper and lower parts (especially the lower) are coarser-grained and ophitic.

The section across the Greenstone flow near Cliff (Fig. 2) and the log of the flow at Delaware (Table 2) are typical of its thicker part. A pegmatitic zone is present in the upper half of the flow from Ojibway (Pl. 1, loc. 9) east to the end of Keweenaw Point, a distance of approximately 30 miles. Between the pegmatitic zone and the amygdaloid at the top of the flow, there is a zone 150 to 200 feet thick that consists in part of fine-grained columnar basalt and in part of fine- to medium-grained ophitic basalt (Fig. 2; Table 2).

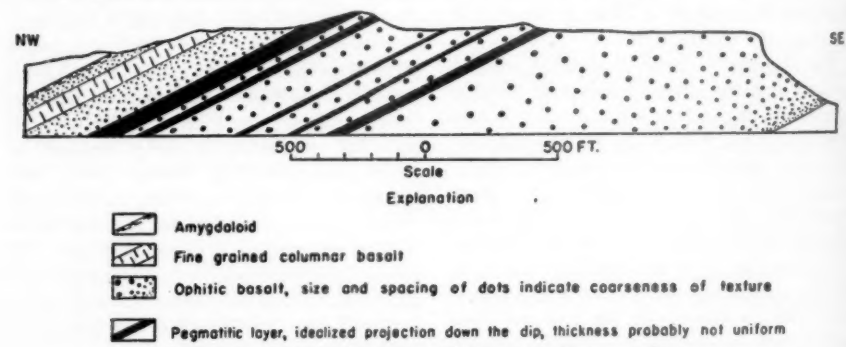

Figure 2.—Section Across the Greenstone Flow at Cliff
Typical of its thicker portion.

Aplitic dikes and interstitial segregations are quite common in the pegmatitic zone of the Greenstone flow, particularly in its upper part. Most of the dikes strike parallel to the flow but dip at right angles to the flow.

Settled blocks.—Irregular, angular blocks of medium-grained ophitic basalt in coarse-grained ophitic basalt (Pl. 2, fig. 4) were noted at locality 11 (Pl. 1), in a zone 25 feet thick, and 250 to 275 feet above the base of the flow at a

TABLE 2.—LOG OF THE GREENSTONE FLOW AT DELAWARE*

Depth (feet)†	
	Top of flow
0–½	Reddish amygdaloid containing abundant ash.
½–23	Amygdaloid in glomeroporphyritic andesite; vesicle fillings of chlorite, calcite, and prehnite.
25–52	Fine-grained andesite.
52–71	Ophitic basalt, 1-mm. augite crystals; contains disseminated pyrite gains.
71–176	Slightly porphyritic, fine-grained basalt.
176–201	Ophitic basalt, 1- to 4-mm. augite crystals; grain size increases downward.
201–202	Pegmatitic facies.
202–203	Ophitic basalt, 6-mm. augite crystals.
203–204	Pegmatitic facies.
204–207	Ophitic basalt, 6-mm. augite crystals.
207–208	Mixed ophitic basalt and pegmatitic facies.
208–841	Medium- to coarse-grained (augite crystals up to 30 mm. in diameter) ophitic basalt containing scattered pegmatitic patches and streaks, and thicker layers as follows:
	262–286 Coarse pegmatitic facies.
	343–347 Coarse pegmatitic facies.
	375–382 Coarse pegmatitic facies.
	419–426 Coarse pegmatitic facies.
	576–581 Coarse pegmatitic facies.
	647–675 Medium- to coarse-grained pegmatitic facies with well developed planar structure due to a preferred orientation of plagioclase laths with the long axes parallel to the base of the flow (and to the plane of the pegmatitic layer).
	681–688 Coarse pegmatitic facies.
841–1205	Ophitic basalt, 30- to 15-mm. augite crystals; grain size decreases downward.
1205–1245	Ophitic basalt, 15- to 8-mm. augite crystals; grain size decreases downward.
1245–1289	Ophitic basalt, 8- to 1-mm. augite crystals; grain size decreases downward.
1289–1299	Ophitic basalt, 1-mm. augite crystals; grades downward to fine-grained basalt at the basal contact, containing scattered minute vesicles filled in part by chlorite.
1299	Base of flow.

TABLE 2.—*Continued*

* Combined log of three overlapping diamond-drill holes, Manitou 3-3 N., 3-4 N., and 3-5 N.

† Stratigraphic depth measured perpendicular to the plane of the flow.

point where the flow is 1400 feet thick. The blocks, ranging in diameter from 1 to 10 feet, are apparently fragments that broke from the roof and sank toward the floor when the flow was partly solidified. Their texture correlates with that of rock near the base of the upper chill zone at a stratigraphic depth of about 200 feet and indicates that, by the time crystals had accumulated at the bottom of the flow to a depth of 250 to 275 feet, the top had frozen to a depth of 200 feet.

Banded ophitic basalt.—Banded ophitic basalt occurs in the lower part of the Greenstone flow at Allouez No. 3 shaft mine (Fig. 1) and for at least a mile to the southwest. The banding is somewhat similar to the primary banding observed by Peoples (1933) and Hess (1938) in the Stillwater Complex, by Grout (1918a) in the Duluth gabbro, and by Coats (1936) experimentally. The bands[1], which occur in a 20-foot zone at the base of the flow, are from less than 1 to 12 inches thick and are due to a gradation in the size of the ophitic pyroxene crystals (Pl. 2, figs. 1, 2, 3). Normally the crystals are largest at the bottom of each band and are successively smaller upward with a sharp contact at the top. Surrounding these ophitic pyroxene crystals are plagioclase laths, chlorite, and more pyroxene. Some of the plagioclase laths tend to be oriented parallel to the banding, and some to the peripheries of the ophitic crystals.

Some of the ophitic crystals have unoriented

[1] The word "layer" is preferable, but the author will use "band" to conform with the usage of the above-mentioned writers.

plagioclase in the core but parallel orientation on the borders, and in some of the smaller crystals the plagioclase laths are parallel to each other throughout. Those pyroxene crystals that contain poikilitically included plagioclase laths of parallel orientation probably formed after most of the crystals had settled into place.

The writer believes that the banded ophitic basalt in the Greenstone flow resulted from differential settling of various sizes of ophitic pyroxene crystals in a manner comparable to that which produces graded bedding in clastic sediments. Like the primary banding described by the authors just cited, it is a phenomenon of crystal sorting by gravity. However, the bands formed because of size sorting, whereas all these authors have described density sorting.

Planar structure of pegmatitic facies.—In practically every section studied across the Greenstone flow along a strike length of 30 miles, the lowermost pegmatitic layers have a strongly developed planar orientation of plagioclase laths. These lowermost layers range from less than 1 to as much as 20 feet thick. The rock is finer-grained than the average. The planar structure is parallel to the plane of the layer and of the flow. No linear parallelism of the plagioclase laths has been observed. The scattered plagioclase phenocrysts in the overlying pegmatitic layers show a slight tendency to be oriented parallel to the layers.

Chalcocite mineralization of the amygdaloid.—Near the center of the NW¼ sec. 36, T. 58 N., R. 32 W. (loc. 10, Pl. 1), the amygdaloid of the Greenstone flow is mineralized for at least 1000 feet along the strike with chalcocite and hematite (variety specularite). The southwestern end of the zone known to be mineralized is approximately 0.4 mile north of the Cliff No. 4 shaft. This deposit, on the property of the Cliff Mining Company now controlled by the Calumet and Hecla Consolidated Copper Company, was discovered by the U. S. Geological Survey party studying the Michigan copper deposits in the summer of 1944. Several trenches were later dug across the mineralized amygdaloid by Calumet and Hecla (Table 3).

In the chalcocite-mineralized area, the 1- to 5-mm. vesicles of the Greenstone amygdaloid are lined with chlorite, and the remaining space is filled with prehnite in radiating clusters, calcite, analcime, chalcocite, and specular hematite. The fine-grained andesite is ophitic, and the principle constituents are augite and albite-oligoclase (An_{10}). Interstitial earthy hematite is abundant.

Chalcocite and specular hematite are for the most part confined to the bottom 5 feet of the 15- to 20-foot amygdaloid. The chalcocite and specular hematite occur as fillings of vesicles 1–5 mm. in diameter, as seams as much as 0.2 mm. wide, and as tiny (0.02 mm.) disseminated grains. The specular hematite occurs in minute plates 0.2 to 1.5 mm. long and 0.02 to 0.2 mm. thick. The space between the plates is commonly filled by chalcocite and small amounts covellite. In addition to the chalcocite, which is orthorhombic, there is a little isometric bluish digenite. Some of the chalcocite has one fairly well developed cleavage. The chalcocite is slightly replaced by covellite, and quite extensively altered to malachite. Small specks of chalcopyrite have been seen in the hand specimens. The basalt below the amygdaloid contains disseminated chalcopyrite and pyrite.

The chemical analyses of Broderick (1935) and the present writer (Fig. 7) indicate that the sulfur in the Greenstone flow is primary and increases directly with the other more volatile constituents. The fine-grained basalt of the upper chill zone, below the amygdaloid and above the pegmatitic zone, contains 0.082 per cent sulfur as compared with Broderick's weighted

PLATE 2.—OPHITIC BASALT

FIGURE 1. BANDED OPHITIC BASALT NEAR THE BASE OF THE GREENSTONE FLOW AT ALLOUEZ NO. 3 SHAFT

FIGURE 2. CLOSE-UP OF LOWER LAYER OF BANDED OPHITIC BASALT IN FIGURE 1
Showing graded layering due to size-sorting of the ophitic pyroxene crystals.

FIGURE 3. IRREGULAR BANDING IN THE OPHITIC BASALT OF THE GREENSTONE FLOW AT ALLOUEZ NO. 3 SHAFT

FIGURE 4. BLOCK OF MEDIUM-GRAINED OPHITIC BASALT, BEHIND HAMMER, WITH COARSER OPHITIC BASALT ABOVE AND BELOW
Greenstone flow (Pl. 1, loc. 11)

FIGURE 1

FIGURE 2

FIGURE 3

FIGURE 4

OPHITIC BASALT

FIGURE 2

FIGURE 4

FIGURE 1

FIGURE 3

PEGMATITIC FACIES

average of 0.023 per cent for the whole flow. Furthermore, basalt in drill core from a depth of 52 to 71 feet below the top contains megascopically visible disseminated grains of pyrite. It seems reasonable to conclude that the pyrite in the upper chill zone at Delaware and Cliff and the chalcocite in the amygdaloid at Cliff were deposited by emanations from the interior of the flow during solidification. Supporting this interpretation, the chalcocite-mineralized area at Cliff coincides with the occurrence in the pegmatitic zone of more deuterically altered rock, aplite, and coarse amygdaloidal pegmatitic material than was noted elsewhere.

Table 3.—Assays of Greenstone Amygdoloid*

Sample	Copper (per cent)
Trench No. 1	
203	0.532
204	2.574
207	1.389
Trench No. 2	
201	0.479
202	1.508
205	0.268
206	0.275

Samples 202 and 204 combined contained 0.006 oz. of gold and 0.82 oz. of silver per ton.

No. 203 Three vertical channels, each about 3½ feet long, across the best part of the mineralized amygdaloid.
204 Selected chips of mineralized rock.
207 Sludge from an 8-inch hole drilled in the floor of the trench.
201 A 10-foot channel along the floor of the trench across the mineralized zone in the amygdaloid.
202 Selected chips of mineralized rock.
205 Two 4-foot channels, 6 feet apart, across the mineralized zone at the base of the amygdaloid.
206 Random chips from the floor of the trench.

* Samples collected and analyzed by the Calumet and Hecla Consolidated Copper Company. Trench No. 1 is located near the southwestern end of the outcrop of mineralized amygdaloid. Trench No. 2 is located 900 feet to the northeast of No. 1. Both trenches cut the amygdaloid at right angles to its strike.

Mandan Flow

The Mandan flow is an ophitic, slightly porphyritic basalt. It has been intersected by underground workings and diamond-drill holes at a number of points between Boston (3 miles northeast of Pl. 1, loc. 6) and Copper Harbor, a distance of 40 miles. Some copper mining has been done on the amygdaloid at Mandan (2 miles west of Lake Medora) where the flow is thickest.

The Mandan flow occurs about 300 feet stratigraphically below the Greenstone flow. It is a typical ophitic basalt with pegmatitic layers in its upper parts (Table 4). It contains scattered plagioclase phenocrysts. Along the strike, the thickness of the flow ranges from a few feet to 400 feet. Locally the variation in thickness is abrupt and may be due to original differences in the thickness of the lava at the periphery of the flow.

Modal analyses (Table 9) were made of samples from diamond-drill hole Clark 11 (Pl. 1, loc. 2) 3 miles south of Copper Harbor. The Mandan flow is 224 feet thick where intersected by this drill hole.

Plate 3.—PEGMATITIC FACIES

Figure 1. Pegmatitic Layer near the Base of the Pegmatitic Zone in Flow at South Range Quarry
Note the straight, even contacts

Figure 2. Pegmatitic Layer near the Base of the Pegmatitic Zone in Flow at South Range Quarry
Note the straight, even contacts and the amygdaloidal character of the pegmatitic facies.

Figure 3. A 1- to 2-Inch Pegmatitic Layer in the Upper Part of the Pegmatitic Zone in the Flow at South Range Quarry
Note flattened amygdules along top of layer, and cross-cutting pegmatitic stringer extending downward near head of hammer.

Figure 4. Partly Coalescing Amygdules of Prehnite and Quartz in One- to Two-Millimeter Ophitic Basalt at Top of the Pegmatitic Zone, Flow at South Range Quarry

Flow above the Kearsarge Conglomerate

An ophitic, glomeroporphyritic basalt flow immediately overlies the Kearsarge conglomerate, 2300 feet stratigraphically below the Greenstone flow where sampled. This flow is part of a series, several hundred feet thick, of ophitic, glomeroporphyritic, pegmatitic basalts that overlie the Kearsarge conglomerate.

TABLE 4.—PEGMATITIC LAYERS IN THE MANDAN FLOW

Depth (feet)	Thickness of pegmatitic layer (inches)
70	1.4 contains a little fine copper
71	0.3
100	3.5 contains a little copper
104	25.0
107	8.5
113	12.7 only moderately pegmatitic
114	1.3 " " "
118	4.2 " " "
121	0.3
Base of flow at 224 feet.	

The writer collected a series of samples of the lowermost flow from the core of diamond-drill hole Delaware 77 (Pl. 1, loc. 3). The flow is 146 feet thick, a typical ophitic basalt, and contains 16 pegmatitic layers, streaks, or spots at depths of 19 to 119 feet below the top (Table 5).

Flow at South Range Quarry

A basalt flow with pegmatitic and ophitic facies is completely exposed on three faces of a quarry 4 miles southwest of Houghton (Pl. 1, loc. 5). The flow is 130 feet thick; it is underlain by a fine-grained basalt flow and overlain by an ophitic basalt flow. This flow occurs stratigraphically about 2100 feet below the Greenstone flow and has been studied and mapped in detail (Pl. 4). Specimens were collected from two complete sections of the flow, and a number of thin sections prepared.

The orderly arrangement of the pegmatitic layers in the flow at South Range quarry is striking (Pl. 4). The thickest (2–4 feet thick), best-developed pegmatitic layer (Pl. 3, figs. 1, 2) occurs near the middle of the flow at the base of the pegmatitic zone. Upward the pegmatitic layers thin from 2 feet to less than 1 inch, are successively more closely spaced, and are increasingly irregular. The layers branch and lense out along the strike and down the dip, and are locally crosscutting (Pl. 3, fig. 3).

TABLE 5.—PEGMATITIC LAYERS IN A FLOW ABOVE THE KEARSARGE CONGLOMERATE

Depth (feet)	Thickness (inches)	
19	6	
27	10	
32	10	
35	7	contains visible native copper
40	10	contains visible native copper
64	8.5	contains visible native copper
47	3.5	
49	3.4	
57	2.3	contains visible native copper
60	3.4	contains visible native copper
66	1.0	contains visible native copper
69	5.7	
71	1.7	
93	0.3	
102	0.6	
119	0.3	

A typical layer in the lower part of the pegmatitic zone has a 2- to 4-inch border at the top and bottom, consisting of a medium- to coarse-grained aggregate to albite-oligoclase, augite, ilmenite, and magnetite, and a 2-inch to 4-foot core of green amygdaloidal rock. No planar or linear parallelism of the constituents was noted.

Toward the top of the flow, the pegmatitic layers are more amygdaloidal. Flattened vesicles that commonly occur at the top of the layer contain quartz, prehnite, and a green or red cherty substance. The top of the pegmatitic zone consists of 15 feet of altered, ophitic basalt containing almond-shaped vesicles filled with prehnite and quartz, strung together in partly coalescing chains in the plane of the flow (Pl. 3, fig. 4). Immediately below the red, fragmental amygdaloid that forms the top of the flow, there is a 1- to 2-foot zone of green, intensely prehnitized and silicified cellular amygdaloid.

"Big" Trap

The "Big" trap is a thick, ophitic, glomeroporphyritic basalt flow that occurs in the lower part of the Keweenawan series. The top of the

flow is about 8000 feet stratigraphically below the Greenstone flow. The flow has been intersected in diamond-drill holes between Calumet and Lake Medora (Pl. 1, loc. 12), a distance of 28 miles. Its maximum thickness is more than 600 feet, at a point 5 miles east of locality 4. The core studied and sampled by the writer came from diamond-drill hole C & H 28 (Pl. 1, loc. 4) where the flow is 402 feet thick (Table 6).

No aplite was found in the drill core. There are, however, three aplite dikes in a large outcrop of the "Big" trap 3 miles east-northeast of Calumet. The dikes are 1–2 inches thick, occur in the pegmatitic zone of the flow, strike roughly parallel to the dip of the flow, and dip vertically. The dikes transect both pegmatitic and ophitic basalt. Two of the dikes are very similar in appearance to the silicic aplite in the Greenstone, and the third dike resembles the chloritic aplite of that flow.

In this outcrop, the pegmatitic layers are roughly parallel to the base of the flow and range up to 4 feet thick. The contacts are sharp and normally smooth, but small pegmatitic stringers have intruded the ophitic basalt locally along the upper contact.

TABLE 6.—LOG OF THE "BIG" TRAP IN DRILL HOLE C & H 28

Depth (feet)	
0–5	Cellular amygdaloid. Vesicles filled with prehnite, calcite, chlorite, and epidote in rock consisting of nearly fresh, 0.25- to 0.50-mm. long slender oligoclase (An_{18}) laths, somewhat glomeroporphyritic, in a matrix of reddish, semiopaque glass.
5–22	Slightly glomeroporphyritic andesite containing cellular amygdaloidal layers.
	9 1-ft. cellular amygdaloidal layer
	14 3-in. cellular amygdaloidal layer
	20 3-in. cellular amygdaloidal layer
22–187	Glomeroporphyritic andesite and basalt containing pegmatitic layers. Rock becomes coarser-grained and increasingly ophitic with greater depth. Ophitic grains attain a maximum size of 13 mm. near the middle of the flow.
	22 3-in. pegmatitic layer
	24 1-ft. of epidotized andesite
	25 6-in. pegmatitic layer
	28 12-in. pegmatitic layer
	31 6-in. pegmatitic layer
	35 8-in. pegmatitic layer
	41–43 epidotized pegmatitic layer
	47–49 epidotized andesite
	51–56 coarse pegmatitic layer
	61–63 intensely epidotized andesite
	68–70 intensely epidotized andesite
	73 6-in. coarse pegmatitic layer
	79–80 epidotized andesite
	92–99 pegmatitic glomeroporphyritic andesite blending into coarse pegmatitic facies; 94–99 ft. coarse pegmatitic facies
	107–108½ epidotized pegmatitic layer
	110 3-in. of epidotized basalt
	115 2-in. coarse pegmatitic layer containing native copper.
	125–126 epidotized pegmatitic layer
	137–138 pegmatitic layer
	154–156 coarse spotty pegmatitic layer
	157 1-in. pegmatitic layer
	183–187 very coarse pegmatitic layer
187–395	Glomeroporphyritic, ophitic basalt; coarseness decreases downward.
395–402	Fine-grained basalt. Base of flow at 402 feet.

DISCUSSION OF MODES

General Statement

A few generalizations can be made about the distribution of minerals in the flows studied, on the basis of the modal analyses (Tables 7–12; Figs. 3–6). In the pegmatitic facies, the percentages of minerals present in one slide may not be representative because of the coarse texture, the rather erratic distribution of minerals and locally intense alteration. Therefore, in the samples chemically analyzed, at least two, and in most instances three, thin sections were used, so the modes should be fairly accurate. The writer has tried to compute the primary mineral content wherever possible even where the alteration has been intense. The modal analyses of the ophitic basalts are more accurate because of the finer texture of the rock and more uniform distribution of minerals.

Plagioclase

With the possible exception of the "Big" trap, plagioclase is not consistently more abundant in the upper parts of the flows, as Walker (1940) reported for the Palisades sill. There

seems to be about the same amount of plagioclase in the pegmatitic facies as in the ophitic basalt except in the "Big" trap where the plagioclase content of the pegmatitic facies is slightly lower than that of the adjacent ophitic basalt. Within the basalt portion of the flows, the plagioclase content of certain zones is above normal. The greatest concentration occurs below the middle of each flow in the upper part of the ophitic basalt zone, as is clearly indicated by the analyses of the Greenstone flow.

A fairly well defined reciprocal relationship exists between the distribution of plagioclase and pyroxene in the Greenstone and Mandan flows, the flow at South Range quarry, and the "Big" trap. In evaluating the significance of this relationship, the following facts must be considered: (1) A large proportion of the plagioclase in the ophitic basalt occurs poikilitically included in augite crystals. (2) An appreciable amount of the plagioclase, however, formed as free, nonpoikilitically included crystals. It is suggested that variations in the rate of crystallization of the two minerals and crystal sorting by differential settling of plagioclase and ophitic pyroxene crystals may have been factors determining their relative distribution in the flows.

The proportion of olivine is reciprocal to that of plagioclase in the Greenstone flow, but the relationship is less apparent in the other flows.

The composition of the plagioclase varies

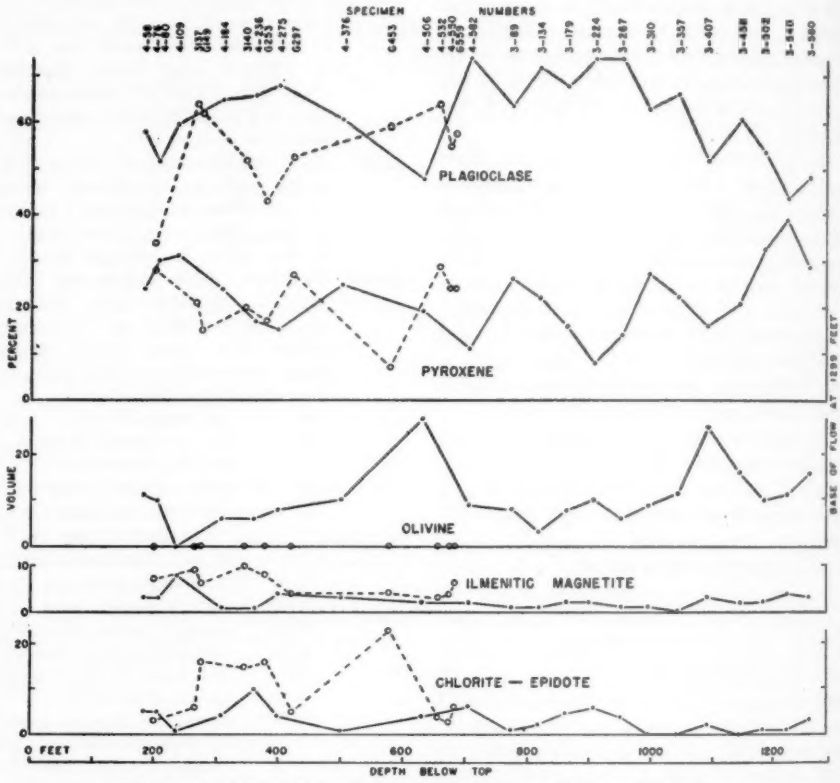

FIGURE 3.—MODAL VARIATION IN THE GREENSTONE FLOW AT DELAWARE

Minor constituents not shown. Dots and solid lines indicate ophitic basalt. Circles and dashed lines indicate pegmatitic facies.

systematically in all the flows (Tables 7–12). In the amygdaloids, the plagioclase is albite or sodic oligoclase (An_{10-15}). The fine-grained andesite immediately underlying the amygdaloids contains plagioclase of intermediate composition, oligoclase-andesine (An_{28-30}), which apparently grades in a short distance downward into labradorite (An_{50-60}). The plagioclase of the ophitic basalt in the pegmatitic zone, which extends downward to nearly the middle of the flows, is normally labradorite (An_{50-62}). In the "Big" trap, however, the plagioclase of the andesite and basalt in the pegmatitic zone ranges from An_{40} to An_{80}, and, in the upper part of the pegmatitic zone of the flow at South Range quarry, the basalt has been intensely albitized. In the ophitic basalt zone of all the flows, the plagioclase is more calcic than that in the overlying pegmatitic zone, having a composition of An_{69} to An_{74} (labradorite-bytownite). The plagioclase of the basal chill zone is somewhat more sodic than that of the overlying ophitic basalt.

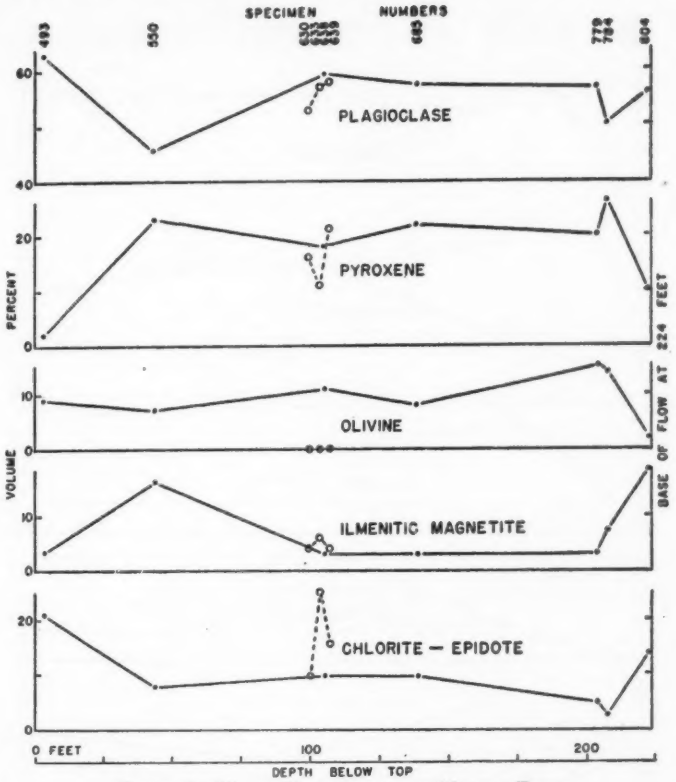

FIGURE 4.—MODAL VARIATION IN THE MANDAN FLOW

Minor constituents not shown. Dots and solid lines indicate ophitic basalt. Circles and dashed lines indicate pegmatitic facies.

Within the pegmatitic layers, the plagioclase has a composition between An_8 and An_{15} (albite to sodic oligoclase). The composition varies irregularly within these limits from layer to layer, as does the degree to which the plagioclase has been altered, with no systematic gradation.

Pyroxene

A marked concentration of pyroxene is found near the base of the Greenstone (Fig. 3) and

Mandan flows (Fig. 4). No similar concentration is apparent in the other flows studied, possibly because of inadequate sampling. In general, the amount of pyroxene decreases from the bottom to the top of the pegmatitic zone in the "Big" trap, both in the andesite-basalt and in the pegmatitic layers (Fig. 6).

In the Greenstone flow the pyroxene content of the ophitic basalt shows cyclic variation (Fig. 3). The highs and lows are nearly equally spaced 200 to 275 feet from high to high or low to low, respectively, and it appears that there is a rhythmic variation in the distribution of the pyroxene. As four to six analyses are involved in each cycle, these results are presumed to represent a real condition.

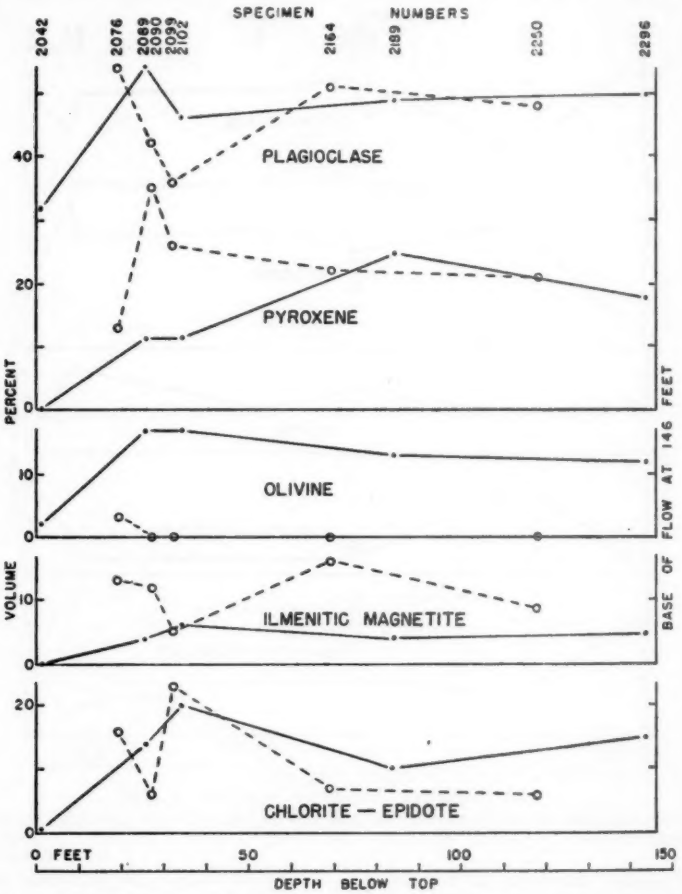

FIGURE 5.—MODAL VARIATION IN A PEGMATITIC FLOW ABOVE THE KEARSARGE CONGLOMERATE
Minor constituents not shown. Dots and solid lines indicate ophitic basalt. Circles and dashed lines indicate pegmatitic facies.

On the whole, there are apparently nearly equal amounts of pyroxene in the ophitic basalts and in the pegmatitic facies of all the flows.

Olivine

Olivine is concentrated near the base of all the flows. The flow immediately above the Kearsarge conglomerate (Fig. 5) has a moderate

olivine concentration in the upper part. No specimen was analyzed from the zone near the base where a concentration would be expected. sampled at two, three, and five points respectively (analyses 1375 and 1381; 1391, 1399, and 1408; 1464, 1472, 1477, 1492, and 1497) to

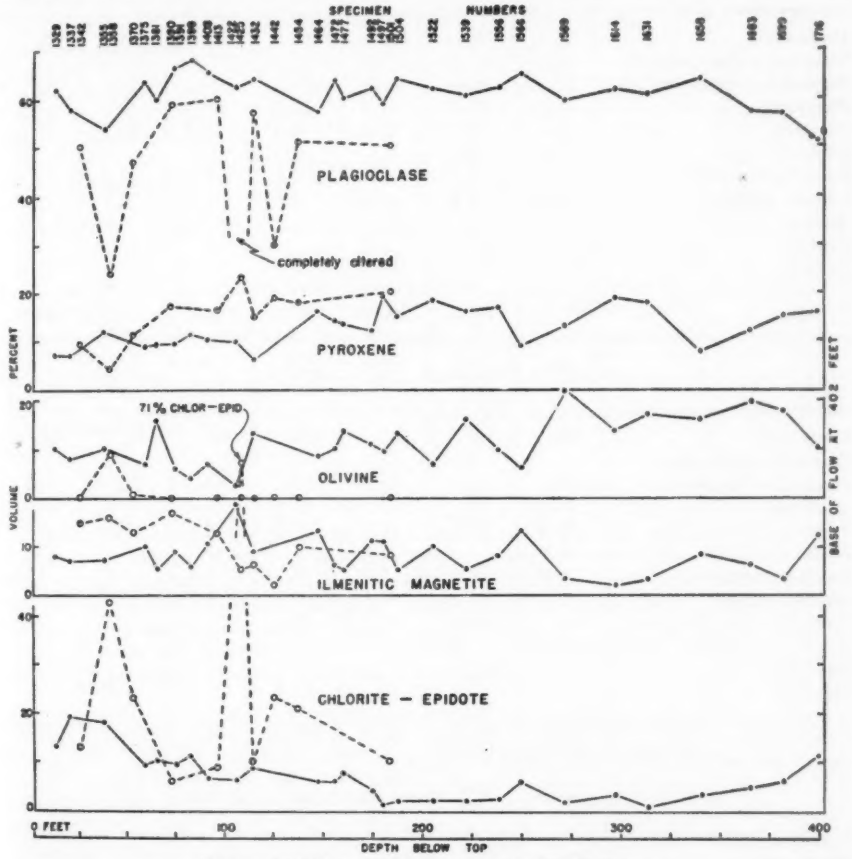

FIGURE 6.—MODAL VARIATION IN THE "BIG" TRAP

Minor constituents not shown. Dots and solid lines indicate ophitic basalt and andesite. Circles and dashed lines indicate pegmatitic facies.

The olivine is also markedly concentrated in the ophitic basalt near the base of the pegmatitic zone in the Greenstone flow and similarly, though less pronouncedly, olivine is concentrated in the ophite near the base of the pegmatitic zone in the Mandan flow (Fig. 4, Table 9). In the pegmatitic zone of the Greenstone, the amount of olivine in the ophitic basalt decreases upward.

Three of the andesite-basalt layers in the pegmatitic zone of the "Big" trap have been determine whether the amount of olivine varies systematically within single layers. Similarly, the ophitic basalt layer near the base of the pegmatitic zone in the Greenstone flow, which contains a high percentage of olivine at a depth of 631 feet (analysis 4-506), was sampled at three points. The results, partly shown by Figure 6, are inconclusive.

In the Greenstone flow (Fig. 3) it will be noted that the intervals from high- to low-olivine in the ophitic basalt zone and in the

TABLE 7.—MODAL ANALYSES OF THE GREENSTONE FLOW*

	4-58 basalt	4-76 pegmatitic facies	4-80 basalt	4-109 basalt	G149 pegmatitic facies	G149 pegmatitic facies
Depth (feet)	183	201	205	234	268	274
Thickness of zone (feet)		1			24	24
Plagioclase composition	An_{56}	An_{7}	An_{60}	An_{62}	An_{10}	An_{10}
Plagioclase	57.5	34.4	52.2	60.1	64.4	61.9
Pyroxene	24.1	27.5	30.4	31.0	20.7	15.0
Olivine	10.8		9.7			
Ilmenite, magnetite	2.8	7.1	3.1	7.8	8.6	6.2
Chlorite, epidote	4.8	2.9	4.6	1.1	6.1	15.6
Apatite		0.1			0.2	0.3
Quartz		1.9				
Prehnite		26.1				1.0
Total	100.0	100.0	100.0	100.0	100.0	100.0

	4-184 basalt	4-220 pegmatitic facies	4-236 basalt	G253 pegmatitic facies	4-275 basalt	G297 pegmatitic facies	4-375 basalt
Depth (feet)	309	345	361	378	400	422	501
Thickness of zone (feet)		4		7		7	
Plagioclase composition	An_{60}	An_{7}	An_{57}	An_{8}	An_{56}	An_{5}	An_{53}
Plagioclase	65.0	49.2	66.1	43.0	68.0	53.4	61.4
Pyroxene	24.0	19.7	17.1	17.2	15.4	27.2	24.6
Olivine	5.9		6.3		8.5		10.1
Ilmenite, magnetite	0.9	10.0	1.0	8.0	3.8	3.8	3.3
Chlorite, epidote	4.2	14.5	9.5	16.1	4.3	5.0	0.6
Apatite		0.4	tr.	0.3			tr.
Quartz		3.0				1.7	
Matrix†		3.2					
Prehnite				15.4		8.9	
Total	100.0	100.0	100.0	100.0	100.0	100.0	100.0

	G453 pegmatitic facies	4-506 basalt	4-532 pegmatitic facies	4-550 pegmatitic facies	G559 pegmatitic facies	4-582 basalt	3-89 basalt
Depth (feet)	578	631	657	675	684	707	774
Thickness of zone (feet)	5		28	6	7		
Plagioclase composition	An_{12}	An_{55}	An_{10}	An_{8}	An_{10}	An_{60}	An_{56}
Plagioclase	59.0	47.8	64.0	55.4	58.4	73.7	64.2
Pyroxene	7.3	18.9	28.7	23.8	24.2	10.5	25.7
Olivine		28.1				8.6	7.7
Ilmenite, magnetite	4.4	1.6	3.1	4.4	6.3	1.6	0.9
Chlorite, epidote	23.2	3.6	3.6	3.2	6.3	5.6	1.5
Apatite	0.7	tr.	0.4	tr.	0.6	tr.	
Quartz	0.6						
Prehnite	4.8		0.2	12.6	4.2		
Analcime				0.6			
Total	100.0	100.0	100.0	100.0	100.0	100.0	100.0

TABLE 7.—*Continued*

	3-134 basalt	3-179 basalt	3-224 basalt	3-267 basalt	3-310 basalt	3-357 basalt
Depth (feet)	819	864	909	952	995	1042
Plagioclase composition	An_{62}	An_{64}	An_{71}	An_{70}	An_{70}	An_{72}
Plagioclase	72.1	68.4	74.3	73.9	62.6	66.1
Pyroxene	21.7	15.9	7.6	14.3	26.6	21.9
Olivine	3.3	8.4	10.1	6.2	9.4	11.3
Ilmenite, magnetite	1.1	2.2	1.7	1.5	1.4	0.5
Chlorite	1.8	5.1	6.3	4.1	0.0	0.2
Total	100.0	100.0	100.0	100.0	100.0	100.0

	3-407 basalt	3-458 basalt	3-502 basalt	3-540 basalt	3-580 basalt
Depth (feet)	1092	1143	1187	1225	1265
Plagioclase composition	An_{68}	An_{74}	An_{69}	An_{65}	An_{48}
Plagioclase	52.5	61.2	54.4	43.9	49.4
Pyroxene	16.1	20.5	32.6	39.3	28.6
Olivine	26.2	16.3	9.9	11.4	15.9
Ilmenite, magnetite	3.2	1.7	2.4	4.0	3.0
Chlorite	2.0	0.3	0.7	1.4	3.1
Total	100.0	100.0	100.0	100.0	100.0

* Samples collected from a series of three diamond drill holes, Manitou 3, 4, and 5 N., which cross the Greenstone at Delaware, Mich. From same holes samples for chemical analyses were obtained by T. M. Broderick and the present writer. Flow is 1299 feet thick at this point; contains pegmatitic layers and streaks at depths of 201 to 841 feet. Deepest well-developed layer is a 7-foot zone at a depth of 684 feet. All depths are stratigraphic and measured from the top of the flow to the middle of the zone sampled.

The plagioclase in the amygdaloid at a depth of 38 feet has a composition of An_{10} (albite).

† Matrix of granophyre, kaolinite, and semiopaque material.

pegmatitic zone are roughly equal (300–400 feet). In the modal analyses of the Greenstone at Lake Medora (Table 8), there are also two concentrations of olivine, one near the base of the ophitic basalt zone at a depth of 1270 feet and one near the base of the pegmatitic zone at a depth of 850 feet. Two other flows and a sill described by Broderick (1935) show similar concentrations of olivine near or above the middle. The writer will consider these apparently anomalous occurrences further in the discussion of the chemical analyses.

Ilmenite and Magnetite

Ilmenite and magnetite are moderately concentrated in the pegmatitic facies. Similar concentrations occur in the basal and upper chill zones. The magnetite in all the flows studied except the Greenstone has been moderately to intensely altered to hematite.

Minor Constituents

Apatite, prehnite, quartz, calcite, and analcime, if present, are mostly confined to the pegmatitic layers, and, except for apatite, to the amygdaloids. Some of the pegmatitic layers contain a reddish matrix of granophyre, kaolinite, and hematite. Epidote occurs for the most part in the pegmatitic facies and as amygdules in the amygdaloids. Chlorite occurs in the pegmatitic facies and amygdaloids, and also in the ophitic basalt, as a replacement and an alteration of plagioclase and olivine respectively, and as amygdules.

As can be seen in the modes, a reciprocal relationship exists between the occurrence of

TABLE 8.—MODAL ANALYSES OF THE GREENSTONE FLOW AT CLIFF AND LAKE MEDORA*

	18-u amygdaloid	18-o basalt	18-o pegmatitic facies	18-k basalt	18-n pegmatitic facies	18-h pegmatitic facies
Depth (feet)	10	210	230	290	420	650
Plagioclase composition	An_{10}	lab.†	An_{12}	lab.†	indet.‡	An_{11}
Plagioclase	49.3	59.3	69.7	61.9	87.4	60.7
Pyroxene	6.6	25.9	6.9	21.6	1.7	31.7
Olivine	1.5	8.5		8.6		
Ilmenite, magnetite	7.2§	2.1	12.4	3.6	1.2	4.2
Chlorite	16.4	4.2	10.8	4.3	9.6	2.9
Apatite			0.2	tr.	0.1	0.5
Prehnite	18.0					
Calcite	0.1					
Analcime	0.9					
Total	100.0	100.0	100.0	100.0	100.0	100.0

	26-a	26-1 pegmatitic facies	26-1 basalt	26-k pegmatitic facies	26-h andesite
Depth (feet)	300	350	350	430	790
Plagioclase composition	An_{16}	An_{8}	lab.†	An_{9}	An_{45}
Plagioclase	60.4	41.8	71.9	51.8	61.7
Pyroxene	16.4	5.0	16.6	23.3	33.6
Olivine	4.4		9.5		0.6
Ilmenite, magnetite	2.2	3.3	1.8	9.9	1.9
Chlorite	14.8	6.5		14.4	0.9
Apatite	0.2	0.9	0.2	0.6	
Quartz		7.2			
Prehnite	1.6				
Analcime					1.3
Matrix		35.3¶			
Total	100.0	100.0	100.0	100.0	100.0

	G-26 aplite	26-g4 aplite	26-g3 basalt
Depth (feet)	800	800	800
Plagioclase composition	An_{12}	An_{15}	lab.†
Plagioclase	49.6	43.2	61.8
Pyroxene		4.7	31.7
Olivine			
Ilmenite, magnetite	0.8	3.0	0.2
Chlorite	6.1		5.9
Apatite			0.4
Quartz	20.6†		
Matrix	21.2‖	49.1**	
Zoisite	1.7		
Total	100.0	100.0	100.0

TABLE 8.—*Continued*

	26-g2 pegmatitic facies	26-g1 basalt	26-f basalt	26-d basalt	26-c basalt	26-b basalt	26-a basalt
Depth (feet)	820	850	880	1270	1300	1330	1370
Plagioclase composition	An_{53}	lab.†	lab.†	lab.†	lab.†	lab.†	lab.†
Plagioclase	67.7	73.4	70.5	59.0	59.7	57.2	60.2
Pyroxene	26.0	5.0	21.0	17.7	18.1	27.9	30.7
Olivine		12.0	3.2	21.2	18.7	8.6	3.0
Ilmenite, magnetite	2.3	1.4	0.9	1.8	1.6	3.4	2.8
Chlorite	4.0	8.2	4.1	0.3	1.9	2.9	3.3
Apatite	tr.		0.3		tr.		
Total	100.0	100.0	100.0	100.0	100.0	100.0	100.0

* Analyses 18h to 18u represent a section across the flow at Cliff (Pl. 1, loc. 10).
Analyses 26a to 26s represent a section across the flow at Lake Medora (Pl. 1, loc. 12).
The flow is about 1400 feet thick at both places.
† Labradorite.
‡ Indeterminable because of alteration.
§ Black and reddish opaque material, probably mostly hematite.
¶ Reddish intergrowth of albite and quartz.
‖ Interstitial granophyre, kaolinite, and semiopaque material.
** Matrix consists of about one half chlorite and one half oligoclase.

pyroxene and that of chlorite-epidote in both the ophitic basalt and the pegmatitic facies. This contrast is most striking in the Greenstone and Mandan flows.

Amygdaloids

The amygdaloids of the flow at South Range quarry, of the flow above the Kearsarge conglomerate, and of the "Big" trap contain no pyroxene and only scattered grains of altered olivine. These amygdaloids consist essentially of glomeroporphyritic plagioclase laths and vesicle fillings of secondary minerals in a matrix of reddish aphanitic material. The amygdaloids of the Mandan and Greenstone flows are holocrystalline and contain small to moderate amounts of pyroxene and altered olivine.

DISCUSSION OF CHEMICAL ANALYSES

Greenstone Flow

Introduction.—Seven chemical analyses (Table 13) of the Greenstone flow were obtained by the writer. Except the aplite (G26), all the samples were obtained from the same core that Broderick (1935) used for his 12 analyses (Figs. 7, 8). The writer sampled five pegmatitic layers, an aplite, and the basal chill zone.

Distribution of elements.—Broderick's findings concerning the relative distribution of elements in the pegmatitic facies and ophitic basalts are confirmed by the writer's analyses. The basal chill zone, which should represent the original composition of the magma, is higher than the overlying ophitic basalt in Fe, Cu, S, Si, K, P, Ti, Mn, CO_2, and H_2O plus. The potash content is very high, however, which probably indicates some deuteric alteration. Fe, Cu, Ti, P, S, combined water, and Mn show a definite tendency to be concentrated in the pegmatitic facies. The writer plotted the amounts of TiO_2 in the chemical analyses against the amounts of ilmenite plus magnetite in the modal analyses. The results indicate that the ilmenite-magnetite ratio is nearly the same for the ophitic basalt and the pegmatitic facies, and this was substantiated by a study of polished sections.

The amount of combined water is very high in one pegmatitic layer, high in two others, and very low in one. It is also above average in the olivine-rich zone 200 feet above the base.

Sulfur, in addition to being concentrated in the pegmatitic facies, definitely trends toward greater abundance in the upper part of the flow. Si, Na, and K tend to be more abundant in the pegmatitic facies. The concentration of Ca is very high in two of the pegmatitic layers, very low in one (and in the basal chill zone), and intermediate in the other analyses. The distribution of Mg is clearly related to the differentiation of the flow as a whole. Mg is relatively more abundant in the ophitic basalt and upper chill zones than in the pegmatitic zone. The greatest concentration of Mg occurs in the ophitic basalt zone 200 feet above the base of the flow. The ratio of MgO to total Fe calculated as FeO shows a trend similar to that for MgO.

Magnesia-iron oxide ratio.—The ratio of MgO to total Fe as FeO furnishes an especially critical indication of the trend of differentiation in successive layers of the pegmatitic zone. There is a definite trend from a low MgO:FeO ratio in the upper pegmatitic layers to a higher ratio in the lower pegmatitic layers. Ophitic basalt between the successive pegmatitic layers shows a similar, but more gradual, downward increase in the MgO:FeO ratio. The ratio is higher in the ophitic basalt than in the pegmatitic layers in the upper part of the zone, but in the lower part it is slightly lower.

TABLE 9.—MODAL ANALYSES OF THE MANDAN FLOW*

	C493 amygdaloid	C550 basalt	C630 pegmatitic facies	C633 pegmatitic facies	C638 basalt	C639 pegmatitic facies
Depth (feet)	3	44	100	104	105.5	107
Thickness of zone (feet)	7		0.3	2.1		0.7
Plagioclase composition	An_{18}	An_{80}	An_{10}	An_{12}	indet.†	An_{12}
Plagioclase	63.6	45.7	52.6	57.4	59.1	57.9
Pyroxene	2.1	22.7	15.6	11.0	17.7	21.1
Olivine	9.4	7.4			10.7	
Ilmenite, magnetite	3.2	15.9	4.1	6.3	2.8	4.4
Chlorite, epidote	21.3	8.3	10.3	25.3	9.7	15.5
Calcite			1.3			1.1
Prehnite	0.4		10.0			
Quartz			6.1			
Total	100.0	100.0	100.0	100.0	100.0	100.0

	C685 basalt	C779 basalt	C784 basalt	C804 basalt (chill zone)
Depth (feet)	139	205	208	223
Plagioclase composition	An_{49}	An_{61}	An_{62}	An_{58}
Plagioclase	57.6	56.8	50.2	56.3
Pyroxene	22.2	20.5	26.3	10.2
Olivine	7.5	14.6	13.7	1.5
Ilmenite, magnetite	2.5	3.0	6.9	17.9‡
Chlorite, epidote	10.2	5.1	2.9	14.1
Total	100.0	100.0	100.0	100.0

* Samples collected from diamond drill hole Clark 11, which intersects the flow 3 miles south of Copper Harbor. The flow is 224 feet thick at this point and contains nine pegmatitic layers at depths of 70 to 121 feet.

† Indeterminable because of alteration.

‡ Ilmenite, magnetite and semiopaque glass.

Aplite.—A crosscutting dike, 1½ feet thick, that occurs near the base of the pegmatitic zone at Lake Medora, (Pl. 1, loc. 12) is an extreme differentiate of the Greenstone flow, very high in silica and very low in magnesia. It is comparable to the pegmatitic facies in its soda content, but notably higher in potash content. Its content of Fe, P, Ti, Mn, and Cu is very low, indicating differentiation beyond the stage at which these elements may have been concentrated in the magma. The writer believes that these elements (Fe, P, Ti, Mn, and Cu) were concentrated in a vapor phase that may in part have co-existed with the residual aplitic magma.

TABLE 10.—MODES OF A FLOW ABOVE THE KEARSARGE CONGLOMERATE*

	2042 amygdaloid	2076 pegmatitic facies	2089 basalt	2090 pegmatitic facies	2099 pegmatitic facies	2102 basalt
Depth (feet)	1	19	26.6	27.2	32	34
Thickness of zone (feet)	1.7	0.3		0.9	0.9	
Plagioclase composition	indet.†	An_{12}	An_{57}	An_{11}	An_{11}	An_{57}
Plagioclase	32.2	53.7	53.8	42.4	36.2	46.2
Pyroxene		12.7	10.9	35.4	26.0	11.0
Olivine	2.0	3.0	17.4			16.8
Ilmenite, magnetite		12.6	3.7	12.5	5.0	5.9
Chlorite, epidote	0.5	16.4	14.2	6.1	22.7	20.1
Quartz	16.5	1.3			4.8	
Prehnite	10.7	0.3		3.6	5.3	
Glass	31.9					
Calcite	6.2					
Total	100.0	100.0	100.0	100.0	100.0	100.0

	2164 pegmatitic facies	2189 basalt	2250 pegmatitic facies	2296 basalt
Depth (feet)	69	84	118	144
Thickness of zone (feet)	0.5		0.1	
Plagioclase composition	An_{12}	An_{49}	An_{15}	An_{48}
Plagioclase	50.6	48.9	29.4	50.1
Pyroxene	21.9	24.6	20.5	18.1
Olivine		12.8		12.1
Ilmenite, magnetite	16.5	4.0	9.5	4.6
Chlorite, epidote	6.5	9.7	5.6	15.1
Quartz	1.7		9.6	
Prehnite	2.8		6.5	
Kaolinite‡			18.9	
Total	100.0	100.0	100.0	100.0

* Samples collected from diamond drill hole Delaware 77 (locality 3, Pl. 1). The flow is 145 feet thick.
† Indeterminable because of alteration.
‡ Mixture of kaolinite and semiopaque material.

Norms (Table 13; Fig. 8).—Normative olivine and quartz have been plotted on the same graph above and below a zero line, with the amount of olivine increasing upward and that of quartz downward. The ophitic basalt of the pegmatitic zone is above average in normative orthoclase, albite, diopside, quartz, ilmenite, magnetite, and apatite; and, in general, the amounts of these normative minerals in the

ophitic basalt increase from the bottom to the top of the pegmatitic zone. Anorthite and hypersthene are deficient in the ophitic basalt of 7; Fig. 3) indicate that olivine actually is concentrated at these points. The concentration near the base of the flow is expectable from

TABLE 11.—MODAL ANALYSES OF THE FLOW AT SOUTH RANGE QUARRY*

	S145a basalt	S142 pegmatitic facies	S132 andesite	S130d andesite	S130a pegmatitic facies
Depth (feet)	46	48	56	58	59
Thickness of zone (feet)		0.2			1.5
Plagioclase composition	indet.†	An_8	An_8	An_{11}	indet.†
Plagioclase	52.3	50.9	58.2	59.4	52.2
Pyroxene	16.9	22.5	13.0	13.5	
Olivine	7.2	0.9	11.4	9.9	1.1
Ilmenite, magnetite	6.5	8.2	4.3	4.7	5.2
Chlorite‡	10.5	11.7	13.1	12.5	17.7
Quartz	4.3	3.1			22.9
Prehnite	2.3	2.7			0.9
Total	100.0	100.0	100.0	100.0	100.0

	S122d pegmatitic facies	S112d pegmatitic facies	S70 basalt
Depth (feet)	64	73	109
Thickness of zone (feet)	1.0	2.5	
Plagioclase composition	An_7	An_8	An_{40}
Plagioclase	61.2	51.8	50.0
Pyroxene	8.4	10.2	14.0
Olivine			7.6
Ilmenite, magnetite	8.7	15.8	12.2
Chlorite‡	20.1	10.8	16.2
Quartz		1.2	
Prehnite	1.6	10.2	
Total	100.0	100.0	100.0

* Samples collected from a road metal quarry at South Range (loc. 5, Pl. 1). The flow is 130 feet thick.
† Indeterminable because of alteration.
‡ Includes some epidote and pumpellyite.

the pegmatitic zone. The pegmatitic facies contains more normative orthoclase, quartz, ilmenite, magnetite, apatite, and diopside than the surrounding ophitic basalt, and less anorthite and hypersthene. Normative albite is more abundant in pegmatitic facies than in ophitic basalt in the upper part of the zone, but the reverse is true in the lower part of the zone.

High-olivine layers.—Normative olivine is concentrated in the ophitic basalt about 200 feet above the base of the flow, and near the middle of the flow, just above the lowermost pegmatitic layers. The modal analyses (Table

the early separation of olivine and from crystal sorting by differential settling, but the concentration near the center is far less readily explained.

This apparently anomalous concentration of olivine is evidently not a freak occurrence; similar concentrations were observed or have been described elsewhere in Keweenawan basaltic extrusives and intrusives. Concentrations of olivine in the central part of the Greenstone were noted both in the section at Delaware and at Lake Medora (Table 8). In the Mandan flow, the flow above the Kearsarge conglom-

TABLE 12.—MODAL ANALYSES OF THE "BIG" TRAP*

	1329 andesite	1337 andesite	1342 pegmatitic facies	1355 basalt	1358 pegmatitic facies	1370 pegmatitic facies	1375 andesite
Depth (feet)	12	20	25	38	41	53	58
Thickness of zone (feet)			0.5		2.0	5.0	
Plagioclase composition	An_{30}	An_{29}	An_{8}	An_{50}	indet.†	An_{11}	An_{40}
Plagioclase	62.3	58.3	49.5	53.5	23.7	47.0	63.4
Pyroxene	6.6	6.8	9.1	11.5	4.3	11.4	9.1
Olivine	9.9	8.5		10.2	9.5	0.6	7.2
Ilmenite magnetite	7.8	7.1	14.6	6.5	16.3	13.1	9.8
Chlorite, epidote	12.9	18.7	13.2	18.3	42.3	23.5	9.3
Quartz	0.5	0.6	12.3		1.2	4.4	
Calcite			1.3		2.7		1.2
Total	100.0	100.0	100.0	100.0	100.0	100.0	100.0

	1381 andesite	1390 pegmatitic facies	1391 basalt	1399 andesite	1408 andesite	1413 pegmatitic facies	1422 andesite
Depth (feet)	64	73	74	82	91	96	105
Thickness of zone (feet)		0.5				5.0	
Plagioclase composition	indet.†	An_{8}	An_{53}	An_{45}	An_{49}	An_{10}	indet.†
Plagioclase	59.6	44.6	66.3	68.1	65.0	60.4	62.3
Pyroxene	9.4	17.5	9.4	11.1	10.7	15.9	9.8
Olivine	15.9		6.2	3.6	7.0		2.6
Ilmenite, magnetite	5.2	17.2	8.6	5.9	10.6	13.3	19.2
Chlorite, epidote	9.9	6.4	9.5	11.3	6.7	8.9	6.1
Apatite		tr.				tr.	
Quartz						1.5	
Kaolinite‡		14.3					
Total	100.0	100.0	100.0	100.0	100.0	100.0	100.0

	1425 pegmatitic facies	1432 basalt	1432 pegmatitic facies	1442 pegmatitic facies	1454 pegmatitic facies	1464 basalt	1472 basalt
Depth (feet)	108	115	115	125	137	147	155
Thickness of zone (feet)	1.5		0.2	1.0	1.0		
Plagioclase composition	indet.†	indet.†	indet.†	An_{12}	indet.†	An_{55}	An_{55}
Plagioclase		63.5	55.0	30.1	51.2	56.8	63.7
Pyroxene	22.5	6.3	14.9	18.7	17.9	15.8	13.7
Olivine		12.7				8.5	10.4
Ilmenite, magnetite	5.0	8.7	6.1	2.4	10.0	12.9	5.9
Chlorite, epidote	71.4	8.8	9.9	22.8	20.9	6.0	6.3
Apatite		tr.	0.3	0.2			
Prehnite			7.4				
Quartz	1.1		2.9	25.8			
Calcite			1.5				
Kaolinite‡			2.0				
Total	100.0	100.0	100.0	100.0	100.0	100.0	100.0

TABLE 12.—*Continued*

	1477 basalt	1492 basalt	1497 basalt	1501 pegmatitic facies	1504 basalt	1522 basalt	1539 basalt
Depth (feet)	160	175	180	184	187	205	222
Thickness of zone (feet)				4.0			
Plagioclase composition	An_{59}	An_{55}	An_{58}	An_{3}	An_{63}	An_{64}	An_{63}
Plagioclase	59.6	61.5	58.5	49.6	64.2	62.2	60.6
Pyroxene	13.7	12.5	19.7	20.4	15.1	18.4	16.1
Olivine	14.1	10.6	9.4		13.6	7.4	16.2
Ilmenite, magnetite	4.7	11.3	10.7	8.4	4.9	10.0	5.5
Chlorite, epidote	7.9	4.1	1.7	10.2	2.2	2.0	1.6
Apatite				0.3			
Prehnite				10.9			
Quartz				0.2			
Total	100.0	100.0	100.0	100.0	100.0	100.0	100.0

	1556 basalt	1566 basalt	1589 basalt	1614 basalt	1631 basalt	1658 basalt
Depth (feet)	239	249	272	297	314	341
Plagioclase composition	An_{70}	An_{70}	An_{68}	An_{67}	An_{67}	An_{68}
Plagioclase	62.3	65.2	59.2	61.5	60.5	64.0
Pyroxene	17.2	9.2	13.2	18.9	17.8	7.7
Olivine	10.3	5.8	22.4	14.0	17.0	16.2
Ilmenite, magnetite	8.0	13.5	3.4	2.0	3.6	8.6
Chlorite, epidote	2.2	6.3	1.8	3.6	1.1	3.5
Total	100.0	100.0	100.0	100.0	100.0	100.0

	1683 basalt	1699 basalt	1716 basalt (chill zone)
Depth (feet)	366	382	400
Plagioclase composition	An_{64}	An_{59}	An_{48}
Plagioclase	56.9	57.4	51.0
Pyroxene	12.4	15.3	15.8
Olivine	19.4	17.9	10.2
Ilmenite, magnetite	5.8	3.3	12.3
Chlorite, epidote	5.5	6.1	10.7
Total	100.0	100.0	100.0

* Samples collected from diamond drill hole C & H 28 (locality 4, Pl. 1). The flow is 402 feet thick, and contains 16 pegmatitic layers.

† Indeterminable because of alteration.

‡ Mixture of kaolinite and semiopaque material.

erate, and in three of the basaltic sheets described by Broderick (1935), similar concentrations of modal or normative occur. The modes of a flow of the Keweenawan series in Wisconsin (Buckstaff, 1923; Broderick, 1935) show a concentration of olivine near the base and another near the middle. The norms of the Kearsarge flow (Broderick, 1935) show normative olivine only in two analyses, one a short distance below the top (3.98 per cent), and the other near the middle (2.43 per cent). A diabase sill on the north shore of Lake Huron (Emmons,

1927) contained normative olivine only in a thin zone a short distance below the top.

These concentrations indicate that at least two periods during solidification were especially

and 16, Analyses 4, 5). These flows are relatively thin and therefore probably relatively undifferentiated. Furthermore, Broderick's sample (Table 15, analysis 4) is a composite from chips

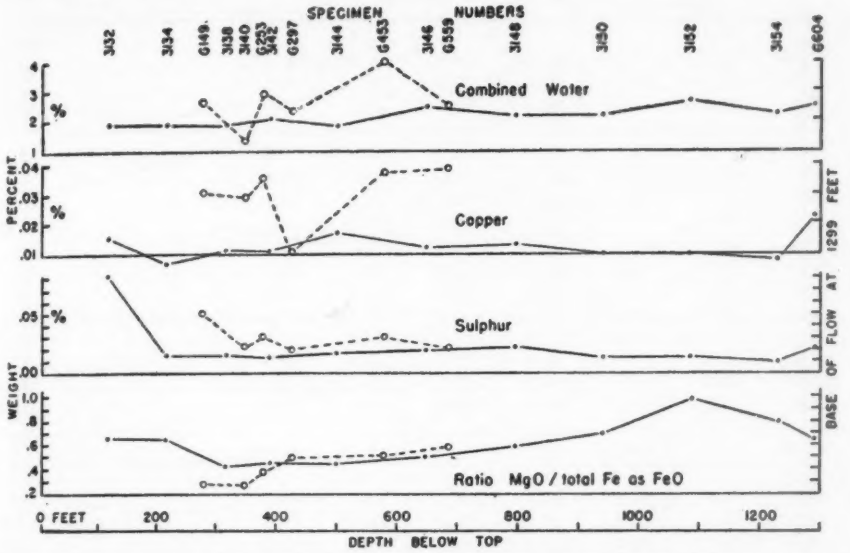

FIGURE 7.—VARIATION IN THE GREENSTONE FLOW OF COMBINED WATER, COPPER, SULPHUR, AND THE RATIO OF MgO TO TOTAL Fe CALCULATED AS FeO

Dots and solid lines indicate ophitic basalt. Circles and dashed lines indicate pegmatititic facies.

favorable for the formation and/or mechanical concentration of olivine. In at least three of the flows or sills for which chemical information is available, the ophitic basalt or diabase that contains the later concentration of olivine also contains a greater amount of soda and potash, and slightly less lime than the underlying ophitic basalt or diabase. The rock containing the late olivine concentration is contrasted with the rock containing the early olivine concentration in this respect, and also it contains less magnesia and somewhat more iron oxide. The analyses also indicate that conditions of crystallization before the second concentration of olivine were not such as to cause notable enrichment of the magma in silica.

Certain of the glomeroporphyritic andesite and dacite flows in the Michigan copper district, like the central olivine-rich layer of the Greenstone, contain a sodic plagioclase and a large ratio of olivine to pyroxene (Tables 15

at uniform intervals from top to bottom of the flow. Analyses 4 and 5 in Table 15, then, should represent approximately the composition of lava which crystallized to form a sodic plagioclase and olivine in preference to pyroxene.

These apparently anomalous occurrences of olivine must be related to: (1) special conditions that caused mechanical concentration; and/or (2) unusual compositions of the magmas from which the rocks formed. In the Greenstone flow, (discussed under differentiation hypothesis A) mechanical processes may have caused the late olivine concentration. In the sodic andesites and dacites, however, olivine must have formed in preference to pyroxene because of special chemical relations in the magmas.

Chemical relations between olivine, pyroxene, and quartz in the system MgO-FeO-SiO_2 have been studied experimentally by Bowen and Schairer (1935). Working with anhydrous

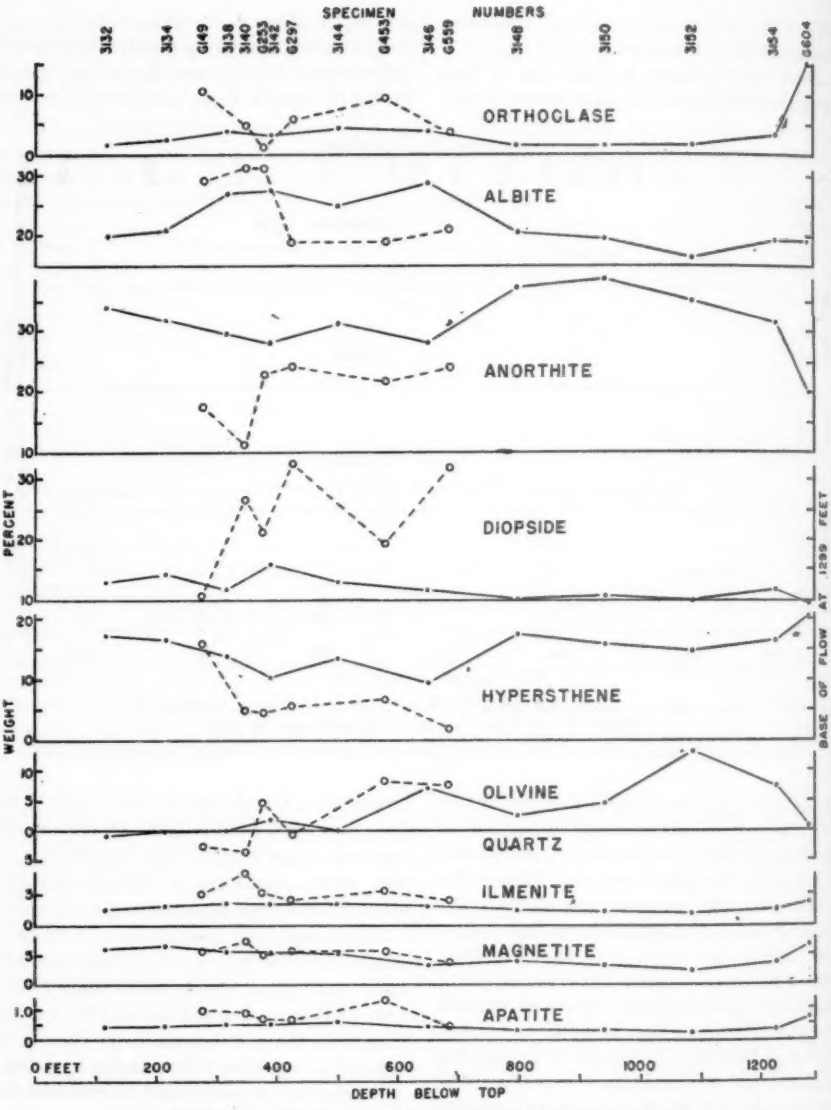

FIGURE 8.—VARIATION OF NORMS IN THE GREENSTONE FLOW
Dots and solid lines indicate ophitic basalt. Circles and dashed lines indicate pegmatitic facies.

melts, they found that with strong fractional crystallization

"the crystalline products—would range all the way trom highly magnesian olivine as the earliest crysafls, through highly magnesian pyroxene accompanied by silica, then more ferriferous pyroxene accompanied by silica, to highly ferriferous olivine again accompanied by silica."

In the Greenstone flow, the writer found by optical methods that the olivine and pyroxene

TABLE 13.—CHEMICAL ANALYSES OF THE GREENSTONE FLOW*

	G149 pegmatitic facies	G253 pegmatitic facies	G297 pegmatitic facies	G453 pegmatitic facies	G559 pegmatitic facies	G26 aplite	G604 basalt (chill zone)
Depth (ft.)	274	378	422	578	684	800	1290
Width (ft.)	24	7	7	5	7	1.5	
SiO_2	50.11	47.30	47.64	45.04	47.56	63.30	48.59
Al_2O_3	13.89	14.72	13.57	13.30	13.60	12.86	13.85
Fe_2O_3	3.75	3.34	3.80	3.89	2.43	3.16	4.64
FeO	10.42	9.23	7.56	9.76	8.95	2.78	7.37
MgO	3.77	4.55	5.39	6.68	6.49	1.76	7.62
CaO	6.56	10.61	13.25	9.90	12.71	5.98	6.96
Na_2O	3.39	3.65	2.24	2.26	2.50	3.35	2.26
K_2O	1.82	0.22	0.90	1.47	0.57	3.61	2.62
H_2O+	2.63	2.94	2.35	3.94	2.56	1.49	2.53
H_2O-	0.39	0.26	0.56	0.46	0.30	0.73	1.14
CO_2	0.02	0.24	0.04	0.04	0.00	0.01	0.12
TiO_2	2.74	2.61	1.99	2.78	2.15	0.85	2.02
P_2O_5	0.43	0.28	0.23	0.48	0.17	0.17	0.23
S	0.05	0.03	0.02	0.03	0.02	0.02	0.02
CuO	0.037	0.044	0.013	0.046	0.048	0.009	0.028
MnO	0.22	0.19	0.19	0.21	0.22	0.11	0.17
Total	100.23	100.21	99.74	100.29	100.28	100.19	100.17
Sp.Gr†	2.98	2.92	3.02	2.98	2.98	2.71	2.90
Total Fe as FeO	13.79	12.24	10.98	13.26	11.14	5.62	11.55
Cu	0.030	0.035	0.010	0.037	0.038	0.007	0.022
MgO/FeO‡	0.273	0.372	0.491	0.504	0.583	0.313	0.660
	G149	G253	G297	G453	G559	G26	G604
Norms							
Quartz	2.40		0.42			18.54	
Orthoclase	10.56	1.11	5.56	8.90	3.34	21.13	15.57
Albite	28.82	30.92	18.86	18.86	20.96	28.30	18.86
Anorthite	17.24	23.07	24.19	21.68	24.19	9.45	20.02
Diopside							
Wo	5.22	10.79	16.59	9.78	16.24	6.15	4.87
En	2.40	5.60	10.00	5.80	9.10	4.40	3.30
Fs	2.77	4.88	5.68	3.70	6.47	1.19	1.19
Hypersthene							
En	7.00	2.50	3.50	4.10	1.20		15.40
Fs	8.84	2.24	2.11	2.64	0.79		5.15
Olivine							
Fo		2.38		4.76	4.20		0.56
Fa		2.24		3.26	3.26		0.20
Wollastonite						2.32	
Apatite	1.01	0.67	0.67	1.34			0.67
Ilmenite	5.17	5.02	3.80	5.32	4.10	1.67	3.80
Magnetite	5.57	4.87	5.57	5.57	3.48	4.64	6.73
Pyrite	0.12						

TABLE 13.—*Continued*

	G149	G253	G297	G453	G559	G26	G604
Norms—*Continued*							
Calcite		0.60					0.30
Water	3.02	3.20	2.91	4.40	2.86	2.22	3.67
Total	100.14	100.09	99.86	100.11	100.19	100.01	100.29
Plagioclase composition	An_{37}	An_{43}	An_{56}	An_{54}	An_{54}	An_{28}	An_{31}
Modes (weight per cent)							
Plagioclase	55.4	37.3	47.7	53.7	51.6	48.0	
Pyroxene	16.7	18.6	30.3	8.3	26.6		
Matrix§						20.5	
Quartz			1.5	0.5		20.3	
Ilmenite, magnetite	10.7	13.3	6.6	7.8	10.7	1.5	
Epidote, chlorite	15.8	15.8	5.1	24.1	6.3	7.7	
Zoisite						2.0	
Apatite	0.4	0.4		0.8	0.7		
Prehnite	1.0	14.6	8.8	4.8	4.1		
Total	100.0	100.0	100.0	100.0	100.0	100.0	
Plagioclase composition	An_{10}	An_{8}	An_{5}	An_{12}	An_{10}	An_{12}	

* All the samples except G26 are of core from diamond drill holes Manitou 3, 4, and 5 N. G26 is from an aplite dike at Lake Medora. Analyses by L. C. Peck, Rock Analysis Laboratory, University of Minnesota. The flow is 1,300 feet thick. All depths are measured to the middle of the zone sampled, and include the amygdaloid and upper basalt zone which Broderick omitted. Corresponding horizons are consequently 60 feet lower by the writer's measurements.

† Specific gravity at 4°C. Determinations by Norman Davidson, Geochemistry and Petrology Branch, U. S. Geological Survey.

‡ Total Fe calculated as FeO.

§ Interstitial, semiopaque material, partly kaolinite.

change composition only slightly from the base to the middle of the flow. The olivine ranges from $Fo_{64}Fa_{36}$ near the base to $Fo_{58}Fa_{42}$ at the middle of the flow. There is no contrast in composition of the early and late phases comparable to that found by Bowen and Schairer. Furthermore, the late concentration of olivine is not accompanied by quartz. To use Bowen and Schairer's data to explain the reappearance of olivine as an important primary phase in the later stages of crystallization in the Greenstone, it will be necessary to postulate changes in the phase relationships owing to the presence of volatiles, Na_2O, K_2O, and other constituents in the magma.

In the Greenstone flow the lower pegmatitic layers are also high in normative olivine, but concentrations of vesiculated vapors, evidenced by their amygdaloidal structure and greater degree of alteration, apparently prevented its formation. Thin sections and modes show that these lower pegmatitic layers differ from the adjacent ophitic basalt in that they contain albite, small amounts of quartz, larger amounts of prehnite and epidote, and no olivine.

"Big" Trap

Six chemical analyses of the "Big" trap were obtained for comparison with the Greenstone (Table 14; Fig. 9). Fe, Ca, Ti, P, and Mn are definitely more abundant in the pegmatitic

facies than in the adjoining andesite and basalt, and, except for Ca, are decidedly concentrated in the upper half of the flow (as is Na also). Na and K (the latter in particular) are more abundant in the andesite at a depth of 82 feet (sample 1399) than would normally be expected. Thin sections of this andesite show that the plagioclase has been intensely altered to sericite and chlorite, and is more sodic than in the normal andesite. The ratio of TiO_2 to modal magnetite was found to be of the same order of magnitude in the andesite-basalt and in the pegmatitic facies.

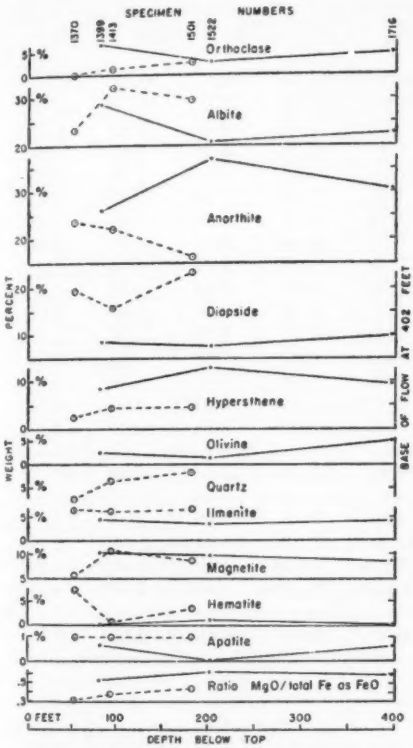

FIGURE 9.—VARIATION OF NORMS IN THE "BIG" TRAP

Dots and solid lines indicate ophitic basalt. Circles and dashed lines indicate pegmatitic facies.

The proportion of MgO to total Fe calculated as FeO is markedly higher in the andesite-basalt than in the pegmatitic facies, and is highest in the ophitic basalt sample at a depth of 205 feet. It increases steadily in the successively deeper pegmatitic layers. Thin sections show that the pegmatitic facies contains considerable epidote and prehnite, which probably accounts for its rather high lime content. Normative quartz occurs only in the pegmatitic facies and decreases in amount downward in the flow. The Greenstone flow shows a similar trend, less pronounced.

Copper is rather uniformly distributed throughout the flow, except that it is very abundant in the basal chill zone, perhaps due in part to the introduction of copper along the contact by later migrating solutions, although there is no direct evidence. Unlike the other pegmatitic layers studied, copper content of the pegmatitic facies in the "Big" trap is lower than in the andesite-basalt.

Relative proportions of FeO to Fe_2O_3 range in the Greenstone from 1.5:1 to 4:1, and in the "Big" trap from 1:1 to almost 1:3.

Silica content of the Greenstone flow ranges from 45 to 50 per cent, and that of the "Big" trap from 44 to 47 per cent. The silica content of the pegmatitic facies averages slightly higher than that of the basalt in both flows; the alumina content is slightly lower.

DIFFERENTIATION

Basic Facts

1. *Chill zones.* Each flow has a thin, slightly amygdaloidal basal chill zone and a much thicker upper chill zone, amygdaloidal toward the top, indicating greater cooling from the top.

2. *Pegmatitic layers.* (a) *Position in flow:* Except for small, scattered, irregular, pegmatitic segregations, the pegmatitic layers occur in a zone whose base lies near the middle of the flow, and whose top is at the base of the upper chill zone.

(b) *Orientation:* With few exceptions, the pegmatitic layers lie in a plane parallel to the flow itself.

(c) *Thickness and spacing* of the successive pegmatitic layers vary irregularly in all the flows studied except the flow exposed at the South Range quarry, where the pegmatitic layers are progressively thinner and closer together from the middle of the flow upward.

(d) *Texture:* The pegmatitic zones are mod-

TABLE 14.—CHEMICAL ANALYSES OF THE "BIG" TRAP*

	T1370 pegmatitic facies	T1399 andesite	T1413 pegmatitic facies	T1501 pegmatitic facies	T1522 basalt	T1716 basalt (chill zone)
Depth (ft.)	53	82	96	184	205	400
Width (ft.)	5		5	4		2
SiO_2	45.84	46.40	47.25	46.14	44.35	44.69
Al_2O_3	13.17	16.36	14.50	12.09	18.10	16.35
Fe_2O_3	11.18	7.28	7.80	9.80	8.02	6.03
FeO	4.65	5.49	6.13	5.70	4.67	6.58
MgO	4.70	6.43	4.72	6.06	7.30	7.25
CaO	10.69	7.85	9.16	9.84	9.38	9.11
Na_2O	2.69	3.44	3.77	3.48	2.43	2.63
K_2O	0.04	1.06	0.24	0.52	0.51	0.76
H_2O+	2.72	2.60	2.69	1.98	2.43	3.30
H_2O-	0.13	0.26	0.10	0.23	0.58	0.76
CO_2	0.19	0.01	0.03	0.06	0.03	0.04
TiO_2	3.47	2.29	3.23	3.52	1.90	2.18
P_2O_5	0.40	0.26	0.35	0.37	0.22	0.26
S	0.02	0.07	0.06	0.02	0.01	0.05
CuO	0.019	0.017	0.018	0.021	0.022	0.060
MnO	0.22	0.17	0.20	0.23	0.15	0.17
Total	100.13	99.99	100.25	100.06	100.10	100.22
Sp.Gr†	2.99	2.95	2.96	3.03	2.87	2.87
Total Fe as FeO	14.71	12.04	13.15	14.52	11.89	12.00
Cu	0.015	0.014	0.014	0.017	0.018	0.048
MgO/FeO‡	0.319	0.534	0.359	0.417	0.614	0.604
	T1370	T1399	T1413	T1501	T1522	T1716
Norms						
Quartz	7.26		3.54	1.62		
Orthoclase		6.67	1.11	2.78	2.78	4.45
Albite	23.06	28.82	31.96	29.34	20.44	22.53
Anorthite	23.63	26.13	21.96	16.12	36.97	30.58
Diopside						
Wo	10.56	4.52	8.70	12.53	4.06	5.34
En	9.10	3.90	7.50	10.80	3.50	4.00
Fs						0.79
Hypersthene						
En	2.70	8.40	4.30	4.40	13.00	7.60
Fs		0.26				2.11
Olivine						
Fo		2.66			1.26	4.48
Fa						0.61
Apatite	1.01	0.67	1.01	1.01		0.67
Ilmenite	6.69	4.41	6.08	6.69	3.65	4.26
Magnetite	5.57	10.67	10.90	8.82	9.98	8.82
Hematite	7.36		0.32	3.68	1.12	
Pyrite		0.12	0.12			

TABLE 14—*Continued*

	T1370	T1399	T1413	T1501	T1522	T1716
Norms—*Continued*						
Calcite	0.50					
Chalcopyrite						0.15
Water	2.85	2.86	2.79	2.21	3.01	4.06
Total	100.09	100.29	100.29	100.00	99.77	100.45
Plagioclase composition	An_{40}	An_{47}	An_{41}	An_{35}	An_{44}	An_{57}
Modes (weight per cent)						
Plagioclase	39.4	62.2	51.1	42.7	43.9	43.0
Pyroxene	12.4	12.7	17.5	22.7	21.6	16.8
Olivine	0.7	4.2			7.4	10.8
Ilmenite, magnetite	21.3	10.2	21.8	13.9	25.4	19.6
Epidote, chlorite	22.5	10.7	8.3	10.0	1.7	9.8
Apatite			tr.	0.3		
Prehnite				10.3		
Quartz	3.7		1.3	0.1		
Total	100.0	100.0	100.0	100.0	100.0	100.0
Plagioclase composition	An_{31}	An_{49}	An_{19}	An_{9}	An_{35}	An_{53}

* Samples obtained from diamond drill hole C & H 28. Analyses by L. C. Peck, Rock Analysis Laboratory, University of Minnesota. All depths are measured to the middle of the horizon sampled. The flow is 402 feet thick.

† Specific gravity at 4°C. Determinations were made by Norman Davidson, Geochemistry and Petrology Branch, U. S. Geological Survey.

‡ Total Fe calculated as FeO.

erately amygdaloidal and coarser-grained than the adjacent ophitic basalt. In the "Big" trap, for example, the plagioclase laths of the pegmatitic facies average 2 times as long and 2½ times as thick as those of the ophitic andesite-basalt, and the interstitial grains of pyroxene, ilmenite, magnetite, chlorite, and other minerals are correspondingly coarser. The texture is only locally ophitic. Pyroxene grains occupy the interstices between plagioclase laths in the same manner as in the ophitic basalt, but each interstitial grain has a different orientation.

(e) *Structure:* In the lowermost pegmatitic layers of the Greenstone flow, the pronounced planar structure is due to a preferred orientation of the plagioclase laths with the long axes parallel to the plane of the layer. No linear parallelism has been noted.

(f) *Composition of plagioclase:* The plagioclase of the pegmatitic facies is albite or albite-oligoclase, but that of the ophitic basalt is labradorite or labradorite-bytownite.

(g) *Chemical composition:* H_2O plus, P, Ti, S, Fe, Cu, Mn, Na, K, and Si tend to be concentrated in the pegmatitic facies whereas Al and Mg are deficient as compared with amounts present in the adjacent ophitic basalt. Variations between pegmatitic facies and adjacent ophitic basalt are only slight in some cases. The ophitic basalt of the pegmatitic zone contains more Fe, Mn, Cu, Ti, Na, K, Si, and volatiles, and less Mg and Al than that of the underlying ophitic basalt zone.

The ratio of MgO to total Fe calculated as FeO, and the amount of normative olivine where present, increase downward in the suc-

cessive pegmatitic layers, and in the intervening ophitic basalt. In the pegmatitic zones of the "Big" trap and in the upper part of the Greenstone, normative quartz decreases in amount downward.

(h) *Alteration and mineral concentrations:* Deuteric alteration, especially of plagioclase, is much more intense in the pegmatitic facies than in the ophitic basalt. Quartz, prehnite, chlorite, epidote, sericite, calcite, analcime, ilmenite, magnetite, apatite, native copper, and copper sulfides are concentrated in the pegmatitic facies.

(i) *Localization of deuteric alteration and aplite dikes:* In the Greenstone flow at Cliff, intensity of deuteric alteration increased toward the top of the pegmatitic zone; aplite dikes and interstitial granophyric segregations are confined to the upper portion. Elsewhere in the Greenstone, aplite dikes have also been found near the base of the pegmatitic zone.

3. *Nonpoikiliticly included plagioclase.* Plagioclase crystals and phenocrysts that are not poikiliticly included in pyroxene crystals are present throughout the ophitic parts of the flows.

4. *Graded layering of ophitic basalt.* Near the base of the Greenstone at Allouez, the ophitic basalt is locally layered. The layers, ranging from less than 1 to 12 inches thick, typically have coarse poikilitic grains at the base grading upward to finer poikilitic grains, and have a sharp contact at the top (Pl. 2, figs. 1, 2). The layers appear to be a phenomenon brought about by the differential settling of varying sizes of poikilitic grains, analogous to graded bedding in sediments.

5. *Concentrations of minerals in the ophitic basalt.* (a) Normally *olivine* is concentrated a short distance above the base of the flow. Olivine is also concentrated in certain zones in the ophitic basalt of the pegmatitic zone, especially in the Greenstone flow (Fig. 3) where there is a pronounced and steady downward increase in the amount of olivine in the ophitic basalt of the pegmatitic zone from none at the top of the zone to more than 20 per cent at the bottom, a trend similar to that in the underlying ophitic basalt zone.

(b) Most of the flows studied have a moderate concentration of *pyroxene* near the base of the flow.

(c) *Plagioclase* is most abundant in the upper part of the ophitic basalt zone above the concentrations of olivine and pyroxene.

6. *Syngenetic copper deposits.* The amygdaloid of the Greenstone flow at Cliff was found to be mineralized with chalcocite and specular hematite. This concentration seems to represent the culmination of an increase in sulfur and ferric iron toward the top of the flow, and is therefore regarded as syngenetic.

Process of Differentiation

The writer believes that at least the first three and perhaps all of the following were primary factors in differentiation of the flows studied: (1) cooling at a moderate rate, and predominantly from the top; (2) differential settling of plagioclase, olivine, and ophitic pyroxene crystals; (3) local concentration of volatiles and transport of materials by migration of the volatiles; (4) periodic convective overturn of the magma during the later stages of crystallization. Two hypotheses appear plausible: Hypothesis A, based on the consideration that convective overturn was important, hypothesis B on the assumption that it was not.

HYPOTHESIS A: The steady increase of the proportion of magnesia to total iron calculated as FeO in the successively deeper pegmatitic layers, and in the intervening ophitic basalt, and other facts about the pegmatitic zone suggest that the order of formation of the pegmatitic layers, and of the intervening ophitic basalt, was from the bottom to the top of the zone in which they occur.

The much thicker upper chill zones of all the flows studied indicates that cooling from the tops of the flows was more rapid than from the bottoms, especially after the early stages of solidification. Cooling from the top, by increasing the density of the upper portion of the magma, would favor the development of convection currents; the uppermost magma, furthermore, being cooler than the underlying magma, would crystallize more rapidly, and therefore contain a greater proportion of crystalline material.

Perret (1913), describing the circulatory system in the Halemaumau lava lake, has presented convincing evidence that the convection currents are caused by the descent of heavier,

cooled, semisolid surface lava, and that the lava, in fact, quite commonly moves down at a point where large bubbles of gas are moving up. Grout (1918b, p. 495) has suggested that the cooler magma (heavier both because of its greater density and because it contains abundant crystals) along the margins of intrusives like the Duluth gabbro may sink and move along the floor of the intrusive, inducing convection currents that aid in crystal sorting and cause banded layering. More recently, Hess (1938), Wager and Deer (1939), and Wahl (1946) have suggested that convection currents may be active in magmas.

Assuming that convection currents were active, the following successive stages are postulated:

(1) Lava, carrying scattered intratelluric crystals of plagioclase and olivine, is extruded and comes to rest on a nearly horizontal land surface.

(2) Cooling and crystallization progress inward from top and bottom. Crystals of olivine, plagioclase, and poikilitic pyroxene form and settle differentially. Volatiles, coming out of solution, stream toward the top. Differential crystal settling causes a moderate concentration of pyroxene and a marked concentration of olivine in the ophitic basalt forming near the base of the flow. A moderate concentration of plagioclase is taking place toward the middle of the flow owing to an accumulation of nonpoikilitically included crystals.

(3) The flow is now about half solidified. The lower part is ophitic basalt; the upper part is magma overlain by a rather thick chill zone of fine-grained, amygdaloidal basalt, grading downward into fine-grained ophitic basalt. At this stage, most of the cooling is from the top and crystallization is more rapid there, too. At the top, therefore, a cooler, viscous layer of magma forms, which contains abundant crystals and becomes increasingly heavier than the underlying magma. This liquid contains more dissolved volatile material because it is cooler. According to Bowen (1928, p. 299), a drop of 50°C. in the temperature of the melt may increase the solubility of volatiles by as much as 1 per cent of the total mass. The increased amount of volatiles in solution in the upper layer, although not greatly changing its density, permits a greater temperature gradient between it and the underlying magma without complete crystallization and freezing to the roof.

Perret's (1913) observations indicate that vapors, coming out of solution as crystallization proceeds, will bubble through the cooler upper layer of magma at the top of the chamber, and form a gaseous layer between it and the roof. If there is an avenue of escape, as there probably was from time to time during the solidification, the gases escape to the surface, forming fumaroles. In fact, as crystallization proceeded, the pressure of the gas in this layer may have increased until it pushed the roof up. If the roof cracked, the gases could escape. It is thus presumed that gases collected and escaped intermittently during crystallization.

(4) Because cooling of the magma column at this stage is predominantly from the top, the upper layer of magma becomes sufficiently denser than the underlying one to overcome the resistance due to viscosity and there is a convective overturn. The cooler, viscous magma, containing abundant crystals and a higher-than-average dissolved gas content, flows to the bottom. Quite probably, when the cooler layer flows downward at one point it will suck down the upper magma over quite a large area (Perret, 1913, p. 343) and induce currents at other points, so that currents are simultaneously active over the whole extent of the thicker parts of the flow.

(5) Hot magma now near the top gradually cools. New crystals grow in this cooling magma and settle differentially, forming a layer of ophitic basalt above the viscous mush that has settled by convection from the top. Olivine is still crystallizing from the magma at this stage in some of the flows at least. Because of stirring of the magma (stage 4), the crystals now settling differentially become sorted according to their sizes and densities as they approach the base of the magma column (Hess, 1938). Olivine, the densest, is concentrated near the base of the layer of ophitic basalt now forming. The olivine concentration may be enhanced at this stage because of an increase in its rate of crystallization. The liquid that is at the top of the magma column after the first convective overturn was originally near the center, or hottest, part of the flow and is probably relatively undifferentiated because crystallization has

been slight in that zone. In its new, cooler environment this liquid starts to crystallize and olivine forms at a rate comparable to that during the early stages when the olivine concentration near the base of the flow formed.

Crystallization in the viscous mush will cease for a time because of its new, warmer environment and the very slow rate of cooling from below. The interstitial liquid of the immediately overlying ophitic basalt, having a somewhat lower volatile content will have become essentially solid before crystallization starts again in the underlying mush. When crystallization does begin in the underlying mush, the volatiles start coming out of solution. They can not escape, however, because of the overlying layer of newly-formed ophitic basalt. Therefore they collect in the top of the mush, alter the plagioclase from labradorite to albite-oligoclase, and cause the formation of epidote, chlorite, prehnite, quartz, and apatite[2]. In this way the volatiles are used up and a pegmatitic layer is formed.

(6) Stages 4 and 5 are repeated successively until the flow has solidified. The uppermost pegmatitic layers contain interstitially a residual liquid rich in silica and a vaporous solution (Fenner, 1933; Morey and Ingerson, 1940). The silicic residual liquid forms interstitial granophyric intergrowths and aplitic dikes. The vapor reacts with the crystalline material and forms amygdaloidal fillings.

Throughout the crystallization of the flow, volatiles containing Fe and Cu may have escaped intermittently through the upper chill zone. Where the conditions of temperature and composition were right (as in the Greenstone at Cliff), deposits of earthy and specular hematite, chalcocite, chalcopyrite, and native copper were formed in the amygdaloid.

HYPOTHESIS B: If convection currents were not active in the flows, Stages 1 and 2 will be the same as in Hypothesis A. Cooling will again be predominantly from the top during the greater part of the solidification of the flow, increasingly so as time goes on. Therefore a temperature gradient is established, the temperature increasing from the top to the bottom of the magma column.

As the magma at the top cools, it takes increasing amounts of volatiles into solution. Crystallization proceeds in all parts of the magma simultaneously. The upward-streaming gas bubbles enrich the upper magma in iron and other more volatile constituents. Therefore, because of a temperature and composition gradient in the magma, crystals forming at the top have a slightly different composition from those forming at the bottom. Crystal settling s inhibited and finally stopped by the increasing proportion of crystals in the magma.

Volatiles may escape intermittently through fractures in the upper chill zone, especially in the earlier stages of solidification. At times, however, vapors become concentrated in the magma at the base of the solid roof. This vapor-rich crystal mush will not solidify completely until some time after the underlying mush because of the lower freezing point of its late fractions. Consequently a solid floor will form beneath a layer of volatile-rich crystal mush, which will solidify sometime later to form a pegmatitic layer.

As crystallization continues in the main body of magma, volatiles stream upward, concentrating beneath the new and lower roof. The process outlined is repeated and another pegmatitic layer is formed, and so on until the last pegmatitic layer solidifies near the middle of the flow. The composition of the residual magma at the center of the flow is in some flows (viz. the Greenstone) such that olivine crystallizes in abundance to form olivine-rich basalt.

Summary

The writer believes that either or both of the hypotheses presented may be correct. It is possible that there was convective overturn in the thicker flows and not in the thinner flows. The magma column may have been too thin and the rate of cooling too rapid for convection in the thinner flows. In the thicker flows, too, the magma column in the late stages of solidification may have been too thin for convective overturn.

[2] Bowen (1933) states that anorthite and pyroxene are unstable in the presence of high concentrations of volatiles in gabbroic Wagma, and that albite is stable. Anorthite yields to albite; anorthite plus Fe-rich pyroxene to epidote and chlorite, and in an excess of volatiles to zeolites, datolite, and thaumasite.

In the flow at South Range quarry, the layers probably formed successively downward at least in the upper part of the pegmatitic zone. Crosscutting pegmatitic veins seem to follow vertical joints and connect one tabular layer with another. The layers are successively closer spaced toward the top, and at the top is a zone of coalescing amygdaloidal ophitic basalt, separated from the overlying fragmental amygdaloid by a sharp contact. The ophitic basalt increases in grain size downward and is intensely altered, especially toward the top of the zone, so that it approaches the pegmatitic facies in mineral composition. None of these features have been noted in the other flows studied. Irregular pegmatitic patches, in places elongated in a plane not parallel to the base, have been noted in all of the flows.

In the Greenstone flow, the residual, interstitial liquid in the upper pegmatitic layers had a granophyric composition. It probably remained fluid long after the rest of the rock solidified, since its temperature of solidification may have been as low as 750°C. This residual liquid crystallized interstitially in the upper pegmatitic layers and invaded the surrounding rock along joints, thus forming aplitic dikes. Crosscutting aplitic dikes have been found throughout the pegmatitic zone, but interstitial granophyre has been found only in the upper pegmatitic layers. These aplite dikes are similar in composition and probably in origin to those in the Palisades sill described by Walker (1940), at Goose Creek, by Shannon (1924) and at North Ulfo, Sweden by von Eckermann (1938). The aplites of the Greenstone flow, however, contain more potash and iron, and less soda and silica.

The presence in the lowermost pegmatitic layers of the Greenstone flow of a pronounced planar structure (already described) must be explained, and the explanation may be different under the two hypotheses. There was evidently deformation in connection with the formation of the planar structures. The plagioclase occurs as idiomorphic laths, as in the ophitic basalt, and interstitial grains of pyroxene and other minerals are present. The individual grains of pyroxene, however, vary somewhat in orientation. It is quite common to find a group of such grains that may have once constituted a single ophitic augite crystal. The individual grains are now oriented in only slightly varying directions, as though a larger crystal had been broken up after formation.

Structural data indicate regional disturbances before and after the extrusion of the Greenstone. If such a disturbance occurred when the lowermost pegmatitic layers were still unsolidified—but surrounded by solid ophitic basalt above and below—the differential movement of the overlying and underlying solid rock probably would have developed a planar structure in the pegmatitic facies.

Another possible explanation of the planar structure is that, while the pegmatitic layer still contained interstitial liquid and vapor, cracks may have opened along that horizon or across the adjacent ophitic basalt, and the liquid and vapor may have been partly squeezed out of its original position by the pressure exerted by the weight of overlying rock. The thinner portions of the flow must have been completely solid by this time, and joints that were developing because of contraction due to cooling may have extended into the thicker part of the flow. The planar structures would have been most pronounced in the lower pegmatitic layers because they were subjected to the greatest load of overlying rock.

These methods are applicable under either hypothesis. In addition, if there were convection currents (hypothesis A), the planar structure may have been developed in the viscous mush of magma and crystals when it flowed down from the top and along the floor of the magma chamber. The preferred orientation of the plagioclase laths may have been more pronounced in the lower pegmatitic layers because the magma chamber was larger at the time, and stronger currents were consequently developed.

Differentiation at Depth

Variation in the Lava Series as a Whole

Broderick (1935) obtained composite samples of 12 mafic to intermediate Keweenawan flows, two felsite bodies (one probably a flow), and a syenodiorite (orthoclase gabbro). The stratigraphic thickness from the lowermost to the uppermost flow sampled is more than 10,000 feet, extending both below the "Big" trap and above the Greenstone flow.

TABLE 15.—NORMS OF REPRESENTATIVE LAVAS OF THE KEWEENAWAN SERIES IN MICHIGAN

Textural classification / Mineralogical classification	(1) ophite basalt	(2) ophite basalt	(3) glomeroporphyrite basalt	(4) glomeroporphyrite andesite	(5) glomeroporphyrite andesite
Quartz		2.16			
Orthoclase	1.67	3.34	3.89	7.78	6.67
Albite	20.96	23.06	23.58	31.96	28.87
Anorthite	33.64	30.58	29.75	23.35	27.80
Diopside	10.07	12.17	8.86	7.29	5.31
Hypersthene	16.35	15.34	12.00	4.19	9.61
Olivine	4.48		3.22	9.68	5.74
Magnetite	5.80	6.73	8.35	8.12	11.60
Hematite			2.08		
Ilmenite	2.74	2.89	2.43	3.19	
Apatite	0.37	0.44	0.30	0.44	
Calcite	0.40	0.43	1.55	0.20	

Textural classification / Mineralogical classification	(6) melaphyre basalt	(7) melaphyre andesite	(8) melaphyre andesite	(9) felsite rhyolite
Quartz	0.84	1.02	4.86	30.30
Orthoclase	1.67	12.79	7.23	48.37
Albite	20.44	24.63	37.73	18.34
Anorthite	33.64	20.85	10.56	
Corundum				0.71
Diopside	15.28	8.99	7.53	
Hypersthene	14.83	12.98	11.77	
Magnetite	7.19	10.21	9.05	0.70
Hematite				0.96
Ilmenite	2.58	4.71	6.08	
Apatite	0.40	0.84	0.91	
Calcite	0.39	0.32	1.02	

(1) Analysis 3095 (Broderick, 1935, p. 536).
(2) Kearsarge flow average (Broderick, 1935, p. 523).
(3) Analysis 3110 (Broderick, 1935, p. 536).
(4) Analysis 3103 (Broderick, 1935, p. 536).
(5) Analysis 2a, Pewabic flow (U. S. Geol. Surv. Prof. Paper 144, 1929, p. 37).
(6) Analysis 3091 (Broderick, 1935, p. 536).
(7) Analysis 3129 (Broderick, 1935, p. 536).
(8) Analysis 3104 (Broderick, 1935, p. 536).
(9) Analysis 3159 (Broderick, 1935, p. 536).

In considering the evidence of a cyclic change in the composition of the magma extruded, he said (1935, p. 553–554):

"In the case of certain of the extensive and best known sediments, characteristically felsite conglomerates, the immediately preceding flow, or group of flows, is of an intermediate type, known as glomeroporphyrite. The immediately succeeding flow is an ophite. As examples, may be mentioned the Allouez and Kearsarge conglomerates and the Wolverine sandstone.

"In these cases and others, including Conglomerates No. 3 and No. 8, the immediately succeeding ophites are exceptionally thick and in many places doleritic [pegmatitic]. Examples of the doleritic ophites which succeed sediments are The Greenstone, St. Louis (Big) Trap, and the flow above the Kearsarge Conglomerate."

The ophitic basalt of the Baltic flow overlies the No. 3 conglomerate, the Kearsarge ophitic basalt overlies the Wolverine sandstone, and the Isle Royale ophitic basalt is part of an

TABLE 16.—MODES IN WEIGHT PER CENT IN FLOWS ABOVE THE GREENSTONE

Textural classification / Mineralogical classification	(1) ophite basalt	(2) ophite basalt	(3) ophite basalt	(4) glomeroporphyrite dacite
Quartz				3.7
Plagioclase	24.9	43.6	52.8	58.6
Pyroxene	14.3	13.0	14.9	1.9
Olivine	43.2	36.5	11.9	8.1
Ilmenite, magnetite	0.5	2.6	1.6	11.4
Chlorite	16.5	4.1	18.1	16.3
Calcite	0.6	0.2	0.5	
Prehnite			0.2	
Total	100.0	100.0	100.0	100.0
Plagioclase composition	An_{60}	An_{55}	An_{55}	An_{10}

Textural classification / Mineralogical classification	(5) glomeroporphyrite Sodic andesite	(6) melaphyre andesite	(7) melaphyre andesite
Quartz		2.6	0.9
Plagioclase	67.3	64.6	71.4
Pyroxene	1.9	16.7	8.8
Olivine	10.8	1.4	
Ilmenite, magnetite	12.1	9.3	10.0
Apatite		0.1	0.8
Chlorite	7.9	5.3	8.1
Total	100.0	100.0	100.0
Plagioclase composition	An_{8}	An_{40}	An_{40}

ophitic basalt series overlying the No. 8 conglomerate.

Broderick also suggests that the felsite conglomerates may have formed by the breaking up of viscous, rhyolitic flows that plugged the volcanic vents, temporarily causing a hiatus in the volcanic extrusions. A typical volcanic cycle, then, would begin with the extrusion of mafic lava, which would be followed by andesitic and rhyolitic lavas.

The norms and modes of flows, selected at scattered points across the entire stratigraphic section (Tables 15, 16), illustrate the relationship between textural characteristics of a flow and its composition. The modes in Table 16, from thin sections of flows above the Greenstone, represent all the main types of rocks. The thin sections of olivine-rich ophitic basalt (analyses 1 and 2) came from two isolated outcrops about 10 miles apart. Both occur a short distance above one of the melaphyres (Table 15, analysis 8) analyzed by Broderick and probably represent a single flow.

The glomeroporphyrites are the most undersaturated of all the rocks, and have a rather wide range in composition, the more calcic varieties overlapping the ophites both in composition and in texture. The "Big" trap and the rock of analysis 3 of Table 15 are examples of the more calcic glomeroporphyrites. The more sodic glomeroporphyrites (sodic andesites and dacites) are characterized by sodic plagioclase and rather abundant olivine (Tables 15 and 16, analyses 4 and 5). The more sodic glomeroporphyrites resemble the ophitic basalt near the middle of the Greenstone (Fig. 8, analysis 3146; Fig. 3, analysis 4–506) with their higher alkali content and abundance of olivine.

The melaphyres tend to be somewhat more silicic than the ophites and glomeroporphyrites,

containing, for the most part, small amounts of free quartz, and little or no olivine. The felsites and felsite conglomerates, constituting only a small fraction of the entire section, are contrasted with the other types of rocks by their extremely silicic character.

General Trends in the Distribution of Elements

In the felsites, as in the aplites within the Greenstone flow, there is a marked concentration of Si and K, no great change in Na, and a deficiency in all other elements. The composition of the felsites and aplites is thus sharply contrasted with that of the nearest genetically related type of rock.

In the remainder of the flows, which constitute the bulk of the section, the more silicic facies generally contain greater amounts of Fe, Mn, Ti, P, S, Cu, Na, and K, and smaller amounts of Ca, Al, and Mg (as within the Greenstone and "Big" trap). However, the proportions of some of these elements—Fe, Mn, Ti, P, S, and Cu—increase only to a certain stage, characterized by sodic glomeroporphyritic andesites and dacites, fine-grained andesites and dacites, and pegmatitic facies; the proportions then fall off sharply in amount in the more siliceous aplites and felsites. It seems reasonable to conclude, therefore, that the copper solutions, whether they formed epigenetic or syngenetic deposits, were concentrated in, and derived from intermediate or rather mafic magmas, and not from the most siliceous magmas that formed the felsites.

Comparison with Greenstone Differentiates

The felsites and felsite conglomerates are similar to, though somewhat more siliceous than, the aplites of the Greenstone. They constitute a small fraction of the total thickness of the section, analogous to the small amount of aplite in the Greenstone as compared to the entire flow. If the conglomerates in upper part of the series are included, however, the proportion of felsitic rock in the section is considerably increased. The sodic glomeroporphyrites (sodic andesites) resemble the pegmatitic basalt near the base of the pegmatitic zone in the Greenstone, and the ophitic basalts of the region can be compared to the ophitic basalt of the ophitic basalt zone in the Greenstone. The olivine-rich ophitic basalt of Table 16 resembles (although it contains more olivine) the olivine-rich ophitic basalt near the base of the Greenstone (Table 7, sample 3–407; Fig. 3), and some of the melaphyres approximate the Greenstone chill zone in composition.

All types of flows present in the lava series, therefore, can be duplicated by differentiation products of the Greenstone, and the proportions of the different types present in the series below the conglomerates in the upper part of the series and in the Greenstone seem roughly comparable. Thus the processes of differentiation responsible for the variety of rocks in the Greenstone could likewise explain the several types of flows. It is difficult, however, to explain repetitions of the different types of flows by simple fractional crystallization, a process that appears to have been important in the Greenstone. Furthermore, if one considers that the parent magma was a basalt, similar to the Greenstone in composition, the more mafic olivine-rich ophitic basalt (similar to analyses 1 and 2 of Table 16) would have formed as a result of differential crystal settling, and should never have been extruded as magma.

Possibly, however, the olivine-rich basaltic magma contained intratelluric crystals of olivine when it was extruded (Bowen, 1947, p. 270). Field data indicate that the lava was quite viscous when it flowed out. The olivine-rich basalt occurs at scattered localities for a strike length of 10 miles. In the individual occurrences, however, the flow is thick (up to 150 feet), and has a short strike length (500 to 1000 feet).

Although the differentiation of the Greenstone demonstrates that it is possible to obtain contrasted types of lava from a primary basaltic magma, it is also possible that the different types were generated at different levels in the earth's crust, and were successively extruded from great depths (Kennedy and Anderson, 1938; Buddington, 1943). The Michigan copper district presents a real opportunity for further study of this intriguing problem.

Origin of the Copper Deposits

Hypotheses

Geologists generally agree that the Michigan copper deposits are genetically related to the

igneous extrusives and intrusives that underlie a large part of the Lake Superior basin. The exact nature of that relationship is, however, still open to debate.

At present, the following hypotheses of origin of the deposits are still open to consideration: (1) The deposits are epigenetic and formed by deposition from hot, ascending solutions (Butler, Burbank, *et al.*, 1929; Broderick, Hohl, and Eidemiller, 1946). (2) The deposits were formed by a combination of syngenetic and epigenetic processes (Lindgren, 1933, p. 523–525). Primary concentrations of copper from fumaroles, thermal springs, or playa lakes on the lavas were later reworked by hot, ascending solutions. (3) The amygdaloidal deposits are primarily syngenetic.

The Michigan copper deposits doubtless formed in part at least by deposition from ascending solutions after the lavas and interbedded sediments had been at least moderately tilted. Two unknown factors are the nature of the solutions, and the source of the copper. The supporters of a purely epigenetic origin, that postulates deposition from ascending solutions, have assumed that the solutions emanated from an underlying intrusive and that the copper was in the solutions when they left the intrusive. The writer prefers the theory that ascending, hydrothermal solutions dissolved primary copper syngenetically concentrated in certain amygdaloids and sediments within the lava series and redeposited the copper, on cooling, to form commercial deposits.

Why does the Michigan copper occur largely in the native state? Most of the important copper deposits in the world consist primarily of copper sulfides. The advocates of a direct magmatic source maintain that copper sulfide solutions emanated from a buried intrusive, and that the sulfur was oxidized by the ferric oxide in the permeable amygdaloids and conglomerates through which the solutions ascended. On cooling, the solutions precipitated native copper.

This hypothesis does not explain at least one important fact: that some of the copper crystallized out of the flows as they solidified, and this copper, too, is mostly native. Both Broderick (1935; Broderick and Hohl, 1935) and the writer found that small amounts of copper are systematically distributed through the flows studied and concentrated in the pegmatitic facies along with other relatively volatile constituents (Fig. 7). This copper was not deposited from copper sulfide solutions that had percolated through the rocks rich in ferric oxide, and yet, in a study of several dozen polished sections, the writer has found that most of it is native copper. The epigenetic theory is thus weakened by the fact that some native copper formed in the Michigan copper district without the aid of magmatic sulfide solutions from a source at depth and without the need of oxidizing the solutions.

The writer prefers the theory that all the copper is native because it crystallized from a solution or liquid that was deficient in sulfur. This theory was favored by Lindgren (1933, p. 418). It is more than a coincidence that, of 17 occurrences of native copper in various parts of the world cited by Butler and Burbank (1929, p. 142–146), 13 occur in the amygdaloids of basaltic lavas. The writer believes that a unique factor, common to lavas in general, accounts for the world-wide association of native copper deposits with basaltic lavas. This unique factor may well be the rapid dissipation of much of the sulfur in a gaseous state as the lava cools at pressures close to atmospheric (Lindgren, 1933, p. 418). Evidence that considerable sulfur boils off at an early state in the consolidation of lava is found in the Michigan copper district and elsewhere.

In the Greenstone flow at Delaware (Pl. 1, loc. 1), the upper chill zone from a depth of 52 to 71 feet (Table 2) contains abundant disseminated pyrite. The fine-grained basalt of the upper chill zone extends to a depth of 176 feet, but no disseminated pyrite is visible below a depth of 71 feet. Broderick's (1935) chemical analysis of the entire upper chill zone is abnormally high in sulfur (Fig. 7), but the sulfur content near the top is probably notably higher than that of the lower part. By examination of outcrops, the writer found that visible disseminated pyrite is likewise concentrated in the upper part of the upper chill zone at Cliff (Pl. 1, loc. 10), and the amygdaloid is mineralized with chalcocite. No signs of mineralization were found along columnar joints that cross the upper chill zone at Cliff; the metallic minerals are in the solid rocks. The fact that the entire upper chill zone of the Greenstone is abnormally high in sulfur indicates that sulfur boiled out of the flow during solidification. The high pyrite

content of the upper part of the upper chill zone, plus the lack of mineralized joints crossing the chill zone where the pyrite occurs, indicates that the sulfur boiled out most rapidly during the early stages of solidification, before the columnar joints had formed.

The Greenstone is the only known flow in the Michigan copper district with pyrite and high sulfur in its upper chill zone and chalcocite mineralization in its amygdaloid. Probably, because of the extraordinary thickness of the Greenstone, the upper chill zone started to freeze before much sulfur had boiled off from the main body of lava. Consequently a large proportion of the sulfur that volatilized and streamed upward through the lava was trapped and deposited in the upper chill zone rather than escaping into the atmosphere, as may have happened with the more normal thinner flows.

Krauskopf (1948) has described the rapid escape of water vapor and sulfur gases by vesiculation as the basaltic lava approaches the surface in the central conduit of Paricutin volcano. Great quantities of gas are emitted from the crater of the volcano, and lava with little gas is simultaneously emitted from fissures near the base of the cone. SO_2 is prominent in the gas from the crater, whereas the small amount of gas emitted from the fissures with the lava contains almost no sulfur, but is rich in HCl. Krauskopf postulates that the lava nearly fills the central conduit, that the lava vesiculates violently in the conduit, and that the less soluble gases (notably the sulfur gases) escape so that the liquid that is ultimately extruded at the vents contains only small amounts of more soluble gases (notably HCl).

The hypothesis that native copper forms where an igneous body solidifies at low pressure and copper sulfides normally form where an igneous body solidifies at moderate to high pressure can be tested by comparing basaltic lavas and genetically associated diabase sills and dikes (Butler and Burbank, 1929, p. 145). In an area near Coppermine River in the Canadian Arctic, native copper occurs uniformly disseminated through individual flows of large extent, whereas copper sulfides occur disseminated through massive sills of diabase, which probably came from the same magma.

If sulfur volatilizes and escapes at low pressures, the sulfur content of basaltic lavas should be less than that of genetically related diabase and gabbro intrusives. The writer has compared the sulfur content of basaltic lavas in the Michigan copper district with that of the Duluth gabbro and of two diabase sills at Duluth. Very little information has been published on the sulfur content of the Duluth gabbro, but two analyses of typical gabbro published by Grout (1918c, p. 646) ran 0.03 per cent and 0.11 per cent S respectively. Three diabase samples (Schwartz and Sandberg, 1940, nos. 1, 3, 14, p. 1144), furnished to the writer by Schwartz, contain 0.04, 0.05, and 0.10 per cent sulfur (analyst, Charlotte M. Warshaw, U. S. Geological Survey). The average for the 13 available composite analyses of basaltic lavas in the Michigan copper district is 0.015 per cent S. Each of the flows sampled averaged less than 0.02 per cent S except the Greenstone, and in the Greenstone sulfur apparently was trapped in the upper chill zone because of the great thickness of the flow.

Another question to be considered is: Did the molten lavas contain enough copper to supply the ascending solutions adequately? To get an idea of the probable range in the primary copper content of the lavas we will consider the composite analyses of the relatively thin flows sampled by Broderick (1935). In using these analyses, we assume that the thin flows chilled rapidly and solidified before much copper escaped with the volatiles.

Three fine-grained flows range from 0.023 per cent to 0.038 per cent copper. A fourth fine-grained flow contains 0.002 per cent copper. The latter flow, along with two thick, fine-grained flows that contain 0.003 per cent copper, occur stratigraphically low in the Keweenawan series, and their low copper content may be related to their stratigraphic position. Two relatively thin, glomeroporphyritic flows contain 0.002 per cent and 0.022 per cent copper respectively. These analyses indicate that the primary copper content of the lavas ranges from almost none to around 0.04 per cent.

Three thick, relatively coarse-grained, ophitic flows, sampled compositely, ranged in copper content from 0.008 per cent to 0.012 per cent. The copper content of these flows is low and

nearly the same for each flow. If these flows originally contained 0.023 per cent to 0.038 per cent copper, like the thin flows mentioned above, they must have lost some two-thirds of it, presumably by boiling out with the volatiles.

The Kearsarge flow, whose amygdaloid is commercially mineralized for a strike-length of 6 miles, is one of the thicker, ophitic flows whose primary copper content is low (0.009 per cent). The flow was compositely sampled (Broderick, 1935; Broderick and Hohl, 1935) in the commercially mineralized zone where the flow is about 190 feet thick. The writer determined the average copper content per square foot of lode area in the commercially mineralized zone, and distributed this copper through a column of Kearsarge rock with dimensions of 1 square foot by 190 feet (the thickness of the flow). To this figure was added the primary copper content of 0.009 per cent determined by Broderick (1935). The average copper content obtained by the above method was 0.043 per cent, only slightly higher than the highest values in the thin flows. It is thus quantitatively possible that the Kearsarge lode was mineralized by pure syngenetic processes with copper derived from the immediately subjacent flow. Other evidence indicates, however, that much of the commercial copper was deposited from, or at least reworked by, hydrothermal solutions.

The writer has shown (1) that the native state of the copper is most readily explained by assuming that the copper was originally a primary constituent of the lavas themselves, and (2) that the amount of copper in the original lava, if accumulated into top top, is quantitatively adequate to explain the concentration in one of the principal ore deposits. The following facts also suggest the importance of syngenetic processes:

(1) The distribution of primary copper in the pegmatitic flows studied by Broderick (1935; Broderick and Hohl, 1935) and the writer, and its concentration along with other relatively volatile elements in the pegmatitic facies, suggests that it was deposited by syngenetic processes in the thicker flows.

(2) In the amygdaloidal deposits, copper is commonly concentrated in the sparsely cellular, relatively impermeable basal portion of the amygdaloid in preference to the more permeable fragmental portion above, and in places the fine-grained rock for 10 feet or more below the amygdaloid contains fine specks of disseminated copper and scattered vesicles filled with copper.

(3) Chemical analyses (Broderick, 1935) show that the fine-grained basalt just below the Kearsarge amygdaloid and the pegmatitic facies both contain greater amounts of the relatively volatile elements than the main body of the flow. The relatively volatile elements, including copper, were probably concentrated by syngenetic processes.

(4) Chalcocite was deposited in the amygdaloid of the Greenstone flow at Cliff, and evidence that this mineralization is syngenetic has been presented.

(5) The two largest amygdaloidal deposits of the district, the Baltic and Kearsarge lodes, occupy the amygdaloids of thick ophitic flows similar in composition to the pegmatitic flows; in the Kearsarge, for which data on thickness are available, the deposit occurs where the flow is thickest. Probably the primary copper was carried to the tops of these relatively coarse-grained, slow-cooling flows by volatile transfer during crystallization. The transfer of copper would have been most pronounced where the flows are thickest.

Conclusions

The potential importance of syngenetic processes in forming at least primary concentrations of copper in the Michigan copper district must be recognized. A world-wide association of native copper with basaltic lavas suggests that some factor common to lavas causes the formation of native copper in preference to copper sulfides. The writer suggests that lavas lose more sulfur by volatilization than intrusive bodies because of the low pressure at which they solidify. Native copper may form in lavas, in preference to sulfides, because there is a deficiency of sulfur. If this hypothesis is valid, the native state of the copper indicates that its immediate source is the lavas in which it occurs, rather than a subjacent intrusive from which the copper was emanated in hydrothermal solution.

Evidence has been presented that there was a concentration of copper in the pegmatitic facies during the solidification of the flows. It has also been shown that copper was probably concentrated by syngenetic processes in the amygdaloid of the Greenstone flow at Cliff. The writer postulates that primary concentrations of copper, either as native copper or as unstable copper salts, formed in the amygdaloids of the flows by syngenetic processes. The primary, syngenetic copper was derived mainly from flows whose original copper content was higher than normal. The primary copper was deposited in the amygdaloids from fumaroles or thermal springs, and in the sediments from playa lakes. The copper was concentrated in the playa lakes by the action of thermal and surface waters that percolated through the amygdaloids.

Some evidence suggests that the amygdaloidal copper deposits are genetically related to the flows in which they occur, and that the copper has been only slightly reworked by later ascending solutions. Several of the important Michigan deposits, however, were formed by deposition from ascending solutions after the lavas and sediments had been at least moderately tilted. Hot, ascending, hydrothermal solutions formed these deposits by reworking earlier syngenetic copper concentrations in amygdaloids and sediments.

References Cited

Bowen, N. L. (1928) *Evolution of igneous rocks*, Princeton Univ. Press, p. 282–302.

—— (1933) *The broader story of magmatic differentiation: Ore Deposits of Western States*, Lindgren Vol., Am. Inst. Min. Met. Eng., p. 106–128.

—— (1947) *Magmas*, Geol. Soc. Am., Bull., vol. 58, p. 263–280.

—— and Schairer, J. F. (1935) *The system MgO—FeO—SiO_2*, Am. Jour. Sci., 5th ser., vol. 29, p. 151–217.

Broderick, T. M. (1935) *Differentiation in lavas of the Michigan Keweenawan*, Geol. Soc. Am., Bull., vol. 46, p. 503–558.

—— and Hohl, C. D. (1935), *Differentiation in traps and ore deposition*, Econ. Geol., vol. 30, p. 301–312.

——, Hohl, C. D., and Eidemiller, H. N. (1946) *Recent contributions to the geology of the Michigan Copper district*, Econ. Geol., vol. 41, p. 675–725.

Buckstaff, S. (1923) *A study of the distribution of magnetite in one of the Keweenawan lava flows*, Univ. Wis., unpub. thesis.

Buddington, A. F. (1943) *Some petrological concepts and the interior of the earth*, Am. Mineral., vol. 28, p. 119–140.

Butler, B. S., Burbank, W. S., *et al.* (1929) *Copper deposits of Michigan*, U. S. Geol. Survey, Prof. Paper 144.

Coats, R. R. (1936) *Primary banding in basic plutonic rocks*, Jour. Geol., vol. 44, p. 407–419.

Emmons, R. C. (1927) *Diabase differentiation*, Am. Jour. Sci., 5th ser., vol. 13, p. 73–82.

Von Eckermann, H. (1938) *A contribution to the knowledge of the late sodic differentiates of basic eruptives*, Jour. Geol., vol. 46, p. 412–437.

Fenner, C. N. (1933) *Pneumatolytic processes in the formation of minerals and ores, Ore Deposits of the Western States*, Lindgren Vol., Am. Inst. Min. Metall. Eng., p. 58–106.

Grout, F. F. (1918a) *Internal structures of igneous rocks*, Jour. Geol., vol. 26, 439–458.

—— (1918b) *Two phase convection in igneous magmas*, Jour. Geol., vol. 26, p. 481–499.

—— (1918c) *A type of igneous differentiation*, Jour. Geol., vol. 26, p. 626–658.

Hess, H. H. (1938) *Primary banding in norite and gabbro*, Am. Geophys. Union, Tr., vol. 19, p. 264–268.

Hubbard, L. L. (1898) *Keweenaw Point with particular reference to the felsites and their associated rocks*, Mich. Geol. Survey Pub., pt. 2.

Irving R. D. (1883) *Copper-bearing rocks of Lake Superior*, U. S. Geol. Survey, Mon. 5.

Johannsen, A. (1939) *Petrography*, Univ. Chicago Press, vols. 1–4.

Kennedy, W. Q. (1933) *Trends of differentiation in basaltic magmas*, Am. Jour. Sci., 5th sec., vol. 25, p. 239–256.

—— and Anderson, E. M. (1938) *Crustal layers and origin of magmas*, Bull. Volcanol., ser. 2, tome 3.

Krauskopf, K. B. (1948) *Lava movement at Paricutin volcano, Mexico*, Geol. Soc. Am., Bull., vol. 59, p. 1267–1283.

Lane, A. C. (1909) *The Keweenawan series of Michigan*, Mich. Geol. Biol. Survey, Pub. 6, ser. 4, vols. 1, 2.

Lindgren, Waldemar (1933) *Mineral deposits*, McGraw-Hill.

Marvine, A. R. (1873) *Correlation of the rocks of Houghton and Keweenaw counties*, Mich. Geol. Survey, vol. 1, pt. 2, p. 47–61, 95–140.

Morey, G. W., and Ingerson, Earl (1940) *On the nature of ore solutions*, Econ. Geol., vol. 35, p. 772–785.

Peoples, J. W. (1933) *Gravity stratification as a criterion in the interpretation of the structure of the Stillwater Complex*, 16th Inter. Geol. Cong., Rept., Washington, D. C., p. 353–360.

Perret, F. A. (1913) *The circulatory system in the Halemaumau lava lake*, Am. Jour. Sci., 4th ser., vol. 35, p. 337–349.

Pumpelly, Raphael (1873) *Copper district*, Mich. Geol. Survey, vol. 1, pt. 2.

Sandell, E. B., and Goldich, S. S. (1943) *The rarer metallic constituents of some American igneous rocks*, Jour. Geol., vol. 51, p. 99–115, 167–189.

Schwartz, G. M., and Sandberg, A. E. (1940) *Rock series in diabase sills at Duluth, Minnesota*, Geol. Soc. Am., Bull., vol. 51, p. 1135–1172.

Shannon, E. V. (1924) *Mineralogy and petrology of intrusive diabase at Goose Creek, Loudoun County, Virginia*, U. S. Nat. Mus., Pr., vol. 66, art. 2, p. 17–18.

Wager, L. R., and Deer W. A. (1939) *Geological investigations in East Greenland*, Medd. Gronland, Bd. 105, Nr. 4.

Wahl, Walter (1946) *Thermal diffusion-convection as a cause of magmatic differentiation I*, Am. Jour. Sci., vol. 244, p. 417–441.

Walker, Frederick (1940) *Differentiation of the Palisades diabase, New Jersey*, Geol. Soc. Am., Bull., vol. 51, pt. 2, p. 1059–1106.

Zies, E. G. (1929) *The Valley of 10,000 Smokes, Alaska*, Nat. Geog. Soc., Contrib., Tech. Papers, Katmai Ser., vol. 1, no. 4.

1 Second Street, Calumet, Michigan

Manuscript Received by the Secretary of the Society, March 24, 1950

Published by Permission of the Director, U. S. Geological Survey

GEOLOGIC MAP AND SECTION OF A PEGMATITIC LAVA FLOW AT SOUTH RANGE QU

Topography and geology by H. R. Cornwall and A. A. Stromqu

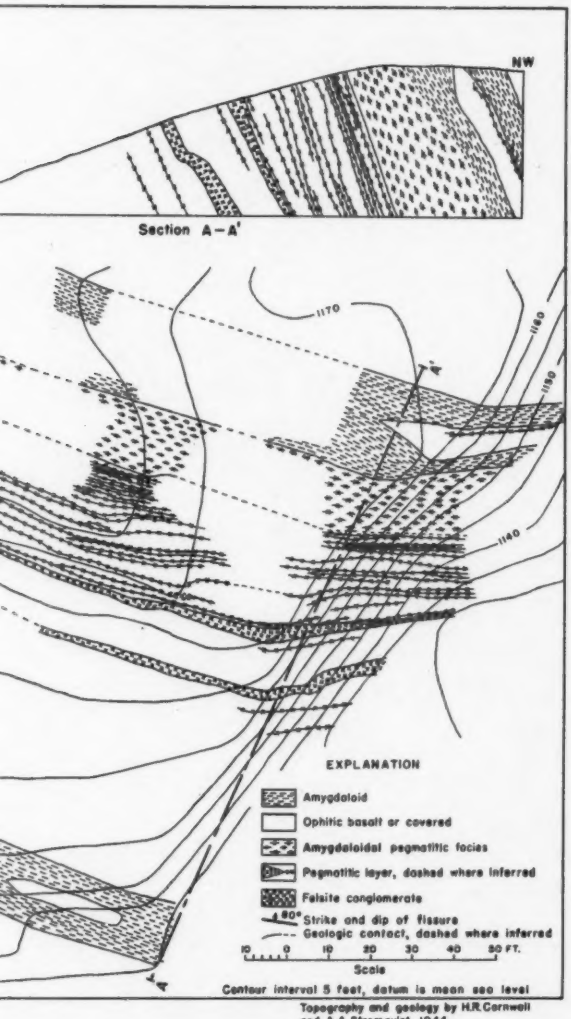

Topography and geology by H.R. Cornwall and A.A. Stromquist, 1944

H RANGE QUARRY, HOUGHTON COUNTY, MICHIGAN
A. A. Stromquist, 1944

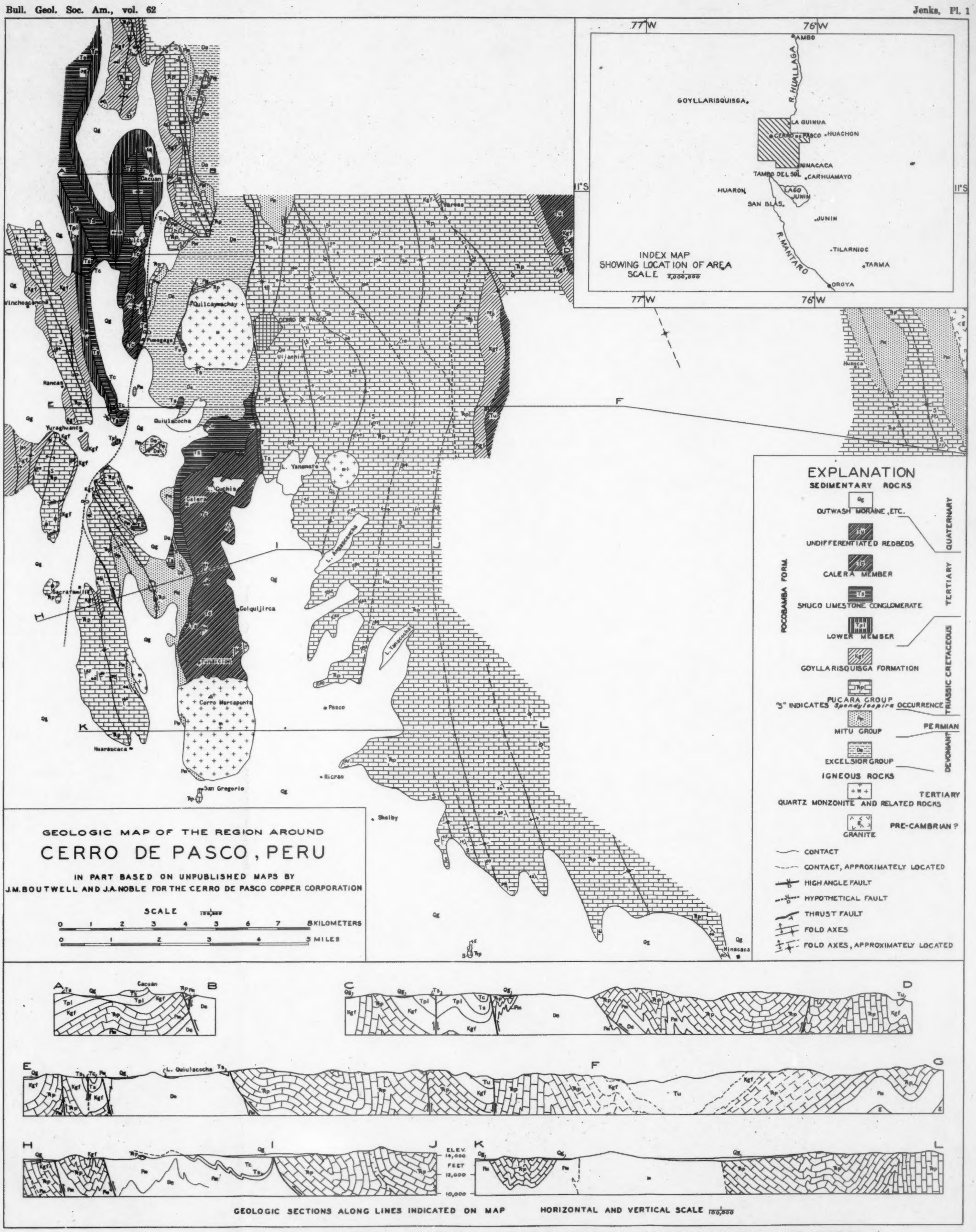

GEOLOGIC MAP AND STRUCTURE SECTIONS OF THE REGION AROUND CERRO DE PASCO

lim
str
as
nor
ishi
int
enc
fau
stu
dic
app

Int
Pro
Pro
Tr

Fig
1.
2.

di
Pe
(M
19
ar
gr
th

Pl

BULLETIN OF THE GEOLOGICAL SOCIETY OF AMERICA
VOLUME 62, PP. 203-220, 2 FIGS., 3 PLS. FEBRUARY 1951

TRIASSIC TO TERTIARY STRATIGRAPHY NEAR CERRO DE PASCO, PERU*

By WILLIAM F. JENKS

ABSTRACT

Near Cerro de Pasco, Peru, thrust faulting and close folding bring an eastern facies of lower Mesozoic limestones, 9500 feet thick, close to beds on the west oe the same age and one quarter as thick. The strata are Upper Triassic and may extend into the lower Liassic. Fossils are abundant but conclusive only as to the oldest beds, of late Triassic age. Original difference in thickness of the two facies is due to abnormal accumulation in a narrow north-trending negative zone east of Cerro de Pasco, with rapidly diminishing thickness and time continuity to the west.

Tertiary strata, which have been confused with the Triassic in recent works, accumulated in low-level intermontane basins on folded and faulted Mesozoic and Paleozoic formations. Strong deformation at the end of the Cretaceous was followed, after the accumulation of Tertiary continental deposits, by thrust faulting and isoclinal folding in the early Tertiary. One member of the Tertiary sequence is a fanglomerate, study of which suggests a short period of movement between the two major ones. Minor warping is indicated toward the close of the Permian and Jurassic periods. Intrusive and extrusive igneous activity apparently closely followed early Tertiary deformation.

CONTENTS

	Page		Page
Introduction	203	Western facies	208
Previous work	204	Cretaceous	211
Pre-Triassic rocks	204	Tertiary	212
Triassic	205	Structural history	215
General discussion	205	References cited	218
Eastern facies	206		

ILLUSTRATIONS

Figure	Page	Plate	Facing page
1. Comparison of eastern and western facies of Pucará group	206	1. Geologic map and structure sections of the region around Cerro de Pasco	203
2. Diagram showing depositional and tectonic history of the Pocobamba formation	215	2. Eastern facies of Pucará group	208
		3. Triassic and Tertiary strata west of Cerro de Pasco thrust fault	209

INTRODUCTION

The geology of the Cerro de Pasco mining district in the Andean highlands of central Peru has been studied and discussed in detail (McLaughlin, 1924; McLaughlin and others, 1933; Moses, 1942). Outside the mineralized area, however, larger structural and stratigraphic features of great complexity, aroused the writer's interest during more than 3 years with the Cerro de Pasco Copper Corporation and led to field work the results of which are described here. Special attention was given to a great limestone sequence of lower Mesozoic age and to continental Tertiary strata, both of which are complexly folded and faulted. In 1940 Boit published articles in w[illegible] he claimed that formations described as probably Tertiary (McLaughlin, 1924) were actually Triassic. Ahlfeld (1932) stated that the strata containing rich silver ores at Colquijirca were Triassic, a claim shown to be in error by McKinstry

* With the support of a grant from the American Philosophical Society.

(1936), who, like McLaughlin assigned these strata tentatively to the Tertiary.

Confusion of the Tertiary sequence of the region with the lower Mesozoic was due to lack of careful structural and stratigraphic studies. Accordingly, during 3 months of 1941, the writer carried on intensive field studies in the hope of clarifying the Mesozoic and Tertiary history of the region.

In order to interpret stratigraphic and structural relationships it was necessary to extend existing geologic maps of the Colquijirca and Cerro de Pasco districts to include other key areas. Geologic mapping was carried out on a scale of 1:20,000. The map (Pl. 1) shows the geology of 630 square miles, more than half of which represents new mapping. Elevations within the region range from 13,800 to 15,200 feet above sea level. Trips were also made to the regions around Goyllarisquisga, Oroya, Carhuamayo, Huachón, and Tilarnioc (index map, Pl. 1) for reconnaissance study of comparable sections.

The work was given impetus by valuable suggestions from Donald H. McLaughlin and was facilitated by the Cerro de Pasco Copper Corporation in many ways. The Corporation allowed free use of all geologic maps in its files and has generously consented to the publication of the geologic map (Pl. 1), parts of which are largely the work of J. M. Boutwell and J. A. Noble, who had previously been on the staff of the Corporation. The manuscript has been critically read by John H. Moses, Chief Geologist of the Corporation, Otto Haas, and Bernhard Kummel. Paleontologic study of numerous fossil collections, made during the field work and presented to the American Museum of Natural History, has been undertaken by Haas, Newell, Wells, and Peck (Haas, 1947).

Previous Work

McLaughlin (1924) noted that in Cerro de Pasco the Triassic Uliachin limestone conformably underlies a sequence of Liassic limestones and dolomites at least 4000 feet thick. Paleontological data at that time were inadequate, but the general section was recognized with remarkable accuracy. McLaughlin pointed out that the youngest folded rocks in the Cerro de Pasco region are probably Tertiary, a conclusion based on structural data particularly in the Goyllarisquisga region.

Steinmann (1929; 1930) tentatively assigned the Uliachin limestones to the Karnian (Upper Triassic). With more assurance he called limestones conformably above the Uliachin, lower and middle Liassic. The first close dating of a part of the Triasic near Cerro de Pasco came when Boit (1940b) reported the discovery of *Entomonotis ochotica*, of Norian age, at San Gregorio. Boit (1945) later reported the presence of Norian limestones with *E. ochotica* east of Carhuamayo. Harrison (1943), in describing the geology of an area in Junin Department south of Cerro de Pasco, noted that a Norian limestone sequence is followed by shale and limestone apparently largely of Liassic age. Cox (1949) considers the whole Uliachin sequence to be Norian.

Pre-Triassic Rocks

The oldest rocks of the general region surrounding Cerro de Pasco are schists cut by granites in a large area around Huachón to the east. These rocks are certainly pre-Permian, and may be as old as Precambrian. There is no evidence that the granitic rocks are Tertiary, as claimed by Welter (1946). Granite of this massif appears at the eastern edge of the geologic map, unconformably covered by Permian strata.

Another pre-Permian formation, the Excelsior group, is exposed in a broad, faulted anticline at Cerro de Pasco, but has not been recognized to the east. The Excelsior group is a series of shales and phyllites with interbedded fine-grained quartzite and some calcareous layers. It is an incompetent formation showing much close folding. No fossils are known from the Excelsior group, but it is tentatively considered Devonian by comparison with lithologically similar strata in the vicinity of Ambo to the north.

In sharp angular unconformity above the Excelsior group is a persistent but extremely variable series of clastics named the Mitu formation by McLaughlin. Dunbar and Newell (1946) described a section of this formation exposed at Tarma, and named it the Yauri

group. Newell, Chronic, and Roberts (1949) demonstrated its Permian age and renamed it the Mitu group.

In the vicinity of Cerro de Pasco the Mitu group is chiefly a conglomerate with pebbles of quartz and Excelsior-type argillaceous material. A short distance to the south, particularly in the valley northwest of San Gregorio, it consists largely of red sandstone, shaly sandstone, and interbedded quartz conglomerate beds. Red clastics also appear abundantly at and beyond the north edge of the present map area. Certain beds in these sequences strongly resemble the red arkosic section at Ambo. Volcanic rocks, prominent in the Mitu 50 miles and more to the south, do not occur around Cerro de Pasco.

Triassic

General Discussion

Along the Andes of central Peru, east of the continental divide, the Mitu group is covered by thick Triassic or Liassic limestones. Recent work has shown that in the region between Oroya and Cerro de Pasco sediments of Norian age are represented in the lower part of the limestone. The Norian pelecypod *Entomonotis ochotica* was found by Boit (1940b; 1944) at San Gregario and Carhuamayo, and by Harrison (1943) near Carhuamayo, Junin, Concepción, and Tarma.

Entomonotis beds have been recorded as well from near Huaira, in the Chinchao valley northeast of Huánuco (Steinmann, 1929). They extend northwest to Leimebamba in the Utcubamba Valley (Steinmann, 1929), and Olmos, east of the Sechura desert of northwest Peru (A. A. Olsson, personal communication). Tschopp (1948) records *E. ochotica* from the lower part of the Santiago formation in eastern Ecuador. Apparently, then, Norian limestones are widely developed along the Cordilleran geosyncline, from a latitude somewhat south of Oroya, north at least as far as Ecuador. No Triassic rocks are known in southern Peru, nor have they been found along the coast.

In the Cerro de Pasco region *E. ochotica* is known only in a mineralized area just west of the bismuth mine at San Gregorio. The fossil is abundant in a single steeply dripping silicified stratum which is close above the contact with the Mitu group. The basal Mesozoic limestones at this locality may therefore be assumed to be Norian.

The age of the whole, thick, remaining sequence of limestones is not exactly known. Exhaustive search for sharply diagnostic ammonites was unsuccesful. Dr. O. H. Haas (personal communication, April 29, 1947) has found the brachiopod genus *Spondylospira* in 16 fossil lots, all from the upper portions of the limestone sequence. Vokes and Haas (1944) demonstrated the presence of certain *Spondylospira* species in the Ladinian (upper Middle Triassic) limestones of the Nevado de Acrotambo, northern Peru (Körner, 1937), but Haas (1946) suggested that the supposedly Ladinian fossils may cover a range wider than Ladinian. In Haas' (personal communication) opinion the presence of several gastropod genera hitherto recorded only from Liassic or even younger Jurassic strata might suggest expansion of the section into the Rhaetian. As undoubted lower Liassic faunas have been described from localities within 50 miles of Cerro de Pasco, part of the continuous limestone sequence east of Cerro de Pasco may be Upper Triassic and part lower Liassic. Separation between the upper and lower parts of the section is not clear cut and exact placing of the boundary will have to await more detailed paleontologic work.

Because age determinations for the lower Mesozoic calcareous sequence of central Peru are still inconclusive, these beds are here considered together as the Pucará group. Pucará was suggested as a regional name by McLaughlin (1924, p. 605). Local names in use at Cerro de Pasco for parts of the limestone sequence (Uliachin limestone for the Triassic and Paria limestone for the Liassic) are not valid stratigraphic terms because their age and limits cannot be determined accurately.

A north-south thrust fault passes through Cerro de Pasco and is lost to the south under the gravels of the Pampa de Junin. It separates distinctly different facies of the limestones within the Cerro de Pasco region (Fig. 1) (Boit, 1940a). Faunas of the two facies are similar, with *Spondylospira* represented in both.

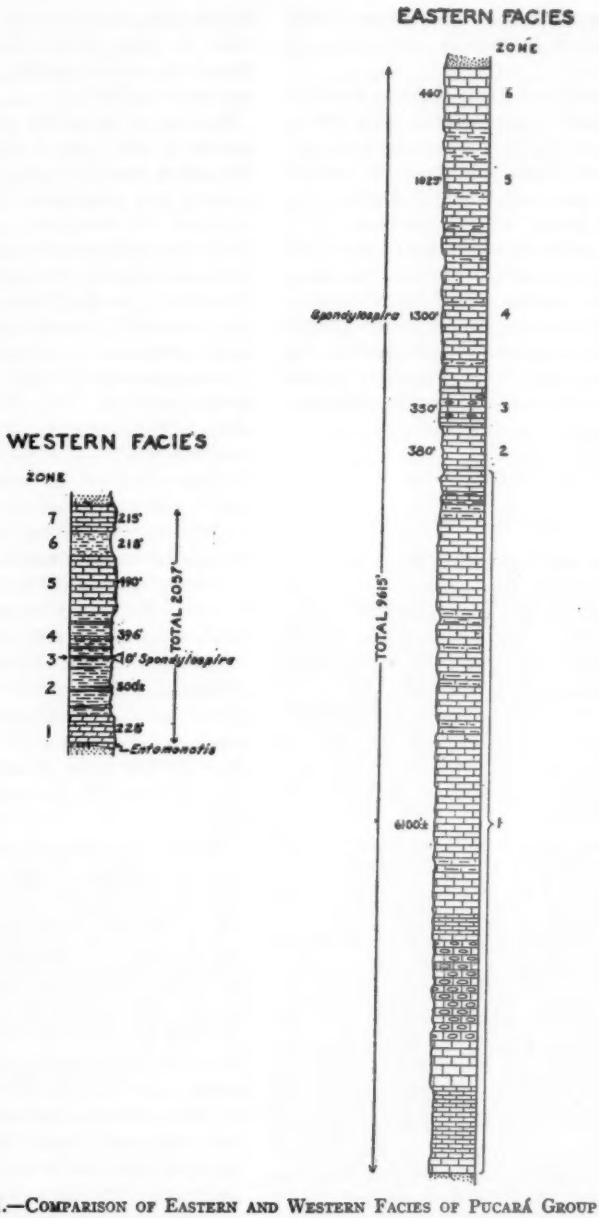

FIGURE 1.—COMPARISON OF EASTERN AND WESTERN FACIES OF PUCARÁ GROUP

Eastern Facies

The eastern facies of the Pucará group within the Cerro de Pasco region underlies an area roughly 7 kilometers (4.3 miles) wide and extending north-south across and beyond the region mapped. The same rocks appear again

at the eastern border of the region just north of the narrow-gauge railway to Huachón.

Section 1 is a generalized section through the Pucará group east of the Cerro de Pasco thrust fault. A compilation of data secured in many places, it is particularly applicable to the area due east from Cerro de Pasco.

SECTION 1.—GENERALIZED SECTION OF PUCARÁ GROUP EAST OF THE CERRO DE PASCO THRUST FAULT, CERRO DE PASCO

Zone	Description	Approximate thickness (feet)
	Lower Cretaceous: Goyllarisquisga formation	
	Discordance	
	Upper Triassic (and Lower Liassic ?): Pucará group	
6	Limestone, thick-bedded, buff, crystalline, with pink to brown fossiliferous bed at base	460
5	Limestone, gray to brownish gray, with soft limy shale interbedded. Near base are several beds with abundant corals	1025
4	Limestone, dark gray to black, weathering bluish gray, some beds highly fossiliferous. All reported *Spondylospira* are from this zone.	1300
3	Limestone, gray brown, massive, with siliceous concretions	350
2	Limestone, interbedded buff and dark gray, with numerous concretionary beds, abundant fossils, and some shale interbeds	380
1	Limestone and dolomite, thick-bedded, largely light gray, crystalline, sparsely fossiliferous, with some shale interbeds	6100
	Total Pucará group	9615 feet
	Discordance	
	Permian: Mitu group.	

The thickness in Section 1 is of the proper order of magnitude but may be in error by 10 per cent due to structural complications. Some idea of the thickness of the Pucará group may be obtained from Figure 1 of Plate 2, which shows a sequence of limestone beds uninterrupted by structural breaks along the ridge between Cerro de Pasco and Vareas' hacienda. At least 4800 feet of the Pucará group are shown, capped by beds containing *Spondylospira* near the axis of a syncline to the east.

The relationship of the Pucará group to the underlying Mitu group east of the Cerro de Pasco thrust fault is not clear except at some distance from the center of the region mapped. At the eastern edge of the area, east of Huanca, brownish-gray massive limestone rests on arkosic sandstone of the Mitu group with slight angular unconformity. Northeast of Carhuamayo, about 30 miles southeast of Cerro de Pasco, basal gray, compact Pucará limestones are essentially parallel to underlying conglomerates and flows of the Mitu group.

In the northern part of the map is a small patch of arkosic red sandstone belonging to the Mitu group and beneath Pucará limestone The structure in the red beds, which are incompetent, is complex, and the actual contact appears to be an angular unconformity. Evidence on this point is inconclusive, as faulting or disharmonic folding may have occurred. At this place 2240 feet of continuous limestone, all within zone 1 of Section 1, were measured. A massive basal limestone here is similar to the basal limestone west of the north-south thrust fault. It also resembles, except in its lack of fossils, the gray basal limestones northeast of Carhuamayo and east of Huanca. These basal beds are probably Norian, although *Entomonotis ochotica* as an index fossil is lacking. From the data assembled it would appear that *E. ochotica* tends to be abundant only in certain limited localities within a single zone close to the base of the Pucará group.

The most widely discussed Triassic section in the region around Cerro de Pasco is that on Cerro Uliachin, close to Cerro de Pasco on the southeast. It has been mentioned that Steinmann (1929) considered this section Karnian. Boit's discovery of Norian strata near the base of the section both east of the fault zone at Carhuamayo and west of it at San Gregorio makes the existence of older strata on Cerro Uliachin unlikely. The limestones on Cerro Uliachin are here considered to be Norian or Rhaetian. The fauna described by Steinmann and found in abundance by the writer is of rather indefinite value as an age determinant. Section 2, measured on Cerro Uliachin, demonstrates the nature of this almost wholly continuous limestone sequence. It is zones 2 and 3 of generalized Section 1.

SECTION 2.—SECTION OF PART OF TRIASSIC LIMESTONE SEQUENCE

Measured with tape and compass along Cerro Uliachin, southeast of Cerro de Pasco. Triangulation station B is at top of bed 4. Section is east of the longitudinal fault.

Bed	Description	Thickness (feet)
Upper Triassic: Pucará group		
17	Limestone, dark gray to black, weathering blue gray; fossiliferous, with large *Myophoria* or *Trigonia* sp.	
16	Limestone, gray brown; massive, with siliceous concretions (Zone 3 of Section 1)	350
15	Limestone, dark gray, nonresistant, fossiliferous (This and underlying beds are zone 2 of Section 1)	40
14	Limestone, dark gray brown, thin-bedded	35
13	Limestone, gray brown, massive, resistant, with chert concretions and lenses of dark-gray limestone	35
12	Limestone, dark gray to black, bituminous, fossiliferous	40
11	Limestone, brown, weathers light gray, nonfossiliferous, thin-bedded, resistant	26
10	Limestone, dark gray, thin-bedded, fossiliferous	11
9	Shale, limy, and thin-bedded limestone, largely covered	40
8	Limestone, dark gray, sandy, banded, nonfossiliferous	22
7	Limestone, dark gray, bituminous, thin-bedded, non-resistant, with few fossils	11
6	Shale, yellow, brown, black, and sandy shale, with thin beds of dark-gray to black bituminous limestone	45
5	Limestone, gray to brownish gray	9
4	Limestone, light grayish tan, massive, resistant, nonfossiliferous, with irregular siliceous concretions	11
3	Dolomite, light yellowish gray, thin-bedded, locally sandy, nonfossiliferous	22
2	Limestone, gray brown, sandy, grading laterally into dark-gray bituminous, fossiliferous limestone	3
1	Limestone, light gray brown, crystalline, massive, non-fossiliferous, with bands of siliceous concretions	35
	Base covered by talus, close to north-south thrust fault	
	Total measured section	730 feet

The kind of alternating rocky and grassy hillsides produced by bands of great and little resistance within this zone of the Pucará group is shown in Figure 3 of Plate 2. Numerous fossil collections from this zone are in the American Museum of Natural History, but none contain the *Spondylospira* fauna. *Spondylospira* so far appears to be limited to the part of zone 4 above bed 17 of Section 2.

No detailed sections were measured in the remaining great expanses of Pucará southeast of Cerro de Pasco, because no clear marker horizons could be traced through. Perhaps the zone which contains *Spondylospira* could have been used as a mappable unit. Several successive belts known to contain *Spondylospira* are interpreted as repetitions due to open or isoclinal folding (Pl. 1). A prolific faunal zone, especially rich in gastropods (Haas, 1946), just north of Ninacaca, is high in the section but cannot be tied accurately to the rest of the Pucará group.

Western Facies

The Pucará group west of the Cerro de Pasco thrust fault is light-colored, thin-bedded limestone with two distinctive shale members, one of which is persistent in the region around

PLATE 2.—EASTERN FACIES OF PUCARÁ GROUP

FIGURE 1.—VIEW SOUTHEAST OF LIMESTONE OF EASTERN FACIES OF PUCARÁ GROUP
Between Cerro de Pasco and Vareas' hacienda.

FIGURE 2.—BASAL PUCARÁ LIMESTONE, MITU GROUP, AND UNDERLYING GRANITE
At Lake Pomacocha, north of railroad to Huachón and east of Huanca. View is northwest.

FIGURE 3.—VIEW SOUTHEAST FROM CERRO ULIACHIN
Showing ridges formed by resistant limestone beds of the eastern facies of Pucará group.

FIGURE 1

FIGURE 2

FIGURE 3

EASTERN FACIES OF PUCARÁ GROUP

FIGURE 1

FIGURE 2

FIGURE 3

TRIASSIC AND TERTIARY STRATA WEST OF CERRO DE PASCO THRUST FAULT

Cerro de Pasco. Peculiarities of deformation have made measurements of the whole group west of the fault impossible. The upper and lower parts of the section are accurately measured, but the middle portion, which may contain some incompetent beds, is broken by sharp folding, faulting, or brecciation. Section 3 is a generalized section through the western facies.

SECTION 3.—GENERALIZED SECTION THROUGH THE WESTERN FACIES

Zone	Description	Approximate Thickness (feet)
Lower Cretaceous: Goyllarisquisga formation		
	Sandstones and conglomerates	
	Disconformity	
Upper Triassic (and lower Liassic?)—Pucará group		
7	Limestone, buff weathering	215
6	Shale, red and green, persistent	218
5	Limestone, white weathering	490
4	Shale and shaly limestone, poorly exposed, apparently not persistent	396
3	Limestone, gray, highly fossiliferous, with *Spondylospira*	10
2	Probably thin-bedded limestone with shales. Largely destroyed by deformation. Estimated	500
1	Dolomite, massive, buff to gray	228
	Total Pucará group	2057
Permian: Mitu group		
	Conglomerates and sandstones	

The western facies is about 7500 feet thinner than the eastern facies just across the fault. The difference in thickness is not imaginary, in spite of the clear element of guesswork in estimating zone 2 in Section 3. Thick sequences, relatively massive and resistant in the eastern facies, are lacking in the western. Thirty miles northwest, at Goyllarisquisga, the Pucará group of the western facies is only 100 to 1000 feet thick (McLaughlin, 1924, p. 604). It is there composed of massive pale-buff and gray limestone without the shale zones present near Cerro de Pasco.

The basal western facies of the Pucará group rests disconformably on the underlying Mitu group. In most places there is no evidence of disconformity although fragments of the underlying conglomerates are now enclosed in the base of the limestone. In a few exposures some evidence of erosion could be detected, although the beds above and below the contact remained approximately parallel. Certainly there is no evidence of a major orogeny at the close of the Paleozoic.

The dolomite of zone 1 is persistent, massive, cliff forming, with bedding obscure except for a few feet at the base. A few poorly preserved pelecypods and brachiopods have been found in this zone, but no trace of the large, easily distinguished *Entomonotis ochotica*. Yet the *E. ochotica* horizon may be projected from San Gregorio northwest to the approximate position of the massive basal dolomite northeast of Huaraucaca (Pl. 1). Either the *Entomonotis* beds lens out northwestward, or this pelecypod was originally erratic in distribution. However, the lowest beds of the western facies may be considered Norian or younger.

The upper part of Section 3, including zones 3 to 7, is well exposed in many places in the hills between Huaraucaca and Yuraghuanca, and in a sharp anticline extending northwest from Yuraghuanca past Rancas and Vinchoscancha. Other excellent exposures are present along the hills east of Cacuan, north to the edge of the map.

Section 4 is a detailed section of this portion of the western facies.

PLATE 3.—TRIASSIC AND TERTIARY STRATA WEST OF CERRO DE PASCO THRUST FAULT

FIGURE 1.—CONTACT BETWEEN WESTERN FACIES OF PUCARÁ GROUP AND GOYLLARISQUISGA FORMATION EAST OF RANCAS

View is southward. Contact is just under projecting slabs of red sandstone. Zone 6 (largely shale) is the grass-covered band between limestones. Strata are vertical to steeply west-dipping.

FIGURE 2.—VIEW WEST ACROSS THE NORTH END OF SOUTHWARD-PLUNGING CACUAN SYNCLINE

Shuco conglomerate caps the hill at left and ridge in distance. Lower member wraps around syncline below the Shuco.

FIGURE 3.—VIEW NORTH FROM HILL OF SHUCO LIMESTONE CONGLOMERATE AT SOUTH END OF PLUNGING CACUAN SYNCLINE

Folded beds are limestone and shale of Calera member.

SECTION 4.—SECTION OF UPPER PORTION OF PUCARÁ GROUP

Measured with tape and compass in low hills south of Yuraghuanca.

Bed	Description	Thickness (feet)	
	Lower Cretaceous: Goyllarisquisga formation		
45	Sandstone, yellow to gray, white weathering, cross-bedded, coarse-grained, with lenses of quartz conglomerate	300	
44	Sandstone, sandy shale, and shale, all red, with lenses of quartz conglomerate	220	
	Unconformity		
	Upper Triassic (and lower Liassic?): Pucará group		
	Zone 7: Buff-weathering limestone		
43	Limestone, brownish pink, nonfossiliferous	11.5	
42	Limestone, buff, compact	4	
41	Limestone, buff, with small solution cavities filled with white calcite	13.9	
40	Limestone, light tan to buff, thin-bedded, with thin shale beds in upper third	27.8	
39	Limestone, tan, with many irregular layers of chert concretions	8.8	
38	Shale, gray, with limestone lenses	11.3	
37	Limestone, tan	9	
36	Limestone, pinkish brown, compact	10.4	
35	Shale	3.2	
34	Limestone, buff	1.4	
33	Shale	5.1	
32	Limestone, light pink to brown, compact, with white chert concretions	7.4	
31	Shale with limestone lenses	8.3	
30	Limestone, tan, with pinkish streaks and chert concretions near top and bottom	28.9	
29	Shale	5	
28	Limestone, gray brown	1.2	
27	Limestone, pink to dull red	0.4	
26	Interbedded gray shale and light gray-brown limestone	22.1	
25	Limestone, light tan, fossiliferous in lower 2 feet, chert nodules in upper part	20.5	
	Total zone 7		214.4
	Zone 6. Chiefly shale		
24	Shale, red and green, with numerous thin beds of buff limestone, green to gray sandstone, and red sandy shale		218
	Zone 5. White-weathering limestone		
23	Limestone, pinkish gray, banded, with gray chert concretions	2.2	
22	Shale	2.2	
21	Limestone, gray brown, thin-bedded, with thin shaly layers	16.1	
20	Limestone, pale yellowish gray, massive	74.2	
19	Limestone, light gray brown with bands of gray chert concretions	62.2	
18	Limestone, gray, sandy	.3	
17	Limestone, light brownish gray, with gray chert concretions in some layers	22.4	
16	Limestone, gray brown, sandy	7	
15	Limestone, light gray to tan, concretionary in middle part	24.7	
14	Limestone, light gray	24	
13	Sandstone, limy, brown, buff weathering	0.7	
12	Limestone, tan to gray brown, in beds 1–2 feet thick	81.4	
11	Limestone, tan, fossiliferous	1.1	
10	Limestone, gray to tan	33.4	
9	Limestone, light gray brown to buff; fossiliferous: poorly preserved brachiopod fauna	1.3	
8	Limestone, buff to gray buff	71	
7	Limestone, light gray brown in part shaly; bituminous odor on fresh fracture	48.3	
6	Limestone, light gray brown, soft, shaly, with thin shale interbeds	17.7	
	Total zone 5		490.2
	Zone 4. Shale and soft limestone		
5	Shale, limy, with thin limestone beds	81	
4	Limestone, dull gray brown, soft, bituminous	136	
3	Shale, yellow and gray, with thin limestone beds	61	
2	Limestone, pale buff, soft	18	
	Total zone 4		296

Zone 3

1	Limestone, gray, massive, with abundant fossils including *Spondylospira* and other brachiopods, gastropods, corals, and large echinoid spines	10
	Total exposed Pucará group	1228.6

Section terminated by strong brecciation along axial plane of isoclinal anticline

Section 5 was measured where the strata are vertical, in the absence of any more open structures in this part of the region. Thickness of incompetent beds is therefore bound to be reduced. A higher percentage of argillaceous beds might be anticipated if the region were not so strongly deformed. A general view of the upper part of the Pucará group is shown in Figure 1 of Plate 3.

The western facies of the Pucará group near Cerro de Pasco somewhat resembles the sections described by Harrison (1943, p. 5–9), in the vicinity of Oroya to the south. He distinguishes three divisions of the Pucará group, as follows:

Upper Calcareous Series (Liassic)

Thin to thick-bedded limestone, with nodular chert bands, oolitic layers, and shale partings. Ranges from 1160 feet thick near Pomacocha to 4400 feet near Oroya.

Lower Liassic shale series

Included in this division are the following strata (east of Oroya)

Shale and green standstone	60
Dark bituminous shales with Sinemurian ammonites	230
Variegated sandstones	265
Thin limestones, sandstones, and shales	620
Dark-red and gray shale	160
Oolitic limestone	460
Shale	5
Total	1800 feet

Lower Calcareous Series (Triassic)

This limestone succession is 2700 feet thick near Huaricolca, 1000 feet thick near Azupite, and missing around Yauli. It is underlain by red and yellow shales up to 360 feet thick. Chert concretions are abundant particularly in the upper part. At least part of this division is Norian.

The western facies near Cerro de Pasco may correspond in part to Harrison's Lower Calcareous series and the lower part of his lower Liassic shale series, which, as he points out, could be Triassic.

To recapitulate, the principal differences between the two facies of the Pucará group, so sharply set apart by the north-south thrust fault through Cerro de Pasco, may be indicated in tabular form.

Eastern facies	*Western facies*
Thickness about 9500 feet	Thickness about 2000 feet
Almost all limestone; little dolomite and shale	Little more than half limestone and dolomite; the rest distinctive, thick shale and sandstone members, one of which is persistent.
Spondylospira zone present. The *Spondylospira* collected appear to be from various horizons in a zone about 1300 feet thick	*Spondylospira* zone present, 10 feet thick
Top of *Spondylospira* zone is about 1500 feet below top of Pucará group	Top of *Spondylospira* zone is about 1320 feet below top of Pucará group

Sharp demarcation of the two facies along the fault is of tectonic origin. In a broader sense, existence of two such different facies in adjacent parts of the lower Mesozoic sea is also tectonic. Discussion of the origin of the facies and of their present juxtaposition is therefore reserved to the section of this paper on structural history of the region.

Cretaceous

The limestones of the Pucará group are overlain by clastics of continental origin which are called the Goyllarisquisga-Jatunhuasi sandstone by McLaughlin (1924). A more appropriate name in view of the varied nature of the deposits is Goyllarisquisga formation, as used in the present work.

Basal red shaly sandstones and associated quartz conglomerates of this formation rest dis-

conformably on the Pucará limestones. Locally slight angular unconformity may be observed. Channelling of the upper surface of the limestone is evident at the contacts east of Vinchoscancha.

Erosion of the uplifted but not strongly distorted surface of the Pucará group must have occurred before the deposition of the Neocomian Goyllarisquisga formation. This probably was a marginal manifestation of the Nevadian disturbance, more strongly evident in southern Peru (Newell, 1949, p. 48).

The Goyllarisquisga formation is developed to about equal extent east and west of the Cerro de Pasco thrust fault. No marked facies changes are evident.

East and northeast of Cerro de Pasco the clastics of the Goyllarisquisga are separated from overlying red beds of probable Tertiary age by one, or in some places two, thin limestone beds which are possibly to be correlated with middle Cretaceous limestones elsewhere in central Peru. These limestones do not appear elsewhere within the area mapped and are not shown on Plate 1.

Tertiary

In the Goyllarisquisga district a thick sequence of red, gray, and gray-green shales and sandstones, with beds of conglomerate and limestone, rests on the Goyllarisquisga formation and middle Cretaceous limestone in angular unconformity. This formation was described by McLaughlin (1924, p. 611) as the Pocobamba formation. Some of the more resistant beds may be traced almost continuously southeast to the Cerro de Pasco district. The Pocobamba formation enters the region of Plate 1 in the northwest corner and may be traced southeastward along a number of folds to the Marcapunta intrusive.

West and south of Cerro de Pasco the Pocobamba formation may be divided conveniently into three members (Section 5).

Section 5.—Pocobamba Formation

	Thickness (feet)
Calera member	
Interbedded dull-gray shale and fine-grained white, pink, and light gray-brown limestone	850–2300
Shuco limestone conglomerate	
Fanglomerate with large subangular boulders of limestone in a limestone matrix	100–550
Lower member	
Shale, sandstone, conglomerate, with several prominent limestone beds and lenses	0–1000
Total exposed thickness Pocobamba formation	1600–2850

The lower member of the Pocobamba formation is well developed in the folded belt west of Quilcaymachay. It is best exposed where it wraps around the north end of the Cacuan syncline (Pl. 3, fig. 2), but its lower contact throughout this area is concealed. This member is soft, nonresistant shale and sandstone, for the most part gray and gray green, but with some pink marl beds and prominent red shales. The sediments of this member appear to be of lacustrine and fluvial origin, but have not yielded confirmatory fossils.

Well down in the shales of the lower member of the Pocobamba formation are two limestone beds somewhat more resistant than the rest of the member. The upper one is a 25-foot bed of soft pale-pink limestone and light-gray limestone mottled with buff and pink and with numerous rounded patches of white crystalline calcite. The lower limestone is about 15 feet thick and is mottled pink and light gray in a manner strongly suggesting algal deposition. Other carbonate beds exist still lower in the formation but are nonpersistent.

The southernmost exposure of the lower member forms a low hill south of the railroad east of Yuraghuanca. In the large area of Tertiary rocks between the Cerro de Pasco and Marcapunta stocks, the succeeding unit, the Shuco limestone conglomerate, rests directly on the Excelsior group, Mitu group, or Pucará group.

The Shuco limestone conglomerate or fanglomerate is one of the spectacular lithologic units of the region (Pl. 3, fig. 3). Outcrops in the vicinity of the Cerro de Pasco stock, and to the south, contain angular to subangular blocks of Pucará limestone ranging up to 12 feet in diameter. The larger blocks are in those outcrops close to the Cerro de Pasco thrust fault. Interstitial to the large boulders are angular to

semirounded limestone boulders, pebbles, and sand grains tightly cemented by fine gray calcium carbonate blotched with pink. With some difficulty irregular lenticular masses of fine-grained conglomerate may be found as a rough indication of bedding.

Farther west the size of boulders abruptly descreases. Boulders are more nearly rounded, and rocks other than limestones of the Pucará group appear. In the plunging syncline northeast of Yuraghuanca the Shuco is distinctly separated into two thick beds on the basis of color of cementing carbonate and on prevalence of Pucará-type boulders. The normal boulder size in this area is 6 to 10 inches. Six miles to the north boulders are in most places 2 to 4 inches in diameter, well rounded, and made up of quartzite, chert, and Mitu conglomerate in excess of Pucará limestones. The Shuco limestone conglomerate thins from about 550 feet between Colquijirca and Cerro de Pasco to about 100 feet in the northwest part of the region mapped. Nearer Goyllarisquisga the Shuco cannot be distinguished from other conglomerates appearing at several places in the Pocobamba formation. The Shuco tongues northwestward into fine shale, siltstone, and sandstone and is lost as a separable member of the formation. Although the conglomerate is conformable with underlying and interfingering beds to the northwest, abrupt disappearance of lower Pocobamba beds toward the east suggests local lack of conformity. Original thinning of the lower member at the east edge of its depositional basin appears to have been accentuated by mild warping and erosion prior to the accumulation of the Shuco conglomerate.

The Shuco limestone conglomerate is a fanglomerate formed in the piedmont belt of new mountains to the east, composed of Pucará limestone. These mountains had come into being just preceding Shuco deposition, for in the lower member of the Pocobamba formation there is no evidence of high topographic relief near by.

Presumably the eastern limestone massif was raised principally along the Cerro de Pasco thrust fault. The assumption is founded on the increase in size and angularity, and the lack of sorting of boulders in the conglomerate as the fault is approached from the west. The Shuco, moreover, is not known east of the fault. Accompanying the faulting, initial slight but general upwarp produced eastward truncation of marginal lower Pocobamba beds.

The coarse and unsorted alluvium of the piedmont was cemented during deposition by carbonate-bearing surface waters from the limestone mountains to the east. Westward from the alluvial fans in front of the thrust, boulders were carried by stream action, reduced and rounded by abrasion and solution, and mixed with an increasing number of boulders from other sources.

It seems unlikely that the Shuco conglomerate itself became involved in the folding or faulting at this time. The conglomerate ends sharply above and is covered in apparent conformity by the Calera member of the Pocobamba formation.

The Calera member, named the Calera limestone by McLaughlin (1924), and Calera formation by McKinstry (1936), is estimated to be about 70 per cent soft shale, siltstone, and sandstone, and 30 per cent limestone. It has yielded a fresh-water flora and fauna which strongly suggest an early Tertiary age.

Limestone beds, in part silicified by hydrothermal solutions from the Marcapunta stock, form the only prominent exposures of the Calera member and suggest that the formation is principally limestone. At the Calera quarry (Pl. 1) and west of Colquirjirca, a clear idea of the lithology of the formation may be obtained (Sections 6, 7).

SECTION 6.—SECTION OF PART OF CALERA MEMBER OF POCOBAMBA FORMATION

Measured with tape in Calera quarry.

Bed No.	*Description*	*Thickness (feet)*
	Tertiary: Pocobamba formation	
	Calera member	
8	Limestone, light brownish gray, fossiliferous, with abundant planorbids, some charophyte oögonia in upper 3 feet (in upper part of southeast corner of quarry)	22
7	Shale, limy, light gray to gray green	14
6	Limestone, fine-grained, light gray brown, with rare and poorly preserved fossils	2.3
5	Shale, green	0.5
4	Marl, light greenish, thin-bedded, soft, with clay bands	17.7

3	Limestone, soft, marly, light greenish gray	16.5
2	Clay, green	5.0
1	Marl, soft, clayey, pale buff, porous	36.0
	Total exposed section	114.0
	Base is covered at level of dump	

SECTION 7.—SECTION OF PART OF CALERA MEMBER OF POCOBAMBA FORMATION

Measured 1 mile west of Colquijirca with tape and compass

Bed No.	*Description*	*Thickness (feet)*	
Tertiary: Pocobamba formation			
	Calera member		
	Chert, gray	2	
12	Limestone, fine-grained, brownish gray with abundant brown chert nodules in some beds. Approximately equivalent to bed 8 of Section 6. (Beds 12 and 13 are the same as the principal mineralized manto in the Colquijirca silver mines, shown in section by McKinstry (1936, p. 621)	15	
11	Shale, gray, limy, with beds of soft limy siltstone and sandstone	22	
10	Limestone, brownish gray, with bands and nodules of brown chert	6	
9	Shale, limy, with two beds of fine-grained gray cherty limestone each a foot thick	43	
8	Limestone, gray, with thin calcite veinlets	3	
7	Shale, with a few lenses of yellow marl	13	
6	Clay, gray green, limy, with several one foot beds of dull yellow limestone	18	
5	Clay, marl, and other soft beds, largely covered	18	
4	Clay (?), largely covered, with a few beds of yellow, cherty limestone 3 to 8 inches thick	10	
3	Limestone, yellow, with many irregular layers of brown chert	8	
2	Shale and sandstone, limy, greenish-gray, soft, largely covered	360	
	Total measured Calera member		518
	Shuco limestone conglomerate		
1	Conglomerate, unsorted, with subanguler boulders of limestones of eastern facies of Pucará group and of Mitu group quartz conglomerate	340	
	Angular unconformity		
Permian: Mitu group			
	Red shale and arkosic sandstone		

Three fossil lots taken at and near Calera quarry yielded poorly preserved fresh-water planorbids. Dr. Henry A. Pilsbry, who has made a provisional examination of the material, writes (letter of Dec. 1, 1947) that there are two species of *Drepanotrema* but that, as these are the first fossil ones ever found they do not help with age determination. In preparing some of this material, Dr. Otto Haas discovered some charophyte oögonia and forwarded them to Dr. Raymond E. Peck. Peck (letter of May 10, 1948) states that because of their poor preservation they are not too diagnostic. He would judge, however, that these charophytes are lower Tertiary or late Upper Cretaceous. They closely resemble *Actochara mitella* Peck and Reker described from the Evanston formation of Wyoming.

The Calera member of the Pocobamba was clearly deposited under conditions largely lacustrine in a region without prominent relief. No conglomerates or coarse sandstones have been detected in it. Certainly, then, the structural activity which produced the relief responsible for the Shuco fanglomerate must have decreased abruptly, or shifted to some other area.

The depositional history of the Pocobamba formation is illustrated schematically in Figure 2. In *A* the lower beds are deposited in a broad shallow basin toward the west, resting unconformably on all older formations. In *B* relief east of the Cerro de Pasco thrust is produced by movement along the fault, giving rise to the Shuco limestone conglomerate. The conglomerate rests conformably on the lower member to the west, but truncates Mesozoic and older beds to the east. It does not occur east of the fault. Lacustrine or fluvial deposition continues in the west, intertonguing with Shuco type conglomerate eastward. Finally, as illustrated in *C*, relief to the east is again reduced, and fine clastics and carbonate deposits are deposited conformably above the conglomerate.

No information is available concerning the subsequent depositional history of the Pocobamba formation in the vicinity of Cerro de Pasco. Erosion may have removed much material above the Calera member as now exposed.

Farther east, however, two faulted synclinal bands of red beds are tentatively correlated with the Pocobamba formation. One is about 5,

and the second about 8 miles due east of Cerro de Pasco. The latter passes just east of La Quinua (index map, Pl. 1). These red beds cover an extensive region east of La Quinua, and actually are preserved on the flanks of a major anticline near Ticlacayan, about 20 miles northeast of Cerro de Pasco. (See Billings, 1942, Pl. V.)

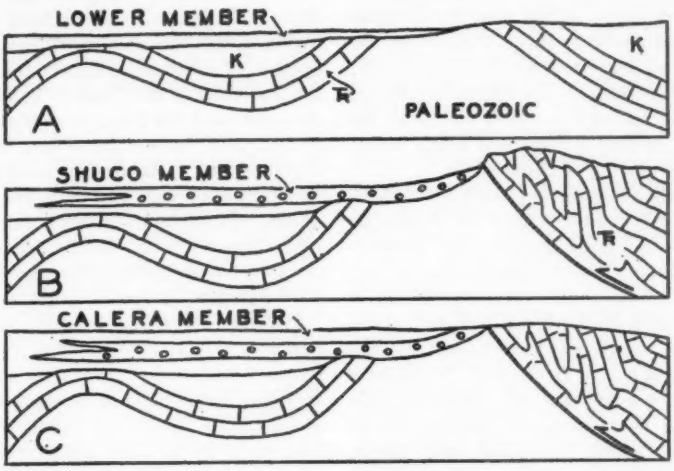

FIGURE 2.—DIAGRAM SHOWING DEPOSITIONAL AND TECTONIC HISTORY OF THE POCOBAMBA FORMATION

The red beds are largely shale, sandstone, and conglomerate of moderate pebble size, with some lenses and persistent beds of limestone, particularly in the lower part. Red colors are much more general than in the Pocobamba formation. Total known thickness is around 3600 feet. It is comparable in many ways to the Casapalca red beds (McKinstry and Noble, 1932, p. 503, 504). Undoubtedly these red beds east and northeast of Cerro de Pasco, the Pocobamba formation, and the Casapalca red beds are roughly equivalent in time. They appear, however, to have accumulated in separate basins and under somewhat different conditions.

Volcanic rocks have not been detected in the Pocobamba formation. Pyroclastics closely associated with the Cerro de Pasco and Marcapunta stocks must have once been much more extensive in the region, resting on the highest Pocobamba beds. As explained in the following structural history, such volcanics would have rested on the Pocobamba and older formations in sharp unconformity.

STRUCTURAL HISTORY

Abrupt changes in thickness of the Pucará limestone sequence cannot be explained wholly by wedging out of the sediments nor by erosion and unconformable overlap of lower Cretaceous strata. Both of these factors play some part in the development of the anomalous stratigraphic data. They are, however, greatly accentuated by a third element, structural in nature, which has had the effect of bringing facies markedly different and formed some distance apart into close juxtaposition.

The lower Mesozoic limestones and shales, considered together as the Pucará group, were deposited in a long, narrow part of the Cordilleran trough between the east side of the Western Cordillera and the crest of the Eastern Cordillera. Within the trough, certain zones, probably elliptical and parallel to the general geosynclinal trend, were consistently negative elements. In these negative areas carbonate sediments accumulated almost to the exclusion of argillaceous or arenaceous clastics. However, clastics appear as persistent interruptions of the carbonate sequence in adjacent more extensive regions. Discrepancies in thickness and lithology suggest that occasional positive movements may have brought about erosion of material deposited in the trough.

The thickest essentially uninterrupted limestone of this age recorded is the eastern facies of the Pucará group east of Cerro de Pasco. The western facies, on the other hand, represents an accumulation much thinner and interrupted by shale and sandstone beds. The thick eastern facies, as now known, appears to be local and limited to a narrow belt about 100 miles long, extending from near Ambo, southward to the vicinity of Carhuamayo.

Deformation subsequent to lower Liassic sedimentation followed the grain of the geosyncline and of the elongated negative and intermittently negative areas of sedimentation. A mild disturbance took place during the middle or upper Jurassic. Emergence of this part of the Cordilleran trough was accompanied by subsidence along a belt to the west. In southern Peru, marine limestones and clastics accumulated along the present coast during Middle and Upper Jurassic (Callovian) time (Jenks, 1948). Marine sedimentation occurred during the Neocomian in the Lima areas (Lisson, 1907). The Nevadian disturbance was stronger in southern than in central Peru, but there is evidence of mild warping and erosion of the Pucará group around Cerro de Pasco prior to the deposition of the Neocomian Goyllarisquisga continental beds.

During the Middle and early Upper Cretaceous that part of the Cordilleran trough including Cerro de Pasco, Oroya, and Huancavelica to the south was again a negative belt. Extensive limestones of this age are the youngest marine formations of the Andes in central Peru.

Between marine sedimentation of early upper Cretaceous age and deposition of the continental Pocobamba formation, most probably of early Tertiary age, strong folding occurred in the Cerro de Pasco and other near-by regions. This manifestation of the Laramide orogeny produced the major anticline which brings up the Excelsior group in the Cerro de Pasco region, and another to the east, much greater in extent, which broadly elevated older schists and granites along the Huachón trend.

Folding at this time produced sharper folds in the zone of the western facies of the Pucará group near Cerro de Pasco than in the thicker eastern facies. Overlying formations were similarly affected. The massive, competent eastern facies acted as a bulwark to strengthen the whole stratigraphic column. Thus, in the vicinity of La Quinua, and southeast of Vareas' hacienda, red beds of probable early Tertiary age rest on Cretaceous strata in apparent conformity. West of the Cerro de Pasco fault, on the other hand, the Pocobamba formation rests on Excelsior, Mitu, and Pucará with sharp angularity (Pl. 1). In the Goyllarisquisga region the Pocobamba rests on Pucará and Goyllarisquisga, with far less angularity than is evident near Cerro de Pasco. Clearly the intensity of the pre-Pocobamba folding dininished somewhat northwestward, and probably westward as well.

Probably the Cerro de Pasco thrust fault began to be active at this time. Pucará limestones, forced westward toward a region where they were far thinner and less competent, broke at the eastern flank of the highest and weakest fold, where the Excelsior group is now exposed. Close folding, and thrusting along the Cerro fault, produced marked shortening of the gap between the eastern and western facies of the Pucará group, a process which was to be accentuated later.

A long interval of quiescence brought about the erosion of the folded Mesozoic and older formations to a condition of moderate relief, close to sea level, before conditions once more became propitious for the preservation of sediments in abundance. In shallow intermontane valleys, early Tertiary lake, river, and alluvial deposits of the Pocobamba formation began to accumulate. In another valley eastward red beds accumulated, as they did along a major broad valley along what is now the western Cordillera.

Intense folding and faulting, undoubtedly accompanied by general upward land movement, ended Pocobamba sedimentation. So great were the compressive stresses that west of the Cerro de Pasco thrust fault isoclinal folds were produced in the upper beds of the Pocobamba formation (Billings, 1942, Pl. VI). The competent Shuco member was less tightly compressed, but did attain vertical dips. The intense compression produced plunging asymmetrical folds in the Shuco limestone conglomerate and, by the squeezing of this competent material, induced disharmonic isoclinal folds

in the extremely incompetent Calera member. Folds west of the Cerro fault tend to be asymmetrical, with axial planes dipping eastward (Sections C-D and H-I-J of Pl. 1).

The large northwestern area of Pocobamba formation shown on Plate 1 is an irregular, canoe-shaped, doubly plunging syncline (Pl. 3, figs. 2, 3).

Offset from the northwestern area just described is the extensive syncline between the Cerro de Pasco and Marcapunta stocks. Though this syncline is more open than that to the northwest, it shows asymmetric folds with eastward-dipping axial planes in the southern portion at Colquijirca. The fold plunges south into the Marcapunta stock. Gravels of the flat pampa conceal any Pocobamba beds which may exist south of the stock.

Intensity of folding in the Tertiary beds increases eastward in both the northwestern (Cacuan-Pumagaga) and eastern (Cerro-Marcapunta) synclines. Shuco conglomerate is overturned just west of the Cerro de Pasco thrust fault between Lakes Quiulacocha and Yanamate as a result of the continued westward thrust of Pucará limestones. That the fault continues south at least to the Marcapunta stock is suggested by the nature of the folding in the Colquijirca Mine. Northward along the fault Pocobamba beds have been removed by erosion because of the south plunge.

A second thrust fault of large displacement is postulated along the east side of the northwest syncline. In places between Cacuan and Pumagaga, and between Pumagaga and the southern outcrop of the synclinal trough, the massive Shuco conglomerate does not outcrop. Apparently this is because the vertical conglomerate member has been thinned or cut out along a thrust. Confirmation is given by an exposure half a mile north of Pumagaga, where brecciated Pucará limestones are in fault contact with the Shuco.

The hypothetical southern extension of the thrust which passes Pumagaga is inserted because of the obvious dislocation of pre-Tertiary folded formations southeast of Yuraghuanca. A second fault must almost inevitably exist between the isoclinal anticlines to the southwest and north of Yuraghuanca. In the absence of confirmatory data this fault was omitted on the map.

North of Pumagaga, the thrust is believed to be offset by an accurately located vertical fault striking northwest. The latter appears to be a tear fault which separates a southern mobile block from a northern relatively stable block. The fault may well have curved around to join the main thrust at a point where the Shuco thins abruptly south of Cacuan. The south side appears to have moved upward to the northwest with a rotational movement which was the result of westward thrusting.

At the north edge of Plate 1 another thrust fault swings abruptly into a tear fault at its south end. In this case Pucará limestone is displaced westward on the north side. Between the two tear faults the thrust is displaced eastward nearly a mile. In this segment basal Pucará beds and the Mitu group on the east are thrust upward against the upper Pucará beds along at least two faults (Pl. 1, Section A-B). Wide zones of brecciation mark these breaks.

The faults of the western thrust zone appear to have been inactive during Pocobamba time. There is no evidence that they in any way limited or controlled facies of the Pocobamba formation. Whether they had been active during the folding which preceded deposition of Pocobamba strata has not been determined.

Movement along the Cerro de Pasco longitudinal thrust fault occurred before, during, and after Pocobamba time. During the last stage of movement Pucará limestones of the eastern facies were thrust westward and upward over older Excelsior shales and younger Pocobamba beds. At the same time massive segments of the Pucará east of the fault were dislocated to form isoclinal folds with axial planes dipping steeply eastward. Folding was accompanied by brecciation along axial planes, as would be expected in the yielding of such a competent sequence. In general, folds may be traced by direct field observation north and east of Cerro de Pasco, but are lost in a sequence of steep east dips 3 miles across the strike at the latitude of Yanamate Lake. Structure in this region is tentatively worked out on the basis of *Spondylospira* occurrences, on the assumption, yet to be proved, that this genus around

Cerro de Pasco marks a distinct stratigraphic unit.

Quartz monzonites and other intrusives which, with associated pyroclastics, make up the Cerro de Pasco, Marcapunta, and Yanamate stocks appear to have been emplaceP after the post-Pocobamba folding and faulting. They do not show strong deformation in a north-south direction, and there is certainly a suggestion that the Cerro stock transects the Cerro de Pasco thrust fault. The two larger stocks appear to be controlled in position by the anticlinal high which brings the Excelsior group to the surface west of the Cerro de Pasco thrust fault. The small Yanamate stock is astride an isoclinal synclinal axis which may have controlled its position.

Following the igneous activity, or perhaps somewhat overlapping it, this region was uplifted to its present elevation. Erosion has removed the Pocobamba formation from anticlinal and upthrust blocks, leaving it only where protected in plunging synclines. Another 2000 feet of erosion which may be anticipated within a relatively short span of geologic time will remove all trace of Tertiary sedimentary rocks from the Cerro de Pasco area. The region would then be relatively uncomplicated by conflicting geological evidence and would perhaps be interpreted by geologists as an area of straightforward, simple folding and faulting of older rocks.

The marked difference in thickness of the Pucará group on opposite sides of the Cerro de Pasco thrust fault is believed to be due to the bringing together of two facies of approximately the same age by sharp folding and by thrust faulting, accentuated by moderate differential erosion during Nevadian time. Tertiary deposits west of the main fault were laid down in a tectonic and erosional basin whose position was largely determined in Laramide time. The main folding and faulting took place during the late Cretaceous and again, after a period of relative quiet, during the early Tertiary. Igneous activity and mineralization followed the last tectonic upheaval. Stratigraphic and structural data clearly distinguish the lower Mesozoic and Tertiary formations.

References Cited

Ahlfeld, F. (1932) *Die Silbererzlaggerstätte Colquijirca, Peru*, Zeit. Prükt. Geol., vol. 40, p. 81–87.

Billings, Marland P. (1942) *Structural geology*, Prentice-Hall, New York, 473 p.

Boit, Bernardo (1940a) *Lineas generales de la estratigrafia de la region de Cerro de Pasco*, Acad. Nac. de Ciencias Exact., Fis. y Nat. de Lima, Actas, vol. 2, Fasc. 4, p. 1–54.

—— (1940b) *Sobre la edad de una formación de la region del centro*, Acad. Nac. de Ciencias Exact., Fis. y Nat. de Lima, Actas, vol. 3, Fasc. 4, p. 212–222.

—— (1944) *Extensión de los terrenos triasicos en la hoya del Marañon*, Acad. Nac. de Ciencias Exact., Fis. y Nat. de Lima, Actas, vol. 7, p. 249–260.

—— (1945) *Geologia post-carbónica de Carhuamayo*, Acad. Nac. de Ciencias Exact., Fis. y Nat. de Lima, Actas, vol. 8, Fasc. 2, p. 69–85.

Cox, L. R. (1949) *Moluscos del Triasico superior del Peru*, Inst. Geol. del Peru, Lima, Bol. 12, 50 p.

Dunbar, Carl O., and Newell, N. D. (1946) *Marine early Permian of the Central Andes and its fusuline faunas*, Am. Jour. Sci., vol. 244, p. 377–402, 457–491.

Haas, Otto (1946) *Triassic gastropod fauna from Cerro de Pasco, central Peru* (Abstract), Geol. Soc. Am., Bull., vol. 57, p. 1198–1199.

—— (1947) *Mesozoic faunas of Peru: Research program*, Science, vol. 106, p. 144.

Harrison, J. V. (1943) *The geology of the central Andes in part of the province of Junin, Peru*, Geol. Soc. London, Quart. Jour., vol. 99, p. 1–36.

Jenks, William F. (1948) *Geology of the Arequipa quadrangle* (*Geologia de la hoja de Arequipa*) (English and Spanish), Inst. Geol. del Peru, Lima, Bol. 9, 204 p.

Körner, Karl (1937) *Marine* (*Cassianer-Raibler*) *Trias am Nevado de Acrotambo* (*Nord-Peru*), Palaeontographica, vol. 86, Abt. A, p. 145–237.

Lisson, C. I. (1907) *Contribución a la geologia de Lima y sus Alrededores*, Lima, 125 p.

—— and Boit, Bernardo (1942) *Edad de los fósiles peruanos y distribución de sus depositos en la republica, con un mapa paleontologico del Peru*, 4th ed., Lima, 320 p.

McKinstry, H. E. (1936) *Geology of the silver deposit at Colquijirca, Peru*, Econ. Geol., vol. 31, p. 619–635.

—— and Noble, J. A. (1932) *The veins of Casapalca, Perú*, Econ. Geol., vol. 27, p. 501–522.

McLaughlin, D. H. (1924) *Geology and physiography of the Peruvian cordillera, Departments of Junin and Lima*, Geol. Soc. Am., Bull., vol. 35, p. 591–632.

——, Graton, L. C., and others (1933) *Copper in the Cerro de Pasco and Morococha districts, Department of Junin, Peru*, Copper Resources of the World, 16th Inter. Geol. Cong., Washington, p. 513–544.

Moses, J. H. (1942) *Recent studies of the geology of the Cerro de Pasco district* (*Perú*), 8th Am. Sci. Cong. (1940), Pr., vol. IV, p. 673–675.

Newell, Norman D. (1949) *Geology of the Lake Titicaca region, Peru and Bolivia*, Geol. Soc. Am., Mem. 36, 111 p.

——, Chronic, B. J., and Roberts, T. G. (1949) *Upper Paleozoic of Peru*, King's Crown Press, 174 p.

Steinmann, G. (1929) *Geologie von Peru*, Heidelberg, 448 p. (Translation in Spanish, Heidelberg, 1930, 448 p.)

Tschopp, H. J. (1948) *Geologische Skizze von Ekuador*, Bull. d. Ver. Schweiz. Petroleumgeol. und -Ing., vol. 15, no. 48, S. 14–45.

Vokes, H. E., and Haas, Otto (1944) *South American and European species of* Spondylospira, Jour. Paleont., vol. 18, p. 283–284.

Welter, Otto A. (1946) *Apuntes sobre la geologia de los alrededores de Huachón*, Inst. Geol. del Peru, Bol. 6, 6 p.

UNIVERSITY OF ROCHESTER, ROCHESTER 3, NEW YORK

MANUSCRIPT RECEIVED BY THE SECRETARY OF THE SOCIETY, NOVEMBER 30, 1949